UiT The Arctic University of Norway

Faculty of Health Science

Exploring and Targeting Novel Cancer Networks in Multidrug Resistant Neuroblastoma

Lotte Olsen

A dissertation for the degree of Philosophiae Doctor, January 2020

Exploring and Targeting Novel Cancer Networks in Multidrug Resistant Neuroblastoma

Lotte Olsen

A dissertation for the degree of Philosophiae Doctor

UiT The Arctic University of Norway

Faculty of Health Sciences

Department of Clinical Medicine

Pediatric Research Group

Tromsø, Norway

JANUARY

2020

Contents

Acknowledgements

This work has been carried out in the Pediatric Research Group, Faculty of Health Sciences, UiT The Arctic University of Tromsø. Finalizing the work for this thesis has been a group-effort, and I would like to express my sincere gratitude to the following people and institutions.

To my main supervisor, prof. Christer Einvik, for his expert advices and guidance through both "Forskerlinjen i medisin" and the PhD course. Your directions and suggestions have been invaluable for my work. Thank you so much for continuing being my supervisor after Forskerlinjen.

To my co-supervisor, prof. M.D. Trond Flægstad for including me in the Pediatric Research Group many years ago, for helping me to stay part of this amazing group and aiding me in my continuing career. To my second co-supervisor, Dr. Sarah Andrea Roth, for propositions and suggestions during work on the manuscripts.

To the amazing laboratory engineer and my good friend, Cecilie Løkke, for her technical assistance and expert advices, for our enjoyable and fruitful conversations, and excellent companionship both in the laboratory and on excursions abroad.

To my former and present laboratory colleagues M.D. Øyvind Hald, Dr. Swapnil Parashram Bhavsar, Dr. Peter Utnes, Dr. Vera Susana Carneiro Maia and Dr. M.D. Bjørn Helge Haug for the interesting discussions and help in the laboratory. A special thanks to Swapnil for helping me during finalization of the thesis.

Also, thanks to Roy Lyså for his helpful assistance with diverse laboratory instruments.

To my wonderful friends outside school and work, who always have a kind and encouraging word at hand, and provide a safe and entertaining environment with activities that help keep my mind of work and performance.

To UiT The Arctic University of Tromsø, The Northern-Norwegian Health Authorities (Helse Nord), The University Hospital of North Norway (UNN), Barnekreftforeningen and Simon Fougner Hartmanns Familiefond who funded my PhD project. In addition, I would like to send my sincere gratitude to all patients and their families for their participation and contribution to neuroblastoma research.

A special thanks to my closest family, for their patience and encouragement. To my mother and father who are always there for me and help me when I need it. You have had a major influence in my life and on my career path, from the very beginning when you aided me with my schoolwork. I am also extremely grateful for my brother and sister who have taught med so much about life, and that I always can count on. Thank you to Anne and Kristian for always being there for us when we need them. Lastly, to the love of my life, Kenneth André Johansen, for sticking with me both in good times, and when things are rough. Thank you so much for blessing me with the most wonderful children I could ever have asked for. You all have made me the person I am today! Love you!

January 2020

Lotte Olsen

Tromsø, Norway

List of Abbreviations

Abbr.	Full name
ABC	ATP-binding cassette
AGO	Argonaute
AKT	AKT Serine/Threonine Kinase 1
ALK	Anaplastic lymphoma kinase
ALL	Acute lymphoblastic leukemia
APAF-1	Apoptotic peptidase activating factor 1
ATM	Ataxia telangiectasia mutated
ATR	ATM and RAD3-related
AURKA	Aurora kinase A
AXL	AXL receptor tyrosine kinase
BAD	BCL2 associated agonist of cell death
BAK	BCL-2 antagonist/killer
BAX	BCL-2 associated X
BCL-B	BCL2 like 10
BCL-W	BCL2 like 2
BCL-X_L	Bcl-2-like 1
BCL-2	B-cell lymphoma 2
BER	Base excision repair
BFL-1	BCL2 related protein A1
BH domain	BCL-2 homology domain
bHLHZip	Basic helix-loop-helix leucine zipper
BIK	BCL2 interacting killer
BIM	BCL2 like 11
BIRC5	Survivin
BMF	Bcl2 modifying factor
BMMSC	Bone marrow-derived mesenchymal stem cell
BRCA1	BRCA1 DNA repair associated

Abbr.	Full name
CAR-T cells	Chimeric antigen receptor T-cells
CCND1, CCND2	Cyclin D1, cyclin D2
CDS	Coding sequence
CHK1, CHK2	Checkpoint kinase 1 and 2
circRNA	Circulatory RNA
CLIP	Crosslink immunoprecipitation
CNS	Central nervous system
COG	Children's Oncology Group
CRISPR	Clustered Regularly Interspaced Short Palindromic Repeats
CYP	Cytochrome P450
DDR	DNA damage response
DGCR8	DiGeorge critical 8
DME	Drug-metabolizing enzyme
DNA	Deoxyribonucleic acid
DSB	Double stranded break
dsRNA	Double stranded RNA
ERK	Extracellular signal-regulated kinase
ETS	External transcribed spacers
EV	Extracellular vesicle
GCR	Gross chromosomal rearrangement
GM-CSF	Granulocyte-macrophage colony stimulating factor
GOLPH3	Golgi phosphoprotein 3
GSK3β	Glycogen synthase kinase 3β
GST	Glutathione S-transferases
HITS	High throughput sequencing
HR	Homologues recombination
HRK	Harakiri, BCL2 interacting protein

HVA	Homovanillic acid
H2AX	H2A.X variant histone
IDRF	Image-Defined Risk Factors
IL	Interleukin
INRG	International Neuroblastoma Risk Group
INRGSS	International Neuroblastoma Risk Group Staging System
INSS	International Neuroblastoma Staging System
ITS	Internal transcribed spacers
JAK	Janus kinase
KDM1A	Lysine demethylase 1A
lincRNA	Long intergenic non-coding RNA
LNA	Locked nucleic acid
lncRNAs	Long noncoding RNAs
LOH	Loss of heterozygosity
MAX	MYC-associated factor X
MCL-1	Myeloid cell leukemia-1
MDM2	MDM2 proto-oncogene
MDR	Multidrug resistance
mIBG	Metaiodobenzylguanidine
miRNA	MicroRNA
MMP-1, MMP2, MMP-14	Matrix metallopeptidase 1, 2 and 14
MMR	Mismatch repair
MNA	*MYCN* amplified
MOM	Mitochondrial outer membrane
MRD	Minimal residual disease
MRE	MicroRNA recognition element
mRNA	Messenger RNA

MRP-1, MRP-4	Multidrug resistance associated protein-1 and 4
mTOR	Mechanistic target of rapamycin kinase
MUC1	Mucin 1, cell surface associated
MYC (C-MYC)	v-Myc avian myelocytomatosis viral oncogene homolog
MYCN	v-Myc avian myelocytomatosis viral oncogene neuroblastoma derived homolog
NAT	N-acetyltransferase
NCC	Neural crest cells
NCL	Nucleolin
ncRNA	Non-coding RNA
NER	Nucleotide excision repair
NHEJ	Non-homologous end joining
NOXA	Phorbol-12-myristate-13-acetate-induced protein 1
NPM1	Nucleophosmin
NSCLC	Non-Small Cell Lung Cancer
Nt	Nucleotide
PARP-1	Poly (ADP-ribose) polymerase-1
P-body	Processing body
PGA	Poly-(α)glutamic acid
piRNA	Piwi-interacting RNA
PI-3	Phosphatidylinositol 3
PLK1	Polo-like kinase 1
Pol (I/II/III)	Polymerase (I/II/III)
Pre-miRNA	Precursor microRNA
Pri-miRNA	Primary microRNA
PTEN	Phosphatase and tensin homolog
PUMA	BCL2 binding component 3

RAN-GTP	RAS-related nuclear protein-guanosine-5'-triphosphate
RAS	Rat sarcoma
RB	Retinoblastoma protein
rDNA	Ribosomal DNA
RISC	RNA-induced silencing complex
RNA	Ribonucleic acid
RNAi	RNA interference
RPs	Ribosomal proteins
rRNA	Ribosomal RNA
RTK	Receptor tyrosine kinase
SCP	Schwann cell precursors
shRNA	short hairpin RNA
sIL-6R	Soluble interleukin-6 receptor
siRNA	Small interfering RNA
SL1	Selectively factor 1
snoRNA	Small nucleolar RNA
snRNA	Small nuclear RNA
SNP	Single nucleotide polymorphism
SNV	Single nucleotide variations
SSBR	Single-strand break repair
ssDNA	Single-stranded DNA
STAT3	Signal transducer and activator of transcription 3
STR	short tandem repeat
TAM	Tumor-associate macrophages
tBID	BH3 interacting domain death agonist
TERF1	Telomeric repeat binding factor 1
TIF1A	Transcription factor 1A
TME	Tumor microenvironment
TNF	Tumor necrosis factor
TPX2	Targeting protein for Xklp2
TP53	Tumor protein P53
TRBP	Transactivation-response element RNA-binding protein
tRNA	Transfer RNA
UBF	Upstream binding factor
UTR	Untranslated region
VEGF	Vascular endothelial growth factor
VMA	Vanillylmandelic acid

Summary

Neuroblastoma is the most common extra-cranial tumor in childhood and accounts for up to 15% of all cancer related deaths in children. Constant efforts have improved therapy, but the mortality is still high for patients with high-risk neuroblastoma. Many possess tumors that are refractory to standard treatment, or they suffer from relapse of multi-resistant disease. Alternative treatment options for these patients are necessary; both to improve survival and to reduce therapy-related adverse effects that often come from the multimodal treatment program these children have to endure.

In this thesis, I will present findings from three scientific works in neuroblastoma model systems that enlighten cellular networks with the potential to be manipulated for anti-tumor effects. MicroRNAs, small endogenous non-coding RNAs, have previously been linked to tumor initiation, progression and therapy resistance, thus manipulation of expression can possibly have clinical implications. In manuscript I and II we show that *miR-323a-3p* and *miR-193b-3p* have tumor suppressive function in neuroblastoma by themselves, and that *miR-193b-3p* additionally can improve sensitivity of neuroblastoma cells to the small molecule inhibitor ABT-737. This compound mimics the pro-apoptotic protein BAD, which sequesters the anti-apoptotic protein BCL-2, thus allowing death signal to be transmitted for induction of apoptosis. We show that selected neuroblastoma cells that are resistant to ABT-737 will become more sensitive in response to upregulation of *miR-193b-3p*.

In paper I, we demonstrate that the small molecule inhibitors of ribosome biogenesis, CX-5461 and quarfloxin, reduce growth and induce DNA damage, G2-cell cycle arrest and downregulate MYCN in neuroblastoma. We propose that they have great potential as therapy in neuroblastomas that carry amplification of the oncogene *MYCN* and have functional p53.

List of Manuscripts and Papers

Manuscript I

***Hsa-miR-323a-3p* Functions as a Tumor Suppressor and Targets *STAT3* in Neuroblastoma Cells**

Swapnil Parashram Bhavsar*, Lotte Olsen*, Cecilie Løkke, Trond Flægstad and Christer Einvik

Manuscript

Manuscript II

***Hsa-miR-193b-3p* Sensitizes MCL-1 Primed Neuroblastoma Cell Lines to the BH3 Mimetic ABT-737**

Lotte Olsen*, Sarah A. Roth*, Cecilie Løkke, Swapnil Parashram Bhavsar, Trond Flægstad and Christer Einvik

Manuscript

Paper I

Inhibitors of Ribosome Biogenesis Repress the Growth of *MYCN*-amplified Neuroblastoma

Øyvind H. Hald, Lotte Olsen, Gabriel Gallo-Oller, Lotta Helena Maria Elfman, Cecilie Løkke, Per Kogner, Baldur Sveinbjörnsson, Trond Flægstad, John Inge Johnsen and Christer Einvik

Oncogene (2019) 38(15): 2800-2813

*The authors have contributed equally to the work

Introduction

Malignancy in Childhood

Every year more than 300.000 children are diagnosed with cancer (1). It is the lead cause of disease-related death in children of western countries and only second to infection worldwide (2, 3). Pediatric malignancy can roughly be divided into hematological malignancy, intra-cranial tumors and extra-cranial tumors (4). In contrast to adult cancers that tend to result from a series of mutational insults, usually due to prolonged exposure to toxins and stressors, childhood cancers typically owe to disturbance in developmental processes.

Since the 1970's incidence rate of childhood cancer has increased, with leukemia and solid tumors in the central nervous system (CNS) being the dominating cancer types. Fortunately, despite increased incidence, there have been a clear decline in cancer related deaths, especially in leukemia, lymphoma and gonad cancers (3, 5-7). This is largely due to improvement of diagnosis and risk stratifications, and multiple clinical trials leading to successful therapy regimens. The advent of technology that enable easy characterization of cytogenetic and biological cancer aberrations from each individual, provided the opportunity to do more precise risk assessment, consequently also more accurate therapy (8).

Leukemia and lymphoma cells generally respond well to standard chemotherapeutic agents, causing a strong increase in survival the last decades to about 90% (3, 5). Improving survival for children with solid tumors has not been equally successful (5). As treatment often involves chemotherapeutic doses up to maximal tolerable capacity, as in e.g. high-risk neuroblastoma, alternative approaches to disseminate disease are urgently needed.

Neuroblastoma

Neuroblastoma is the most common solid tumor in early childhood (1, 6, 9, 10), with a median age at diagnosis of 18 months (11). Although neuroblastoma account for merely 6-8% of all pediatric cancers (3, 9, 12), it is responsible for up to 15% of all cancer related deaths in children (7). Therapy improvement have increased survival (5, 13), and favorable neuroblastoma have an excellent prognosis (14, 15). Unfortunately, about half of all patients are classified as high-risk patients at diagnosis (16), with an overall survival of only 50% (15) despite aggressive treatment.

Origin

Neuroblastoma originates from developing neural crest cells (NCC) which, under normal circumstances, give rise to various tissues (17). A recent theory suggest that the

sympathoadrenal lineage of NCCs diverge in early embryonic state: One differentiate into sympathetic neurons which forms suprarenal sympathetic ganglions and a small chromaffin cell population in the adrenal medulla; another differentiate into schwann cell precursors (SCPs), which develop into chromaffin cells that comprise the majority of the adrenal medulla (**figure 1**) (18). Neuroblastoma can originate from both paths, and the source reflects the localization of the tumors, which can be anywhere along the sympathetic chain, and in the adrenal glands (**figure 2**) (19). Single-cell examination have revealed that neuroblastoma tumors compose of distinct cellular subtypes, alone or in combination, which have the same genetic profile, but different transcriptome and regulation of super-enhancers (20, 21). The possibility of switching between these subtypes (21), combined with the low frequency of mutations in neuroblastoma (22, 23), suggest that epigenetic modification has a pivotal role in tumor initiation.

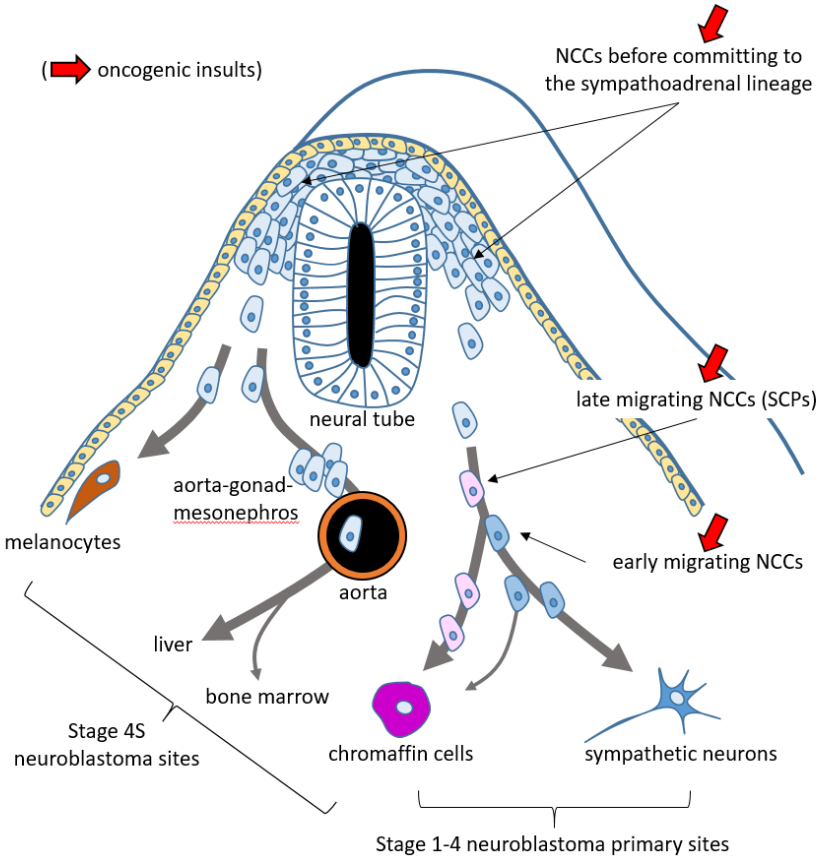

Figure 1: Origin of neuroblastoma reflects the localization of tumors. Neural crest cells (NCC) migrate and differentiate into sympathetic neurons and a small proportion of the chromaffin cells in the adrenal medulla (early migrating NCCs) or become the larger part of the chromaffin cells in the adrenal medulla (late migrating cells). An alternative route for NCCs is to differentiate into melanocytes, or cells in the liver and bone marrow via the aorta-gonad-mesenephros. This route is probably the source for 4S tumors. The figure is reprinted with permission from (24).

Interestingly, it appears that stage 4S neuroblastoma can be initiated even before the NCC stem cells commit to the sympathoadrenal linage. This is a special stage in neuroblastoma

where patients with disseminate disease can have an excellent prognosis. NCC stem cells that migrate to the skin or the transient embryonal tissue aorta-gonad-mesonephros are probably the source of stage 4S tumors in the skin, liver and bone marrow (**figure 1**) (24). Hence, opposed to the severe stage 4 tumor, these tumors arise from developmental cells rather than being metastatic tumors from a primary source.

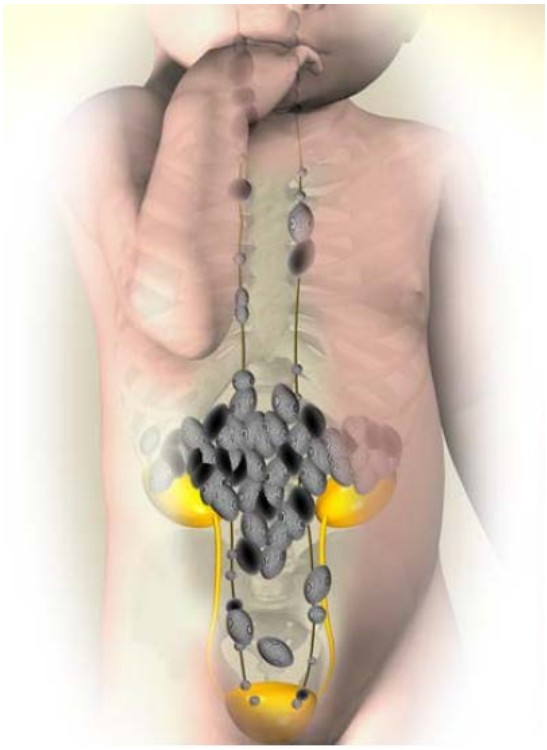

Figure 2: Distribution of tumors. Primary neuroblastoma tumors arise along the sympathetic chain and in the adrenal glands. The figure is reprinted with permission from (2).

Symptoms and Signs

Neuroblastoma can present with palpable tumors anywhere from the neck to the pelvis, and localization of the tumors can dictate the perceptible symptoms and signs (25, 26). Involvement of nerve roots in the neck or pelvis can cause Horner syndrome or bladder dysfunction, obstipation or lower extremity pain, respectively. Abdominal primary tumors or liver metastases may manifest as belly distention or dysfunction of the liver, lung or kidneys. More customary malignancy signs like fever and weight loss are common, and hypertension, flushing and tachycardia triggered by release of catecholamines can occur. Actually, 90% of all children suffering from neuroblastoma have elevated levels of catecholamines or the catecholamine metabolites homovanillic acid (HVA) and vanillylmandelic acid (VMA) in blood or urine (27, 28). About 40% of all patients present metastatic disease at the time of diagnosis (29), with lymph nodes, bone marrow and bone being the most common sites (29,

30). Bone marrow lesions can disturb blood cell production, resulting in anemia or thrombocytopenia, while severe pain or periorbital bruising can be signs of bone metastases. A special symptom exclusive for 4S disease is palpable lesions in the skin (25, 26). This can be explained by the new theory of origin (24) described in the previous section.

Staging and Risk Group Classification

To evaluate tumor dissemination, two different staging systems are used, the International Neuroblastoma Staging System (INSS) and the International Neuroblastoma Risk Group Staging System (INRGSS). INSS is a post-resection system applied for decades to categorize tumors into stage 1-4 or 4S according to localization of primary tumor and metastatic lesions (31). The newer INRGSS is a pretreatment, non-invasive system that stages the disease according to Image-Defined Risk Factors (IDRFs) into L1, L2, M and MS (32, 33).

These staging systems are incorporated into risk group classification systems together with other prognostic factors, in order to specialize treatment. In the Children's Oncology Group (COG) risk assessment form, patients are stratified into risk groups low, intermediate or high based on age at diagnosis, INSS stage, *MYCN*-copy number, ploidy and pathological classification (**supplementary table 1**) (34). There is a clear difference pertaining age at diagnosis. Children under 18 months often have much better prognosis than older kids and adults (11, 35). However, amplification of the *MYCN* (v-Myc avian myelocytomatosis viral oncogene neuroblastoma derived homolog) oncogene, one of the strongest prognostic factors in neuroblastoma (36, 37), almost automatically classifies patients into high-risk group, irrespective of other features (32, 34). Low differentiation status and diploid chromosome content are also associated with worse outcome (32, 38-40). Age, *MYCN*-copy number, ploidy and histopathological features are also included in INRG classification system; however, they use INRGSS and include 11q aberrations (41-43) in their form to divide into very low-, low-, intermediate- and high-risk groups (32) (**supplementary table 2**). There are other chromosome aberrations, not included in these classification systems, which are frequently observed, such as 1p and 14q loss of heterozygosity (LOH), and gain of chromosome 17q (42, 44).

MYCN Amplification in Neuroblastoma

The *MYCN* gene encodes the 60-63 kDa MYCN oncoprotein, a basic helix-loop-helix leucine zipper (bHLHZip) transcription factor in the MYC-family. To initiate transcription, it forms a heterodimer with MYC-associated factor X (MAX) and binds E-box sequences (variations of CANNTG) in the promoter region of target genes. It shares gene sequence and

protein structure homology and have several mutual targets with another MYC family member C-MYC, also referred to as MYC (v-myc avian myelocytomatosis viral oncogene homolog) (45). However, whereas MYC normally is ubiquitously expressed in proliferating cells, MYCN is restricted to embryonic development of neural tissue (45, 46).

MYCN amplification (MNA) is found in 20-25% of all neuroblastoma cases, while 40-50% of all high-risk patient carry such aberration (32, 47-50), usually combined with high expression of MYCN or MYCN signature genes (50, 51). MNA has been considered one of the most powerful prognostic factors in neuroblastoma for decades (36, 37) and it is involved in tumor initiation and progression of neuroblastoma (52). MYCN is a master regulator of many important pathways, for example the p53 pathway. Despite a functional p53, MYCN can alter the p53 response to DNA damage and sustain proliferation (53).

Interestingly, a neuroblastoma tumor can consist of a heterogeneous mixture of MNA cells and non-MNA cells. A recent study therefore advocates that tumors with such heterogeneity should be individually considered to avoid over-treatment (54). Other *MYCN*/*MYC*-related abnormalities can also have clinical implication, despite a lack of MNA. *MYCN* gain of function mutation is not that common, but it does occur (22) and can produce similar phenotypic alterations as amplification in neuroblastoma. Additionally, high expression of MYC is associated with bad prognosis (50, 55), and there is even evidence of MYC having neuroblastoma initiating capacity (56). Although amplification of the *MYC* gene is rare in neuroblastoma (22, 23), amplification of enhancer regions that promote MYC expression probably occurs (56). In all, the heterogeneity of neuroblastoma makes it challenging to stratify patients into risk groups. It is a continues work to find reliable prognostic factors and improve current stratification systems (34). It also emphasizes the need for personalized treatment, at patient group- and individual level.

Treatment

Tailored treatment after risk stratification has been applied for decades. Children with low-risk 4S neuroblastoma can benefit from merely observation (14, 57), as spontaneous regression of tumors are frequently seen, while other low-risk patients get complete surgical tumor resection (35, 58). For intermediate-risk patients, cycles of chemotherapy treatment are included (59, 60). High-risk patients, on the other hand, require intensive multimodal treatment regimen (61, 62). An induction phase comprises chemotherapy and surgical resection, before the consolidation phase is initiated by myeloablative therapy with autologous stem cell

transplantation followed by radiotherapy. To tackle minimal residual disease (MRD) a maintenance phase, with immune- and differentiation therapy, is also necessary. The differentiation inducing agent isotretinoin has proven to increase survival for children with progressive disease (61), and has for the last ten years been part of standard treatment. GD2, a disialoganglioside found almost exclusively on the surface of neuroectodermal tumors like neuroblastoma (63), provides a tumor specific target site for immunotherapy. The anti-GD2 chimeric antibody ch14.18 (dinutuximab) was shown to improve survival rates in combination with interleukin-2 (IL-2) and granulocyte-macrophage colony-stimulating factor (GM-CSF) (64). This regimen was part of the maintenance phase until recently, when exclusion of IL-2 was recommended since it does not appear to provide additional survival advantage (65, 66). Ongoing trials strive to find the ideal treatment regime for anti-GD2 administration to minimize adverse effects (66, 67), and see whether anti-GD2 antibodies could be beneficial as adjuvant treatment in other therapy settings (62, 68, 69).

Nearly half of all neuroblastoma patients experience recurrent tumors after initial treatment (15, 70). Patients with refractory or relapse disease are rarely cured (70), and the main objective is often just to get therapy response to relieve tumor burden and enhance quality of life. Chemotherapy regimens (71, 72) and radiation therapy with ^{131}I-mIBG (16, 73, 74) is the current treatment approach for these patients. However, many tumors become insensitive to most chemotherapeutic agents (75) rendering a necessity for alternate experimental protocols. Small molecule inhibitors against ALK (37) and aurora kinases (76) are being tested, and immunotherapy using patients own T-cells modified to express chimeric antigen receptors (CAR T-cells) that target tumor cells are part of several clinical trials (77). Most neuroblastoma patients with refractory or relapsed disease are enrolled into diverse clinical trials. This makes it pivotal to share information across borders and provide a general consensus about how to report and conduct such trials, as low incidence of solid tumors outside the CNS causes a natural limitation of available subjects for clinical testing.

Drug Resistance

Irrespective of risk factors, patients with neuroblastoma generally respond well to initial treatment (49, 75). Unfortunately, the majority of high-risk patients will suffer relapsed disease (13) that often is resistant to structurally and chemically unrelated drugs; so-called multidrug resistance (MDR). As the cellular subtypes of neuroblastoma show different sensitivity to chemotherapeutic agents (21), drug resistance can be a result of selection and expansion of intrinsically resistant tumor clones (intrinsic resistance) (78). On the other hand, tumor cells

can acquire resistance mechanisms to become refractory to therapy (acquired resistance). This can be due to genetic (gene mutation or amplification, chromosome aberrations) or epigenetic (methylation, histone modification) changes in the tumor DNA or post-transcriptional modifications (miRNA regulation, alternative splicing) (79).

Chemotherapy resistance is a major obstacle in treatment of most cancers, not only neuroblastoma. Overall, 90% of treatment failure in metastatic cancer can be attributed to resistance against standard treatments (80). To overcome this, or at least provide a broader selection of therapy choices, it is important to recognize the mechanisms causing the phenomenon. In the following sections, a number of possible explanations for drug resistance are presented (**figure 3**), with a special focus on neuroblastoma.

Altered Transmembrane Drug Transport

Inhibition or inactivation of transmembrane transporters that a drug depends on or upregulation of transporters that actively eject the drug consequently lower its intracellular concentration. ATP-binding cassette (ABC)-transporter proteins comprise a family of efflux pumps with a wide array of substrates, which is often related to intrinsic and acquired drug resistance. Both multidrug resistance protein 1 (MRP1) and MRP4 are ABC-transporter family members found associated with MNA and poor clinical outcome in neuroblastoma (81, 82). Conjugated and unconjugated substances are substrates for MRP1 (83, 84), including drugs normally used in neuroblastoma treatment like vincristine, doxorubicin, and etoposide (85). Downregulation of MRP1 has been shown to increase sensitivity for these drugs in neuroblastoma, both *in vitro* and *in vivo* (86-88). MRP4 has a broad substrate specificity and transports antiviral, antibiotic, cardiovascular and cytotoxic drugs across the cellular membrane (89). In neuroblastoma cells and xenografts, high levels of MRP4 cause resistance to irinotecan (81, 90), a drug used for treatment of relapsed or refractory disease (72). The extensive range of substrates for this transporter family explain why aberrant expression may cause multidrug resistance. Thus, considerable efforts are invested in exploring the possibility of inhibiting these proteins. ABC-transporter family members are also shown to be regulated by miRNAs (91, 92). Co-delivery of chemotherapeutic drugs and miRNAs that downregulate these ABC-transporter proteins might help overcome this resistance mechanism.

Most conventional chemotherapeutic agents have targets within the nucleus, but other substances can work in the cytosol, mitochondria, golgi apparatus, endoplasmatic reticulum or endosomes. The ability of drugs to access and accumulate in the correct compartments will

consequently influence their efficacy. Indeed, differences in drug localization have been observed between sensitive and drug resistant cells (93), suggesting a role of compartmentalization in drug resistance. Sequestration of drugs can be due to pH- or electrochemical gradients across membranes or binding to endogenous molecules which changes the drug's permeability capability or translocate it to specific sites (93). An emerging number of biomolecules are being developed and subjected to clinical testing. Design of novel compounds thus have to be well reasoned and accurate to maximize their anti-proliferative effect. Like for the mitochondria targeting TPP-conjugated cisplatin compound that showed superior effect in resistant neuroblastoma compared to conventional cisplatin (94).

Metabolic Activation and Elimination

When drugs are distributed throughout the body, they are subjected to drug-metabolizing enzymes (DME) in the liver, vascular system or the cells, which can either activate pro-drugs or deactivate/eliminate active drugs. Cytochrome P450s (CYPs), glutathione S-transferases (GSTs) and N-acetyltransferases (NATs) are all enzyme families involved in drug metabolism (95). It is important to recognize that many of the chemotherapeutic agents regularly used in neuroblastoma treatment are substrates of such enzymes (96). Therefore, inherited polymorphism or acquired alterations within these genes, which consequently speed up elimination of drugs, can reduce the therapeutic effect. However, there are limited publications explicit in neuroblastoma regarding this phenomenon, and drugs not currently used in a clinical setting are mostly studied (97, 98).

Changing the Therapeutic Target

Epigenetic modifications or gene mutations can lead to altered expression or conformational modifications of a therapeutic target, which can alter drug sensitivity. Likewise, will compensatory activation of alternative pathways or changes to the target's regulators be mechanisms of drug resistance. Comparing expression profiles between drug resistant cells or tumors and corresponding sensitive samples have confirmed differential expression with prognostic implication in numerous studies.

Anaplastic lymphoma kinase (ALK) is often found highly expressed in neuroblastoma and other neuroectodermal tumors (99), and gain-of-function germline and somatic mutations are recurrent events in neuroblastoma (100-105). This receptor tyrosine kinase (RTK) is considered a potential druggable target, and several inhibitory compounds are currently in clinical testing. However, spontaneous acquisition of somatic *ALK* mutations have been linked

to resistance to ALK inhibitors such as crizotinib and ceritinib (106-109). A preclinical study has also demonstrated compensatory upregulation of another RTK, AXL, as a mechanism of ALK-inhibitor resistance (110).

Concomitant mutation or gene amplification in several oncogenes challenges single target therapies. For example, will phosphorylated ALK activate the PI3K-AKT-mTOR/GSK3β-pathways, which are important for stabilization of MYCN (111, 112). Thus, simultaneous MNA and *ALK* mutation/amplification is characterized as ultra-high-risk neuroblastoma (100, 101, 113). Even though amplification of *MYCN* has been used as a prognostic indicator for years, targeting MYCN has proven difficult. It is challenging to create specific MYCN inhibitors, because, like MYC, it lacks enzymatic activity and well-defined hubs for inhibitors that can perturb the interactions between MYCN and DNA or other proteins (114). Actually, at this point there are no drugs selectively directed against MYCN available in the clinic (115). An indirect approach is probably more likely to succeed, such as targeting MYCN stabilizers like phosphoinositide 3-kinase (PI3K), mechanistic target of rapamycin kinase (mTOR), aurora kinase A (AURKA) or polo-like kinase 1 (PLK1) (112, 113, 116, 117). Disturbing MYCN/MAX interaction or *MYCN* transcription are also conceivable alternatives (118).

Although mutations in the tumor suppressor gene *TP53* are common in adult cancers, they are rarely found in neuroblastoma. As little as 2% of newly diagnosed neuroblastoma tumors carry such mutation (119), compared to more than half in many other cancers (120). However, alternative inactivation of p53 is more common, and defective p53 probably plays a role in relapse and progression of neuroblastoma (121, 122). The SK-N-BE(2)-C cell line derived from a patient with relapsed neuroblastoma has gained a *TP53* mutation that the cells isolated from the primary tumor of the same patient before treatment (SK-N-BE(1)) does not have (122). The acquired multidrug resistant phenotype of this cell line (75) can be partially due to the defective p53 pathway, as many chemotherapeutic agents regularly used in neuroblastoma work through p53-dependent mechanisms (123).

Evading Apoptosis

A tumor cell has the ability to evade apoptosis and promote survival. In chemo-sensitive malignant cells, efficacious anti-cancer drugs cause cellular stress, which induces apoptosis through upregulation of pro-apoptotic proteins or downregulation of anti-apoptotic proteins. Tumor cells that harbor a resistant profile typically have strategies to evade and block apoptosis.

One strategy is to upregulate anti-apoptotic proteins, which can repeal the drug-induced activation of pro-apoptotic proteins. This cause for a discriminating dependence on one or a few anti-apoptotic proteins, a so-called “primed” state, a feature that can differ between tumors (124, 125). A thorough review of the apoptotic process is presented later in this thesis.

The Microenvironment

Multicellular organisms are highly sophisticated machineries with a microenvironment that allows for cooperation and communication between cells and tissue. The tumor microenvironment (TME) comprise different cells, extracellular matrix, signaling molecules and blood vessels. Cells in the TME communicate through direct cell-to-cell interaction, via signaling molecules such as cytokines and growth factors, or by exchanging extracellular vesicles (EVs) containing e.g. proteins, lipids and nucleic acids. Such intercellular communication can promote proliferation and protect neighboring cells from drug induced death (126). Furthermore, budding of EVs from the tumor cell can serve as decoys for immuno-based drugs as they are covered by the same surface antigens as the cellular membrane (126).

Exchange of miRNAs through specialized EVs called exosomes has been linked to chemotherapy resistance in neuroblastoma. Transfer of *miR-155-5p* from monocytes to tumor cells promote resistance to cisplatin, most likely through a diminution of the telomerase inhibitor telomeric repeat binding factor 1 (TERF1). Introduction of an exosome inhibitor restored sensitivity, both *in vitro* and *in vivo*, providing a rationale for this treatment strategy (127).

When metastasized to the bone marrow, neuroblastoma cells can be subjected to interleukin 6 (IL-6) and soluble IL-6 receptor (sIL-6R) from bone marrow-derived mesenchymal stem cells (BMMSC) and tumor-associated macrophages (TAMs). This activates the IL-6-JAK-STAT3 pathway, which gives the cell a survival advantage and decreased drug sensitivity due to activated signal transducer and activator of transcription 3 (STAT3) (128, 129). There is also evidence for activation of the pathway independent of IL-6 in non-MNA neuroblastoma. Paracrine signaling from TAMs activate the JAK-STAT3 pathway, whereby transcriptional upregulation of MYC causes enhanced tumor growth (130).

Response to DNA Damage

Detection and repair of DNA damage are essential for a cells’ homeostasis, and a complex DNA damage response (DDR) machinery has evolved. Specific DNA-repair pathways deal with the many types of lesions. Single-strand errors involve mismatch repair (MMR), base

excision repair (BER), single-strand break repair (SSBR) and nucleotide excision repair (NER), while double stranded break (DSB) repair uses either non-homologues end-joining (NHEJ) or homologues recombination (HR) (131). The phosphatidylinositol 3 (PI-3) kinases ATM and ATR are the key signaling components in human DDR. In response to DNA damage they phosphorylate targets such as CHK1, CHK2, p53, BRCA1 and H2AX (132). This will halt the cell cycle allowing time for repair or, in case of unrepairable damage, lead cells into apoptosis. Components in this machinery are regularly compromised during cancer development, causing an accumulation of tumor driving mutations and accelerated proliferation. Since many chemotherapeutic drugs induce DNA damage, the cells capacity to repair this can influence its sensitivity to the drugs. In some circumstances, defects in DDR pathways that normally would deal with drug induced DNA-insults can cause an increased drug-sensitivity because of an extreme load of damage and genomic instability (133, 134). Other times defects can cause increased drug resistance by avoidance of apoptosis due to inability to detect DNA damage or because of overactive DDR components that favor DNA repair.

Depletion of *ATM* in MYC-driven tumors promote tumor progression (135-137), and display a drug resistant phenotype due to decreased apoptosis (136). *ATM* is located on chromosome 11q. Deletion of this region in neuroblastoma is linked to disease relapse and associated with haploinsufficiency of ATM (138). Copy number alterations and rare single nucleotide variations (SNVs) in *ATM* are observed in all neuroblastoma stages, but in stage III and IV in particular. The majority of these alterations cause a nonfunctional gene (139). Additionally, MYCN upregulates *miRNA-421*, which in turn suppresses *ATM* expression (140). All these findings indicate that aberrations in ATM can be of importance in neuroblastoma tumorigenesis.

Moreover, a recent study has demonstrated how damaged DNA in neuroblastoma cells can cause a DDR where golgi phosphoprotein 3 (GOLPH3) and targeting protein for Xklp2 (TPX2) are upregulated and promote DNA repair, rather than apoptosis, thereby protecting cells from dying (141). Upregulation of other proteins that favor repair over death, such as Poly (ADP-ribose) polymerase-1 (PARP-1), are also seen in various cancers (142). This can be exploited in combating drug resistance, as acquired depletion of *ATM* in combination with inhibition of PARP-1 will cause synthetic lethality in neuroblastoma (138, 139), especially in combination with a DNA damaging agent (138). Interestingly, in breast- and ovarian cancer, some tumors can counteract this strategy by reinstating a former nonfunctional DDR gene, rendering the tumor resistant yet again (143, 144).

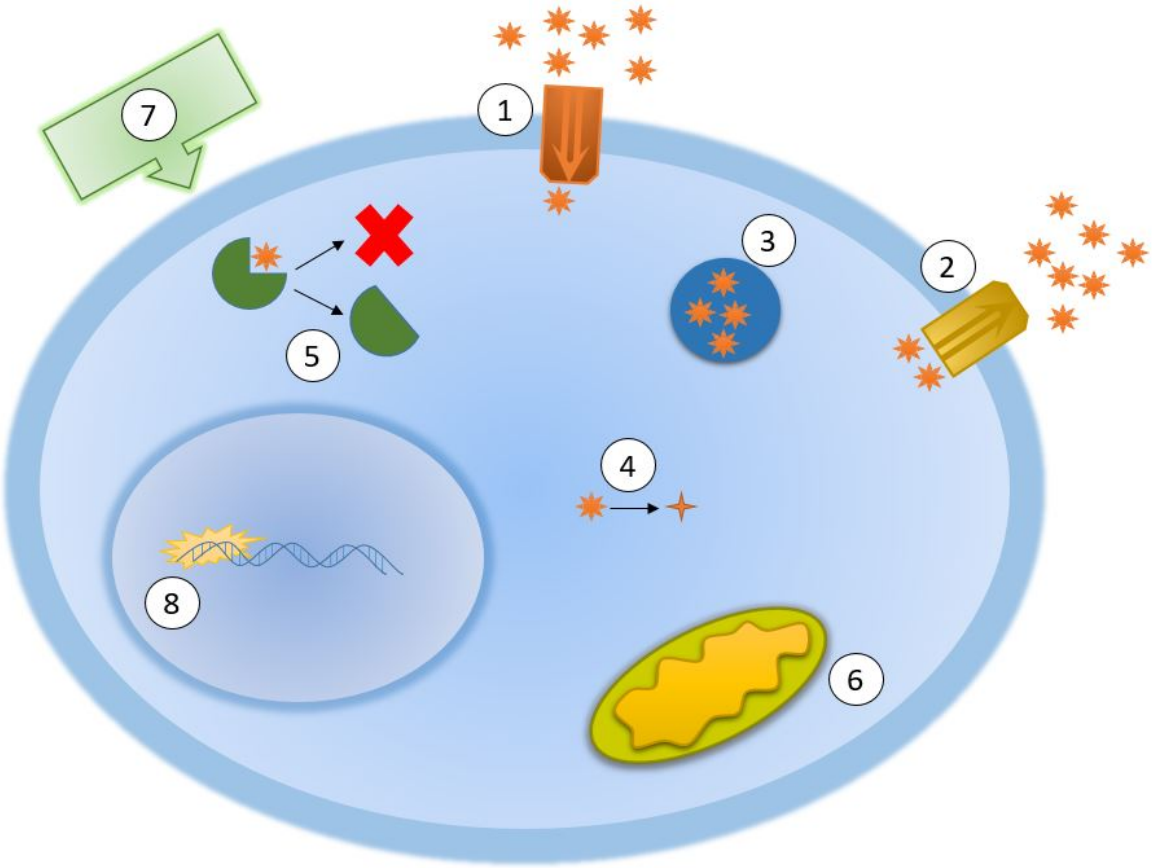

Figure 3: Presentations of drug resistance mechanisms in a cell. 1) Preventing drug influx. 2) Active efflux of drug. 3) Compartmentalization of drug. 4) Changing drug metabolism. 5) Altering the expression or conformation of the drug target. 6) Evading apoptosis. 7) Influence from the tumor microenvironment. 8) Altered DNA damage response.

Non-Coding RNA

In the central dogma of molecular biology, DNA is transcribed into mRNA, which subsequently is translated into a functional protein. However, this is a major simplification of the genomic enigma. Of the roughly 200.000 genes in the human genome that are transcribed into RNA, only 20.000 are protein-coding (145, 146). The large amount of RNAs that do not translate into proteins are now recognized as functional, and considered to have important biological implications. Interestingly, the proportions of some of these non-coding RNAs (ncRNAs) are greater in highly developed species (147), and their targetome is larger (148), suggesting that they contribute to biological complexity. Furthermore, they have an impact on cell identity because the expression of these genes are highly cell and tissue specific (149, 150).

The ncRNAs are divided into small ncRNAs (sncRNAs; <200 nt in length) and long ncRNAs (lncRNA; ≥200 nt in length), which comprise a number of RNA classes with different origin and a plethora of functions. Increasing knowledge suggest that virtually all biological processes are, to some extent, regulated by these RNA molecules (36). Among the sncRNAs

the best known are microRNA (miRNA), small interfering RNA (siRNA), transfer RNA (tRNA), piwi-interacting RNA (piRNA), small nucleolar RNA (snoRNA) and small nuclear RNA (snRNA), while some of the most abundant lncRNA are circulatory RNA (circRNA) and long intergenic non-coding RNA (lincRNA).

When the first miRNA was found in the *Caenorhabditis elegans* genome (151) it led to the revolutionizing discovery of RNA interference (RNAi) (152). RNAi comprise the mechanistically related pathways of miRNA, siRNAs and piRNAs. They form functional RNA-argonaute complexes called RNA-induced silencing complexes (RISCs) that impose post-transcriptional inhibition of mRNAs and transposons (153, 154). Insight into how gene expression is silenced by these sncRNA molecules have led to a better understanding of gene regulation and opened a new and important field of research. We now know that approximately 1-5% of the human genome encode miRNA, which subsequently regulate at least 25-30%, but possibly up to 90%, of all protein-coding genes (155-159).

MicroRNAs

Almost 2000 human miRNAs are registered in miRBase at date (mirbase.org, accessed 06.12.2019). With an average of ~19-24 nucleotides in length they are amongst the smallest naturally occurring RNA molecules. Their canonical function is post-transcriptional regulation of protein-coding genes, as they bind mRNA and cause translational inhibition or degradation (160). Each miRNA may have several target mRNAs and an mRNA is usually targeted by more than one miRNA, consequently miRNAs orchestrate numerous cellular processes. They are vital for fetal development, survival and reproduction, being involved in stem cell differentiation, proliferation, modulation and organ development (150).

MicroRNA Biogenesis and Function

Approximately half of all miRNAs are located in introns or exons of other known genes, and are often transcribed together with the host gene, before being processed separately. The other half are transcribed from previously unannotated genomic regions (161). The most common and recognized biogenesis pathway of miRNAs (reviewed in (153, 162, 163)) starts when RNA polymerase II (or III) (Pol II/III) enhances transcription activity of miRNA in the nucleus (**figure 4**), which results in a primary miRNA transcript (pri-miRNA). The pri-miRNA converts to a miRNA precursor molecule (pre-miRNA) by forming a stem-loop structure with the help of the microprocessor complex comprising the RNase III enzyme Drosha and the DiGeorge critical region 8 (DGCR8) protein. Exportin 5 and RAS-related nuclear protein-

guanosine-5'-triphosphate (RAN-GTP) transport the pre-miRNA to the cytoplasm where the terminal loop is excised by the RNase III enzyme Dicer with the aid of the transactivation-response element RNA-binding protein (TRBP). This results in a double stranded RNA (dsRNA) with 2-nucleotide (nt) 3'overhangs. The miRNA is associated with an argonaute (AGO) protein to form the core of the miRNA-induced silencing complex (miRISC), where the guide strand (the functional miRNA) dissociates from the passenger strand and form a mature miRNA. The guide strand can be either from the 5'-strand (denoted 5p) of the pre-miRNA hairpin, or from the complementary 3'-strand (3p). The selection of 5p or 3p strands for the mature miRNA is not fully understood, but is partially dependent on the thermodynamic stability of the 5' ends of the miRNA duplex (164). The scaffold protein GW182 associates with miRNA-AGO to form the complete miRISC complex, and the mature miRNA binds to (partially) complementary sequences on an mRNA. MiRISC exerts its silencing function either through AGO2-induced cleavage of the target (165) or through non-endonucleolytic mRNA repression (153, 166). In the latter, downstream effectors are recruited, which is usually followed by loading into processing (P-)bodies where the mRNA is provisionally translational silenced or marked for deadenylation and degradation (153, 166, 167).

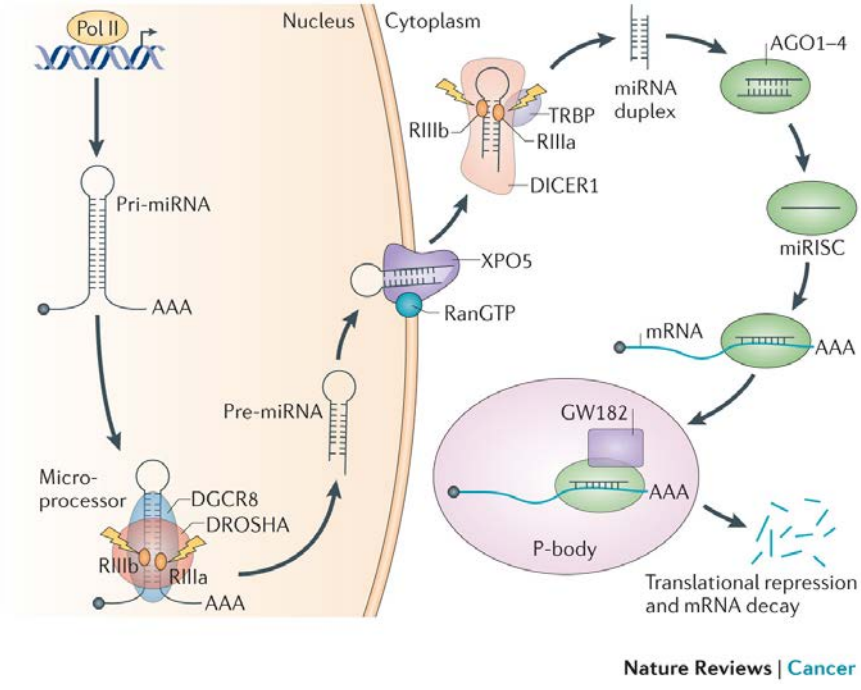

Figure 4: Biogenesis of miRNAs. Polymerase II engage biogenesis of miRNA genes by transcribing a pri-miRNA, which is further processed by drosha and DGCR8 into a pre-miRNA. The miRNA precursor is transported into the cytoplasm where the stem-loop structure is removed by dicer. In the cytoplasm the miRNA duplex is loaded into the miRISC where the functional single stranded miRNA is selected and guided to its target mRNA. The figure is reprinted with permission from (168).

Specific selection of target mRNA is executed by the seed-region of the miRNA, which is the 2-8 residues at the 5'-region (169). This section binds to perfect or imperfect complementary sequences on the mRNA, called miRNA recognition elements (MRE), usually in the 3'-untranslated region (UTR) (160). Additionally, there are growing evidence of binding and regulation within the 5'UTR and the coding sequence (CDS) as well (158, 169, 170).

MicroRNA and Cancer

Most cancer associated single nucleotide polymorphisms (SNPs) are located outside the coding region of proteins (171), hence it is not surprising that dysregulation of ncRNAs are found in virtually all cancers. Since 2002, when miRNAs were first associated with cancer (172), numbers of miRNAs have been found to cause malignant formation and tumor progression. An oncogene-inhibiting miRNA is characterized as a tumor suppressor miRNA, whereas miRNAs that silence tumor suppressor mRNAs are oncogenic miRNAs ("oncomiRs"). Aberrant miRNA expression can originate from disruption of epigenetic or transcriptional regulation of miRNAs, perturbation in genes and proteins involved in miRNA maturation or as a consequence of genomic localization of the miRNA to cancer associate sites (36, 79).

A wide range of miRNAs have been found implicated in pediatric tumorigenesis (36). Some regulate important oncogenes like *MYC*, *MYCN* and *RAS*, while others can be downstream effectors of some of the same proteins. For example, the well-studied tumor suppressor miRNAs *let-7* and *miR-34a* both target *MYCN* (173), whereas MYCN controls transcription of numerous miRNAs (174). The latter helps explain why several miRNAs have been found differentially expressed in MNA tumors compared to less aggressive neuroblastoma (174, 175). As mentioned earlier, miRNAs also appear to contribute to chemotherapy resistance in several cancers, including neuroblastoma (91, 127, 140, 176-178). Reinstating tumor suppressor miRNAs or inhibiting oncomiRs thus provide a therapeutic opportunity in cancer. There are, however, evidence of miRNAs that function as both oncomiRs and tumor suppressor miRNAs depending on cell- or drug type (179, 180). For instance, in hepatocellular carcinoma and neuroblastoma, high levels of *miR-363-3p* reduce proliferation and metastatic formation (181, 182), whereas in gastric cancer cells downregulation of the same miRNA show anti-tumor effects (183). Considering the magnitude of possible targets per miRNA it is only logical that a miRNA can silence both anti-proliferative and tumor promoting mRNAs.

Techniques to characterize the genome, transcriptome and proteome are becoming more accessible, and open up former intangible opportunities. Clinical trials accessing miRNA

profiles in body fluids and tissue, have demonstrated that single miRNAs or panels of miRNAs can be highly valuable to determine disease classification, prognosis, aid in choice of therapy and assessing therapy response (150, 184). In one study, a miRNA microarray library was actually proven more accurate in tumor classification than an mRNA library (185). Perhaps because of entrapment in EVs, miRNAs have the advantage of being relatively stable in body fluids and tissue compared to mRNAs, and the fact that they can be found in among others plasma, serum, saliva and urine (150, 160, 184) makes them readily accessible. However, before we are able to use miRNAs as biomarkers, validated disease specific panels of miRNAs have to be generated, and good sample preparation techniques have to be established.

MicroRNAs Investigated in This Thesis

Our laboratory possesses cell lines harvested from six patients at diagnosis and at relapse after treatment. This provides a valuable opportunity for investigating how expression profiles are altered in a relapse setting. We have used next generation sequencing to identify 42 differentially expressed miRNAs, out of which 8 were upregulated and 34 downregulated (186). A selection of these have been investigated more profoundly, two of which are presented in this thesis: *miR-323a-3p* and *miR-193b-3p*.

Mir-323a is located on the chromosome region 14q32, together with a cluster of other miRNAs often dysregulated in cancers (187-192). Deep sequencing revealed that a total of 22 RNAs from this region are downregulated in relapsed disease, *miR-323a* being one of them (186). Downregulation of this miRNA is observed in multiple other cancers as well (193-196), which may suggest that it has a tumor suppressive function. However, in prostate cancer *miR-323* is upregulated and appears to promote tumorigenesis (197, 198). The latter studies do not designate if this is *miR-323a* or *-b*, though. Therefore, the results can either indicate a dual, tissue-specific role of *miR-323a* or show different properties for the two isoforms.

In several cancers, *miR-193b* has been characterized as a tumor suppressor miRNA. Decreased expression in malignant versus normal tissue have been found in many cancers (199-201), and expression profiling revealed downregulation in chemotherapy resistant esophageal cancer cells compared to sensitive cells (202). In neuroblastoma, we have shown that *miR-193b-3p* also is downregulated in cells from patients with relapsed disease (186). Furthermore, several studies have demonstrated that this miRNA can increase sensitivity to chemotherapeutic drugs (202), kinase inhibitors (203) and BH3-mimicking drugs (204).

Oncogenic Pathways

A cell's biology involves a myriad of different pathways that allow this fine-tuned machinery to sustain homeostasis. Dysregulation of cellular pathways can cause malignant transformation, continuous proliferation, invasion and metastasis. In this thesis, I will focus on two pathways that can be subjected to oncogenic alteration: The apoptotic pathway and ribosome biogenesis. Manuscript II and paper I will demonstrate how these pathways potentially can be targeted in neuroblastoma.

Apoptosis

During development, and to maintain homeostasis, the process of programmed cell death (apoptosis) is essential. It allows for a controlled eradication of damaged or redundant cells without distressing the surrounding cells. Failure in this process can have dire consequences, one of them being cancer development.

Apoptosis can occur through two distinct pathways: The extrinsic and the intrinsic pathway (reviewed in (125, 205-208)). The extrinsic pathway is initiated when members in the tumor necrosis factor (TNF) superfamily bind cell surface receptors. These receptors convey signals to intracellular pathways through a characteristic death domain. The intrinsic pathway is triggered through non-receptor mediated stimuli that initiate transcription or posttranscriptional activation of pro-apoptotic proteins, and involves an intricate interaction between several pro- and anti-apoptotic proteins. Activation is either due to loss of factors that suppress apoptosis, like hormones, cytokines and growth factors, or presence of factors that positively regulate apoptosis, such as radiation, hypoxia, hyperthermia, viral infections, toxins and free radicals. Activation ultimately cause permeabilization of the mitochondrial outer membrane (MOM), which in turn leads to efflux of among others cytochrome c. Both pathways result in caspase activation, and thereafter apoptosis.

The highly conserved BCL-2-family (208) of anti- and pro-apoptotic proteins is the major player in the intrinsic pathway. The anti-apoptotic members are e.g. BCL-2, BCL-X_L, BCL-W, BCL-B, BFL-1 and MCL-1, while the pro-apoptotic proteins are divided into two groups: The first group consists of BAX and BAK; the other of e.g. PUMA, tBID, BIM, NOXA, HRK, BMF, BIK and BAD. They all share a certain homology via the presence of BCL-2 homology (BH) domains, but the latter group differs from the others as they only contain the BH3 domain ("BH-only" proteins) (209). The fate of the cell rests on the balance between these proteins. Commitment to apoptosis occur when activated BAX and BAK form homo-

oligomeric complexes that cause permeabilization of the MOM. The other family members regulate apoptosis by either promoting (BH3-only proteins) or inhibiting (anti-apoptotic proteins) this oligomerization (205, 210). Of the BH3-only proteins BIM, PUMA and tBID are classified as "activators" because of their ability to directly activate BAX and BAK (211, 212). The anti-apoptotic proteins exert their functions by either binding directly to monomeric BAX/BAK or to the "activators" at the BH3 domain. Conversely, the remaining BH3-only proteins (termed sensitizers) attenuate the effect of the anti-apoptotic proteins by competing with the activators for binding, thus neutralizing them (213, 214). Changed permeability of the MOM causes release of among others cytochrome c into the cytoplasm. Cytochrome c forms a complex called apoptosome with oligomerized apoptotic peptidase activating factor 1 (APAF-1), creating a hub for caspase-9 activation which initiate the caspase cascade, in turn leading to apoptotic cell death (212, 214, 215).

Binding affinities between the pro- and anti-apoptotic proteins differ somewhat. BIM and PUMA bind all the anti-apoptotic proteins, while BCL-2, BCL-W and BCL-X_L have a qualitatively related profile, and are bound by BMF and BAD in particular. NOXA on the other hand exclusively binds to MCL-1; in contrast to BAD, that does not bind MCL-1 at all (214, 216).

Apoptosis and Cancer

Evading apoptosis is a hallmark of cancer (217). Malignant cells are constantly subjected to stressors that will provoke death signals, such as upregulated oncogenes, high proliferation rate, genomic instability, oxidative stress and more (125, 214). In order to bypass the apoptotic program, cancer cells can mitigate distinct apoptotic pathways, which cause for a dependence on selected cellular features. Localizing the specific apoptosis blocks and subsequently avert them, makes it possible to overcome drug resistance (125).

The concept of cells being "primed for death" was introduced in the mid-2000. It proposes that anti-apoptotic proteins sequester activator proteins to counteract the constant death signals that the tumor cells encounter (214, 218). However, if these activator proteins are released, a rapid induction of apoptosis may occur (219, 220). The majority (81%) of high-risk neuroblastoma express BCL-2 and/or MCL-1 (221). Interestingly, even if cells have multiple anti-apoptotic protein sequestering BIM (which is the primary activator in neuroblastoma (124)), a preferential dependence on one is often present (e.g. either BCL-2 or MCL-1) (222). This provides the opportunity to target these proteins specifically with components resembling

sensitizer BH3-only proteins. Common aberrations in neuroblastoma, like *MYCN* amplification, *ALK* mutations and 11q LOH, appear to be independent of the mitochondrial profile (124).

ABT-737 is a BAD mimetic with the potential to antagonize binding of BCL-2, BCL-X_L and BCL-W to BIM, thereby indirectly inducing BAX/BAK-mediated cell killing (**figure 5**) (223, 224). The selective affinity of the compound is probably the reason why cancers with a discriminating dependence on MCL-1 ("MCL-1 primed") are more resistant to ABT-737 than BCL-2 primed cells and tumors (124, 218, 221, 223). Contrariwise, the MCL-1 antagonist AT-101 shows superior effect in MCL-1 primed cells (218). To overcome the resistance of MCL-1 primed cells to ABT-737, knockdown of MCL-1 have proven effective in several studies, either using RNAi or drugs (221, 223, 225-227).

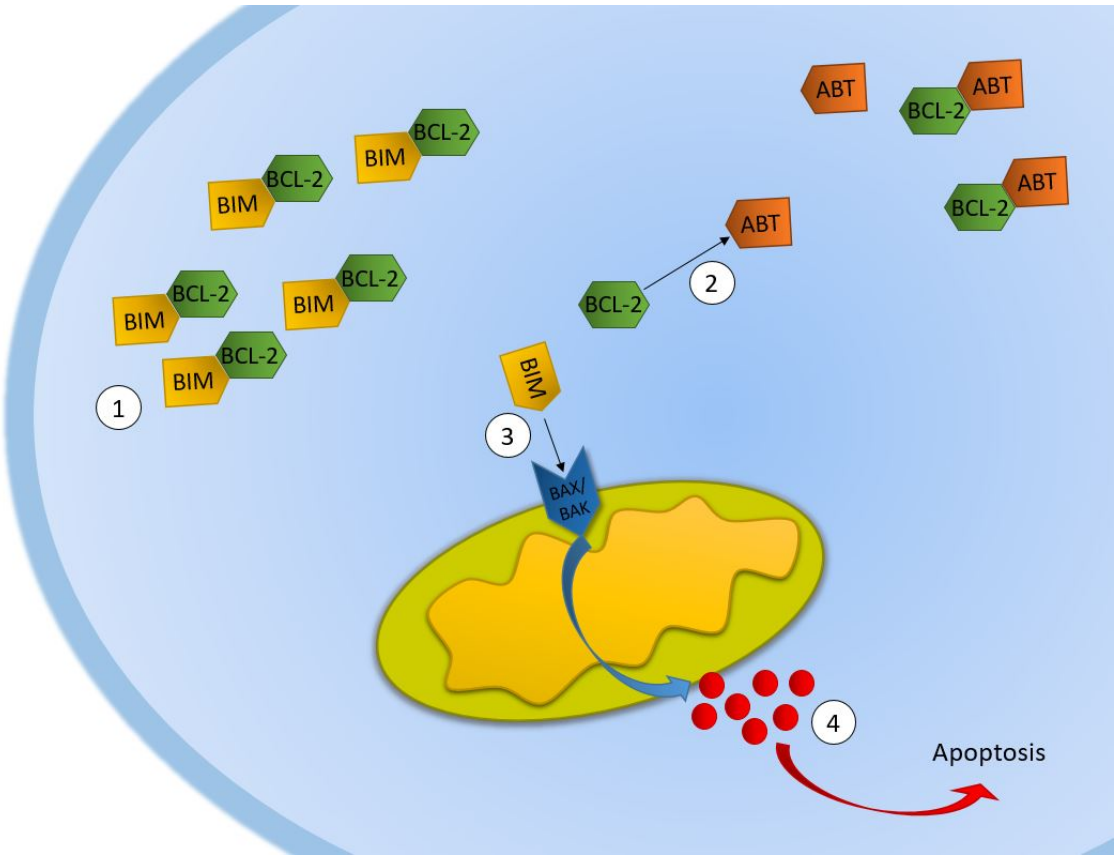

Figure 5: Overview of how ABT-737 sequesters BCL-2, allowing BIM-induced apoptosis in BCL-2 primed cells. 1) A tumor cell constantly endure death signaling that upregulates pro-apoptotic proteins (e.g. BIM). BCL-2 binds BIM to prevent conduction of the death signal. 2) BCL-2 is sequestered by ABT-737, thus releasing BIM. 3) BIM cause oligomerization of BAX/BAK, which results in permeabilization of the mitochondrial outer membrane. 4) Cytochrome C is released from the mitochondria, inducing a caspase-cascade that leads to apoptosis.

Ribosome Biogenesis

Translation of mRNA into protein take place on the ribosome, a ribonucleoprotein comprising ribosomal RNA (rRNA) and ribosomal proteins (RPs). The availability of ribosomes is a key regulator of cell growth and proliferation. Ribosome biogenesis (reviewed in (228-231)) is a multistep process initiated by recruitment of proteins to the ribosomal DNA (rDNA) promotor in the nucleolus (**figure 6**). Binding of upstream binding factor (UBF) and selectively factor 1 (SL1) to the promotor activates transcription factor 1A (TIF1A), which in turn interacts with polymerase I (Pol I) to commence transcription of rDNA to a 47S pre-rRNA. External (ETS) and internal (ITS) transcribed spacers are removed from the 47S rRNA as it is cleaved into three mature rRNA transcripts, 28S, 18S and 5,8S. Together with 5S rRNA (transcribed by Pol III) and a selection of roughly 80 RPs, they will form two ribosomal complexes, 60S and 40S, which will assemble into a mature ribosome during protein synthesis. The 60S ribosomal subunit comprises 5.8S and 28S rRNAs, while the 18S rRNA is in the 40S ribosomal subunit. RPs are transcribed by Pol II in the nucleus and translated into proteins in the cytoplasm. To regulate and assemble with the maturing rRNA they translocate to the nucleus, where they stabilize and promote correct rRNA folding and guide precursor rRNA transport.

Ribosome Biogenesis and Cancer

To sustain growth and survival, cancer cells in general have a high demand for proteins, which is met by an increase in synthesis of ribosomes. Pol I-dependent transcription is considered the rate-limiting step of ribosome biogenesis (232), and altered expression of Pol I regulators can cause accelerated ribosome biogenesis (233, 234). To be self-sufficient, cancer cells circumvent normal regulation of ribosome biogenesis and become independent on extracellular growth signaling through upregulation of proteins involved in promotion of rRNA synthesis, like ERK, mTOR, MYC, RAS and NPM1, and through epigenetic regulation, like hypomethylation of rDNA genes. Conversely, several tumor suppressor genes that normally would constrain ribosome biogenesis are frequently mutated, like *TP53*, *RB* and *PTEN* (233-235). As a consequence of dysregulation, prominent nucleoli are regularly observed in cancer (50, 55, 236). Actually, altered nucleolar morphology and quantity have been used to assess tumor aggressiveness for decades (237). In neuroblastoma, prominent nucleoli are associated with poor prognosis and high expression of MYC family members (50, 55, 238). MYCN and MYC actually enhance the expression of several genes functioning in ribosome biogenesis, like

NCL, *NPM1* and genes encoding RPs (239). Perturbing rDNA transcription, either by targeting oncogenic pathways or by direct inhibition of Pol I, has emerged as an intriguing concept.

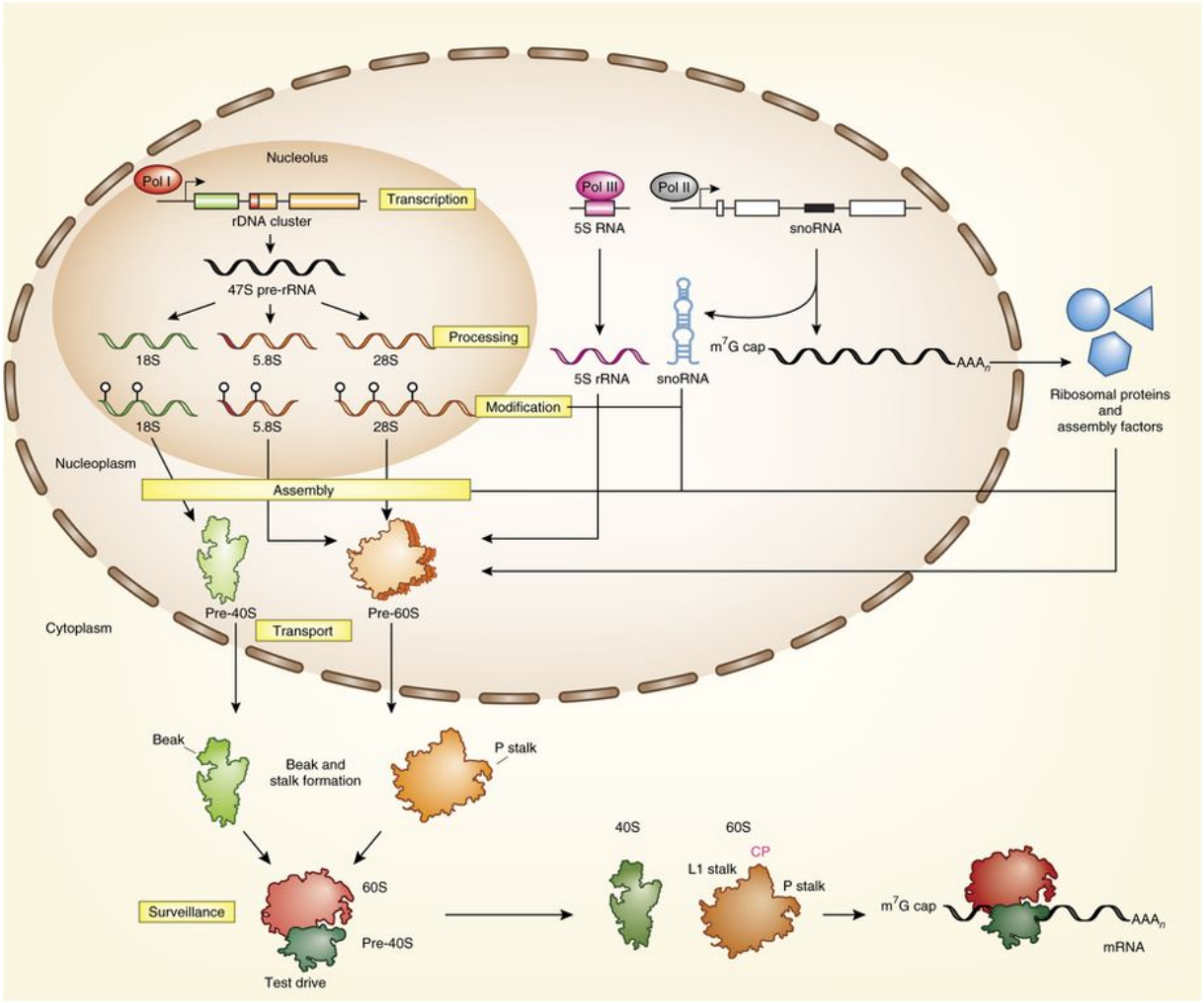

Figure 6: **Ribosome biogenesis**. In the nucleolus, polymerase I transcribes rDNA into a 47S pre-rRNA, which is cleaved into 18S, 5.8S and 28S rRNAs. These rRNAs are assembled together with ribosomal proteins into two subunits, pre-40S and pre-60S. After transportation to the cytoplasm, the subunits are combined in order to form a mature ribosome. The figure is reprinted with permission from (240)

G-quadruplexes are structures in DNA or RNA derived from folding of guanine (G)-rich single nucleotide strands. They consist of stacked G-quartets that are bound together by hydrogen bonds. Stacks of G-quartets are stabilized by central cations and can generate different topologies (**figure 7**) (241), which have been identified in telomere regions, promoters, introns and rDNA (46, 230, 242, 243). Human rDNA is G-rich, and transcription of these sites are accompanied by the formation of G-quadruplexes in the non-template strand. This in turn prevents renaturation of the template strand, promoting Pol I-induced transcription of rDNA (244). The phosphoprotein NCL will further stabilize these G-quadruplexes, causing increased pre-rRNA levels (230). It has been proposed that G-quadruplexes might be therapeutic targets

in cancer. For instance, small molecule targeting of these structures have demonstrated inhibition of telomerase function and disruption of the telomere ends (245). To date, there are several telomere ligands suggested to convey their effect through G-quadruplex interaction (246).

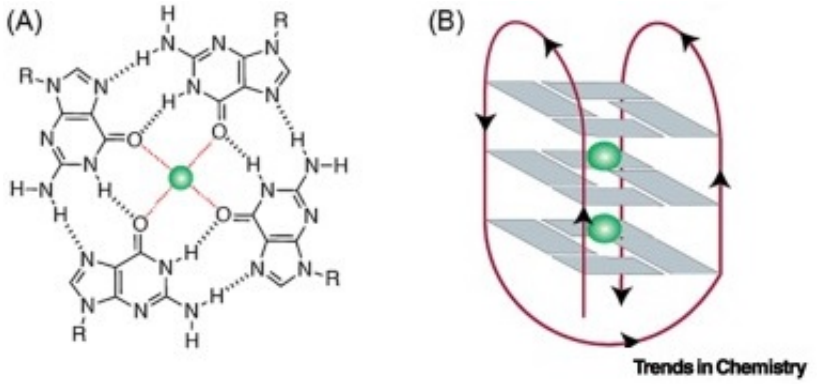

Figure 7: Structure of G-quadruplex. A) Guanine molecules are arranged in quartets bound together by hydrogen bonds. A central cation is involved in stabilization of the structure. **B)** Stacks of G-quartets form the structure of the entire G-quadruplex. The figure is reprinted with slight modifications after permission from (241).

Inhibitors of Ribosome Biogenesis

CX-5461 and CX-3543 (quarfloxin) were initially described as inhibitors of ribosome biogenesis. CX-5461 outcompetes SL1 binding in the Pol I promoter (247), while quarfloxin can disrupt the interaction between G-quadruplex structures and nucleolin (NCL) (230), thereby inhibiting Pol I induced transcription of rDNA. Preclinical studies have shown anti-tumor effect of the compounds in several cancers (230, 248, 249) and level of Pol I activity has been linked to efficacy of CX-5461 in ovarian cancer (236). MYC is, as mentioned, a positive regulator of rDNA transcriptions (250). That is probably one of the reasons why increased sensitivity to CX-5461 have been seen in cancers with elevated MYC.

Other studies have revealed novel mechanisms of action besides inhibition of ribosome biogenesis. Both CX-5461 and quarfloxin can bind G-quadruplex structures and cause DNA damage (230, 251). Repair of such DNA damage rely on HR or NHEJ. Therefore, since CX-5461 has been shown to cause gross chromosomal rearrangement (GCR) in G-quadruplex foci, cells with defective DDR are especially sensitive to the drugs (251). Furthermore, CX-5461 appears to target G-quadruplexes in telomeres. Telomeres are repeat segments that protect human chromosomal ends by preventing them from being recognized as double strand breaks (DSB). With every cell division, the telomeres shorten, in the end limiting the replication capacity of the cell. Telomere maintenance is conducted by telomerase; its catalytic domain, hTERT, adds repeated sequences and caps telomere ends (246). Because unlimited proliferation

is another hallmark of cancer (217), high telomerase activity is found in the vast majority of cancer cells (252, 253). Furthermore, since telomeres are sequences packed with GC-rich sites, *in vitro* experiments have shown that CX-5461 can compromise telomerase integrity most likely through binding of G-quadruplex structures (251). The latter has not been shown for short-term treatment with quarfloxin (230). In ALL, another anti-proliferative effect of CX-5461 is G2-arrest, prompted by activation of ATR. Negi *et al.* have demonstrated a synergistic effect of CX-5461 and an inhibitor of ATR, leading to enhanced cell death (248). Disruption of the nucleolar structures by CX-5461 (249), causing the release of sequestered proteins important in cell cycle regulation (254, 255), may be part of the explanation for induction of G2-arrest. In conclusion, the different anti-tumor mechanisms attributed to CX-5461 and quarfloxin in different cancers suggest that the therapeutic response to these compounds might be disease specific and depend on the biological makeup of the malignant cells.

Aim of Study

The work presented in this thesis have a dual objective. Firstly, we sought to elucidate the role of selected miRNAs in neuroblastoma, revealing their functional properties and potential targets. Secondly, by targeting known tumorigenic pathways, we wanted to examine novel therapeutic opportunities for high-risk neuroblastoma. Collectively, these investigations can help illuminate biological alterations in neuroblastoma cells important for cancer development and progression, and give incentive for further investigation of specific drugs.

Specific Aims for the Manuscripts/Paper

Manuscript I

In this study, we wanted to expose specific functions of the miRNA *Hsa-miR-323a-3p* in high-risk neuroblastoma.

Manuscript II

After discovering that *Hsa-miR-193b-3p* downregulates *MCL-1*, we aimed to see if this miRNA consequently would increase sensitivity in MCL-1 primed neuroblastoma cells for the BCL-2 antagonist ABT-737.

Paper I

The objective of this study was to investigate the effect of the ribosome biogenesis inhibitors CX-5461 and quarfloxin on high-risk neuroblastoma, both *in vitro* and *in vivo.*

Results

In this section, the main results from the three works are briefly presented. Detailed description of our findings are presented in the individual manuscripts and paper.

Manuscript I

Hsa-miR-323a-3p Functions as a Tumor Suppressor and Targets *STAT3* in Neuroblastoma Cells

Enforced expression of *miR-323a-3p* in neuroblastoma cell lines SK-N-BE(2)C, SH-SY5Y and Kelly led to significant decrease in cell viability. In Kelly and SH-SY5Y *miR-323a-3p* overexpression caused G1-cell cycle arrest and apoptosis, while SK-N-BE(2)C showed only increased apoptosis. Additionally, ectopic *miR-323a-3p* expression decreased STAT3 mRNA and protein levels, and co-transfection of *miR-323a-3p* mimics and a plasmid containing the *STAT3* 3'UTR sequence cloned downstream of a luciferase reporter, resulted in decreased luciferase activity compared to transfection with negative control mimics. Mutation of a predicted target sequence for *miR-323a-3p* on *STAT3* 3'UTR abolished this effect and confirmed that *STAT3* is a direct target of *miR-323a-3p* in neuroblastoma cells.

Manuscript II

Hsa-miR-193b-3p Sensitizes MCL-1 primed Neuroblastoma Cells to the BH3-mimetic ABT-737

Consistent with previous work, the MCL-1 primed neuroblastoma cell lines SH-SY5Y and NLF are relatively resistant to the BCL-2 antagonist ABT-737, while the BCL-2 primed cell lines SMS-KAN and CHLA-20 have a more sensitive profile. SK-N-AS is, as anticipated, highly ABT-737-resistant. After transient transfection of *miR-193b-3p* mimics, the MCL-1 primed cells and CHLA-20 become more sensitive to the inhibitor, demonstrated as reduced viability and increased apoptosis. Also, the BH3-resistant cell line SK-N-AS get more sensitive to the inhibitor, but only at high ABT-737 concentrations and prolonged exposure. Contrary to this, the sensitivity profile of SMS-KAN is unchanged upon *miR-193b-3p* overexpression. The change in sensitivity is in part due to *miR-193b-3p* induced downregulation of *MCL-1*, since MCL-1 primed cells regain their resistance to ABT-737 when transfecting with MCL-1 lacking the 3'UTR or antisense oligonucleotide that prevent the miRNA-mRNA interaction.

Paper I

Inhibitors of Ribosome Biogenesis Repress the Growth of *MYCN*-amplified Neuroblastoma

Oncogene (2019) 38(15): 2800-2813

In neuroblastoma, there is a strong correlation between high-risk disease, *MYCN* expression, poor survival and increased ribosome biogenesis, providing a rationale for testing inhibitors of ribosome biogenesis in this malignancy. Here we show that the RNA polymerase I inhibitors CX-5461 and quarfloxin induce DNA damage in *MYCN* amplified (MNA) neuroblastoma cell lines, leading to p53 activation, cell cycle arrest and apoptosis. Exclusive to cell lines with MNA and a functional p53, MYCN protein levels are reduced after treatment with CX-5461 and quarfloxin. In murine neuroblastoma xenograft models, CX-5461 shows a clear anti-tumor effect, especially in tumors with *MYCN* amplification and wild-type *TP53*.

Discussion

Discussion of Materials and Methods

The following section provide an overview of a selection of methods used in the manuscripts and paper, along with some considerations regarding choice of methods and potential weaknesses. Vastly used standardized methods are not included here. Detailed materials and method-descriptions are presented in the manuscripts and paper.

Cell Lines

In general, most *in vitro* studies on neuroblastoma were conducted on commercially available cell lines harvested from patients decades ago. These immortalized cells are valuable models to study specific characteristics that represent different biological traits of neuroblastoma, like MNA, death priming, p53 status and more. Widespread use of well-characterized cells ensure reproducible and consistent results. Furthermore, these cells often grow fast and robustly, making it an easy-to-work-with model that quickly can produce enough material to analyze phenotypic effects of treatment (256), and the possibility of manipulating gene expression to create gene knockout or gene overexpressing clones.

On the downside of using immortalized cell, continuous passaging will inevitably cause genetic alterations that can generate unique expression patterns that will differ from native tumors (256). Another obvious weakness is the lack of tumor microenvironment and immune system. Despite these drawbacks, cultured cells are a useful model to study biological functions and theoretical hypothesis that later have to be validated in patient material and *in vivo* models. Although primary cell cultures could have been an alternative to immortalized cells, they are hard to obtain from rare diseases such as neuroblastoma, ethical working guidelines apply, and even at low passaging there is a chance of genetic variations (78).

To minimize genotypic changes, a low passage number was favored and cell authenticity was regularly confirmed by short tandem repeat (STR) profiling performed by the Center of Forensic Genetics, University of Tromsø. Habitual testing of mycoplasma contamination was also done. Since antibiotics can cause genetic, morphological and functional changes to cultured cells (257, 258) all cell lines are routinely grown without antibiotics in the medium. Cell lines used in the following studies are all from patients suffering from high-risk neuroblastoma.

In Vivo Studies

In vivo studies for paper I were done at Karolinska Institutet (Sweden) after approval by the regional ethics committee for animal research (approval N231/14), and conducted in accordance with national legislations and regulations (SFS 1988:534, SFS 1988:539 and SFS 1988:541). Neuroblastoma xenografts were established in 4-6-week-old NMRI nu/nu mice. These mice are well suited for formation of tumors from cancer cells because of a non-functional *FOXN1* gene, which leads to functional athymia and subsequent defective T-cell immunity (259-262). IMR-32 and SK-N-BE(2)-C were considered appropriate models for *MYCN*-amplified tumors that represent *TP53* wild-type and *TP53* mutated genotype, respectively. For IMR-32 we used matrigel, as this has been shown to enhance implantation and growth of tumor cells (263), and a pilot study indicated superior tumor development of matrigel-diluted IMR-32 compared to direct implantation. Careful consideration is advised when using this compound if the objective is to analyze extracellular components, as growth factors in the matrigel can influence the result (264, 265). Since our main objective was to evaluate tumor progression after treatment, rather than examining different factors, robust establishing of tumors was considered beneficial. CX-5461 is an orally bioavailable drug (266) that has shown anti-tumor effect in other murine cancers models (247, 251). In our study, CX-5461 was given by oral gavage, which is a more precise oral administration technique than through feed (267) and preferred over parenteral delivery. Drug dosages were adopted from another study (251).

An appealing alternative approach would be to treat immunocompetent mice with *MYCN*-driven tumors. In the transgenic TH-MYCN mouse strain (52) a thyroxine hydroxylase promoter drives *MYCN* expression in neuroectodermal cells and causes formation of tumors that closely resembles neuroblastoma (268-270). This would allow us to investigate the efficacy of CX-5461 in an immune proficient model. Additionally, creating tumor models with deletion in *TP53* (52, 271) in order to evaluate the impact of *TP53* deficiency would also be of value.

MicroRNA Target Prediction

Finding targets for miRNAs can help reveal their functions. However, as one miRNA can have numerous targets and most miRNAs' seed region are only partially complementary to the mRNA sequence, target identification can be a challenging task. Multiple target prediction softwares have been created, all with distinct algorithms that can define slightly different predictions. Some algorithms only allow perfect Watson-Crick base paring between miRNAs and the corresponding targetome. Unfortunately, not permitting G:U wobbles and/or bulges in

the binding will most certainly miss targets (272). Requiring 8 nt pairing increases specificity, but since most miRNA have a 7 nt seed match, this renders a lot of missed miRNA-mRNA interaction when implying such conditions (159). Furthermore, not all prediction algorithms include sites in the CDS, even though it is clear that some miRNAs bind extensively to the CDS (273). In addition to missed targets, the softwares can have a false positive rate somewhere between 24-70% (274). Factors that can affect the possibility that a recognized site actually is functional are: The 3'UTR sequence composition and position of the site; the immediate environment of the putative site; the base paring pattern; structural accessibility to the site; presence of multiple target sites and the proximity between them (275, 276); and sites conserved between species (277).

Validating *bona fide* miRNA-mRNA interactions is typically done using a luciferase reporter gene cloned in proximity to the sequence harboring the putative binding site. Direct binding of the miRNA will reduce luminescence, which again will be rescued if the target site is mutated. A novel approach recently available uses locked nucleic acid (LNA)-enhanced antisense oligonucleotides ("Target Site Blockers") to block a predicted seed sequence for a specific miRNA on a given mRNA. This will explicitly perturb the miRNA effect on this mRNA if the region is indeed a functional binding site (278). For both techniques, the predicted target sites are found through the aforementioned bioinformatic softwares. However, when using these to locate miRNAs that regulate a specific gene, it can create bias towards only recognizing certain predicted sites, leaving out actual miRNAs that the software cannot find. To overcome this incongruity, we usually search through multiple softwares, but could also have perform high-throughput luciferase reporter screen. Using a library of several hundred miRNA, and co-transfect it with a luciferase reporter construct with the desired gene, one is able to find miRNA-mRNA interactions that can be overlooked using only target prediction software (174). Alternatively, performing crosslink immunoprecipitation (CLIP), preferentially combined with high throughput sequencing (HITS-CLIP) (279) , is an alternative.

Apoptosis

There are different strategies to assess apoptosis in cells: Looking for typical morphological changes in the microscope; assessing DNA fragmentation on agarose gels; measuring annexin V, a phosphatidylserine-binding protein, by flow cytometry; assessing caspase activity with luciferase assay or immunodetection of cleaved caspase; or detection of cleaved PARP-1 using immunoblotting or immunohistochemistry.

Morphological changes include cell shrinking and pyknosis, thus, most cells are small, have a distinct dense fragmented nucleus and a circular shape. Further, as the cells cytoskeleton breaks up, the membrane starts to bleb. This process is called “budding” and results in formation of small apoptotic bodies containing cytoplasm and tightly packed organelles to be engulfed by phagocytes (206).

PARP-1 is the best-studied member of a superfamily of enzymes capable of catalyzing poly ADP-ribosylation. It has several important roles, one being in DNA damage response, where it facilitates BER and NER after single strand breaks (280). During apoptosis PARP-1 is cleaved by caspases, (e.g. caspase 3 or 7), into two fragments of 89 and 24 kDa. The 24 kDa fragment is retained in the nucleus where it binds to DNA and inhibits DNA repair mechanisms, among others active PARP-1. The second fragment is translocated into the cytosol (281). Detection of the 89 kDa fragment on western blot is a well-established marker for initiated apoptosis, and one of the most used methods in our lab; usually combined with a brief detection of some morphological changes. Of course, it is valuable to add a second method to strengthen the results, and we strive to do so in most cases.

Manipulating Gene Expression

In Vitro Studies

In vitro manipulation of gene expression is an essential part of biological research. Editing the DNA or transferring foreign genetic material or mature gene products are all ways of achieving altered expression.

For miRNA gain-of-function studies, we transiently transfected cells with miRNA mimics. These are dsRNAs, analogous to endogenous miRNAs, but chemically modified so that the favored guide strand is selected when loaded into the miRISC. This allows us to see how the miRNA influence biological functions in the cell and identify potential targets. However, as for all experiments with forced overexpression, it is important to keep in mind that we are possibly introducing supraphysiological levels of the molecule, thus non-specific changes is consequently a concern (282).

Another typical approach to gene overexpression is introduction of plasmid or viral vectors with the desired protein-coding gene driven by a constitutively active promoter (usually viral). Such vectors can exploit the recipient cell’s own transcription and translation machinery. Viral vectors can even incorporate genes into the host’s genome for stable expression. Endocytotic delivery of lipid-enclosed RNA or DNA is a fast, easy and robust transfection

method that we frequently utilize in our laboratory. Efficiency of single compound transfection is usually high; however, co-transfection of two or more can be a bit challenging. There is a limit for how much nucleic acid the liposomes can contain and it can be difficult to assure that the same amount will be transfected at all time. Providing the optimal conditions is therefore vital, such as healthy cells, correct cell confluence, not too high passaging and optimized DNA/RNA concentrations.

Stably transfected genes with inducible promoters can be extremely useful. In paper I, we used the *MYCN* inducible cell line SHEP-TET21N (283), where *MYCN* is under the influence of an E.coli tetracycline repressor. In the absence of tetracycline, *MYCN* is constitutively expressed, while introduction of tetracycline "turns off" the gene. This allows us to control *MYCN* expression and exclusively test the functional implication of elevated MYCN.

Whilst miRNAs can have imperfect binding to multiple targets, siRNAs have one specific target mRNA with perfect complementarity (284). This makes them suitable for silencing specific genes. siRNA can be introduced to the cell as oligonucleotides or endogenously derived from short hairpin RNA (shRNA), which is transported into the cell by transfection of a plasmid vector or by transduction of a viral vector (285). Efficiency of an siRNA is not always 100%; therefore, we often use a pool of four siRNAs. This will target several sites in the mRNA, often both in the UTR and CDS, and ensure strong silencing (286). It also limits the chance of off-target effects, since the specificity of an siRNA is not always absolute. For instance, if the siRNA is too similar to a miRNA it can mimic the miRNA effect (284).

After being discovered in bacteria as a virus defense mechanism (287), the revolutionizing technique of CRISPR/cas9 gene editing system has gained augmented attention the last years. It is a fast, accurate and efficient system to add, remove or alter specific locations in the genome. Clustered Regularly Interspaced Short Palindromic Repeats (CRISPR) is repetitive sequences separated by unique spacers that can detect highly specific gene sequences. Complimentary binding to these genome sites allows precise nuclease cleavage by cas9 (288, 289). The double-strand break can be exploited for gene editing, before the DNA repair system in the cell will repair the break and simultaneously permanently introduce alteration to the genome. This technique can potentially substitute or complement most of the previous methods described. Although we have not used this system in the work presented in this thesis, we are

in the process of establishing the method in the laboratory. It will surely be employed much more in the future.

General Discussion

The word “cancer” will forever be associated with fear, anguish and loss. Circumstances are even more devastating when children are victims of this disease, like in neuroblastoma, where the majority of patients are under 5 years of age (1). Evolvement the past decades have improved therapy, but still, only 50% of those with high-risk disease will survive (15). Many get tumors refractory to standard treatment, while others initially respond before relapsing at a later stage. Chemotherapy is a cornerstone in treatment of pediatric malignancies, and patients with high-risk neuroblastoma receive accumulating doses of chemotherapeutic drugs in combination with other medications and therapies. Unfortunately, this high treatment load also causes deaths due to adverse effects or treatment related morbidity (290-292). Alternatives for high-risk patients are therefore critically needed.

In this thesis, I present insight into how reintroduction of tumor suppressor miRNAs can suppress growth of cancer cells (manuscript I) and increase sensitivity to small molecule inhibitors (manuscript II). Furthermore, I show how treatment with small molecule drugs formerly characterized as inhibitors of ribosome biogenesis have solid anti-tumor effect in neuroblastoma with specific biological features. The following section will comprise a discussion of the work in specific and considerations about its potential for clinical use.

Discussion of Results

MicroRNAs and ABT-737

When examining differential miRNA expression patterns in neuroblastoma cell lines, our group discovered that *miR-323a* and *miR-193b-3p* were downregulated in relapsed neuroblastoma compared to cells harvested at diagnosis (186). Since *miR-323a* previously have been found implicated in tumorigenesis in other cancers, we set out to scrutinize the role of *miR-323a-3p* in neuroblastoma, as presented in manuscript I. *MiR-323a-3p* is, as mentioned earlier, part of a miRNA cluster located on chromosome 14q32 in humans. In clusters, several miRNA genes are juxtaposed on a chromosome. They frequently share a promoter and can be transcribed together as a long pri-miRNA, before being processed into individual pre-miRNAs. Often these clusters originate from one gene that has been duplicated and mutated. Accordingly, the miRNAs within a cluster commonly have high sequence homology, and they often target several mRNAs within the same pathway (293). Since our laboratory have found 22 of the

miRNAs within the 14q32 cluster to be downregulated in relapsed neuroblastoma (186), we postulate that they have a tumor suppressor function in this malignancy. This assumption is corroborated by various studies conducted on a selection of these miRNAs. The work presented in manuscript I shows that ectopic expression of *miR-323a-3p* can reduce viability by induction of G1-arrest and apoptosis in neuroblastoma cells. A former study from our laboratory have demonstrated that *miR-376c-3p* also caused G1-arrest and reduced viability in neuroblastoma cells, by targeting *CCND1* (294). Furthermore, *miR-329* has been shown to possess an anti-proliferative function and reduced migration and invasiveness through *KDM1A*-targeting (295); while *miR-337-3p* reduced growth, migration, invasion and angiogenesis in both cells and tumors of neuroblastoma, through transcriptional inhibition of matrix metallopeptidase 14 (*MMP-14*) (296). Additionally, Gattolliat *et al.* have proposed that two of the downregulated cluster-members, *miR-487b* and *miR-410*, can be prognostic factors for relapse of favorable neuroblastoma (297). A widespread downregulation of miRNAs from the same cluster can suggest that common transcriptional regulators are altered. Perhaps can simultaneous upregulation of several of these miRNAs through activation of positive transcriptional regulators (with e.g. CRISPR technology) (192) present a more powerful anti-tumor effect than either alone?

We also show that *STAT3* evidently is a direct target for *miR-323a-3p* in neuroblastoma. STAT3 is a transcription factor for genes that promote proliferation (*CCND1*, *CCND2*, *MYC*), invasiveness (*MMP-1*, *MMP-2*, *MUC1*), angiogenesis (*VEGF*), inflammation and resistance to apoptosis (*BCL2*, *BCL-X_L*, *MCL-1*, *BIRC5*) (298). The oncogenic role of STAT3 is well established, and numerous cancers have constitutively active STAT3 (299). There are also evidence of its involvement in chemotherapy- and radiotherapy resistance (128, 300-303). Targeting STAT3 have demonstrated anti-tumor effects, both in development of carcinogenesis and in tumor progression (298, 304). Whether silencing of *STAT3* is the cause of the phenotypic alterations we observe upon enforced expression of *miR-323a-3p* has yet to be determined. Attempts to phenocopy the miRNA-effect with siRNA-induced knockdown of *STAT3* have shown that the majority of the cell lines transfected suffer reduction in viability. However, SH-SY5Y appeared to be unaffected. Additional experiments have to be conducted to elucidate this question, such as co-transfection of *miR-323a-3p* mimics and a STAT3 overexpression plasmid without the MRE for *miR-323a-3p* to observe if this will rescue the miRNA's effect on cell viability. Obviously, there are other possible reasons for the *miR-323a-3p*-effect, considering that a single miRNA can have several target mRNAs and affect various pathways. Actually,

highly conserved mammalian miRNA families are predicted to average about 300 targets (159). We are therefore looking into other potential pathways. Although it is intriguing to think that one miRNA's regulatory effect on a single target can change the cells phenotype, it is most likely a coordinated regulation of several miRNAs. This theory helps explain why some targets are only partially regulated, since the sum of all target disruptions could cause the changed phenotype (305).

The question of multiple target regulation is also relevant for our discoveries in manuscript II. In this manuscript we show that reintroduction of *miR-193b-3p* enhances sensitivity to the BH3-mimetic ABT-737 in cells with preferential dependence on MCL-1. We postulate that this is partly due to *MCL-1* repression by the miRNA. Inhibiting *MCL-1* with siRNA have previously shown reduction in resistance to ABT-737 in neuroblastoma (227, 306, 307), and, since our laboratory have demonstrated that *miR-193b-3p* downregulates *MCL-1*, we hypothesized that upregulation of *miR-193b-3p* would present similar results. Indeed, compared to negative control, transfection of *miR-193b-3p* prior to ABT-737-treatment reduced viability through induction of apoptosis in MCL-1 primed cells. Our results corroborate comparable research done in melanoma, where the authors showed that *miR-193b* generated increased PARP-1 cleavage when combined with treatment of ABT-737, an effect which was partially rescued by MCL-1 overexpression (204).

ABT-737 has affinity towards BCL-2, BCL-X_L and BCL-W. In our study, we have focused solely on MCL-1 and BCL-2, since these appear to be the key anti-apoptotic proteins in death-priming of neuroblastoma. Studies on neuroblastoma cell lines indicate that BIM is the primary death signal, and that it predominantly is sequestered by BCL-2 and MCL-1, while BCL-X_L hardly binds BIM at all (218). However, due to technical difficulties the authors could not definitively say if BIM also can be sequestered by BCL-W (124). Even though we have not tested the other BCL-2 proteins, previous findings from other laboratories and the magnitude of change we see after BCL-2 antagonism and MCL-1 knockdown indicate a dominant role of BCL-2 and MCL-1 in death-priming of neuroblastoma. Our results corroborate previous stories that the small molecule inhibitor ABT-737 is more effective in cell lines with a preferential dependence on BCL-2, while MCL-1 primed cell lines are more resistant (308, 309).

MCL-1 has a fully complimentary predicted MRE for *miR-193b-3p* in its 3'UTR, according to TargetScan (310) (targenscan.org) and miRDB (311, 312) (mirdb.org). Introducing *MCL-1* without the 3'UTR to the cells partially reinstated resistance to ABT-737

in NLF cells when co-transfected with *miR-193b-3p*. This demonstrates that binding of *miR-193b-3p* to the 3'UTR of *MCL-1* is partly the reason for increased sensitivity to ABT-737. Remaining viability loss compared to negative control can indicate other involved targets for the miRNA or additional sites within the 5'UTR or CDS of *MCL-1*. In SH-SY5Y the relative difference between cells with and without augmented MCL-1 was unchanged. However, overall viability increased in cells with MCL-1 overexpression, perhaps representing binding of endogenous *miR-193b-3p* to the 3'UTR. Lower transfection efficiency is perhaps an issue in this cell line, because we observe a smaller difference in ABT-737 sensitivity between negative control and *miR-193b-3p* in cells co-transfected with control plasmid than cells merely transfected with mimics.

In breast cancer, luciferase assay has confirmed the putative MRE from the target prediction softwares to be functional (313). On the other hand, others have attempted the same in melanoma and embryonic kidney without being able to fully reverse the *miR-193b-3p* induced silencing by mutation of the binding site (203, 204). The authors propose that there are both seeded and unseeded binding sites in the 3'UTR that account for the down-regulatory effect (204). If we disregard the likelihood of technical reasons for this discrepancy, the miRNA-mRNA interaction appears to be cell type dependent. Designing LNA antisense oligonucleotides that specifically block the interaction between *miR-193b-3p* and *MCL-1* at the predicted site would theoretically overturn any effects of this interaction if it indeed was a functional site. Surely, the variance in viability between negative control mimics and *miR-193b-3p* after ABT-737 is repealed upon site blocking in both NLF and SH-SY5Y cells. We have to gauge the expression of *MCL-1* after using this target site blocker to confirm that its influence on viability indeed is attributed miRNA-induced repression of *MCL-1* and not an off-target effect. For now, it supports our assumption that *miR-193b-3p* increases sensitivity to ABT-737 in MCL-1 primed cells through silencing of *MCL-1*.

Increased sensitivity to ABT-737 in CHLA-20 cells upon overexpression of *miR-193b-3p* was somewhat unexpected, since the CHLA-20 cell line has been reported to be BCL-2 primed (124). The *miR-193b-3p/MCL-1* interaction is probably not the sole reason for our observations. A miRNA has the potential to pleiotropically target a vast number of mRNAs, so the increased sensitivity can be due to its influence on other targets and cellular pathways. Nevertheless, some contribution to increased ABT-737 sensitivity can presumably be attributed to MCL-1 suppression, considering that siRNA directed against *MCL-1* also increased sensitivity in this cell line, to some extent. Others have shown that even though a cell line is

primed, there can still be some dependence on the other factors (221) and combinational inhibition will result in less viability than either alone (216). A compensatory increase in MCL-1 from ABT-737 treatment, which we observed in CHLA-20 but not in SMS-KAN, can indicate that this anti-apoptotic protein is of importance in CHLA-20. A shift in priming state resulting from selection of clones has previously been reported (124, 222). However, this is probably not the reason in our studies due to short drug exposure time. The phenotypic alterations seen from ectopic *miR-193b-3p* expression is similar to that of specific *MCL-1* knockdown using siRNA, but they are not identical. In SH-SY5Y, increased sensitivity is more pronounced using siRNA, while in CHLA-20 it is the opposite. This can reflect the difference in priming state between these two cell lines. SH-SY5Y is clearly more dependent on MCL-1 for survival, thus highly specific downregulation with siRNA present a more profound impact on the cell than that of a miRNA with several other targets (314). Conversely, in CHLA-20, MCL-1 is not equally important and compromising MCL-1 will not have that strong impact. Moreover, in addition to its role in averting apoptosis, there are considerable evidence that MCL-1 helps maintain mitochondrial function (315, 316). Compromised mitochondria can perhaps make cells more vulnerable to small molecule inhibitors like ABT-737.

Increasing knowledge gained through genome wide sequencing and functional studies indicate that miRNA expression and regulation can be highly tissue- and cell specific (317), thus, results obtained in one cell type is not necessarily directly transmissible to another. This implies that the functional roles of miRNAs have to be investigated before being applied in the clinic, especially since a single miRNA can have both oncogenic and tumor suppressive properties, depending on the disease. Furthermore, it creates new opportunities for the use of miRNA as markers for risk profiling (36).

CX-5461 and Quarfloxin

Evading apoptosis is one of the many ways cancer cells promote proliferation. Increased ribosome biogenesis, to meet the cell's protein demand, is another feature of rapidly dividing cancer cells, thus several inhibitors of this pathway have been made (233). Frequent observation of prominent nucleoli and evidence of increased ribosome biogenesis in high-risk neuroblastoma (50, 55, 238) encouraged us to investigate the two small molecule inhibitors of ribosome biogenesis, CX-5461 and quarfloxin. In paper I, we demonstrate their anti-proliferating effect on MNA neuroblastoma, both *in vitro* and *in vivo*, through introduction of DNA damage, apoptosis and G2-cell cycle arrest. Moreover, both CX-5461 and quarfloxin downregulate MYCN in MNA cell lines and tumors.

In selected neuroblastoma cell lines (IMR-32, CHP-134 and CHLA-20), we observed that CX-5461 and quarfloxin caused phosphorylation of H2AX (γH2AX), which is a widely used biomarker of DNA damage and repair (318). Similar observations have been made in adult cancers (230, 248, 251). Both colorectal adenocarcinoma cells and osteosarcoma cells show elevated levels of γH2AX in response to CX-5461- and quarfloxin treatment (251), while H2AX is phosphorylated in lung carcinoma cells in response to quarfloxin (230). Additionally, in acute lymphoblastic leukemia (ALL) cells, ATR and CHK1 are activated due to CX-5461 treatment, also indicative of DNA damage (248). Xu *et al.* propose that the inhibitors prevent function of DNA replication forks, which result in single-stranded DNA (ssDNA) gaps or breaks (251). Drygin *et al*. attribute elevated γH2AX to apoptosis, characterizing it as a secondary event (230). This can surely be the explanation for our findings as well, since augmented γH2AX solely occurs in cell lines with massive CX-5461/quarfloxin-induced PARP-1- and caspase 3 cleavage. In addition to DNA damage, we show that CX-5461 and quarfloxin induce G2-cell cycle arrest in SK-N-BE(2)-C and SK-N-AS, which can explain the viability loss in these cell lines in the absence of apoptosis. In relation to our study, G2-arrest have also been observed in lung carcinoma cells in response to quarfloxin (230), ALL cells due to CX-5461 (248), and in colorectal cancer cells in response to either of the inhibitors (251).

Exclusive to MNA neuroblastoma with wild-type *TP53*, nanomolar concentrations of CX-5461 and quarfloxin strongly downregulate MYCN protein levels. This observation is supported by another study (319). They demonstrate that four times the amount of CX-5461 had to be subjected to non-MNA cells with functional p53 or MNA cells with *TP53* mutation to produce equivalent MYCN/MYC downregulation that was observed in MNA cells with wild-type *TP53*. Interestingly, our unpublished preliminary data indicate that, despite low protein expression, mRNA levels are actually slightly elevated in IMR-32 cells treated with CX-5461 and quarfloxin (**figure 8**). This suggests a post-transcriptional silencing mechanism of MYCN. Induction of autophagy, proteasome degradation or translational inhibition by other proteins, ncRNAs or modulation of G-quadruplexes can all be reasons for this observation. In fact, two independent DNA G-quadruplexes have been reported in the 5'UTR of *MYCN* (46, 242). Further investigations to enlighten this relationship are being conducted in our laboratory.

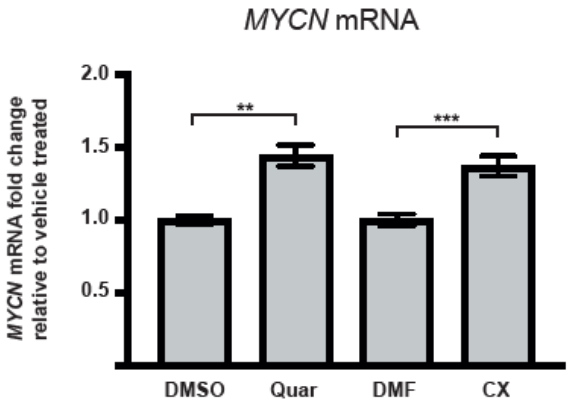

Figure 8: Expression of *MYCN* mRNA in IMR-32 cells after treatment with CX-5461 or quarfloxin. After 48 hours, treatment with CX-5461 or quarfloxin the expression level of mRNA is elevated compared to vehicle.

Downregulation of MYCN can be an indirect way that CX-5461 and quarfloxin inhibit ribosome biogenesis, since MYCN previously has been shown to upregulate several genes involved in the process (239). Nucleolar stress, induced by aberrant expression of either rRNAs or RPs, leads to nucleolar efflux of selected RPs that will bind and inactivate MDM2 proto-oncogene (MDM2) (249, 320, 321). This nucleolar surveillance network is an important mechanism to monitor the integrity of ribosome biogenesis. Disruption of MDM2 stabilizes and activates p53, as MDM2 normally prevents p53-induced transcription initialization or cause ubiquitination and degradation of p53 (320). MDM2 is often elevated in MNA neuroblastoma with a consequent upregulation of p53 and prevention of apoptosis (322). Furthermore, MDM2 regulates *MYCN* mRNA stabilization and translation, thus abolishing it leads to destabilization and decreased expression of MYCN in MNA neuroblastoma (323). We have not investigated if CX-5461 or quarfloxin affect MDM2, although MDM2 downregulation could explain both reduction in MYCN and increased p53.

Regardless of explanation, we show that induction of apoptosis exclusively occurs in cells with functional p53, and knockdown of p53 inhibits this process. Failure to reinstate functional p53 into SK-N-BE(2)-C could be due to a dominant negative p53 mutation in this cell line (324). Thus, an alternative cell line should have been used for this experiment. Irrespectively, our observations coincide with a study in lymphoma where rate of apoptotic death caused by CX-5461 *in vitro*, was dependent on functional p53 (249). Anti-tumor effect in murine wild-type *TP53* xenografts were also profound, with a clear upregulation of the p53 target p21. However, they did not test CX-5461 on *TP53*-mutated tumors *in vivo*. Though limited by a small population size, a phase I clinical trial using CX-5461 in adult cancer further supports our presumption that *TP53* status is of clinical relevance (235). Four out of five

patients with *TP53*-mutated malignancies suffered from disease exacerbation, while the last experienced stable disease. In contrast, the patient with best response had functional p53, and p53-expression levels were elevated in response to treatment with CX-5461. However, another *in vitro* study in adult cancer conflicts with our observations (247). Analyzing several malignancies, they did not observe a significant difference in efficacy of CX-5461 between cells with wild-type and mutated *TP53*. Still, it is interesting that, while CX-5461 show a similar activity in all mutated tumors, there are higher variations between the samples with wild-type *TP53*. Biological features can vary between cancer types and perhaps are there common denominators in the outliers with wild-type *TP53* that should have been further investigated. Nevertheless, our *in vivo* experiments emphasize our *in vitro* findings; CX-5461 has greater anti-tumorigenic effect in the wild-type *TP53* (IMR-32) than the *TP53*-mutated (SK-N-BE(2)-C) xenograft model. Additional studies on MNA neuroblastoma xenograft models, comparing effects on tumors with functional and defective p53, would help clarify this question.

Potential for Clinical Use

RNA Interference (RNAi)

RNAi has great therapeutic potential to combat cancer. While small molecule and protein-based drugs have a limited substrate diversity, siRNAs and miRNAs can specifically target most genes. The fact that miRNAs can silence various mRNAs simultaneously can be an advantage in treatment of multigene disorders, like cancer. However, compared to most small molecule drugs that are stable and relatively easy to deliver, siRNAs and miRNAs are more volatile and can rapidly degrade in the circulation (284). Many hurdles have to be overcome for a miRNA to be successfully delivered to a solid tumor: Avoid immune reaction, enzymatic degradation and entrapment by phagocytes; minimize renal clearance; be delivered to the correct site and extravagate efficiently; get into the tumor cells, escape from the endosome and be loaded successfully into the RISC (325). Of course, a majority of these obstacles apply to most drugs, so the right method just have to be found. Several carrier methods for delivery of miRNAs and siRNA have been evaluated, such as viral vectors, lipidic or polymeric scaffolds, poly-(α)glutamic acid (PGA)-based nanocarriers and bacteria-derived minicells (326, 327). Furthermore, for therapeutic purposes miRNA duplexes (pri-, pre- or mature miRNA) are better suited than single stranded miRNA oligos because of greater stability (284).

Intravenous liposomal delivery of *miR-34a* was the first miRNA mimicking drug to be tested in a stage I clinical trial (ClinicalTrials.gov Identifier: NCT01829971). Unfortunately, adverse effects forced early discontinuation in several individuals. If this was due to the miRNA

itself or the delivery method is unclear, and further studies are warranted (328). The pleiotropic nature of miRNA will surely raise the possibility of adverse effects. *MiR-34a* has multiple recognized targets important in critical pathways (329), and, although this could be valuable in suppressing tumorigenesis, it can increase the risk for adverse effects. However, off-target effects can also be observed when targeting single genes, and studies show that novel multi-target drugs can have low toxicity towards normal cells (330).

Other miRNA replacement drugs are currently being tested. "TargomiRs" are bacteria derived minicells with an antibody moiety for tumor specificity that encapsulate miRNA mimics. A phase I trial treating mesothelioma and non-small cell lung cancer (NSCLC) with *miR-16* TargomiRs (NCT02369198) show an encouraging toxicity profile and further testing of efficacy is warranted (327). Additionally, the pharmacodynamic and –kinetic properties of the *miR-29* mimicking drug MRG-201 (Remlarsen) are being tested (NCT03601052).

Small Molecule Inhibitors

The low solubility of ABT-737 cause poor bioavailability, limiting its use *in vivo* (207, 331). To improve uptake a clinical analogue of ABT-737, ABT-263 (Navitoclax), was constructed (331). Unfortunately, it induced a drop in peripheral platelet count when tested in adult patients (332, 333). Platelets are dependent on BCL-X_L for survival (334), therefore, it is presumed that therapeutic doses of ABT-263 sequester BCL-X_L and generate an increased risk of bleeding. ABT-199 (Venetoclax) is derived from ABT-263, but modified to bind BCL-2 selectively, thereby reducing thrombocytopenia (335). Clinical trials have led to the approval of ABT-199 for oral treatment of chronic lymphocytic leukemia and small lymphocytic lymphoma (336, 337), and ongoing studies investigate its potential as monotherapy in other cancers or look into a possible synergic effect of combination treatment (207, 338, 339). Perhaps can concurrent sensitization of the apoptotic pathway augment the possibility for chemotherapy-induced death? Indeed, in neuroblastoma and lymphoma, preclinical trials have demonstrated an advantage of co-treatment with BCL-2 inhibitors and chemotherapeutic drugs in BCL-2 primed cells (124, 222, 331). Since ABT-737 and ABT-199 hardly affect MCL-1 primed neuroblastoma xenografts (222, 308) combination with drugs that can neutralize MCL-1 is a compelling strategy, such as siRNAs, miRNAs or other small molecule inhibitors.

One important aspect to keep in mind is that MCL-1 has vital functions in several cell lineages (315, 316, 340-343). Consequently, abrogating MCL-1 might cause severe side effects. AT-101, a drug that inhibits MCL-1, has a toxicity profile that caused it to fail in clinical trials

(344). It is not certain if this was exclusively due to downregulation of MCL-1, or caused by off-target effects that have been seen for this compound (344). Treatment that incorporate MCL-1 downregulation and another mechanism of action preferentially targeting tumor cells can hopefully achieve a synergistic or additive effect, while sparing non-tumorous tissue. At least, to avoid unnecessary adverse effects, it is important to distinguish between patients that will benefit from MCL-1 downregulation, and the ones that will not.

G-quadruplexes are located throughout the genome and transcriptome, including the promoter region of several cancer related genes, such as *BCL2*, *MYC*, *VEGF*, *kRAS* and *RB* (230, 345). This could cause apprehension about targeting them. However, there are structural differences between G-quadruplexes, specifically between loop lengths or strand orientations (241). This may allow for more specific, or even unique drug targeting. Moreover, since both inhibitors evidently have other functions than targeting G-quadruplexes and ribosome biogenesis, the therapeutic response might be somewhat disease specific. In general, affecting normal cells is a concern when attempting to disrupt important biological processes. Fortunately, whereas inhibition of ribosome biogenesis cause apoptosis in cancer cells, normal cells appear to tolerate a reduction in rRNA (247, 249). Clinical trials have demonstrated low toxicity of both CX-5461 and quarfloxin (235, 346). Quarfloxin has successfully completed clinical I/II trials (NCT00955786 and NCT00780663), and progression into phase II is also planned for CX-5461, treating breast cancer patients (346). In rats, radiolabeled quarfloxin accumulate in tissue that originates from neural crests (347), potentially making it a valuable drug for targeting neuroectodermal cancers like neuroblastoma. A promising preclinical study has also tested localized management of the drug using CX-5461-loaded silk film (319). This has potential of minimizing systemic toxicity while maximizing confined anti-tumor effects.

Targeted Therapy

The heterogeneity of tumors, both morphological, biological and in regard to therapy responsiveness, underscores the importance of methodical tumor characterization. Both the studies on small molecule inhibitors presented in this thesis highlight how biological features such as apoptotic priming state, *MYCN* status and p53 functioning significantly distinguish drug sensitivity. Sequencing tumor material prior to treatment can be useful to identify individuals who would benefit from more personalized therapy. Several molecular profiling studies have been launched that also include pediatric patients, such as MOSCATO-02 (NCT01566019; (348)), MAPPYACTS (NCT02613962) and INFORM (349). These lay the foundation for mutation-matched therapy trials for patients with refractory or relapsed disease, like INFORM2

(NCT03838042), ESMART (NCT02813135), the "Next Generation Personalized Neuroblastoma Therapy"-study (NCT02780128) and "The Pediatric MATCH Screening Trial" (NCT03155620). Now, also newly diagnosed patients with high-risk disease can be enrolled in targeted induction treatment after prior tumor profiling in trials like PEDS-PLAN (NCT02559778) or the ALK-targeting trial NCT03126916. The era of constantly trying to improve standard therapy in neuroblastoma (chemotherapy, surgery, radiation and stem cell transplantation) has perhaps culminated, and we now move into a time where we find targeted therapy based on biological features more fruitful.

Finding the major apoptosis patterns in neuroblastoma is an important step in the work of overcoming drug resistance. Seeing that a functional mitochondrial apoptosis is required for chemotherapy induced cell death to occur, profiling tumors to determine death priming can therefore be of value for treatment stratification (124). In theory, any cell that the mitochondria can be isolated from can be assessed for priming state (214) using BH3-profiling (219). As others and we have presented, priming state can also be valuable in response stratification for small molecule BCL-2 antagonist used with or without adjuvant treatment.

Lastly, the equivocal treatment response for CX-5461 and quarfloxin indicate that if they were to be incorporated into neuroblastoma treatment, the genetic profile of the patients' tumors ought to be investigated. Our findings argue for discriminating between those with MNA tumors with wild-type *TP53* and those with other genetic profiles.

Conclusion

In addition to challenges related to chemotherapy resistance, standard treatment for high-risk neuroblastoma involves chemotherapy doses up to maximal tolerable capacity; making alternative approaches to severe disseminate neuroblastoma a necessity. This thesis presents novel insights into the function of selected miRNA in neuroblastoma and demonstrate a possibility of using small molecule inhibitors of oncogenic pathways to challenge treatment-refractory neuroblastoma.

The Author's Contribution

In this section, I briefly present my contribution to the published and unpublished work of this thesis.

In manuscript I (*Hsa-miR-323a-3p* Functions as a Tumor Suppressor and Targets *STAT3* in Neuroblastoma Cells), I contributed to the design of the research. Swapnil Parashram Bhavsar performed the majority of the experimental work that has been included in the final manuscript, but I have performed several additional experiments that are not presented at this time. Together with Bhavsar, I have written and edited the final manuscript. Bhavsar and I have contributed equally to the work and share 1st authorship.

To manuscript II (*Hsa-miR-193b-3p* Sensitizes MCL-1 Primed Neuroblastoma Cell Lines to the BH3 Mimetic ABT-737), my work has been to design the research, perform the majority of the experiments, and write and edit the final manuscript. Sarah Andrea Roth and I have contributed equally to the work and share 1st authorship.

In paper I (Inhibitors of Ribosome Biogenesis Repress the Growth of MYCN-amplified Neuroblastoma) I have conducted some experiments, contributed in discussion of the results and critically amended the final manuscript. My involvement qualified for 2nd authorship for this paper.

Supplemental Material

INSS*	**Age** (days)	***MYCN***	**DNA index**	**INCP**	**Other**	**Risk group**
1	Any	Any	Any	Any		Low
2A/B	Any	NA	Any	Any	Resection ≥50%, asymptomatic	Low
					Resection ≥50%, symptomatic	Intermediate
					Resection <50%	Intermediate
					Biopsy only	Intermediate
		Amp			Any degree of resection	High
3	<547	NA	Any	Any		Intermediate
	>547			Favorable		Intermediate
	Any	Amp		Any		High
	>547	NA		Unfavorable		High
4	<365	Amp	Any	Any		High
		NA				Intermediate
	365 to <547	Amp				High
		Any	DI = 1			High
			Any	Unfavorable		High
		NA	DI > 1	Favorable		Intermediate
	>547	Any	Any	Any		High
4S	<365	NA	DI > 1	Favorable	Asymptomatic	Low
			DI = 1	Any	Asymptomatic or symptomatic	Intermediate
		Missing	Missing	Missing	Too sick to undergo biopsy	Intermediate
		NA	Any	Any	Symptomatic	Intermediate
				Unfavorable	Asymptomatic or symptomatic	Intermediate
		Amp		Any		High

Abbreviations: Abbreviations: Amp, amplified; NA, not amplified; INPC, International Neuroblastoma Pathology Classification; DI >1, hyperdiploid; DI = 1, diploid.

*INSS is in the progress of being replaced by INRGSS (34).

Supplementary table 1: Children's oncology group risk assessment form (34).

INRG Stage	Age (months)	Histology	Tumor diff	*MYCN*	11q aberration	Ploidy	Pretreatment Risk Group
L1/L2	Any	GN maturing, GNB intermixed	Any	Any	Any	Any	Very low
L1	Any	Any, exc. GN mat., GNB interm.	Any	NA	Any	Any	Very low
				Amp			High
L2	<18	Any, exc. GN mat., GNB interm.	Any	NA	No	Any	Low
					Yes		Intermediate
	≥18	GNB nodular; NB	Diff	NA	No	Any	Low
					Yes		Intermediate
			Poorly diff. or undiff.	NA	Any	Any	
			Any	Amp			High
M	<18	Any	Any	NA	Any	DI >1	Low
	<12					DI = 1	Intermediate
	12-<18						Intermediate
	<18			Amp	Any	Any	High
	≥18			Any			High
MS	<18	Any	Any	NA	No	Any	Very low
					Yes		High
				Amp	Any		High

Abbreviations: GN, ganglioneuroma; GNB, ganglioneuroblastoma; Exc, except; Diff, differentiated; Amp, amplified; NA, not amplified; DI > 1, hyperdiploidy; DI = 1, diploid.

Supplementary table 2: International neuroblastoma risk group classification system (INRGCS) (32).

References

1. Steliarova-Foucher E, Colombet M, Ries LAG, Moreno F, Dolya A, Bray F, et al. International incidence of childhood cancer, 2001–10: a population-based registry study. The Lancet Oncology. 2017;18(6):719-31.

2. Johnsen JI, Kogner P, Albihn A, Henriksson MA. Embryonal neural tumours and cell death. Apoptosis. 2009;14(4):424-38.

3. Siegel RL, Miller KD, Jemal A. Cancer statistics, 2019. CA: A Cancer Journal for Clinicians. 2019;69(1):7-34.

4. Chen X, Pappo A, Dyer MA. Pediatric solid tumor genomics and developmental pliancy. Oncogene. 2015;34(41):5207-15.

5. Smith MA, Seibel NL, Altekruse SF, Ries LAG, Melbert DL, O'Leary M, et al. Outcomes for Children and Adolescents With Cancer: Challenges for the Twenty-First Century. Journal of Clinical Oncology. 2010;28(15):2625-34.

6. Ries LAG, Smith MA, Gurney J, Linet M, Tamra T, Young J, et al. Cancer Incidence and Survival among Children and Adolescents: United States SEER Program 1975-1995. National Cancer Institute, SEER Program NIH Pub. 1999;99-4649.

7. WHO. World Cancer Report 2014. International Agency for Research on Cancer; 2014.

8. Sweet-Cordero EA, Biegel JA. The genomic landscape of pediatric cancers: Implications for diagnosis and treatment. Science. 2019;363(6432):1170.

9. Kaatsch P. Epidemiology of childhood cancer. Cancer Treatment Reviews. 2010;36(4):277-85.

10. NOPHO. Annual report 2014. Nopho.org; 2014.

11. London WB, Castleberry RP, Matthay KK, Look AT, Seeger RC, Shimada H, et al. Evidence for an Age Cutoff Greater Than 365 Days for Neuroblastoma Risk Group Stratification in the Children's Oncology Group. Journal of Clinical Oncology. 2005;23(27):6459-65.

12. Maris JM, Hogarty MD, Bagatell R, Cohn SL. Neuroblastoma. The Lancet. 2007;369(9579):2106-20.

13. Maris JM. Recent Advances in Neuroblastoma. New England Journal of Medicine. 2010;362(23):2202-11.

14. Nuchtern JG, London WB, Barnewolt CE, Naranjo A, McGrady PW, Geiger JD, et al. A Prospective Study of Expectant Observation as Primary Therapy for Neuroblastoma in Young Infants: A Children's Oncology Group Study. Annals of Surgery. 2012;256(4):573-80.

15. Pinto NR, Applebaum MA, Volchenboum SL, Matthay KK, London WB, Ambros PF, et al. Advances in Risk Classification and Treatment Strategies for Neuroblastoma. Journal of Clinical Oncology. 2015;33(27):3008-17.

16. Zhou MJ, Doral MY, DuBois SG, Villablanca JG, Yanik GA, Matthay KK. Different outcomes for relapsed versus refractory neuroblastoma after therapy with 131I-metaiodobenzylguanidine (131I-MIBG). European Journal of Cancer. 2015;51(16):2465-72.

17. Shakhova O, Sommer L. Neural crest-derived stem cells. StemBook [Internet]: Cambridge (MA): Harvard Stem Cell Institute; 2010.

18. Tsubota S, Kadomatsu K. Origin and initiation mechanisms of neuroblastoma. Cell and Tissue Research. 2018;372(2):211-21.

19. Vo KT, Matthay KK, Neuhaus J, London WB, Hero B, Ambros PF, et al. Clinical, Biologic, and Prognostic Differences on the Basis of Primary Tumor Site in Neuroblastoma: A Report From the International Neuroblastoma Risk Group Project. Journal of Clinical Oncology. 2014;32(28):3169-76.

20. Boeva V, Louis-Brennetot C, Peltier A, Durand S, Pierre-Eugène C, Raynal V, et al. Heterogeneity of neuroblastoma cell identity defined by transcriptional circuitries. Nature Genetics. 2017;49:1408.

21. van Groningen T, Koster J, Valentijn LJ, Zwijnenburg DA, Akogul N, Hasselt NE, et al. Neuroblastoma is composed of two super-enhancer-associated differentiation states. Nature Genetics. 2017;49:1261.

22. Pugh TJ, Morozova O, Attiyeh EF, Asgharzadeh S, Wei JS, Auclair D, et al. The genetic landscape of high-risk neuroblastoma. Nature Genetics. 2013;45:279.

23. Molenaar JJ, Koster J, Zwijnenburg DA, van Sluis P, Valentijn LJ, van der Ploeg I, et al. Sequencing of neuroblastoma identifies chromothripsis and defects in neuritogenesis genes. Nature. 2012;483(7391):589-93.

24. Tsubota S, Kadomatsu K. Origin and mechanism of neuroblastoma. Oncoscience. 2017;4(7-8):70-2.

25. Tolbert VP, Matthay KK. Neuroblastoma: clinical and biological approach to risk stratification and treatment. Cell and Tissue Research. 2018;372(2):195-209.

26. Kushner BH. Neuroblastoma: A Disease Requiring a Multitude of Imaging Studies*. Journal of Nuclear Medicine. 2004;45(7):1172-88.

27. Strenger V, Kerbl R, Dornbusch HJ, Ladenstein R, Ambros PF, Ambros IM, et al. Diagnostic and prognostic impact of urinary catecholamines in neuroblastoma patients. Pediatric Blood & Cancer. 2007;48(5):504-9.

28. Tuchman M, Ramnaraine MLR, Woods WG, Krivit W. Three Years of Experience With Random Urinary Homovanillic and Vanillylmandelic Acid Levels in the Diagnosis of Neuroblastoma. Pediatrics. 1987;79(2):203.

29. Morgenstern DA, London WB, Stephens D, Volchenboum SL, Simon T, Nakagawara A, et al. Prognostic significance of pattern and burden of metastatic disease in patients with stage 4 neuroblastoma: A study from the International Neuroblastoma Risk Group database. European Journal of Cancer. 2016;65:1-10.

30. DuBois SG, Kalika Y, Lukens JN, Brodeur GM, Seeger RC, Atkinson JB, et al. Metastatic Sites in Stage IV and IVS Neuroblastoma Correlate With Age, Tumor Biology, and Survival. Journal of Pediatric Hematology/Oncology. 1999;21(3):181-9.

31. Brodeur GM, Pritchard J, Berthold F, Carlsen NL, Castel V, Castelberry RP, et al. Revisions of the international criteria for neuroblastoma diagnosis, staging, and response to treatment. Journal of Clinical Oncology. 1993;11(8):1466-77.

32. Cohn SL, Pearson ADJ, London WB, Monclair T, Ambros PF, Brodeur GM, et al. The International Neuroblastoma Risk Group (INRG) Classification System: An INRG Task Force Report. Journal of Clinical Oncology. 2009;27(2):289-97.

33. Monclair T, Brodeur GM, Ambros PF, Brisse HJ, Cecchetto G, Holmes K, et al. The International Neuroblastoma Risk Group (INRG) staging system: an INRG Task Force report.

Journal of clinical oncology : official journal of the American Society of Clinical Oncology. 2009;27(2):298-303.

34. Naranjo A, Irwin MS, Hogarty MD, Cohn SL, Park JR, London WB. Statistical Framework in Support of a Revised Children's Oncology Group Neuroblastoma Risk Classification System. JCO Clinical Cancer Informatics. 2018(2):1-15.

35. Strother DR, London WB, Schmidt ML, Brodeur GM, Shimada H, Thorner P, et al. Outcome After Surgery Alone or With Restricted Use of Chemotherapy for Patients With Low-Risk Neuroblastoma: Results of Children's Oncology Group Study P9641. Journal of Clinical Oncology. 2012;30(15):1842-8.

36. Smith CM, Catchpoole D, Hutvagner G. Non-Coding RNAs in Pediatric Solid Tumors. Frontiers in genetics. 2019;10:798-.

37. Trigg RM, Turner SD. ALK in Neuroblastoma: Biological and Therapeutic Implications. Cancers. 2018;10(4):113.

38. Shimada H, Ambros IM, Dehner LP, Hata J-i, Joshi VV, Roald B, et al. The International Neuroblastoma Pathology Classification (the Shimada system). Cancer. 1999;86(2):364-72.

39. Shimada H, Umehara S, Monobe Y, Hachitanda Y, Nakagawa A, Goto S, et al. International neuroblastoma pathology classification for prognostic evaluation of patients with peripheral neuroblastic tumors. Cancer. 2001;92(9):2451-61.

40. Kaneko Y, Knudson AG. Mechanism and relevance of ploidy in neuroblastoma. Genes, Chromosomes and Cancer. 2000;29(2):89-95.

41. Taggart DR, London WB, Schmidt ML, DuBois SG, Monclair TF, Nakagawara A, et al. Prognostic Value of the Stage 4S Metastatic Pattern and Tumor Biology in Patients With Metastatic Neuroblastoma Diagnosed Between Birth and 18 Months of Age. Journal of Clinical Oncology. 2011;29(33):4358-64.

42. Attiyeh EF, London WB, Mossé YP, Wang Q, Winter C, Khazi D, et al. Chromosome 1p and 11q Deletions and Outcome in Neuroblastoma. New England Journal of Medicine. 2005;353(21):2243-53.

43. Spitz R, Hero B, Simon T, Berthold F. Loss in Chromosome 11q Identifies Tumors with Increased Risk for Metastatic Relapses in Localized and 4S Neuroblastoma. Clinical Cancer Research. 2006;12(11):3368.

44. Colon NC, Chung DH. Neuroblastoma. Advances in pediatrics. 2011;58(1):297-311.

45. Huang M, Weiss WA. Neuroblastoma and MYCN. Cold Spring Harb Perspect Med. 2013;3(10):a014415-a.

46. Trajkovski M, Webba da Silva M, Plavec J. Unique Structural Features of Interconverting Monomeric and Dimeric G-Quadruplexes Adopted by a Sequence from the Intron of the N-myc Gene. Journal of the American Chemical Society. 2012;134(9):4132-41.

47. Brodeur GM, Seeger RC, Schwab M, Varmus HE, Bishop JM. Amplification of N-myc in untreated human neuroblastomas correlates with advanced disease stage. Science. 1984;224(4653):1121.

48. Seeger RC, Brodeur GM, Sather H, Dalton A, Siegel SE, Wong KY, et al. Association of Multiple Copies of the N-myc Oncogene with Rapid Progression of Neuroblastomas. New England Journal of Medicine. 1985;313(18):1111-6.

49. Lee JW, Son MH, Cho HW, Ma YE, Yoo KH, Sung KW, et al. Clinical significance of MYCN amplification in patients with high-risk neuroblastoma. Pediatric Blood & Cancer. 2018;65(10):e27257.

50. Wang LL, Teshiba R, Ikegaki N, Tang XX, Naranjo A, London WB, et al. Augmented expression of MYC and/or MYCN protein defines highly aggressive MYC-driven neuroblastoma: a Children's Oncology Group study. British journal of cancer. 2015;113(1):57-63.

51. Valentijn LJ, Koster J, Haneveld F, Aissa RA, van Sluis P, Broekmans MEC, et al. Functional MYCN signature predicts outcome of neuroblastoma irrespective of MYCN amplification. Proceedings of the National Academy of Sciences. 2012;109(47):19190.

52. Weiss WA, Aldape K, Mohapatra G, Feuerstein BG, Bishop JM. Targeted expression of MYCN causes neuroblastoma in transgenic mice. The EMBO Journal. 1997;16(11):2985-95.

53. Tweddle DA, Malcolm AJ, Cole M, Pearson AD, Lunec J. p53 cellular localization and function in neuroblastoma: evidence for defective G(1) arrest despite WAF1 induction in MYCN-amplified cells. The American journal of pathology. 2001;158(6):2067-77.

54. Berbegall AP, Bogen D, Pötschger U, Beiske K, Bown N, Combaret V, et al. Heterogeneous MYCN amplification in neuroblastoma: a SIOP Europe Neuroblastoma Study. British Journal of Cancer. 2018;118(11):1502-12.

55. Wang LL, Suganuma R, Ikegaki N, Tang X, Naranjo A, McGrady P, et al. Neuroblastoma of undifferentiated subtype, prognostic significance of prominent nucleolar formation, and MYC/MYCN protein expression: A report from the Children's Oncology Group. Cancer. 2013;119(20):3718-26.

56. Zimmerman MW, Liu Y, He S, Durbin AD, Abraham BJ, Easton J, et al. MYC Drives a Subset of High-Risk Pediatric Neuroblastomas and Is Activated through Mechanisms Including Enhancer Hijacking and Focal Enhancer Amplification. Cancer Discovery. 2018;8(3):320.

57. Hero B, Simon T, Spitz R, Ernestus K, Gnekow AK, Scheel-Walter H-G, et al. Localized Infant Neuroblastomas Often Show Spontaneous Regression: Results of the Prospective Trials NB95-S and NB97. Journal of Clinical Oncology. 2008;26(9):1504-10.

58. De Bernardi B, Mosseri V, Rubie H, Castel V, Foot A, Ladenstein R, et al. Treatment of localised resectable neuroblastoma. Results of the LNESG1 study by the SIOP Europe Neuroblastoma Group. British journal of cancer. 2008;99(7):1027-33.

59. Baker DL, Schmidt ML, Cohn SL, Maris JM, London WB, Buxton A, et al. Outcome after Reduced Chemotherapy for Intermediate-Risk Neuroblastoma. New England Journal of Medicine. 2010;363(14):1313-23.

60. Bernardi BD, Gerrard M, Boni L, Rubie H, Cañete A, Cataldo AD, et al. Excellent Outcome With Reduced Treatment for Infants With Disseminated Neuroblastoma Without MYCN Gene Amplification. Journal of Clinical Oncology. 2009;27(7):1034-40.

61. Matthay KK, Villablanca JG, Seeger RC, Stram DO, Harris RE, Ramsay NK, et al. Treatment of High-Risk Neuroblastoma with Intensive Chemotherapy, Radiotherapy, Autologous Bone Marrow Transplantation, and 13-cis-Retinoic Acid. New England Journal of Medicine. 1999;341(16):1165-73.

62. Talleur AC, Triplett BM, Federico S, Mamcarz E, Janssen W, Wu J, et al. Consolidation Therapy for Newly Diagnosed Pediatric Patients with High-Risk Neuroblastoma Using

Busulfan/Melphalan, Autologous Hematopoietic Cell Transplantation, Anti-GD2 Antibody, Granulocyte-Macrophage Colony–Stimulating Factor, Interleukin-2, and Haploidentical Natural Killer Cells. Biology of Blood and Marrow Transplantation. 2017;23(11):1910-7.

63. Schulz G, Cheresh DA, Varki NM, Yu A, Staffileno LK, Reisfeld RA. Detection of Ganglioside GD2 in Tumor Tissues and Sera of Neuroblastoma Patients. Cancer Research. 1984;44(12 Part 1):5914.

64. Yu AL, Gilman AL, Ozkaynak MF, London WB, Kreissman SG, Chen HX, et al. Anti-GD2 Antibody with GM-CSF, Interleukin-2, and Isotretinoin for Neuroblastoma. New England Journal of Medicine. 2010;363(14):1324-34.

65. Ladenstein R, Pötschger U, Valteau-Couanet D, Luksch R, Castel V, Yaniv I, et al. Interleukin 2 with anti-GD2 antibody ch14.18/CHO (dinutuximab beta) in patients with high-risk neuroblastoma (HR-NBL1/SIOPEN): a multicentre, randomised, phase 3 trial. The Lancet Oncology. 2018;19(12):1617-29.

66. Ladenstein RL, Pötschger U, Valteau-Couanet D, Gray J, Luksch R, Balwierz W, et al. Randomization of dose-reduced subcutaneous interleukin-2 (scIL2) in maintenance immunotherapy (IT) with anti-GD2 antibody dinutuximab beta (DB) long-term infusion (LTI) in front–line high-risk neuroblastoma patients: Early results from the HR-NBL1/SIOPEN trial. Journal of Clinical Oncology. 2019;37(15_suppl):10013-.

67. Siebert N, Eger C, Seidel D, Jüttner M, Zumpe M, Wegner D, et al. Pharmacokinetics and pharmacodynamics of ch14.18/CHO in relapsed/refractory high-risk neuroblastoma patients treated by long-term infusion in combination with IL-2. mAbs. 2016;8(3):604-16.

68. Federico SM, McCarville MB, Shulkin BL, Sondel PM, Hank JA, Hutson P, et al. A Pilot Trial of Humanized Anti-GD2 Monoclonal Antibody (hu14.18K322A) with Chemotherapy and Natural Killer Cells in Children with Recurrent/Refractory Neuroblastoma. Clinical Cancer Research. 2017;23(21):6441.

69. Mody R, Naranjo A, Van Ryn C, Yu AL, London WB, Shulkin BL, et al. Irinotecan–temozolomide with temsirolimus or dinutuximab in children with refractory or relapsed neuroblastoma (COG ANBL1221): an open-label, randomised, phase 2 trial. The Lancet Oncology. 2017;18(7):946-57.

70. Garaventa A, Parodi S, De Bernardi B, Dau D, Manzitti C, Conte M, et al. Outcome of children with neuroblastoma after progression or relapse. A retrospective study of the Italian neuroblastoma registry. European Journal of Cancer. 2009;45(16):2835-42.

71. Di Giannatale A, Dias-Gastellier N, Devos A, Mc Hugh K, Boubaker A, Courbon F, et al. Phase II study of temozolomide in combination with topotecan (TOTEM) in relapsed or refractory neuroblastoma: A European Innovative Therapies for Children with Cancer-SIOP-European Neuroblastoma study. European Journal of Cancer. 2014;50(1):170-7.

72. Bagatell R, London WB, Wagner LM, Voss SD, Stewart CF, Maris JM, et al. Phase II Study of Irinotecan and Temozolomide in Children With Relapsed or Refractory Neuroblastoma: A Children's Oncology Group Study. Journal of Clinical Oncology. 2011;29(2):208-13.

73. George SL, Falzone N, Chittenden S, Kirk SJ, Lancaster D, Vaidya SJ, et al. Individualized 131I-mIBG therapy in the management of refractory and relapsed neuroblastoma. Nuclear Medicine Communications. 2016;37(5):466-72.

74. French S, DuBois SG, Horn B, Granger M, Hawkins R, Pass A, et al. 131I-MIBG followed by consolidation with busulfan, melphalan and autologous stem cell transplantation for refractory neuroblastoma. Pediatric Blood & Cancer. 2013;60(5):879-84.

75. Keshelava N, Seeger RC, Groshen S, Reynolds CP. Drug Resistance Patterns of Human Neuroblastoma Cell Lines Derived from Patients at Different Phases of Therapy. Cancer Research. 1998;58(23):5396.

76. DuBois SG, Mosse YP, Fox E, Kudgus RA, Reid JM, McGovern R, et al. Phase II Trial of Alisertib in Combination with Irinotecan and Temozolomide for Patients with Relapsed or Refractory Neuroblastoma. Clinical Cancer Research. 2018;24(24):6142.

77. Richards RM, Sotillo E, Majzner RG. CAR T Cell Therapy for Neuroblastoma. Front Immunol. 2018;9:2380-.

78. Mora J, Cheung NK, Gerald WL. Genetic heterogeneity and clonal evolution in neuroblastoma. British journal of cancer. 2001;85(2):182-9.

79. Giovannetti E, Erozenci A, Smit J, Danesi R, Peters GJ. Molecular mechanisms underlying the role of microRNAs (miRNAs) in anticancer drug resistance and implications for clinical practice. Critical Reviews in Oncology/Hematology. 2012;81(2):103-22.

80. Longley D, Johnston P. Molecular mechanisms of drug resistance. The Journal of Pathology. 2005;205(2):275-92.

81. Norris MD, Smith J, Tanabe K, Tobin P, Flemming C, Scheffer GL, et al. Expression of multidrug transporter MRP4/ABCC4 is a marker of poor prognosis in neuroblastoma and confers resistance to irinotecan in vitro. Molecular Cancer Therapeutics. 2005;4(4):547.

82. Norris MD, Bordow SB, Marshall GM, Haber PS, Cohn SL, Haber M. Expression of the Gene for Multidrug-Resistance–Associated Protein and Outcome in Patients with Neuroblastoma. New England Journal of Medicine. 1996;334(4):231-8.

83. Borst P, Evers R, Kool M, Wijnholds J. A Family of Drug Transporters: the Multidrug Resistance-Associated Proteins. JNCI: Journal of the National Cancer Institute. 2000;92(16):1295-302.

84. Hipfner DR, Deeley RG, Cole SPC. Structural, mechanistic and clinical aspects of MRP1. Biochimica et Biophysica Acta (BBA) - Biomembranes. 1999;1461(2):359-76.

85. Coughlan D, Gianferante M, Lynch CF, Stevens JL, Harlan LC. Treatment and survival of childhood neuroblastoma: Evidence from a population-based study in the United States. Pediatric Hematology and Oncology. 2017;34(5):320-30.

86. Kuss BJ, Corbo M, Lau WM, Fennell DA, Dean NM, Cotter FE. In vitro and in vivo downregulation of MRP1 by antisense oligonucleotides: A potential role in neuroblastoma therapy. International Journal of Cancer. 2002;98(1):128-33.

87. Burkhart CA, Watt F, Murray J, Pajic M, Prokvolit A, Xue C, et al. Small-Molecule Multidrug Resistance–Associated Protein 1 Inhibitor Reversan Increases the Therapeutic Index of Chemotherapy in Mouse Models of Neuroblastoma. Cancer Research. 2009;69(16):6573.

88. Norris MD, Madafiglio J, Gilbert J, Marshall GM, Haber M. Reversal of multidrug resistance-associated protein-mediated drug resistance in cultured human neuroblastoma cells by the quinolone antibiotic difloxacin. Medical and Pediatric Oncology. 2001;36(1):177-80.

89. Russel FGM, Koenderink JB, Masereeuw R. Multidrug resistance protein 4 (MRP4/ABCC4): a versatile efflux transporter for drugs and signalling molecules. Trends in Pharmacological Sciences. 2008;29(4):200-7.

90. Murray J, Valli E, Yu DMT, Truong AM, Gifford AJ, Eden GL, et al. Suppression of the ATP-binding cassette transporter ABCC4 impairs neuroblastoma tumour growth and sensitises to irinotecan in vivo. European Journal of Cancer. 2017;83:132-41.

91. Guo J, Jin D, Wu Y, Yang L, Du J, Gong K, et al. The miR 495-UBE2C-ABCG2/ERCC1 axis reverses cisplatin resistance by downregulating drug resistance genes in cisplatin-resistant non-small cell lung cancer cells. EBioMedicine. 2018;35:204-21.

92. Xie Y, Shao Y, Deng X, Wang M, Chen Y. MicroRNA-298 Reverses Multidrug Resistance to Antiepileptic Drugs by Suppressing MDR1/P-gp Expression in vitro. Frontiers in Neuroscience. 2018;12(602).

93. Duvvuri M, Krise JP. Intracellular drug sequestration events associated with the emergence of multidrug resistance: a mechanistic review. Frontiers in bioscience : a journal and virtual library. 2005;10:1499-509.

94. Marrache S, Pathak RK, Dhar S. Detouring of cisplatin to access mitochondrial genome for overcoming resistance. Proceedings of the National Academy of Sciences. 2014;111(29):10444.

95. Daly AK. Pharmacogenetics of the major polymorphic metabolizing enzymes. Fundamental & Clinical Pharmacology. 2003;17(1):27-41.

96. de Man FM, Goey AKL, van Schaik RHN, Mathijssen RHJ, Bins S. Individualization of Irinotecan Treatment: A Review of Pharmacokinetics, Pharmacodynamics, and Pharmacogenetics. Clinical Pharmacokinetics. 2018;57(10):1229-54.

97. Ogawa M, Hori H, Ohta T, Onozato K, Miyahara M, Komada Y. Sensitivity to Gemcitabine and Its Metabolizing Enzymes in Neuroblastoma. Clinical Cancer Research. 2005;11(9):3485.

98. Poljaková J, Eckschlager T, Hraběta J, Hřebačková J, Smutný S, Frei E, et al. The mechanism of cytotoxicity and DNA adduct formation by the anticancer drug ellipticine in human neuroblastoma cells. Biochemical Pharmacology. 2009;77(9):1466-79.

99. Lamant L, Pulford K, Bischof D, Morris SW, Mason DY, Delsol G, et al. Expression of the ALK Tyrosine Kinase Gene in Neuroblastoma. The American Journal of Pathology. 2000;156(5):1711-21.

100. Bresler Scott C, Weiser Daniel A, Huwe Peter J, Park Jin H, Krytska K, Ryles H, et al. ALK Mutations Confer Differential Oncogenic Activation and Sensitivity to ALK Inhibition Therapy in Neuroblastoma. Cancer Cell. 2014;26(5):682-94.

101. De Brouwer S, De Preter K, Kumps C, Zabrocki P, Porcu M, Westerhout EM, et al. Meta-analysis of neuroblastomas reveals a skewed ALK mutation spectrum in tumors with MYCN amplification. Clinical Cancer Research. 2010;16(17):4353.

102. Chen Y, Takita J, Choi YL, Kato M, Ohira M, Sanada M, et al. Oncogenic mutations of ALK kinase in neuroblastoma. Nature. 2008;455(7215):971-4.

103. George RE, Sanda T, Hanna M, Fröhling S, Ii WL, Zhang J, et al. Activating mutations in ALK provide a therapeutic target in neuroblastoma. Nature. 2008;455(7215):975-8.

104. Janoueix-Lerosey I, Lequin D, Brugières L, Ribeiro A, de Pontual L, Combaret V, et al. Somatic and germline activating mutations of the ALK kinase receptor in neuroblastoma. Nature. 2008;455(7215):967-70.

105. Mossé YP, Laudenslager M, Longo L, Cole KA, Wood A, Attiyeh EF, et al. Identification of ALK as a major familial neuroblastoma predisposition gene. Nature. 2008;455(7215):930-5.

106. Bresler SC, Wood AC, Haglund EA, Courtright J, Belcastro LT, Plegaria JS, et al. Differential Inhibitor Sensitivity of Anaplastic Lymphoma Kinase Variants Found in Neuroblastoma. Science Translational Medicine. 2011;3(108):108ra14.

107. Mossé YP, Lim MS, Voss SD, Wilner K, Ruffner K, Laliberte J, et al. Safety and activity of crizotinib for paediatric patients with refractory solid tumours or anaplastic large-cell lymphoma: a Children's Oncology Group phase 1 consortium study. The Lancet Oncology. 2013;14(6):472-80.

108. Sasaki T, Okuda K, Zheng W, Butrynski J, Capelletti M, Wang L, et al. The Neuroblastoma-Associated F1174L ALK Mutation Causes Resistance to an ALK Kinase Inhibitor in ALK-Translocated Cancers. Cancer Research. 2010;70(24):10038.

109. Wang HQ, Halilovic E, Li X, Liang J, Cao Y, Rakiec DP, et al. Combined ALK and MDM2 inhibition increases antitumor activity and overcomes resistance in human ALK mutant neuroblastoma cell lines and xenograft models. eLife. 2017;6:e17137.

110. Debruyne DN, Bhatnagar N, Sharma B, Luther W, Moore NF, Cheung NK, et al. ALK inhibitor resistance in ALKF1174L-driven neuroblastoma is associated with AXL activation and induction of EMT. Oncogene. 2016;35(28):3681-91.

111. Vaughan L, Clarke PA, Barker K, Chanthery Y, Gustafson CW, Tucker E, et al. Inhibition of mTOR-kinase destabilizes MYCN and is a potential therapy for MYCN-dependent tumors. Oncotarget. 2016;7(36):57525-44.

112. Chesler L, Schlieve C, Goldenberg DD, Kenney A, Kim G, McMillan A, et al. Inhibition of Phosphatidylinositol 3-Kinase Destabilizes Mycn Protein and Blocks Malignant Progression in Neuroblastoma. Cancer Research. 2006;66(16):8139.

113. Berry T, Luther W, Bhatnagar N, Jamin Y, Poon E, Sanda T, et al. The ALKF1174L Mutation Potentiates the Oncogenic Activity of MYCN in Neuroblastoma. Cancer Cell. 2012;22(1):117-30.

114. Johnsen JI, Dyberg C, Fransson S, Wickström M. Molecular mechanisms and therapeutic targets in neuroblastoma. Pharmacological Research. 2018;131:164-76.

115. Tucker ER, Poon E, Chesler L. Targeting MYCN and ALK in resistant and relapsing neuroblastoma. Cancer Drug Resistance. 2019;2:803-12.

116. Brockmann M, Poon E, Berry T, Carstensen A, Deubzer HE, Rycak L, et al. Small molecule inhibitors of aurora-a induce proteasomal degradation of N-myc in childhood neuroblastoma. Cancer cell. 2013;24(1):75-89.

117. Xiao D, Yue M, Su H, Ren P, Jiang J, Li F, et al. Polo-like Kinase-1 Regulates Myc Stabilization and Activates a Feedforward Circuit Promoting Tumor Cell Survival. Molecular Cell. 2016;64(3):493-506.

118. Barone G, Anderson J, Pearson ADJ, Petrie K, Chesler L. New Strategies in Neuroblastoma: Therapeutic Targeting of MYCN and ALK. Clinical Cancer Research. 2013;19(21):5814.

119. Tweddle DA, Pearson ADJ, Haber M, Norris MD, Xue C, Flemming C, et al. The p53 pathway and its inactivation in neuroblastoma. Cancer Letters. 2003;197(1):93-8.

120. Harris CC, Hollstein M. Clinical Implications of the p53 Tumor-Suppressor Gene. New England Journal of Medicine. 1993;329(18):1318-27.

121. Carr-Wilkinson J, Toole K, Wood KM, Challen CC, Baker AG, Board JR, et al. High Frequency of p53/MDM2/p14ARF Pathway Abnormalities in Relapsed Neuroblastoma. Clinical Cancer Research. 2010;16(4):1108.

122. Tweddle DA, Malcolm AJ, Bown N, Pearson ADJ, Lunec J. Evidence for the development of p53 mutations after cytotoxic therapy in a neuroblastoma cell line. Cancer Research. 2001;61(1):8.

123. Hientz K, Mohr A, Bhakta-Guha D, Efferth T. The role of p53 in cancer drug resistance and targeted chemotherapy. Oncotarget. 2017;8(5):8921-46.

124. Goldsmith KC, Gross M, Peirce S, Luyindula D, Liu X, Vu A, et al. Mitochondrial Bcl-2 family dynamics define therapy response and resistance in neuroblastoma. Cancer Research. 2012;72(10):2565-77.

125. Montero J, Letai A. Why do BCL-2 inhibitors work and where should we use them in the clinic? Cell Death And Differentiation. 2017;25:56.

126. Maacha S, Bhat AA, Jimenez L, Raza A, Haris M, Uddin S, et al. Extracellular vesicles-mediated intercellular communication: roles in the tumor microenvironment and anti-cancer drug resistance. Molecular Cancer. 2019;18(1):55.

127. Challagundla KB, Wise PM, Neviani P, Chava H, Murtadha M, Xu T, et al. Exosome-Mediated Transfer of microRNAs Within the Tumor Microenvironment and Neuroblastoma Resistance to Chemotherapy. JNCI: Journal of the National Cancer Institute. 2015;107(7).

128. Ara T, Nakata R, Sheard MA, Shimada H, Buettner R, Groshen SG, et al. Critical Role of STAT3 in IL-6–Mediated Drug Resistance in Human Neuroblastoma. Cancer Research. 2013;73(13):3852.

129. Ara T, Song L, Shimada H, Keshelava N, Russell HV, Metelitsa LS, et al. Interleukin-6 in the Bone Marrow Microenvironment Promotes the Growth and Survival of Neuroblastoma Cells. Cancer Research. 2009;69(1):329.

130. Hadjidaniel MD, Muthugounder S, Hung LT, Sheard MA, Shirinbak S, Chan RY, et al. Tumor-associated macrophages promote neuroblastoma via STAT3 phosphorylation and up-regulation of c-MYC. Oncotarget. 2017;8(53):91516-29.

131. Jackson SP, Bartek J. The DNA-damage response in human biology and disease. Nature. 2009;461(7267):1071-8.

132. Maréchal A, Zou L. DNA Damage Sensing by the ATM and ATR Kinases. Cold Spring Harbor Perspectives in Biology. 2013;5(9):a012716.

133. Furuta T, Ueda T, Aune G, Sarasin A, Kraemer KH, Pommier Y. Transcription-coupled Nucleotide Excision Repair as a Determinant of Cisplatin Sensitivity of Human Cells. Cancer Research. 2002;62(17):4899.

134. Tassone P, Di Martino MT, Ventura M, Pietragalla A, Cucinotto I, Calimeri T, et al. Loss of BRCA1 function increases the antitumor activity of cisplatin against human breast cancer xenografts in vivo. Cancer Biology & Therapy. 2009;8(7):648-53.

135. Pusapati RV, Rounbehler RJ, Hong S, Powers JT, Yan M, Kiguchi K, et al. ATM promotes apoptosis and suppresses tumorigenesis in response to Myc. Proceedings of the National Academy of Sciences. 2006;103(5):1446.

136. Reimann M, Loddenkemper C, Rudolph C, Schildhauer I, Teichmann B, Stein H, et al. The Myc-evoked DNA damage response accounts for treatment resistance in primary lymphomas in vivo. Blood. 2007;110(8):2996-3004.

137. Maclean KH, Kastan MB, Cleveland JL. Atm Deficiency Affects Both Apoptosis and Proliferation to Augment Myc-Induced Lymphomagenesis. Molecular Cancer Research. 2007;5(7):705.

138. Sanmartín E, Muñoz L, Piqueras M, Sirerol JA, Berlanga P, Cañete A, et al. Deletion of 11q in Neuroblastomas Drives Sensitivity to PARP Inhibition. Clinical Cancer Research. 2017;23(22):6875.

139. Takagi M, Yoshida M, Nemoto Y, Tamaichi H, Tsuchida R, Seki M, et al. Loss of DNA Damage Response in Neuroblastoma and Utility of a PARP Inhibitor. JNCI: Journal of the National Cancer Institute. 2017;109(11).

140. Hu H, Du L, Nagabayashi G, Seeger RC, Gatti RA. ATM is down-regulated by N-Myc–regulated microRNA-421. Proceedings of the National Academy of Sciences. 2010;107(4):1506.

141. Ognibene M, Podestà M, Garaventa A, Pezzolo A. Role of GOLPH3 and TPX2 in Neuroblastoma DNA Damage Response and Cell Resistance to Chemotherapy. International journal of molecular sciences. 2019;20(19):4764.

142. Shah N. Dodging the bullet: therapeutic resistance mechanisms in pediatric cancers. Cancer Drug Resistance. 2019;2:428-46.

143. Sakai W, Swisher EM, Karlan BY, Agarwal MK, Higgins J, Friedman C, et al. Secondary mutations as a mechanism of cisplatin resistance in BRCA2-mutated cancers. Nature. 2008;451(7182):1116-20.

144. Swisher EM, Sakai W, Karlan BY, Wurz K, Urban N, Taniguchi T. Secondary BRCA1 mutations in BRCA1-mutated ovarian carcinomas with platinum resistance. Cancer Research. 2008;68(8):2581.

145. Salzberg SL. Open questions: How many genes do we have? BMC Biology. 2018;16(1):94.

146. International Human Genome Sequencing C. Finishing the euchromatic sequence of the human genome. Nature. 2004;431(7011):931-45.

147. Kapusta A, Feschotte C. Volatile evolution of long noncoding RNA repertoires: mechanisms and biological implications. Trends in Genetics. 2014;30(10):439-52.

148. Moran Y, Agron M, Praher D, Technau U. The evolutionary origin of plant and animal microRNAs. Nature Ecology & Evolution. 2017;1(3):0027.

149. Fernandes JCR, Acuña SM, Aoki JI, Floeter-Winter LM, Muxel SM. Long Non-Coding RNAs in the Regulation of Gene Expression: Physiology and Disease. Non-Coding RNA. 2019;5(1):17.

150. Bhaskaran M, Mohan M. MicroRNAs:History, Biogenesis, and Their Evolving Role in Animal Development and Disease. 2014;51(4):759-74.

151. Lee RC, Feinbaum RL, Ambros V. The C. elegans heterochronic gene lin-4 encodes small RNAs with antisense complementarity to lin-14. Cell. 1993;75(5):843-54.

152. Fire A, Xu S, Montgomery MK, Kostas SA, Driver SE, Mello CC. Potent and specific genetic interference by double-stranded RNA in Caenorhabditis elegans. Nature. 1998;391:806.

153. Wilson RC, Doudna JA. Molecular Mechanisms of RNA Interference. Annual Review of Biophysics. 2013;42(1):217-39.

154. Weick E-M, Miska EA. piRNAs: from biogenesis to function. Development. 2014;141(18):3458.

155. Berezikov E, Guryev V, van de Belt J, Wienholds E, Plasterk RHA, Cuppen E. Phylogenetic Shadowing and Computational Identification of Human microRNA Genes. Cell. 2005;120(1):21-4.

156. Lewis BP, Burge CB, Bartel DP. Conserved Seed Pairing, Often Flanked by Adenosines, Indicates that Thousands of Human Genes are MicroRNA Targets. Cell. 2005;120(1):15-20.

157. Rajewsky N. microRNA target predictions in animals. Nature Genetics. 2006;38(6):S8-S13.

158. Miranda KC, Huynh T, Tay Y, Ang Y-S, Tam W-L, Thomson AM, et al. A Pattern-Based Method for the Identification of MicroRNA Binding Sites and Their Corresponding Heteroduplexes. Cell. 2006;126(6):1203-17.

159. Bartel DP. MicroRNAs: Target Recognition and Regulatory Functions. Cell. 2009;136(2):215-33.

160. O'Brien J, Hayder H, Zayed Y, Peng C. Overview of MicroRNA Biogenesis, Mechanisms of Actions, and Circulation. Frontiers in Endocrinology. 2018;9(402).

161. Liu B, Shyr Y, Cai J, Liu Q. Interplay between miRNAs and host genes and their role in cancer. Briefings in Functional Genomics. 2019;18(4):255-66.

162. Choudhuri S. Small noncoding RNAs: Biogenesis, function, and emerging significance in toxicology. Journal of Biochemical and Molecular Toxicology. 2010;24(3):195-216.

163. Winter J, Jung S, Keller S, Gregory RI, Diederichs S. Many roads to maturity: microRNA biogenesis pathways and their regulation. Nat Cell Biol. 2009;11(3):228-34.

164. Khvorova A, Reynolds A, Jayasena SD. Functional siRNAs and miRNAs Exhibit Strand Bias. Cell. 2003;115(2):209-16.

165. Pillai RS, Artus CG, Filipowicz W. Tethering of human Ago proteins to mRNA mimics the miRNA-mediated repression of protein synthesis. 2004;10(10):1518-25.

166. Fabian MR, Sonenberg N, Filipowicz W. Regulation of mRNA Translation and Stability by microRNAs. Annual Review of Biochemistry. 2010;79(1):351-79.

167. Kulkarni M, Ozgur S, Stoecklin G. On track with P-bodies. Biochemical Society Transactions. 2010;38(1):242.

168. Lin S, Gregory RI. MicroRNA biogenesis pathways in cancer. Nature Reviews Cancer. 2015;15:321.

169. Kloosterman WP, Wienholds E, Ketting RF, Plasterk RHA. Substrate requirements for let-7 function in the developing zebrafish embryo. Nucleic Acids Research. 2004;32(21):6284-91.

170. Forman JJ, Legesse-Miller A, Coller HA. A search for conserved sequences in coding regions reveals that the let-7 microRNA targets Dicer within its coding sequence. 2008;105(39):14879-84.

171. Cheetham SW, Gruhl F, Mattick JS, Dinger ME. Long noncoding RNAs and the genetics of cancer. British Journal of Cancer. 2013;108(12):2419-25.

172. Calin GA, Dumitru CD, Shimizu M, Bichi R, Zupo S, Noch E, et al. Frequent deletions and down-regulation of micro- RNA genes miR15 and miR16 at 13q14 in chronic lymphocytic leukemia. Proceedings of the National Academy of Sciences. 2002;99(24):15524.

173. Buechner J, Einvik C. N-myc and Noncoding RNAs in Neuroblastoma. Molecular Cancer Research. 2012;10(10):1243.

174. Beckers A, Van Peer G, Carter DR, Mets E, Althoff K, Cheung BB, et al. MYCN-targeting miRNAs are predominantly downregulated during MYCN-driven neuroblastoma tumor formation. Oncotarget. 2014;6(7):5204-16.

175. Chen Y, Stallings RL. Differential Patterns of MicroRNA Expression in Neuroblastoma Are Correlated with Prognosis, Differentiation, and Apoptosis. Cancer Research. 2007;67(3):976.

176. Chen Y, Tsai Y-H, Fang Y, Tseng S-H. Micro-RNA-21 regulates the sensitivity to cisplatin in human neuroblastoma cells. Journal of Pediatric Surgery. 2012;47(10):1797-805.

177. Ryan J, Tivnan A, Fay J, Bryan K, Meehan M, Creevey L, et al. MicroRNA-204 increases sensitivity of neuroblastoma cells to cisplatin and is associated with a favourable clinical outcome. British Journal of Cancer. 2012;107(7):1203-.

178. Fontana L, Fiori ME, Albini S, Cifaldi L, Giovinazzi S, Forloni M, et al. Antagomir-17-5p Abolishes the Growth of Therapy-Resistant Neuroblastoma through p21 and BIM. PLOS ONE. 2008;3(5):e2236.

179. Li H, Yang BB. Friend or foe: the role of microRNA in chemotherapy resistance. Acta Pharmacologica Sinica. 2013;34(7):870-9.

180. Gu S, Chan W-Y. Flexible and versatile as a chameleon-sophisticated functions of microRNA-199a. International journal of molecular sciences. 2012;13(7):8449-66.

181. Han H, Sun D, Li W, Shen H, Zhu Y, Li C, et al. A c-Myc-MicroRNA functional feedback loop affects hepatocarcinogenesis. Hepatology. 2013;57(6):2378-89.

182. Qiao J, Lee S, Paul P, Theiss L, Tiao J, Qiao L, et al. miR-335 and miR-363 regulation of neuroblastoma tumorigenesis and metastasis. Surgery. 2013;154(2):226-33.

183. Hsu K-W, Wang A-M, Ping Y-H, Huang K-H, Huang T-T, Lee H-C, et al. Downregulation of tumor suppressor MBP-1 by microRNA-363 in gastric carcinogenesis. Carcinogenesis. 2013;35(1):208-17.

184. Hanna J, Hossain GS, Kocerha J. The Potential for microRNA Therapeutics and Clinical Research. Frontiers in Genetics. 2019;10(478).

185. Lu J, Getz G, Miska EA, Alvarez-Saavedra E, Lamb J, Peck D, et al. MicroRNA expression profiles classify human cancers. Nature. 2005;435(7043):834-8.

186. Roth SA, Knutsen E, Fiskaa T, Utnes P, Bhavsar S, Hald ØH, et al. Next generation sequencing of microRNAs from isogenic neuroblastoma cell lines isolated before and after treatment. Cancer Letters. 2016;372(1):128-36.

187. González-Vallinas M, Rodríguez-Paredes M, Albrecht M, Sticht C, Stichel D, Gutekunst J, et al. Epigenetically Regulated Chromosome 14q32 miRNA Cluster Induces Metastasis and Predicts Poor Prognosis in Lung Adenocarcinoma Patients. Molecular Cancer Research. 2018;16(3):390.

188. Nadal E, Zhong J, Lin J, Reddy RM, Ramnath N, Orringer MB, et al. A MicroRNA Cluster at 14q32 Drives Aggressive Lung Adenocarcinoma. Clinical Cancer Research. 2014;20(12):3107.

189. Zehavi L, Avraham R, Barzilai A, Bar-Ilan D, Navon R, Sidi Y, et al. Silencing of a large microRNA cluster on human chromosome 14q32 in melanoma: biological effects of mir-376a and mir-376c on insulin growth factor 1 receptor. Molecular Cancer. 2012;11(1):44.

190. Zhang L, Huang J, Yang N, Greshock J, Megraw MS, Giannakakis A, et al. microRNAs exhibit high frequency genomic alterations in human cancer. Proceedings of the National Academy of Sciences. 2006;103(24):9136.

191. Hoshi M, Otagiri N, Shiwaku HO, Asakawa S, Shimizu N, Kaneko Y, et al. Detailed deletion mapping of chromosome band 14q32 in human neuroblastoma defines a 1.1-Mb region of common allelic loss. British Journal of Cancer. 2000;82(11):1801-7.

192. Nayak S, Aich M, Kumar A, Sengupta S, Bajad P, Dhapola P, et al. Novel internal regulators and candidate miRNAs within miR-379/miR-656 miRNA cluster can alter cellular phenotype of human glioblastoma. Scientific Reports. 2018;8(1):7673.

193. Chen H, Gao S, Cheng C. MiR-323a-3p suppressed the glycolysis of osteosarcoma via targeting LDHA. Human Cell. 2018;31(4):300-9.

194. Li J, Xu X, Meng S, Liang Z, Wang X, Xu M, et al. MET/SMAD3/SNAIL circuit mediated by miR-323a-3p is involved in regulating epithelial-mesenchymal transition progression in bladder cancer. Cell death & disease. 2017;8(8):e3010-e.

195. Shahar T, Granit A, Zrihan D, Canello T, Charbit H, Einstein O, et al. Expression level of miRNAs on chromosome 14q32.31 region correlates with tumor aggressiveness and survival of glioblastoma patients. Journal of Neuro-Oncology. 2016;130(3):413-22.

196. Wang C, Liu P, Wu H, Cui P, Li Y, Liu Y, et al. MicroRNA-323-3p inhibits cell invasion and metastasis in pancreatic ductal adenocarcinoma via direct suppression of SMAD2 and SMAD3. Oncotarget. 2016;7(12):14912-24.

197. Gao Q, Yao X, Zheng J. MiR-323 Inhibits Prostate Cancer Vascularization Through Adiponectin Receptor. Cellular Physiology and Biochemistry. 2015;36(4):1491-8.

198. Gao Q, Zheng J. microRNA-323 upregulation promotes prostate cancer growth and docetaxel resistance by repressing p73. Biomedicine & Pharmacotherapy. 2018;97:528-34.

199. Li J, Kong F, Wu K, Song K, He J, Sun W. miR-193b directly targets STMN1 and uPA genes and suppresses tumor growth and metastasis in pancreatic cancer. Molecular Medicine Reports. 2014;10:2613-20.

200. Mu Y-P, Tang S, Sun W-J, Gao W-M, Wang M, Su X-L. Association of miR-193b Down-regulation and miR-196a up-Regulation with Clinicopathological Features and Prognosis in Gastric Cancer. Asian Pacific Journal of Cancer Prevention. 2014;15(20):8893-900.

201. Xu C, Liu S, Fu H, Li S, Tie Y, Zhu J, et al. MicroRNA-193b regulates proliferation, migration and invasion in human hepatocellular carcinoma cells. European Journal of Cancer. 2010;46(15):2828-36.

202. Nyhan MJ, O'Donovan TR, Boersma AWM, Wiemer EAC, McKenna SLJBC. MiR-193b promotes autophagy and non-apoptotic cell death in oesophageal cancer cells. 2016;16(1):101.

203. Mao K, Zhang J, He C, Xu K, Liu J, Sun J, et al. Restoration of miR-193b sensitizes Hepatitis B virus-associated hepatocellular carcinoma to sorafenib. Cancer Letters. 2014;352(2):245-52.

204. Chen J, Zhang X, Lentz C, Abi-Daoud M, Paré GC, Yang X, et al. miR-193b Regulates Mcl-1 in Melanoma. The American Journal of Pathology. 2011;179(5):2162-8.

205. Quinn BA, Dash R, Azab B, Sarkar S, Das SK, Kumar S, et al. Targeting Mcl-1 for the therapy of cancer. Expert opinion on investigational drugs. 2011;20(10):1397-411.

206. Elmore S. Apoptosis: A Review of Programmed Cell Death. Toxicologic Pathology. 2007;35(4):495-516.

207. Suvarna V, Singh V, Murahari M. Current overview on the clinical update of Bcl-2 anti-apoptotic inhibitors for cancer therapy. European Journal of Pharmacology. 2019;862:172655.

208. Delbridge ARD, Strasser A. The BCL-2 protein family, BH3-mimetics and cancer therapy. Cell death and differentiation. 2015;22(7):1071-80.

209. Warren CFA, Wong-Brown MW, Bowden NA. BCL-2 family isoforms in apoptosis and cancer. Cell Death & Disease. 2019;10(3):177.

210. Pistritto G, Trisciuoglio D, Ceci C, Garufi A, D'Orazi G. Apoptosis as anticancer mechanism: function and dysfunction of its modulators and targeted therapeutic strategies. Aging. 2016;8(4):603-19.

211. Letai A, Bassik MC, Walensky LD, Sorcinelli MD, Weiler S, Korsmeyer SJ. Distinct BH3 domains either sensitize or activate mitochondrial apoptosis, serving as prototype cancer therapeutics. Cancer Cell. 2002;2(3):183-92.

212. Ren D, Tu H-C, Kim H, Wang GX, Bean GR, Takeuchi O, et al. BID, BIM, and PUMA Are Essential for Activation of the BAX- and BAK-Dependent Cell Death Program. Science. 2010;330(6009):1390.

213. Green Douglas R, Fitzgerald P. Just So Stories about the Evolution of Apoptosis. Current Biology. 2016;26(13):R620-R7.

214. Certo M, Moore VDG, Nishino M, Wei G, Korsmeyer S, Armstrong SA, et al. Mitochondria primed by death signals determine cellular addiction to antiapoptotic BCL-2 family members. Cancer Cell. 2006;9(5):351-65.

215. Cai J, Yang J, Jones D. Mitochondrial control of apoptosis: the role of cytochrome c. Biochimica et Biophysica Acta (BBA) - Bioenergetics. 1998;1366(1):139-49.

216. Chen L, Willis SN, Wei A, Smith BJ, Fletcher JI, Hinds MG, et al. Differential Targeting of Prosurvival Bcl-2 Proteins by Their BH3-Only Ligands Allows Complementary Apoptotic Function. Molecular Cell. 2005;17(3):393-403.

217. Hanahan D, Weinberg Robert A. Hallmarks of Cancer: The Next Generation. Cell. 2011;144(5):646-74.

218. Goldsmith KC, Lestini BJ, Gross M, Ip L, Bhumbla A, Zhang X, et al. BH3 Response Profiles From Neuroblastoma Mitochondria Predict Activity of Small Molecule Bcl-2 Family Antagonists. Cell death and differentiation. 2010;17(5):872-82.

219. Chonghaile TN, Sarosiek KA, Vo T-T, Ryan JA, Tammareddi A, Moore VDG, et al. Pretreatment Mitochondrial Priming Correlates with Clinical Response to Cytotoxic Chemotherapy. Science. 2011;334(6059):1129.

220. Sarosiek KA, Fraser C, Muthalagu N, Bhola PD, Chang W, McBrayer SK, et al. Developmental Regulation of Mitochondrial Apoptosis by c-Myc Governs Age- and Tissue-Specific Sensitivity to Cancer Therapeutics. Cancer Cell. 2017;31(1):142-56.

221. Lestini BJ, Goldsmith KC, Fluchel MN, Liu X, Chen NL, Goyal B, et al. Mcl1 downregulation sensitizes neuroblastoma to cytotoxic chemotherapy and small molecule Bcl2-family antagonists. Cancer biology & therapy. 2009;8(16):1587-95.

222. Tanos R, Karmali D, Nalluri S, Goldsmith KC. Select Bcl-2 antagonism restores chemotherapy sensitivity in high-risk neuroblastoma. BMC Cancer. 2016;16:97.

223. van Delft MF, Wei AH, Mason KD, Vandenberg CJ, Chen L, Czabotar PE, et al. The BH3 mimetic ABT-737 targets selective Bcl-2 proteins and efficiently induces apoptosis via Bak/Bax if Mcl-1 is neutralized. Cancer Cell. 2006;10(5):389-99.

224. Oltersdorf T, Elmore SW, Shoemaker AR, Armstrong RC, Augeri DJ, Belli BA, et al. An inhibitor of Bcl-2 family proteins induces regression of solid tumours. Nature. 2005;435(7042):677-81.

225. Keuling AM, Felton KEA, Parker AAM, Akbari M, Andrew SE, Tron VA. RNA Silencing of Mcl-1 Enhances ABT-737-Mediated Apoptosis in Melanoma: Role for a Caspase-8-Dependent Pathway. PLoS ONE. 2009;4(8):e6651.

226. Boiani M, Daniel C, Liu X, Hogarty MD, Marnett LJ. The Stress Protein BAG3 Stabilizes Mcl-1 Protein and Promotes Survival of Cancer Cells and Resistance to Antagonist ABT-737. Journal of Biological Chemistry. 2013;288(10):6980-90.

227. Klymenko T, Brandenburg M, Morrow C, Dive C, Makin G. The Novel Bcl-2 Inhibitor ABT-737 Is More Effective in Hypoxia and Is Able to Reverse Hypoxia-Induced Drug Resistance in Neuroblastoma Cells. Molecular Cancer Therapeutics. 2011;10(12):2373.

228. Crossland H, Timmons JA, Atherton PJ. A dynamic ribosomal biogenesis response is not required for IGF-1–mediated hypertrophy of human primary myotubes. The FASEB Journal. 2017;31(12):5196-207.

229. Figueiredo VC, Caldow MK, Massie V, Markworth JF, Cameron-Smith D, Blazevich AJ. Ribosome biogenesis adaptation in resistance training-induced human skeletal muscle hypertrophy. American Journal of Physiology-Endocrinology and Metabolism. 2015;309(1):E72-E83.

230. Drygin D, Siddiqui-Jain A, Brien S, Schwaebe M, Lin A, Bliesath J, et al. Anticancer Activity of CX-3543: A Direct Inhibitor of rRNA Biogenesis. Cancer Research. 2009;69(19):7653.

231. Bursac S, Brdovcak MC, Donati G, Volarevic S. Activation of the tumor suppressor p53 upon impairment of ribosome biogenesis. Biochimica et Biophysica Acta (BBA) - Molecular Basis of Disease. 2014;1842(6):817-30.

232. Kopp K, Gasiorowski JZ, Chen D, Gilmore R, Norton JT, Wang C, et al. Pol I Transcription and Pre-rRNA Processing Are Coordinated in a Transcription-dependent Manner in Mammalian Cells. Molecular Biology of the Cell. 2007;18(2):394-403.

233. Drygin D, Rice WG, Grummt I. The RNA Polymerase I Transcription Machinery: An Emerging Target for the Treatment of Cancer. Annual Review of Pharmacology and Toxicology. 2010;50(1):131-56.

234. Bywater MJ, Pearson RB, McArthur GA, Hannan RD. Dysregulation of the basal RNA polymerase transcription apparatus in cancer. Nature Reviews Cancer. 2013;13(5):299-314.

235. Khot A, Brajanovski N, Cameron DP, Hein N, Maclachlan KH, Sanij E, et al. First-in-Human RNA Polymerase I Transcription Inhibitor CX-5461 in Patients with Advanced Hematological Cancers: Results of a Phase I Dose Escalation Study. Cancer Discovery. 2019:CD-18-1455.

236. Cornelison R, Dobbin ZC, Katre AA, Jeong DH, Zhang Y, Chen D, et al. Targeting RNA-Polymerase I in Both Chemosensitive and Chemoresistant Populations in Epithelial Ovarian Cancer. Clinical Cancer Research. 2017;23(21):6529.

237. Stacher A, Lutz D, Varbiro M, Aichinger A, Nowotny H. Morphology and index of nucleoli in malignant lymphomas. Folia Haematol Int Mag Klin Morphol Blutforsch. 1980;107(4):548-58.

238. Niemas-Teshiba R, Matsuno R, Wang LL, Tang XX, Chiu B, Zeki J, et al. MYC-family protein overexpression and prominent nucleolar formation represent prognostic indicators and potential therapeutic targets for aggressive high-MKI neuroblastomas: a report from the children's oncology group. Oncotarget. 2017;9(5).

239. Boon K, Caron HN, van Asperen R, Valentijn L, Hermus M-C, van Sluis P, et al. N-myc enhances the expression of a large set of genes functioning in ribosome biogenesis and protein synthesis. The EMBO Journal. 2001;20(6):1383-93.

240. Lafontaine DLJ. Noncoding RNAs in eukaryotic ribosome biogenesis and function. Nature Structural &Amp; Molecular Biology. 2015;22:11.

241. Spiegel J, Adhikari S, Balasubramanian S. The Structure and Function of DNA G-Quadruplexes. Trends in Chemistry. 2019.

242. Benabou S, Ferreira R, Aviñó A, González C, Lyonnais S, Solà M, et al. Solution equilibria of cytosine- and guanine-rich sequences near the promoter region of the n-myc gene that contain stable hairpins within lateral loops. Biochimica et Biophysica Acta (BBA) - General Subjects. 2014;1840(1):41-52.

243. Chang C-C, Kuo IC, Ling IF, Chen C-T, Chen H-C, Lou P-J, et al. Detection of Quadruplex DNA Structures in Human Telomeres by a Fluorescent Carbazole Derivative. Analytical Chemistry. 2004;76(15):4490-4.

244. Duquette ML, Handa P, Vincent JA, Taylor AF, Maizels N. Intracellular transcription of G-rich DNAs induces formation of G-loops, novel structures containing G4 DNA. Genes & Development. 2004;18(13):1618-29.

245. Sun D, Thompson B, Cathers BE, Salazar M, Kerwin SM, Trent JO, et al. Inhibition of Human Telomerase by a G-Quadruplex-Interactive Compound. Journal of Medicinal Chemistry. 1997;40(14):2113-6.

246. De Cian A, Lacroix L, Douarre C, Temime-Smaali N, Trentesaux C, Riou J-F, et al. Targeting telomeres and telomerase. Biochimie. 2008;90(1):131-55.

247. Drygin D, Lin A, Bliesath J, Ho CB, Brien SE, Proffitt C, et al. Targeting RNA Polymerase I with an Oral Small Molecule CX-5461 Inhibits Ribosomal RNA Synthesis and Solid Tumor Growth. Cancer Research. 2011;71(4):1418.

248. Negi SS, Brown P. rRNA synthesis inhibitor, CX-5461, activates ATM/ATR pathway in acute lymphoblastic leukemia, arrests cells in G2 phase and induces apoptosis. Oncotarget. 2015;6(20):18094-104.

249. Bywater Megan J, Poortinga G, Sanij E, Hein N, Peck A, Cullinane C, et al. Inhibition of RNA Polymerase I as a Therapeutic Strategy to Promote Cancer-Specific Activation of p53. Cancer Cell. 2012;22(1):51-65.

250. van Riggelen J, Yetil A, Felsher DW. MYC as a regulator of ribosome biogenesis and protein synthesis. Nat Rev Cancer. 2010;10(4):301-9.

251. Xu H, Di Antonio M, McKinney S, Mathew V, Ho B, O'Neil NJ, et al. CX-5461 is a DNA G-quadruplex stabilizer with selective lethality in BRCA1/2 deficient tumours. Nature Communications. 2017;8:14432.

252. Kim NW, Piatyszek MA, Prowse KR, Harley CB, West MD, Ho PL, et al. Specific association of human telomerase activity with immortal cells and cancer. Science. 1994;266(5193):2011.

253. Shay JW, Bacchetti S. A survey of telomerase activity in human cancer. European Journal of Cancer. 1997;33(5):787-91.

254. Andersen JS, Lam YW, Leung AKL, Ong S-E, Lyon CE, Lamond AI, et al. Nucleolar proteome dynamics. Nature. 2005;433(7021):77-83.

255. Andersen JS, Lyon CE, Fox AH, Leung AKL, Lam YW, Steen H, et al. Directed Proteomic Analysis of the Human Nucleolus. Current Biology. 2002;12(1):1-11.

256. Carter M, Shieh J. Chapter 14 - Cell Culture Techniques. In: Carter M, Shieh J, editors. Guide to Research Techniques in Neuroscience (Second Edition). San Diego: Academic Press; 2015. p. 295-310.

257. Ryu AH, Eckalbar WL, Kreimer A, Yosef N, Ahituv N. Use antibiotics in cell culture with caution: genome-wide identification of antibiotic-induced changes in gene expression and regulation. Scientific Reports. 2017;7(1):7533.

258. Kuhlmann I. The prophylactic use of antibiotics in cell culture. Cytotechnology. 1995;19(2):95-105.

259. Nehls M, Pfeifer D, Schorpp M, Hedrich H, Boehm T. New member of the winged-helix protein family disrupted in mouse and rat nude mutations. Nature. 1994;372(6501):103-7.

260. Pantelouris EM. Absence of Thymus in a Mouse Mutant. Nature. 1968;217(5126):370-1.

261. Pantelouris EM, Hair J. Thymus dysgenesis in nude (nu nu) mice. Journal of Embryology and Experimental Morphology. 1970;24(3):615.

262. Frank J, Pignata C, Panteleyev AA, Prowse DM, Baden H, Weiner L, et al. Exposing the human nude phenotype. Nature. 1999;398(6727):473-4.

263. Mullen P. The Use of Matrigel to Facilitate the Establishment of Human Cancer Cell Lines as Xenografts. In: Langdon SP, editor. Cancer Cell Culture: Methods and Protocols. Totowa, NJ: Humana Press; 2004. p. 287-92.

264. Vukicevic S, Kleinman HK, Luyten FP, Roberts AB, Roche NS, Reddi AH. Identification of multiple active growth factors in basement membrane matrigel suggests caution in interpretation of cellular activity related to extracellular matrix components. Experimental Cell Research. 1992;202(1):1-8.

265. Stevenson CS, Marshall LA, Morgan DW. In Vivo Models of Inflammation. 2 ed: Birkhäuser Basel; 2006.

266. Haddach M, Schwaebe MK, Michaux J, Nagasawa J, O'Brien SE, Whitten JP, et al. Discovery of CX-5461, the First Direct and Selective Inhibitor of RNA Polymerase I, for Cancer Therapeutics. ACS Med Chem Lett. 2012;3(7):602-6.

267. Hoggatt AF, Hoggatt J, Honerlaw M, Pelus LM. A spoonful of sugar helps the medicine go down: a novel technique to improve oral gavage in mice. J Am Assoc Lab Anim Sci. 2010;49(3):329-34.

268. Hackett CS, Hodgson JG, Law ME, Fridlyand J, Osoegawa K, de Jong PJ, et al. Genome-wide Array CGH Analysis of Murine Neuroblastoma Reveals Distinct Genomic Aberrations which Parallel those in Human Tumors. Cancer Research. 2003;63(17):5266.

269. Cheng AJ, Ching Cheng N, Ford J, Smith J, Murray JE, Flemming C, et al. Cell lines from MYCN transgenic murine tumours reflect the molecular and biological characteristics of human neuroblastoma. European Journal of Cancer. 2007;43(9):1467-75.

270. Teitz T, Stanke JJ, Federico S, Bradley CL, Brennan R, Zhang J, et al. Preclinical Models for Neuroblastoma: Establishing a Baseline for Treatment. PLOS ONE. 2011;6(4):e19133.

271. Chesler L, Goldenberg DD, Collins R, Grimmer M, Kim GE, Tihan T, et al. Chemotherapy-induced apoptosis in a transgenic model of neuroblastoma proceeds through p53 induction. Neoplasia. 2008;10(11):1268-74.

272. Mogilyansky E, Rigoutsos I. The miR-17/92 cluster: a comprehensive update on its genomics, genetics, functions and increasingly important and numerous roles in health and disease. Cell Death And Differentiation. 2013;20:1603.

273. Hausser J, Syed AP, Bilen B, Zavolan M. Analysis of CDS-located miRNA target sites suggests that they can effectively inhibit translation. Genome Research. 2013;23(4):604-15.

274. Thomson DW, Bracken CP, Goodall GJ. Experimental strategies for microRNA target identification. Nucleic Acids Research. 2011;39(16):6845-53.

275. Hausser J, Landthaler M, Jaskiewicz L, Gaidatzis D, Zavolan M. Relative contribution of sequence and structure features to the mRNA binding of Argonaute/EIF2C–miRNA complexes and the degradation of miRNA targets. Genome Research. 2009;19(11):2009-20.

276. Schnall-Levin M, Zhao Y, Perrimon N, Berger B. Conserved microRNA targeting in Drosophila is as widespread in coding regions as in 3'UTRs. 2010;107(36):15751-6.

277. Fang Z, Rajewsky N. The Impact of miRNA Target Sites in Coding Sequences and in 3′UTRs. PLOS ONE. 2011;6(3):e18067.

278. Louloupi A, Ørom UAV. Inhibiting Pri-miRNA Processing with Target Site Blockers. In: Ørom UAV, editor. miRNA Biogenesis: Methods and Protocols. New York, NY: Springer New York; 2018. p. 63-8.

279. Darnell RB. HITS-CLIP: panoramic views of protein-RNA regulation in living cells. Wiley interdisciplinary reviews RNA. 2010;1(2):266-86.

280. Morales J, Li L, Fattah FJ, Dong Y, Bey EA, Patel M, et al. Review of poly (ADP-ribose) polymerase (PARP) mechanisms of action and rationale for targeting in cancer and other diseases. Crit Rev Eukaryot Gene Expr. 2014;24(1):15-28.

281. Chaitanya GV, Steven AJ, Babu PP. PARP-1 cleavage fragments: signatures of cell-death proteases in neurodegeneration. Cell Commun Signal. 2010;8:31-.

282. Jin HY, Gonzalez-Martin A, Miletic AV, Lai M, Knight S, Sabouri-Ghomi M, et al. Transfection of microRNA Mimics Should Be Used with Caution. Frontiers in Genetics. 2015;6(340).

283. Lutz W, Stöhr M, Schürmann J, Wenzel A, Löhr A, Schwab M. Conditional expression of N-myc in human neuroblastoma cells increases expression of α-prothymosin and ornithine decarboxylase and accelerates progression into S-phase early after mitogenic stimulation of quiescent cells. Oncogene. 1996;13, No. 4(4):803-12.

284. Lam JKW, Chow MYT, Zhang Y, Leung SWS. siRNA Versus miRNA as Therapeutics for Gene Silencing. Molecular Therapy - Nucleic Acids. 2015;4:e252.

285. Taxman DJ, Moore CB, Guthrie EH, Huang MT-H. Short Hairpin RNA (shRNA): Design, Delivery, and Assessment of Gene Knockdown. In: Sioud M, editor. RNA Therapeutics: Function, Design, and Delivery. Totowa, NJ: Humana Press; 2010. p. 139-56.

286. Parsons BD, Schindler A, Evans DH, Foley E. A Direct Phenotypic Comparison of siRNA Pools and Multiple Individual Duplexes in a Functional Assay. PLOS ONE. 2010;4(12):e8471.

287. Wiedenheft B, Sternberg SH, Doudna JA. RNA-guided genetic silencing systems in bacteria and archaea. Nature. 2012;482(7385):331-8.

288. Hoy MA. Chapter 9 - CRISPR-Cas Genome Editing: Another Revolution in Molecular Biology. In: Hoy MA, editor. Insect Molecular Genetics (Fourth Edition): Academic Press; 2019. p. 345-61.

289. Jinek M, Chylinski K, Fonfara I, Hauer M, Doudna JA, Charpentier E. A Programmable Dual-RNA–Guided DNA Endonuclease in Adaptive Bacterial Immunity. Science. 2012;337(6096):816.

290. Applebaum MA, Vaksman Z, Lee SM, Hungate EA, Henderson TO, London WB, et al. Neuroblastoma survivors are at increased risk for second malignancies: A report from the International Neuroblastoma Risk Group Project. European Journal of Cancer. 2017;72:177-85.

291. Berthold F, Spix C, Kaatsch P, Lampert F. Incidence, Survival, and Treatment of Localized and Metastatic Neuroblastoma in Germany 1979-2015. Paediatr Drugs. 2017;19(6):577-93.

292. Kubota M, Okuyama N, Hirayama Y, Asami K, Ogawa A, Watanabe A. Mortality and morbidity of patients with neuroblastoma who survived for more than 10 years after treatment—Niigata Tumor Board Study. Journal of Pediatric Surgery. 2010;45(4):673-7.

293. Khuu C, Utheim TP, Sehic A. The Three Paralogous MicroRNA Clusters in Development and Disease, miR-17-92, miR-106a-363, and miR-106b-25. Scientifica. 2016;2016:10.

294. Bhavsar SP, Lokke C, Flaegstad T, Einvik C. Hsa-miR-376c-3p targets Cyclin D1 and induces G1-cell cycle arrest in neuroblastoma cells. Oncol Lett. 2018;16(5):6786-94.

295. Yang H, Li Q, Zhao W, Yuan D, Zhao H, Zhou Y. miR-329 suppresses the growth and motility of neuroblastoma by targeting KDM1A. FEBS Letters. 2014;588(1):192-7.

296. Xiang X, Mei H, Zhao X, Pu J, Li D, Qu H, et al. miRNA-337-3p suppresses neuroblastoma progression by repressing the transcription of matrix metalloproteinase 14. Oncotarget. 2015;6(26).

297. Gattolliat CH, Thomas L, Ciafrè SA, Meurice G, Le Teuff G, Job B, et al. Expression of miR-487b and miR-410 encoded by 14q32.31 locus is a prognostic marker in neuroblastoma. British Journal of Cancer. 2011;105(9):1352-61.

298. Aggarwal BB, Kunnumakkara AB, Harikumar KB, Gupta SR, Tharakan ST, Koca C, et al. Signal Transducer and Activator of Transcription-3, Inflammation, and Cancer. Annals of the New York Academy of Sciences. 2009;1171(1):59-76.

299. Frank DA. STAT3 as a central mediator of neoplastic cellular transformation. Cancer Letters. 2007;251(2):199-210.

300. Lee H-J, Zhuang G, Cao Y, Du P, Kim H-J, Settleman J. Drug Resistance via Feedback Activation of Stat3 in Oncogene-Addicted Cancer Cells. Cancer Cell. 2014;26(2):207-21.

301. Otero DC, Poli V, David M, Rickert RC. Cutting edge: inherent and acquired resistance to radiation-induced apoptosis in B cells: a pivotal role for STAT3. J Immunol. 2006;177(10):6593-7.

302. Real PJ, Sierra A, de Juan A, Segovia JC, Lopez-Vega JM, Fernandez-Luna JL. Resistance to chemotherapy via Stat3-dependent overexpression of Bcl-2 in metastatic breast cancer cells. Oncogene. 2002;21(50):7611-8.

303. Zhao C, Li H, Lin H-J, Yang S, Lin J, Liang G. Feedback Activation of STAT3 as a Cancer Drug-Resistance Mechanism. Trends in Pharmacological Sciences. 2016;37(1):47-61.

304. Yu H, Pardoll D, Jove R. STATs in cancer inflammation and immunity: a leading role for STAT3. Nature Reviews Cancer. 2009;9:798.

305. Carleton M, Cleary MA, Linsley PS. MicroRNAs and Cell Cycle Regulation. Cell Cycle. 2007;6(17):2127-32.

306. Lestini BJ, Goldsmith KC, Fluchel MN, Liu X, Chen NL, Goyal B, et al. Mcl1 downregulation sensitizes neuroblastoma to cytotoxic chemotherapy and small molecule Bcl2-family antagonists. Cancer Biol Ther. 2009;8(16):1587-95.

307. Boiani M, Daniel C, Liu X, Hogarty MD, Marnett LJ. The stress protein BAG3 stabilizes Mcl-1 protein and promotes survival of cancer cells and resistance to antagonist ABT-737. The Journal of biological chemistry. 2013;288(10):6980-90.

308. Goldsmith KC, Gross M, Peirce S, Luyindula D, Liu X, Vu A, et al. Mitochondrial Bcl-2 family dynamics define therapy response and resistance in neuroblastoma. Cancer research. 2012;72(10):2565-77.

309. Goldsmith KC, Lestini BJ, Gross M, Ip L, Bhumbla A, Zhang X, et al. BH3 response profiles from neuroblastoma mitochondria predict activity of small molecule Bcl-2 family antagonists. Cell death and differentiation. 2010;17(5):872-82.

310. Agarwal V, Bell GW, Nam J-W, Bartel DP. Predicting effective microRNA target sites in mammalian mRNAs. eLife. 2015;4:e05005.

311. Liu W, Wang X. Prediction of functional microRNA targets by integrative modeling of microRNA binding and target expression data. Genome Biology. 2019;20(1):18.

312. Wong N, Wang X. miRDB: an online resource for microRNA target prediction and functional annotations. Nucleic Acids Research. 2014;43(D1):D146-D52.

313. Long J, Ji Z, Jiang K, Wang Z, Meng G. miR-193b Modulates Resistance to Doxorubicin in Human Breast Cancer Cells by Downregulating MCL-1. Biomed Res Int. 2015;2015:373574-.

314. Roth SA, Hald ØH, Fuchs S, Løkke C, Mikkola I, Flægstad T, et al. MicroRNA-193b-3p represses neuroblastoma cell growth via downregulation of Cyclin D1, MCL-1 and MYCN. Oncotarget. 2018;9(26):18160-79.

315. Wang X, Bathina M, Lynch J, Koss B, Calabrese C, Frase S, et al. Deletion of MCL-1 causes lethal cardiac failure and mitochondrial dysfunction. Genes & development. 2013;27(12):1351-64.

316. Thomas RL, Roberts DJ, Kubli DA, Lee Y, Quinsay MN, Owens JB, et al. Loss of MCL-1 leads to impaired autophagy and rapid development of heart failure. Genes & Development. 2013;27(12):1365-77.

317. Mestdagh P, Lefever S, Pattyn F, Ridzon D, Fredlund E, Fieuw A, et al. The microRNA body map: dissecting microRNA function through integrative genomics. Nucleic Acids Research. 2011;39(20):e136-e.

318. Mah LJ, El-Osta A, Karagiannis TC. γH2AX: a sensitive molecular marker of DNA damage and repair. Leukemia. 2010;24(4):679-86.

319. Taylor JS, Zeki J, Ornell K, Coburn J, Shimada H, Ikegaki N, et al. Down-regulation of MYCN protein by CX-5461 leads to neuroblastoma tumor growth suppression. Journal of Pediatric Surgery. 2019.

320. Zhang Y, Lu H. Signaling to p53: ribosomal proteins find their way. Cancer cell. 2009;16(5):369-77.

321. Zheng J, Lang Y, Zhang Q, Cui D, Sun H, Jiang L, et al. Structure of human MDM2 complexed with RPL11 reveals the molecular basis of p53 activation. Genes & Development. 2015;29(14):1524-34.

322. Gamble LD, Kees UR, Tweddle DA, Lunec J. MYCN sensitizes neuroblastoma to the MDM2-p53 antagonists Nutlin-3 and MI-63. Oncogene. 2012;31(6):752-63.

323. Gu L, Zhang H, He J, Li J, Huang M, Zhou M. MDM2 regulates MYCN mRNA stabilization and translation in human neuroblastoma cells. Oncogene. 2012;31(11):1342-53.

324. Goldschneider D, Horvilleur E, Plassa L-F, Guillaud-Bataille M, Million K, Wittmer-Dupret E, et al. Expression of C-terminal deleted p53 isoforms in neuroblastoma. Nucleic acids research. 2006;34(19):5603-12.

325. Kim HJ, Kim A, Miyata K, Kataoka K. Recent progress in development of siRNA delivery vehicles for cancer therapy. Advanced Drug Delivery Reviews. 2016;104:61-77.

326. Gibori H, Eliyahu S, Krivitsky A, Ben-Shushan D, Epshtein Y, Tiram G, et al. Amphiphilic nanocarrier-induced modulation of PLK1 and miR-34a leads to improved therapeutic response in pancreatic cancer. Nature Communications. 2018;9(1):16.

327. van Zandwijk N, Pavlakis N, Kao SC, Linton A, Boyer MJ, Clarke S, et al. Safety and activity of microRNA-loaded minicells in patients with recurrent malignant pleural mesothelioma: a first-in-man, phase 1, open-label, dose-escalation study. The Lancet Oncology. 2017;18(10):1386-96.

328. Beg MS, Brenner AJ, Sachdev J, Borad M, Kang Y-K, Stoudemire J, et al. Phase I study of MRX34, a liposomal miR-34a mimic, administered twice weekly in patients with advanced solid tumors. 2017;35(2):180-8.

329. Farooqi AA, Tabassum S, Ahmad A. MicroRNA-34a: A Versatile Regulator of Myriads of Targets in Different Cancers. International journal of molecular sciences. 2017;18(10):2089.

330. Raghavendra NM, Pingili D, Kadasi S, Mettu A, Prasad SVUM. Dual or multi-targeting inhibitors: The next generation anticancer agents. European Journal of Medicinal Chemistry. 2018;143:1277-300.

331. Tse C, Shoemaker AR, Adickes J, Anderson MG, Chen J, Jin S, et al. ABT-263: A Potent and Orally Bioavailable Bcl-2 Family Inhibitor. Cancer Research. 2008;68(9):3421.

332. Gandhi L, Camidge DR, Oliveira MRd, Bonomi P, Gandara D, Khaira D, et al. Phase I Study of Navitoclax (ABT-263), a Novel Bcl-2 Family Inhibitor, in Patients With Small-Cell Lung Cancer and Other Solid Tumors. Journal of Clinical Oncology. 2011;29(7):909-16.

333. Rudin CM, Hann CL, Garon EB, Ribeiro de Oliveira M, Bonomi PD, Camidge DR, et al. Phase II Study of Single-Agent Navitoclax (ABT-263) and Biomarker Correlates in Patients with Relapsed Small Cell Lung Cancer. Clinical Cancer Research. 2012;18(11):3163.

334. Zhang H, Nimmer PM, Tahir SK, Chen J, Fryer RM, Hahn KR, et al. Bcl-2 family proteins are essential for platelet survival. Cell Death & Differentiation. 2007;14(5):943-51.

335. Souers AJ, Leverson JD, Boghaert ER, Ackler SL, Catron ND, Chen J, et al. ABT-199, a potent and selective BCL-2 inhibitor, achieves antitumor activity while sparing platelets. Nature Medicine. 2013;19(2):202-8.

336. US.FDA. FDA approves venetoclax for CLL and SLL: U.S. Food and Drug Administration; 2019 [Available from: https://www.fda.gov/drugs/resources-information-approved-drugs/fda-approves-venetoclax-cll-and-sll.

337. EMA. Venclyxto: European Medicines Agency; 2019 [Available from: https://www.ema.europa.eu/en/medicines/human/summaries-opinion/venclyxto.

338. Deeks ED. Venetoclax: First Global Approval. Drugs. 2016;76(9):979-87.

339. Delbridge ARD, Grabow S, Strasser A, Vaux DL. Thirty years of BCL-2: translating cell death discoveries into novel cancer therapies. Nature Reviews Cancer. 2016;16:99.

340. Opferman JT, Iwasaki H, Ong CC, Suh H, Mizuno S-i, Akashi K, et al. Obligate Role of Anti-Apoptotic MCL-1 in the Survival of Hematopoietic Stem Cells. Science. 2005;307(5712):1101.

341. Opferman JT, Letai A, Beard C, Sorcinelli MD, Ong CC, Korsmeyer SJ. Development and maintenance of B and T lymphocytes requires antiapoptotic MCL-1. Nature. 2003;426(6967):671-6.

342. Vikstrom I, Carotta S, Lüthje K, Peperzak V, Jost PJ, Glaser S, et al. Mcl-1 Is Essential for Germinal Center Formation and B Cell Memory. Science. 2010;330(6007):1095.

343. Arbour N, Vanderluit JL, Le Grand JN, Jahani-Asl A, Ruzhynsky VA, Cheung ECC, et al. Mcl-1 Is a Key Regulator of Apoptosis during CNS Development and after DNA Damage. The Journal of Neuroscience. 2008;28(24):6068.

344. Guo Z, Song T, Xue Z, Liu P, Zhang M, Zhang X, et al. Using CETSA assay and a mathematical model to reveal dual Bcl-2/Mcl-1 inhibition and on-target mechanism for ABT-199 and S1. European Journal of Pharmaceutical Sciences. 2019:105105.

345. Brooks TA, Hurley LH. Targeting MYC Expression through G-Quadruplexes. Genes & Cancer. 2010;1(6):641-9.

346. Hilton J, Cescon DW, Bedard P, Tu D, Ritter H, Soong J, et al. 44OCCTG IND.231: A phase 1 trial evaluating CX-5461 in patients with advanced solid tumors. Annals of Oncology. 2018;29(suppl_3).

347. Lim J, Padgett C, Von Hoff D, Rice W, Darjania L, Phung J, et al. Abstract #3599: Quarfloxin phase I clinical data and scientific findings supporting the selection of carcinoid/neuroendocrine tumors as the phase II indication. Cancer Research. 2009;69(9 Supplement):3599.

348. Geoerger B, Deschamps F, Puget S, Koubi-Pick V, Lacroix L, Vielh P, et al. Molecular screening for cancer treatment optimization (MOSCATO 01) in pediatric patients: First feasibility results of a prospective molecular stratification trial. Journal of Clinical Oncology. 2014;32(15_suppl):10050-.

349. Deutsches-Krebsforschungszentrum. INFORM – INdividualized Therapy FOr Relapsed Malignancies in Childhood https://www.dkfz.de/en/inform/index.html2019 [

Manuscript I

Hsa-miR-323a-3p Functions as a Tumor Suppressor and Targets *STAT3* in Neuroblastoma Cells

Swapnil Parashram Bhavsar[1*], Lotte Olsen[1*], Cecilie Løkke[1], Trond Flægstad[1, 2] and Christer Einvik[1, 2]

[1] Pediatric Research Group, Department of Clinical Medicine, Faculty of Health Science, UiT The Arctic University of Norway, NO-9037 Tromsø, Norway

[2] Department of Pediatrics, Division of Child and Adolescent Health, UNN–University Hospital of North-Norway, NO-9038 Tromsø, Norway

*Authors have contributed equally to this work.

Abstract

Background: Studies conducted the last decades have revealed a role for the non-coding microRNAs (miRNAs) in cancer development and progression. Several miRNAs within the chromosome region 14q32, a region commonly deleted in cancers, are associated with poor clinical outcome in the childhood cancer neuroblastoma. We have previously identified *miR-323a-3p* from this region to be downregulated in chemotherapy treated neuroblastoma cells compared to pre-treatment cells from the same patients. Furthermore, in neuroblastoma tumors, this miRNA is downregulated in advanced stage 4 disease compared to stage 1-2. In this study, we attempt to delineate the unknown functional roles of *miR-323a-3p* in neuroblastoma.

Methods: Synthetic mimics were used to overexpress *miRNA-323a-3p* in neuroblastoma cell lines. To investigate the functional roles of *miR-323a-3p*, cell viability assay, flow cytometry, reverse transcription-quantitative polymerase chain reaction, luciferase reporter assay and western blot were conducted on the neuroblastoma cell lines Kelly, SH-SY5Y and SK-N-BE(2)-C.

Results: Ectopic expression of *miR-323a-3p* resulted in marked reduction of cell viability in Kelly, SH-SY5Y and SK-N-BE(2)-C by causing G1-cell cycle arrest in Kelly, SH-SY5Y and apoptosis in all cell lines tested. Furthermore, mRNA and protein levels of signal transducer and activator of transcription 3 (*STAT3*) were reduced upon *miR-323a-3p* overexpression. A direct binding of the miRNA to the 3'UTR of *STAT3* was experimentally validated by luciferase

reporter assay, where *miR-323a-3p* reduced luminescent signal from full length *STAT3* 3'UTR luciferase reporter, but not from a reporter with mutation in the predicted seed sequence.

Conclusions: *miR-323a-3p* inhibits growth of neuroblastoma cell lines through G1-cell cycle arrest and apoptosis, and the well-known oncogene *STAT3* is a direct target of this miRNA.

Background

Neuroblastoma is one of the most common embryonal malignancies among children and 40% of all children diagnosed with neuroblastoma are designated as high-risk patients (1) with poor clinical outcome (2). Multiple treatment modalities are available, including intensive chemotherapy with autologous stem-cell rescue, surgery, radiation and immunotherapy, which have improved the survival rate of high-risk neuroblastoma patients. However, many high-risk patients ultimately relapse and eventually die from disease progression. Treatment failure is mainly attributed to the development of drug resistance and is one of the major clinical obstacles in treatment of high-risk neuroblastoma (1, 3). Thus, development of more effective targeted therapies are required to address this issue.

MicroRNAs (miRNAs) are evolutionary conserved, endogenously expressed, small non-coding RNAs (~19-24 nucleotides) that regulate gene expression by translation inhibition or degradation of mRNA. They are subsequently responsible for regulating expression of genes involved in a myriad of cellular processes (4). In addition, miRNAs are shown to modulate drug resistance in multiple cancers. Several research groups have identified a differential expression of miRNAs in parental (chemo-sensitive) vs resistant (chemo-resistant) cancer cells (5, 6). Moreover, some molecular mechanisms underlying drug resistance have also been elucidated (7).

Mir-323a is located on the chromosome region 14q32, a region frequently dysregulated in cancers (8-12). Several miRNAs from this cluster, including *miR-323a-3p,* have been found downregulated in neuroblastoma cells from patients with relapsed disease (6). An aberrant expression of *miR-323a-3p* is observed in multiple other cancers as well. In glioblastoma (13), osteosarcoma (14), pancreatic ductal adenocarcinoma (PDAC) (15) and bladder cancer (16) it was found downregulated. Whereas in prostate cancer, *miR-323* was upregulated and promoted cell proliferation (17, 18). The role of *miR-323a-3p* in neuroblastoma is unknown and investigation is warranted given the role of the miRNA in other cancers.

STAT3 is one of seven members (STAT1, STAT2, STAT3, STAT4, STAT5A, STAT5B and STAT6) of the signal transducer and activator of transcription (STAT) protein family (19, 20). This protein was initially shown to be activated in response to binding of cytokines and growth factors to cellular receptors, which activates membrane-associated janus kinases (JAK). JAK in turn phosphorylates STAT3 at specific residues to form homo/heterodimers and translocate to the cell nucleus. In the nucleus, STAT3 acts as a transcription factor, regulating the expression of a wide range of genes involved in survival,

proliferation, invasion, metastasis, angiogenesis, and immunosuppression (21). Moreover, Zhou C. and colleagues have shown that downregulation of STAT3 induces G1-cell cycle arrest and apoptosis in esophageal carcinoma (22). Accumulating evidence suggest that STAT3 is activated by numerous activators (e.g. cytokines, growth factors, toll-like receptors, etc.). Hence, dysregulation of *STAT3* can lead to oncogenesis through various mechanisms. Several studies have identified different miRNAs having reciprocal interactions with JAK-STAT3 signaling pathway in different cancer types, for example, *let-7* (23), *miR-9* (24), *miR-337* (25), *miR-26a* (26) and *miR-135a* (27). However, the role of miRNA directly targeting STAT3-3'UTR is not yet demonstrated in neuroblastoma.

We have previously observed downregulation of *miR-323a-3p* in post-chemotherapy neuroblastoma cell lines as compared to matched pre-chemotherapy neuroblastoma cell lines (6). In this study, we set out to understand the functional role of *miR-323a-3p* in neuroblastoma. Therefore, gain-of-function studies were done by overexpressing *miR-323a-3p* in candidate neuroblastoma cell lines, which had significant effect on growth and survival by inducing G1-cell cycle arrest and apoptosis. Furthermore, we demonstrate *STAT3* as a novel target of *miR-323a-3p*.

Materials and Methods

Cell Lines and Cell Culture

The neuroblastoma cell lines Kelly, SH-SY5Y and SK-N-BE(2)-C (BE(2)-C) were all maintained at 37°C in RPMI-1640 medium with 2 mM L-Glutamine (Sigma-Aldrich) supplemented with 10% fetal bovine serum (Sigma-Aldrich), in a humidified incubator with 5% CO_2 atmosphere. In collaboration with the Center of Forensic Genetics (UiT The Arctic University of Norway, Norway), we authenticated the cell lines using short tandem repeat (STR) profiling. We confirmed absence of mycoplasma contamination in the cell lines using MycoAlert™ Mycoplasma Detection Kit (Lonza).

Transfections

For ectopic expression, 25-40 nM of *miRNA-323a-3p* or negative control (NC) mirVana® miRNA mimics (Ambion, Thermo Fisher Scientific) were transfected using Invitrogen™ Lipofectamine™ 2000 Transfection Reagent (Fisher Scientific) in OptiMEM medium (Thermo Fisher Scientific) according to the manufacturer's instructions.

Cell Viability

Cell viability was assessed using alamarBlue® (Thermo Fisher Scientific) cell viability assay according to the manufacturer's instructions. 25 nM *miR-323a-3p* or NC mimics were reverse transfected into Kelly, SH-SY5Y and BE(2)-C cells seeded in 24-well plates. Cell viability 24, 48, 72 and 96 hours after transfection were measured in a CLARIOstar microplate reader (BMG LABTECH), and calculated as the percentage of NC transfected cells set to 100 percent.

Flow Cytometry

For determining cell cycle distribution Kelly, SH-SY5Y and BE(2)-C cells were first reverse transfected with 25 nM *miR-323a-3p* or NC mimics in 25 cm^2 culture flasks. After 72 hours, the cells were detached by trypsin, centrifuged and washed with 1x phosphate-buffered saline (PBS). An overnight incubation at -20°C in 70% ethanol was performed to fixate the cells. After 10 minutes centrifugation at 850 g, and a subsequent wash with 1x PBS, fixated cells were added DNA-staining solution consisting of PBS with 50 µg/ml propidium iodide (PI) and 100 µg/ml RNase (Life technologies). Cells were protected from light and stored on ice during a 30 minutes incubation period prior to flow cytometry measurement of PI-stained DNA in a BD LSRFortessa™ cell analyzer (BD Bioscience). The Dean-Jett-Fox model for cell cycle evaluation was used for analysis in the FlowJo 7.6.5 software.

MicroRNA Target Prediction

A computational approach with miRDB algorithm (available at http://www.mirdb.org/) was used to identify *miR-323a-3p* targets (28).

RNA Extraction, Reverse Transcription and Quantitative PCR

Kelly, SH-SY5Y and BE(2)-C cells were transfected with 25 nM *miR-323a-3p* or NC mimics in 6-well plates. The QIAzol®Lysis Reagent (QIAGEN) was used for isolation of total RNA 24 hour later according to the manufacturer's instructions. Quantity and purity of total RNA was assessed with NanoDrop™ 2000 spectrophotometer (Thermo Fisher Scientific).

For miRNA and mRNA expression analysis, complementary DNA (cDNA) synthesis from total RNA, and successive qPCR measurements, were performed as previously described (29). The qPCR cycling was carried out in a Light Cycler 96 SW 1.1 (Roche). For miRNA analyzation the miScript primer assays Hs_miR-323-3p_2 (cat. no MS00037219) and Hs_miR-4286_1 (cat. no MS00021371) (QIAGEN) were used for *miR-323a-3p* quantification and as a reference gene, respectively. Using the LinRegPCR software (Version 11.0; http: //LinRegPCR.HFRC.nl.) we generated mean efficiency for each amplicon group and deducted baseline corrected Cq-values. Expression of *miR-323a-3p* relative to *miR-4286* was calculated as: Expression = E(GOI)^ -Cq(GOI) / E(REF)^ -Cq(REF) (E, efficiency; GOI, gene of interest; REF, reference gene) (30). The following primers were used for mRNA expression analysis: *STAT3* (forward: 5'-CAG CAG CTT GAC ACA CGG TA-3'; reverse: 5'- AAA CAC CAA AGT GGC ATG TGA -3') and *SDHA* (forward: 5'-CTG ATG AGA CAA GAT GTG GTG-3'; reverse: 5'-CAA TCT CCC TTC AAT GTA CTC C-3'). *SDHA* functioned as a reference gene. Expression of *STAT3* was assessed by the ΔΔCq comparative cycle threshold method (31).

All RT-qPCR reactions were performed in triplicates on at least two independent biological replicates. Standard deviations were calculated taking into account the principle of error propagation (including technical and biological replicates).

Western Blot Analysis

Cells were seeded in 6-well plates, and, 72 hours later, trypsinized and lysed in 40 µl RIPA buffer (50 mM Tris-HCL pH 8, 150 mM NaCl, 1% NP-40, 0.5% sodium deoxycholate, 0.1% SDS) containing 1x Protein Inhibitor Cocktail (Roche) and 1 mM dithiothreitol (DTT) (Sigma-Aldrich). For PARP cleavage analysis, floating cells were included. Total protein concentrations were determined using DC™Protein Assay Kit (Bio-Rad) according to the manufacturer's instructions, and 40 µg protein was separated on a NuPAGE® Novex 4-12%

Bis-Tris precast polyacrylamide gel (Thermo Fisher Scientific) before blotted onto Immobilon-FL PVDF membrane (Millipore). Prior to fluorescence detection, the membrane was blocked for 1 hour at room temperature in 5 ml Odyssey Blocking Buffer (LI-COR Biosciences) followed by overnight incubation at 4°C with primary antibodies: Stat3 (C-20): sc-482, rabbit, polyclonal (1:1000) (Santa Cruz Biotechnology); PARP: 9542, rabbit, polyclonal (1:1000) (Cell Signaling Technology); and Anti-Actin antibody [ACTN05 (C4)]: ab3280, mouse, monoclonal (1:1000) (Abcam). After four (5 minutes) washes with 0,1% PBST, the membrane was incubated with secondary antibodies Rabbit IgG (H&L) Antibody DyLight™ 800 Conjugated (1:5000) (Rockland Immunochemicals) and goat anti-mouse-Alexa Fluor 680 (1:5000) (Thermo Fisher Scientific) and scanned in the Odyssey CLx Infrared Imaging System (LI-COR Biosciences). Actin was used as loading control. For quantification of protein, the ImageJ software was used (32) (available on imagej.net).

Reporter Constructs and Dual Luciferase Assay

The cells were grown on a 12-well plate and co-transfected with 40 nM mimics, 50 ng/ml pMIR-Report-Firefly construct (Ambion) and 100 ng/ml mutated (pLightSwitch-STAT3-3'UTR-mut) or wild-type (pLightSwitch-STAT3-3'UTR-wt) luciferase constructs harboring full-length STAT3-3'UTR.

The pLightSwitch-STAT3-3'UTR-wt construct was obtained from SwitchGear Genomics (Product ID: S813664). pLightSwitch-STAT3-3'UTR-mut construct with a mutation in the putative *miR-323a-3p* seed sequence was generated using QuickChange II Site-Directed Mutagenesis kit (Agilent Technologies). The primers used for mutagenesis were: Forward: 5'-CTG CCC AGC CTT ACT CAC TAA AAG GCC AAT AGC GGA CAA AGG AAA ATA AGT CTA TTT ATA A -3'; reverse: 5'-TTA TAA ATA GAC TTA TTT TCC TTT GTC CGC TAT TGG CCT TTT AGT GAG TAA GGC TGG GCA G -3'. To confirm mutation in the seed sequence, the mutant plasmid was sequenced using sequencing primer 5'- GAA ACG GGC TTC AGG TCA AAC CC-3'.

After incubation for 24 hours at 37°C, luciferase activity was measured using the Dual-Luciferase Reporter Assay (Promega), according to the manufacturer's instructions. The renilla luciferase activity was normalized to the firefly luciferase activity.

MicroRNA Expression Data

A subset of 226 primary neuroblastoma tumors from the 'Tumor Neuroblastoma NRC Compendium-NRC-364-mirg' miRNA dataset was used to obtain miRNA expression data. The

dataset was generated using multiplex RT-qPCR assays and consist of tumors from The Neuroblastoma Research Consortium (NRC), a collaboration between laboratories in Dublin, Amsterdam, Essen and Ghent (33). The R2: Genomics Analysis and Visualization Platform (http://r2.amc.nl) was used to generate Kaplan-Meier overall survival curves for patients with high and low expression of *miR-323a.* Analyzation using the Mann–Whitney test determined the differential expression of miRNAs at different tumor stages. Differential analysis between *MYCN* amplified (MNA) and non-MNA tumors was done using the Kruskal–Wallis test.

Statistical Analysis

The GraphPad Prism (version 5.00) software for Windows (GraphPad Software) (available at www.graphpad.com) was used for all statistical analyses unless stated otherwise. Analyses are based on at least three independent experiments and presented as mean ± standard deviation (SD). Student's t-test was used to calculate statistical differences between means (n=3) of control and treated cells. P values *P<0.05, **P<0.01 were considered to indicate statistically significant results.

Results

MiR-323a is Differentially Expressed in Neuroblastoma Cell Line Pairs and Primary Tumors

In our previous study, we reported a reduced expression of 22 miRNAs from the chromosome 14q32 miRNA cluster (including *miR-323a*) in post-chemotherapy neuroblastoma cell lines as compared to matched pre-chemotherapy neuroblastoma cell lines (***supplementary figure 1***) (6). When analyzing neuroblastoma tumor data we observed an association between low expression of *miR-323a* and a poor overall survival (***figure 1A***). Further investigations also revealed that *miR-323a* expression was reduced in advanced stage 4 tumors as compared to stage 1-2 (***figure 1B, left panel***), and in MNA neuroblastoma tumors as compared to non-MNA (***figure 1B, right panel***). Others have reported that *miR-323a-3p* is downregulated and acts as a tumor suppressor in various cancers (13-16). Given these findings, we sought out to elucidate *miR-323a-3p* functional role in aggressive neuroblastoma.

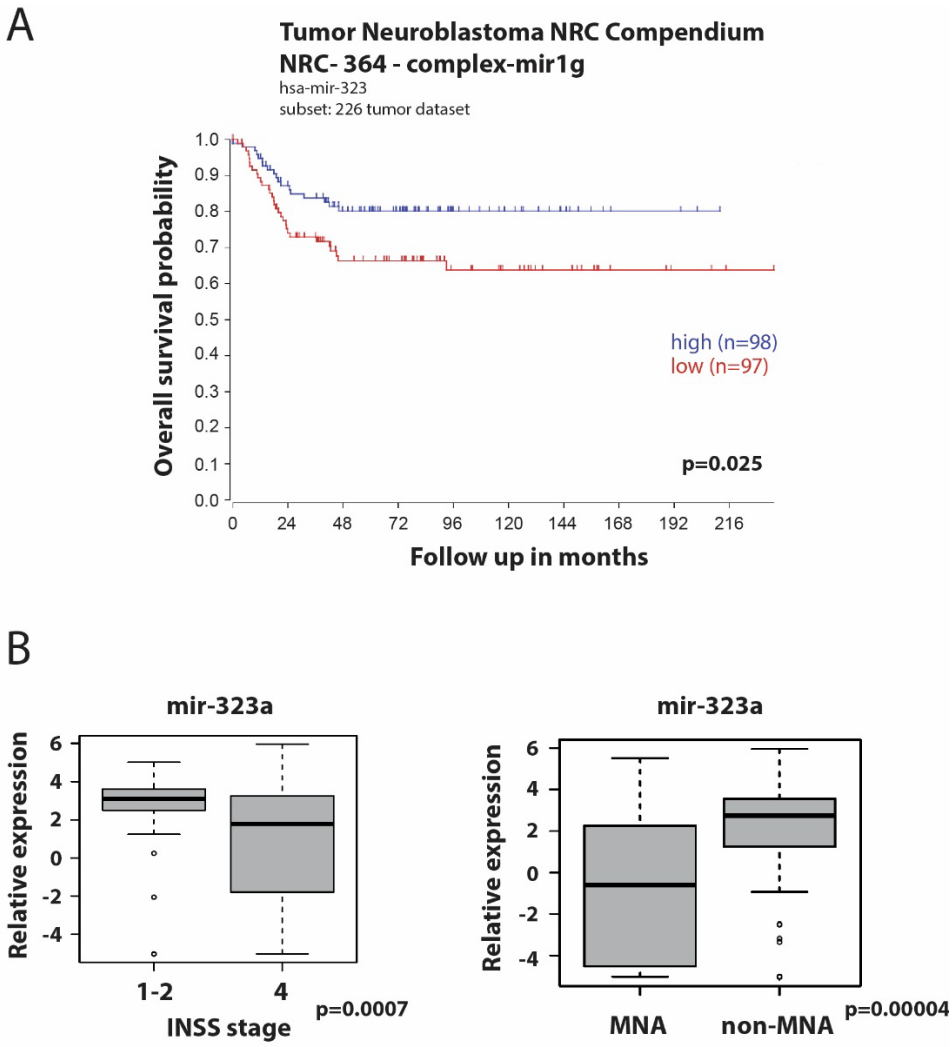

Figure 1: Low expression of *miR-323a* is associated with poor overall survival, high stage disease and MNA in primary tumors. A) Kaplan-Meier overall survival curve for patients with high (blue, n=98) and low (red, n=97) expression of *miR-323a*. **B)** Reduced expression of *miR-323a* in advanced stage 4 (n=92) vs stage 1-2 (n=57) (left) and in MNA (n=40) vs non-MNA (n=160) neuroblastoma tumors (right). The boxes represent the 25%–75% quartiles. The horizontal line in the boxes represents the median level. Whiskers represent the non-outlier range and open circles represent the outliers.

MiR-323a-3p Inhibits Growth and Survival of Neuroblastoma Cells

To examine the relationship between reduced expression of *mir-323a-3p* and cell survival, we first evaluated the basic expression of *miR-323a-3p* relative to endogenous *miR-4286* in Kelly, SH-SY5Y and BE(2)-C neuroblastoma cell lines by RT-qPCR. *MiR-4286* is stably expressed in these neuroblastoma cell lines as reported previously (6). We observed very low levels of *miR-323a-3p* in Kelly and SH-SY5Y as compared to BE(2)-C cell line (***figure 2A***).

Next, to check the transfection efficiency, we transfected Kelly, SH-SY5Y and BE(2)-C cell lines with negative control (NC) or *miR-323a-3p* miRNA mimics. RT-qPCR analysis demonstrated that the expression of *miR-323a-3p* was significantly increased in *miR-323a-3p* transfected cells compared to NC transfected cells (***supplementary figure 2***).

The overexpression of *miR-323a-3p* in Kelly, SH-SY5Y and BE(2)-C cell lines caused markedly lower cell viability than in NC transfected cells as measured by alamarBlue cell viability assay performed at 24, 48, 72 and 96 h post-transfection (***figure 2B***). Collectively, these results demonstrated that overexpression of *miR-323a-3p* affect the growth of neuroblastoma cells.

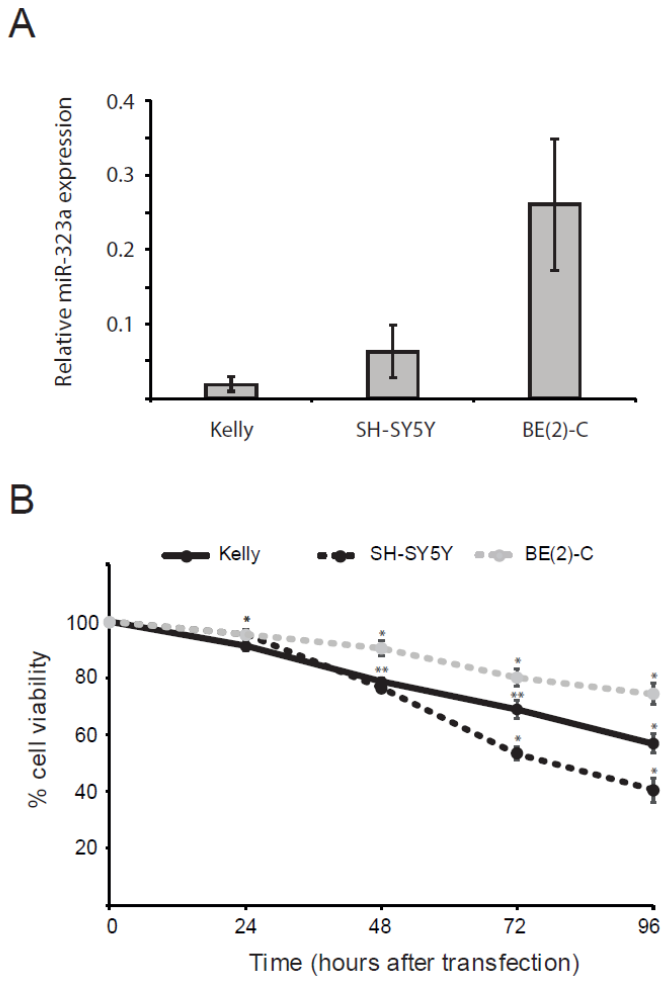

Figure 2: *miR-323a-3p* overexpression suppressed the growth and survival of neuroblastoma cells. A) The basic expression of *miR-323a-3p* with respect to stably expressed *miR-4286* in Kelly, SH-SY5Y and BE(2)-C cell lines were detected by RT-qPCR analysis. Data is presented as mean ± SD. of at least two independent experiments, each repeated in triplicates. **B)** The alamarBlue cell viability assay indicated that overexpression of *miR-323a-3p* markedly reduces the growth and survival of neuroblastoma cells at 24h, 48h, 72h and 96h post transfection. Data are presented as mean ± SD. of three independent experiments, each repeated in triplicates. *P<0.05, **P<0.01 vs. the NC. RT-qPCR, reverse transcription-quantitative polymerase chain reaction; NC, negative control; miR, microRNA; SD, standard deviation.

MiR-323a-3p Affects G1-cell Cycle Arrest and Apoptosis in Neuroblastoma Cells

As cell growth is associated with the cell cycle, we analyzed the effect of *miR-323a-3p* overexpression on the cell cycle distribution in Kelly, SH-SY5Y and BE(2)-C by flow cytometry assay. Whereas, *miR-323a-3p* expression did not affect cell cycle distribution in BE(2)-C, it significantly induced G1-arrest in Kelly and SH-SY5Y by 13.6% (p=0.0042) and 17.5% (p=0.0181), respectively (***figure 3A***).

To further assess the ability of *miR-323a-3p* to induce apoptosis, we transfected Kelly, SH-SY5Y and BE(2)-C with NC or *miR-323a-3p* mimics and determined the induction of PARP-cleavage on western blot. The western blot analysis revealed PARP-cleavage in Kelly, SH-SY5Y and BE(2)-C by 197% (p=0.0443), 671% (p=0.0365) and 175% (p=0.0079),

respectively, as compared to NC transfected cells (***figure 3B and 3C***). Taken together, we show that *miR-323a-3p* reduces cell viability by inducing G1-cell cycle arrest and apoptosis in neuroblastoma cells.

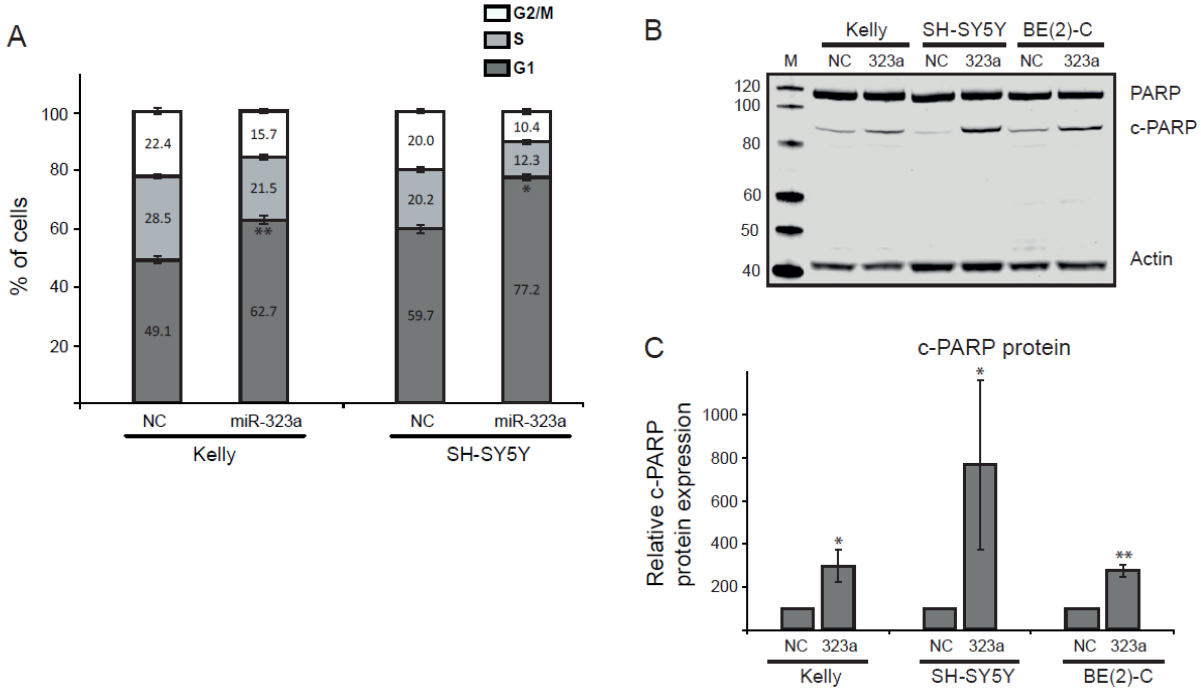

Figure 3: *miR-323a-3p* induces G1-cell cycle arrest and apoptosis in neuroblastoma cells. A) Kelly and SH-SY5Y cell lines were transfected with *miR-323a-3p* or NC mimics and cell cycle distribution was measured by flow cytometry assay. Data are presented as mean ± SD. of three independent experiments, each repeated in triplicates. **B)** Western blot assay indicated that PARP-cleavage (represents apoptosis) was increased in Kelly, SH-SY5Y and BE(2)-C cell lines transfected with *miR-323a-3p* or NC mimics. **C)** Quantification of c-PARP protein expression on the western blots (n=3). Data are presented as mean ± SD. of three independent experiments. *P<0.05, **P<0.01 vs. the NC. SD, standard deviation; NC, negative control; miR, microRNA.

MiR-323a-3p Targets *STAT3* in Neuroblastoma

We used bioinformatics target prediction algorithm miRDB (mirdb.org) to find mRNA binding sequences for *miR-323a-3p.* The miRDB database revealed 793 predicted targets for *miR-323a-3p*. Additionally, a literature search was performed to check previously validated targets of *miR-323a-3p,* in other cancers (***supplementary figure 3A***). We used RT-qPCR to scan through a subset of these mRNAs in Kelly cells transfected with *miR-323a-3p* mimics. Compared to NC mimic transfected cells, we observed several mRNAs that were downregulated. *STAT3,* which has not previously been validated as a direct target of *miR-323a-3p*, was consistently downregulated by more than 40 % (***supplementary figure 3B***).

miRDB database identified a putative binding site for *miR-323a-3p* in the 3'UTR of *STAT3* (***figure 4A***). Thus, to confirm that *STAT3* is a direct target of *miR-323a-3p*, we performed luciferase reporter assay by co-transfecting luciferase construct containing wild-type

or mutant 3'UTR of *STAT3* with *miR-323a-3p* or NC mimics. The results showed that overexpression of *miR-323a-3p* suppressed the luciferase activity of wild-type construct by 30.7% (p=0.0014), but not the mutant construct, in SH-SY5Y cells (***figure 4B***). Together, these data demonstrated that *STAT3* is a direct target of *miR-323a-3p* in neuroblastoma.

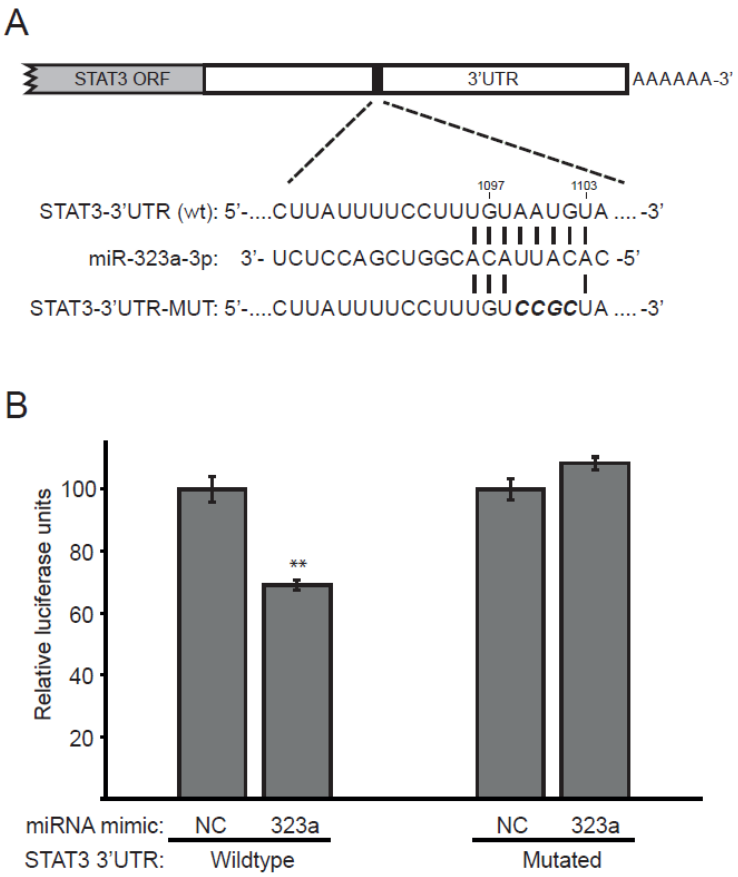

Figure 4: *STAT3* is a direct target of *miR-323a-3p* in neuroblastoma. A) The putative binding site of *miR-323a-3p* (nucleotides 1,097 to 1,103) in the 3'UTR of *STAT3* was mutated as shown in the figure with bold and italics. **B)** A dual-luciferase reporter assay demonstrated that *miR-323a-3p* suppressed the luciferase activity of wild-type construct with 3'UTR of *STAT3*, but not the mutated construct in SH-SY5Y transfected with *miR-323a-3p* or NC mimics. Data are presented as mean ±SD. of three independent experiments, each repeated in triplicates. **P<0.01 vs. the NC. SD, standard deviation; miR, microRNA; NC, negative control; STAT3, signal transducer and activator of transcription; ORF, open reading frame; UTR, untranslated region; wt, wild-type; MUT, mutated.

STAT3 mRNA and Protein Levels are Regulated by *MiR-323a-3p*

We next investigated whether *miR-323a-3p* could regulate *STAT3* at mRNA and protein levels. The *miR-323a-3p* or NC mimics were transfected into neuroblastoma cell lines and the expression levels of *STAT3* mRNA and protein was examined by RT-qPCR and western blot analysis, respectively. Overexpression of *miR-323a-3p* led to significant decrease of *STAT3* mRNA in Kelly, SH-SY5Y and BE(2)-C by 42% (p=0.0049), 31% (p=0.0137) and 43% (p=0.0039), respectively, as compared to NC transfected cells (***figure 5A***). Moreover, STAT3 protein levels were also significantly decreased upon *miR-323a-3p* overexpression in Kelly,

SH-SY5Y and BE(2)-C by 60% (p=0.0079), 64% (p=0.0070) and 75% (p=0.0023), respectively, as compared to NC transfected cells (***figure 5B and 5C***). Altogether, these data suggest that *miR-323a-3p* directly binds and inhibits the expression of *STAT3* mRNA and protein levels in neuroblastoma cells.

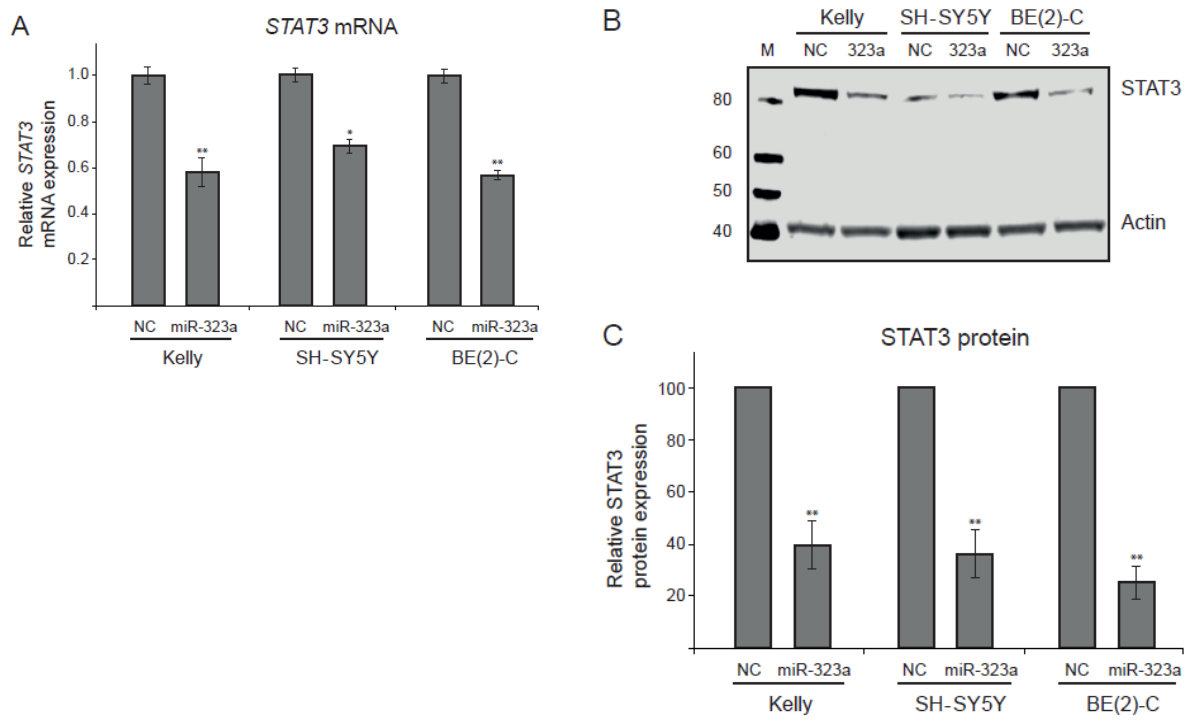

Figure 5: *miR-323a-3p* reduces mRNA and protein levels of STAT3 in neuroblastoma cells. A) The RT-qPCR analysis indicated that *STAT3* mRNA levels were significantly downregulated in Kelly, SH-SY5Y and BE(2)-C cell lines transfected with *miR-323a-3p*. Data are presented as mean ±SD. of three independent experiments, each repeated in triplicates. **B)** Western blot assay demonstrated that STAT3 protein levels were significantly reduced in Kelly, SH-SY5Y and BE(2)-C cell lines transfected with *miR-323a-3p*. **C)** Quantification of STAT3 protein expression on the western blots (n=3). Data are presented as mean ±SD. of three independent experiments. *P<0.05, **P<0.01 vs. the NC. RT-qPCR, reverse transcription-quantitative polymerase chain reaction; SD, standard deviation; miR, microRNA; NC, negative control; STAT3, signal transducer and activator of transcription.

Discussion

Several miRNA-profiling studies have demonstrated differential expression of miRNAs across normal vs cancerous tissues or parental vs resistant tumors. In neuroblastoma, differential patterns of miRNA expression have been reported in favorable vs unfavorable disease, and many of these deregulated miRNAs are shown to correlate with prognosis, differentiation, apoptosis and survival (34-36). In our previous study, we observed expression variations in several miRNAs when comparing post-chemotherapy neuroblastoma cell lines to matched pre-chemotherapy neuroblastoma cell lines. Interestingly, downregulation of several genes in the chromosome 14q32 cluster of miRNAs was evident in post-chemotherapy neuroblastoma cell lines and it correlated with poor prognostic factors (6). In other malignancies, this appear to be an unstable region with frequent loss of heterozygosity (LOH), deletions (37, 38) and dysregulation of miRNAs from the cluster (8, 11, 39). Furthermore, DNA methylation screening has shown that several miRNAs, including miRNAs from the chromosome 14q32 cluster, are epigenetically silenced in neuroblastoma (33). We have previously shown that *miR-376c-3p* located on the 14q32 cluster can affect cell viability and drug resistance in neuroblastoma (29).

Analyzing neuroblastoma tumor data of another downregulated miRNA from the cluster, *miR-323a*, revealed that this miRNA is reverse correlated with MNA and high-stage disease. We also observed a significant association between low *miR-323a* levels and poor overall survival. However, the dataset from NRC was generated using RT-qPCR assays that do not discriminate between the 3p and the 5p version of *miR-323a*, but reflects the expression of the pre-miRNA. Soriano *et al.* has previously demonstrated that *miR-323a-5p* also has anti-tumor effect in neuroblastoma (40). To analyze association between low *miR-323a-5p* expression and poor overall survival they used the same dataset as us, but neither they nor we can be confident that the results reflect the impact of either mature miRNA. Furthermore, Soriano *et al*. analyzed their data using the KaplanScan function in R2 (41), while we have analyzed the median. We chose to use the 'median' to split high and low *miR-323a* expression, since the scan function divides the tumors into two very unequal sized groups (25 vs 228) and there are no obvious reasons to use the scan function. Observing low expression of *miR-323a-3p* in neuroblastoma cell lines from patients with relapsed neuroblastoma and tumors from high-risk patients led us to hypothesize that overexpression of *miR-323a-3p* could have positive phenotypic effect on neuroblastoma cell lines. Indeed, cell viability was clearly reduced upon transient transfection with *miR-323a-3p* due to G1-arrest and apoptosis. This is in line with

several other studies that show a tumor suppressive role of *miR-323a-3p*. Recently, *miR-323a-3p* was found downregulated in glioblastoma cells and overexpression of *miR-323a-3p* led to inhibition of proliferation and migration. In addition, *in vivo* studies on mice implanted with *miR-323a-3p* overexpressing glioblastoma cells showed prolonged survival as compared to control mice (13). A study by Chen *et al.*, reported significant downregulation of *miR-323a-3p* in osteosarcoma tissues and cell lines as compared to adjacent normal tissue and normal cells, respectively (14). Transfection of osteosarcoma cell lines with *miR-323a-3p* targeted lactate dehydrogenase (LDHA), which resulted in induction of apoptosis and decreased cell viability and colony formation. A low expression of *miR-323a-3p* have also been observed in cells and tissue of pancreatic ductal adenocarcinoma (PDAC) and lower expression of *miR-323a-3p* correlated with poor prognosis in patients with PDAC (10). By transfecting with *miR-323a-3p*, the invasion and migration abilities of PDAC cells were inhibited both *in vitro* and *in vivo*. Also in bladder cancer, *miR-323a-3p* was downregulated and associated with poor overall survival (11). Overexpression of *miR-323a-3p* inhibited epithelial-mesenchymal (EMT) transition via regulating the MET/SMAD/SNAIL circuit.

Contrary to these studies, *miR-323a-3p* was upregulated and shown to promote cell proliferation and growth of xenograft tumors by targeting *p73* in prostate cancer (17, 18). A dual role of miRNAs reflects their intricate way of regulating several targets within a cell, which can produce different phenotypes in different cells and diseases, and even within the same disease (42, 43). Therefore, understanding the cell- or disease specific mechanisms of a miRNA through functional studies are imperative to develop targeted therapies. From the previous studies, we conclude that *miR-323a-3p* may have disease specific function as tumor suppressive or oncogenic miRNA by regulating growth, apoptosis, invasion and migration. Our study suggests a tumor suppressive function of *miR-323a-3p* in neuroblastoma.

Further elucidating the role of *miR-323a-3p*, we searched for unknown targets. Expression of a selection of genes involved in proliferation, cell cycle and apoptosis were screened using RT-qPCR in neuroblastoma cells transfected with either *miR-323a-3p* or negative control mimics. *STAT3*, a gene well known to function in apoptosis (36) and that induces G1-arrest when silenced in esophageal carcinoma (17), was significantly reduced by *miR-323a-3p* in all three cell lines. Although other genes that could contribute to the observed biological effects mediated by exogenous expression of *miR-323a-3p* were observed downregulated (particularly *SMAD2*, *TGFA* and *TGFB2*), the levels of these were low (Cq-values >31) and therefore not studied further. The miRDB miRNA target prediction algorithm

found a putative binding site for *miR-323a-3p* in the 3'UTR of *STAT3*. A direct regulation of *STAT3* was confirmed by dual-luciferase reporter assay, when *miR-323a-3p* reduced luciferase activity of wild-type STAT3-3'UTR, but not a construct with mutation in the predicted seed sequence. Additionally, we showed that protein levels of *STAT3* were significantly reduced in *miR-323a-3p* transfected cells compared to negative control, further confirming the effect of *miR-323a-3p* on *STAT3*. Target prediction software RNA22 (https://cm.jefferson.edu/rna22/) indicated another putative binding site for *miR-323a-3p* in the *STAT3* 3'UTR. However, luciferase assay on a construct with mutation in this sequence did not indicate this as a direct target site (data not shown).

The oncogenic role of *STAT3* is well established (44), and therapeutic strategies that inhibit the oncogene are promising. A recent study from Odate *et al*. demonstrated that STAT3 inhibition with the antisense oligonucleotide AZD9150 in murine neuroblastoma models reduced tumor growth and sensitized tumors to cisplatin (45). In addition, STAT3 inhibitors and several tyrosine kinase inhibitors, which can target JAK-STAT3 signaling indirectly, are also developed and some are available in the clinic (46). Interestingly, when analyzing neuroblastoma tumor data, we did not observe a reverse correlation between STAT3 and *miR-323a* (data not shown). This underscores the importance of conducting further investigations to establish if the phenotypic effect we observe from upregulation of *miR-323a-3p* is indeed functionally linked to inhibition of *STAT3*.

MYCN amplification (MNA) is one of the most powerful biological markers indicating poor prognosis in neuroblastoma (47). Analyzing tumor data, we see a lower *miR-323a-3p* expression in MNA tumors compared to non-amplified tumors, further supporting the assumption that *miR-323a-3p* is a tumor suppressor in this malignancy. Basic expression of *miR-323a-3p* in the three cell lines we have tested do not fully coincide with the tumor data. As expected, the MNA cell line Kelly shows less expression than the non-MNA cell line SH-SY5Y. However, the MNA cell line BE(2)-C have the highest levels. Considering the heterogeneous nature of neuroblastoma, variations between single cell lines will occur. Various biological factors, like chromosomal aberrations or gene mutations can alter the miRNA expression, thus accounting for the higher expression in BE(2)-C. As the number of cell lines in this study is limited, generalization of gene expression is restricted. Furthermore, compared to its isogenic counterpart, SK-N-BE(1), expression of *miR-323a-3p* in BE(2)-C is indeed downregulated (6).

The documented role of miRNAs to act as either oncogenes (oncomiRs) or tumor suppressor genes in multiple cancers has led to clinical trials aiming to reconstitute downregulated tumor suppressor miRNAs or inhibit highly expressed miRNAs. *MiR-34* (MRX34) has entered phase-I clinical trial (ClinicalTrials.gov Identifier: NCT01829971) for treating solid tumors and *miR-122* entered phase-II trial (ClinicalTrials.gov Identifier: NCT01200420) for treating hepatitis (48-50). Thus, strategies involving manipulating expression of miRNAs can be an important approach in treatment of cancers or other diseases. As our study suggest a tumor suppressive function of *miR-323a-3p* in neuroblastoma, it is intriguing to consider it valid for further testing. Although the number of cell lines used limits our study, it is indicative of the biological functions of *miR-323a-3p* in neuroblastoma, and provide novel knowledge about the neuroblastoma targetome.

Conclusions

In conclusion, our study provides new insights into the functional roles of *miR-323a-3p* in neuroblastoma. We demonstrate that *miR-323a-3p* is downregulated in resistant neuroblastoma cell lines as compared to matched parental cell lines, and in tumors with high-risk features. In addition, ectopic expression of *miR-323a-3p* in neuroblastoma cell lines lead to reduced cell viability, G1-cell cycle arrest and apoptosis, and cause reduced expression of *STAT3* because of direct binding of *miR-323a-3p* to the 3'UTR of *STAT3* mRNA.

Declarations

Funding

This study was supported by grants from the UiT The Arctic University of Norway, Children's Cancer Association Troms and Finnmark, Helse Nord and Simon Fougner Hartmanns Familiefond. The publication charges for this article have been funded by a grant from the publication fund of UiT The Arctic University of Norway. The funding organizations have no role in the design of the study, analysis, and interpretation the data and in writing the manuscript.

Authors' Contributions

SPB, LO, TF and CE designed the research. SPB performed most of the experimental work. LO and CL performed some experiments. CE, TF and CL supervised the experimental work. SPB and LO wrote the manuscript. CE critically amended the manuscript. The final manuscript was read and approved by all of the authors.

Acknowledgements

We thank Professor Pieter Mestdagh, Ghent University, Belgium for providing us with miRNA expression data from primary neuroblastoma tumors obtained through the Neuroblastoma Research Consortium (NRC) initiative. We thank Dr. John Inge Johnsen, Childhood Cancer Research Unit, Department of Women's and Children's Health, Karolinska Institutet, 171 76 Stockholm, Sweden for providing us with SK-N-BE(2)-C, Kelly and SH-SY5Y.

References

1. Wagner LM, Danks MK. New therapeutic targets for the treatment of high-risk neuroblastoma. J Cell Biochem. 2009;107(1):46-57.

2. Smith V, Foster J. High-Risk Neuroblastoma Treatment Review. Children (Basel). 2018;5(9).

3. Pugh TJ, Morozova O, Attiyeh EF, Asgharzadeh S, Wei JS, Auclair D, et al. The genetic landscape of high-risk neuroblastoma. Nat Genet. 2013;45(3):279-84.

4. Croce CM, Calin GA. miRNAs, cancer, and stem cell division. Cell. 2005;122(1):6-7.

5. Ayers D, Mestdagh P, Van Maerken T, Vandesompele J. Identification of miRNAs contributing to neuroblastoma chemoresistance. Comput Struct Biotechnol J. 2015;13:307-19.

6. Roth SA, Knutsen E, Fiskaa T, Utnes P, Bhavsar S, Hald OH, et al. Next generation sequencing of microRNAs from isogenic neuroblastoma cell lines isolated before and after treatment. Cancer Lett. 2016;372(1):128-36.

7. Baker DL, Schmidt ML, Cohn SL, Maris JM, London WB, Buxton A, et al. Outcome after Reduced Chemotherapy for Intermediate-Risk Neuroblastoma. New England Journal of Medicine. 2010;363(14):1313-23.

8. González-Vallinas M, Rodríguez-Paredes M, Albrecht M, Sticht C, Stichel D, Gutekunst J, et al. Epigenetically Regulated Chromosome 14q32 miRNA Cluster Induces Metastasis and Predicts Poor Prognosis in Lung Adenocarcinoma Patients. Molecular Cancer Research. 2018;16(3):390.

9. Hoshi M, Otagiri N, Shiwaku HO, Asakawa S, Shimizu N, Kaneko Y, et al. Detailed deletion mapping of chromosome band 14q32 in human neuroblastoma defines a 1.1-Mb region of common allelic loss. British Journal of Cancer. 2000;82(11):1801-7.

10. Nadal E, Zhong J, Lin J, Reddy RM, Ramnath N, Orringer MB, et al. A MicroRNA Cluster at 14q32 Drives Aggressive Lung Adenocarcinoma. Clinical Cancer Research. 2014;20(12):3107.

11. Zehavi L, Avraham R, Barzilai A, Bar-Ilan D, Navon R, Sidi Y, et al. Silencing of a large microRNA cluster on human chromosome 14q32 in melanoma: biological effects of mir-376a and mir-376c on insulin growth factor 1 receptor. Molecular Cancer. 2012;11(1):44.

12. Zhang L, Huang J, Yang N, Greshock J, Megraw MS, Giannakakis A, et al. microRNAs exhibit high frequency genomic alterations in human cancer. Proceedings of the National Academy of Sciences. 2006;103(24):9136.

13. Shahar T, Granit A, Zrihan D, Canello T, Charbit H, Einstein O, et al. Expression level of miRNAs on chromosome 14q32.31 region correlates with tumor aggressiveness and survival of glioblastoma patients. J Neurooncol. 2016;130(3):413-22.

14. Chen H, Gao S, Cheng C. MiR-323a-3p suppressed the glycolysis of osteosarcoma via targeting LDHA. Hum Cell. 2018;31(4):300-9.

15. Wang C, Liu P, Wu H, Cui P, Li Y, Liu Y, et al. MicroRNA-323-3p inhibits cell invasion and metastasis in pancreatic ductal adenocarcinoma via direct suppression of SMAD2 and SMAD3. Oncotarget. 2016;7(12):14912-24.

16. Li J, Xu X, Meng S, Liang Z, Wang X, Xu M, et al. MET/SMAD3/SNAIL circuit mediated by miR-323a-3p is involved in regulating epithelial-mesenchymal transition progression in bladder cancer. Cell Death Dis. 2017;8(8):e3010.

17. Gao Q, Yao X, Zheng J. MiR-323 Inhibits Prostate Cancer Vascularization Through Adiponectin Receptor. Cell Physiol Biochem. 2015;36(4):1491-8.

18. Gao Q, Zheng J. microRNA-323 upregulation promotes prostate cancer growth and docetaxel resistance by repressing p73. Biomed Pharmacother. 2018;97:528-34.

19. Copeland NG, Gilbert DJ, Schindler C, Zhong Z, Wen Z, Darnell JE, Jr., et al. Distribution of the mammalian Stat gene family in mouse chromosomes. Genomics. 1995;29(1):225-8.

20. Darnell JE, Jr. STATs and gene regulation. Science. 1997;277(5332):1630-5.

21. Yu H, Lee H, Herrmann A, Buettner R, Jove R. Revisiting STAT3 signalling in cancer: new and unexpected biological functions. Nat Rev Cancer. 2014;14(11):736-46.

22. Zhou C, Ma J, Su M, Shao D, Zhao J, Zhao T, et al. Down-regulation of STAT3 induces the apoptosis and G1 cell cycle arrest in esophageal carcinoma ECA109 cells. Cancer Cell Int. 2018;18:53.

23. Sugimura K, Miyata H, Tanaka K, Hamano R, Takahashi T, Kurokawa Y, et al. Let-7 expression is a significant determinant of response to chemotherapy through the regulation of IL-6/STAT3 pathway in esophageal squamous cell carcinoma. Clin Cancer Res. 2012;18(18):5144-53.

24. Zhuang G, Wu X, Jiang Z, Kasman I, Yao J, Guan Y, et al. Tumour-secreted miR-9 promotes endothelial cell migration and angiogenesis by activating the JAK-STAT pathway. EMBO J. 2012;31(17):3513-23.

25. Du L, Subauste MC, DeSevo C, Zhao Z, Baker M, Borkowski R, et al. miR-337-3p and its targets STAT3 and RAP1A modulate taxane sensitivity in non-small cell lung cancers. PLoS One. 2012;7(6):e39167.

26. Yang X, Liang L, Zhang XF, Jia HL, Qin Y, Zhu XC, et al. MicroRNA-26a suppresses tumor growth and metastasis of human hepatocellular carcinoma by targeting interleukin-6-Stat3 pathway. Hepatology. 2013;58(1):158-70.

27. Navarro A, Diaz T, Martinez A, Gaya A, Pons A, Gel B, et al. Regulation of JAK2 by miR-135a: prognostic impact in classic Hodgkin lymphoma. Blood. 2009;114(14):2945-51.

28. Liu W, Wang X. Prediction of functional microRNA targets by integrative modeling of microRNA binding and target expression data. Genome Biol. 2019;20(1):18.

29. Bhavsar SP, Lokke C, Flaegstad T, Einvik C. Hsa-miR-376c-3p targets Cyclin D1 and induces G1-cell cycle arrest in neuroblastoma cells. Oncol Lett. 2018;16(5):6786-94.

30. Ramakers C, Ruijter JM, Deprez RH, Moorman AF. Assumption-free analysis of quantitative real-time polymerase chain reaction (PCR) data. Neurosci Lett. 2003;339(1):62-6.

31. Livak KJ, Schmittgen TD. Analysis of relative gene expression data using real-time quantitative PCR and the 2(-Delta Delta C(T)) Method. Methods. 2001;25(4):402-8.

32. Schindelin J, Arganda-Carreras I, Frise E, Kaynig V, Longair M, Pietzsch T, et al. Fiji: an open-source platform for biological-image analysis. Nature Methods. 2012;9(7):676-82.

33. Das S, Bryan K, Buckley PG, Piskareva O, Bray IM, Foley N, et al. Modulation of neuroblastoma disease pathogenesis by an extensive network of epigenetically regulated microRNAs. Oncogene. 2013;32(24):2927-36.

34. Schulte JH, Marschall T, Martin M, Rosenstiel P, Mestdagh P, Schlierf S, et al. Deep sequencing reveals differential expression of microRNAs in favorable versus unfavorable neuroblastoma. Nucleic Acids Res. 2010;38(17):5919-28.

35. Chen Y, Stallings RL. Differential patterns of microRNA expression in neuroblastoma are correlated with prognosis, differentiation, and apoptosis. Cancer Res. 2007;67(3):976-83.

36. Bray I, Bryan K, Prenter S, Buckley PG, Foley NH, Murphy DM, et al. Widespread dysregulation of MiRNAs by MYCN amplification and chromosomal imbalances in neuroblastoma: association of miRNA expression with survival. PLoS One. 2009;4(11):e7850.

37. Felsberg J, Yan PS, Huang TH, Milde U, Schramm J, Wiestler OD, et al. DNA methylation and allelic losses on chromosome arm 14q in oligodendroglial tumours. Neuropathol Appl Neurobiol. 2006;32(5):517-24.

38. Zhang L, Huang J, Yang N, Greshock J, Megraw MS, Giannakakis A, et al. microRNAs exhibit high frequency genomic alterations in human cancer. Proc Natl Acad Sci U S A. 2006;103(24):9136-41.

39. Geraldo MV, Nakaya HI, Kimura ET. Down-regulation of 14q32-encoded miRNAs and tumor suppressor role for miR-654-3p in papillary thyroid cancer. Oncotarget. 2017;8(6):9597-607.

40. Soriano A, Masanas M, Boloix A, Masiá N, París-Coderch L, Piskareva O, et al. Functional high-throughput screening reveals miR-323a-5p and miR-342-5p as new tumor-suppressive microRNA for neuroblastoma. Cellular and Molecular Life Sciences. 2019;76(11):2231-43.

41. R2-support. R2 Tutorials. 2019(Release 4.3.1).

42. Roth SA, Hald OH, Fuchs S, Lokke C, Mikkola I, Flaegstad T, et al. MicroRNA-193b-3p represses neuroblastoma cell growth via downregulation of Cyclin D1, MCL-1 and MYCN. Oncotarget. 2018;9(26):18160-79.

43. Roth SA. MicroRNAs and Drug Resistance in Neuroblastoma [PhD]. Tromsø: University of Tromsø; 2016.

44. Wake MS, Watson CJ. STAT3 the oncogene - still eluding therapy? FEBS J. 2015;282(14):2600-11.

45. Odate S, Veschi V, Yan S, Lam N, Woessner R, Thiele CJ. Inhibition of STAT3 with the Generation 2.5 Antisense Oligonucleotide, AZD9150, Decreases Neuroblastoma Tumorigenicity and Increases Chemosensitivity. Clin Cancer Res. 2017;23(7):1771-84.

46. Yu H, Pardoll D, Jove R. STATs in cancer inflammation and immunity: a leading role for STAT3. Nat Rev Cancer. 2009;9(11):798-809.

47. Matthay KK, Maris JM, Schleiermacher G, Nakagawara A, Mackall CL, Diller L, et al. Neuroblastoma. Nat Rev Dis Primers. 2016;2:16078.

48. Bouchie A. First microRNA mimic enters clinic. Nat Biotechnol. 2013;31(7):577.

49. Janssen HL, Reesink HW, Lawitz EJ, Zeuzem S, Rodriguez-Torres M, Patel K, et al. Treatment of HCV infection by targeting microRNA. N Engl J Med. 2013;368(18):1685-94.

50. Beg MS, Brenner AJ, Sachdev J, Borad M, Kang YK, Stoudemire J, et al. Phase I study of MRX34, a liposomal miR-34a mimic, administered twice weekly in patients with advanced solid tumors. Invest New Drugs. 2017;35(2):180-8.

Supplementary Materials

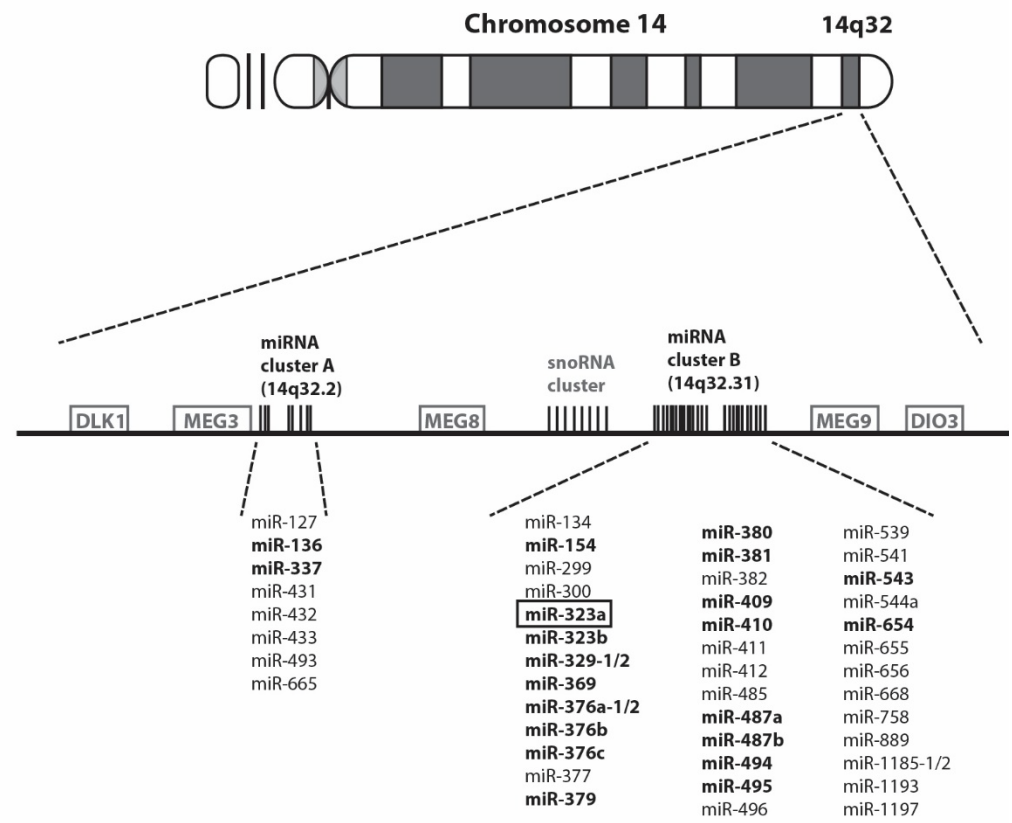

Supplementary figure 1: *Mir-323a*, located on chromosome 14q32, is differentially expressed in neuroblastoma cell line pairs. The miRNAs located on chromosome 14q32 region are upregulated or downregulated (bold type) in neuroblastoma cell line pairs. The miRNA of interest, *miR-323a* is highlighted in rectangular box. MEG, Maternally expressed; SnoRNA, Small nucleolar RNAs; DLK1, Delta like non-canonical notch ligand 1; DIO3, Iodothyronine deiodinase 3; miR, microRNA.

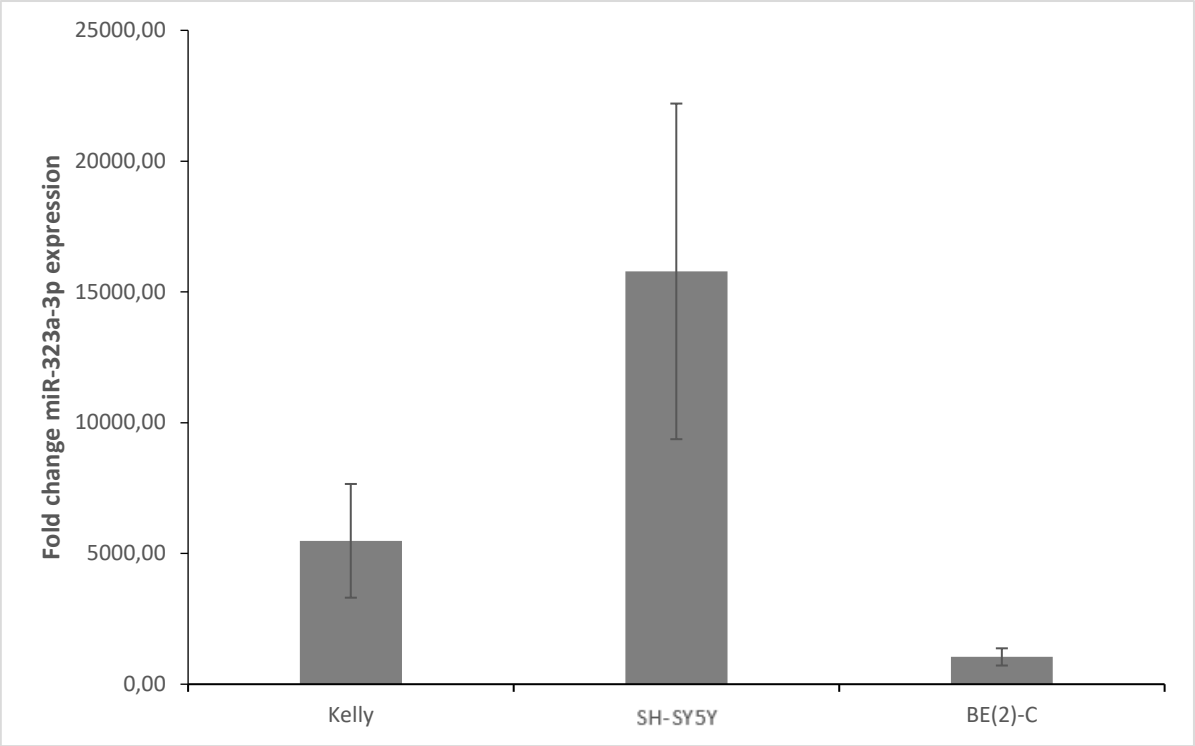

Supplementary figure 2: Transfection efficiency of *miR-323a-3p* in neuroblastoma cells. RT-qPCR analysis for confirmation of *miR-323a-3p* overexpression in Kelly, SH-SY5Y and BE(2)-C cell lines transfected with NC or *miR-323a-3p*. The expression of *miR-323a-3p* in NC transfected cells was set to 1 and *miR-4286* served as an endogenous control for miRNAs. Data are presented as mean ± SD. of two independent experiments, each repeated in triplicates.

A

miRNA	Gene	Gene description	Pred.	Valid.	Refs.
hsa-miR-323a-3p	BMP1	Bone morphogenetic protein 1	X		miRDB
hsa-miR-323a-3p	BMP3	Bone morphogenetic protein 3	X		miRDB
hsa-miR-323a-3p	BRI3	Brain protein I3		X	(1, 2)
hsa-miR-323a-3p	CDK6	Cyclin dependent kinase 6		X	(2)
hsa-miR-323a-3p	CDKN1B	Cyclin dependent kinase inhibitor 1B	X		miRDB
hsa-miR-323a-3p	CDK19	Cyclin dependent kinase 19	X		miRDB
hsa-miR-323a-3p	SMAD2	SMAD family member 2		X	(3-5)
hsa-miR-323a-3p	SMAD3	SMAD family member 3		X	(4, 5)
hsa-miR-323a-3p	SMAD5	SMAD family member 5	X		miRDB
hsa-miR-323a-3p	TGFA	Transforming growth factor alpha		X	(3)
hsa-miR-323a-3p	TGFB2	Transforming growth factor beta 2	X		miRDB
hsa-miR-323a-3p	STAT3	Signal transducer and activator of transcription 3	X		miRDB

Abbreviations: Pred., predicted; Valid., validated; Refs., references

B

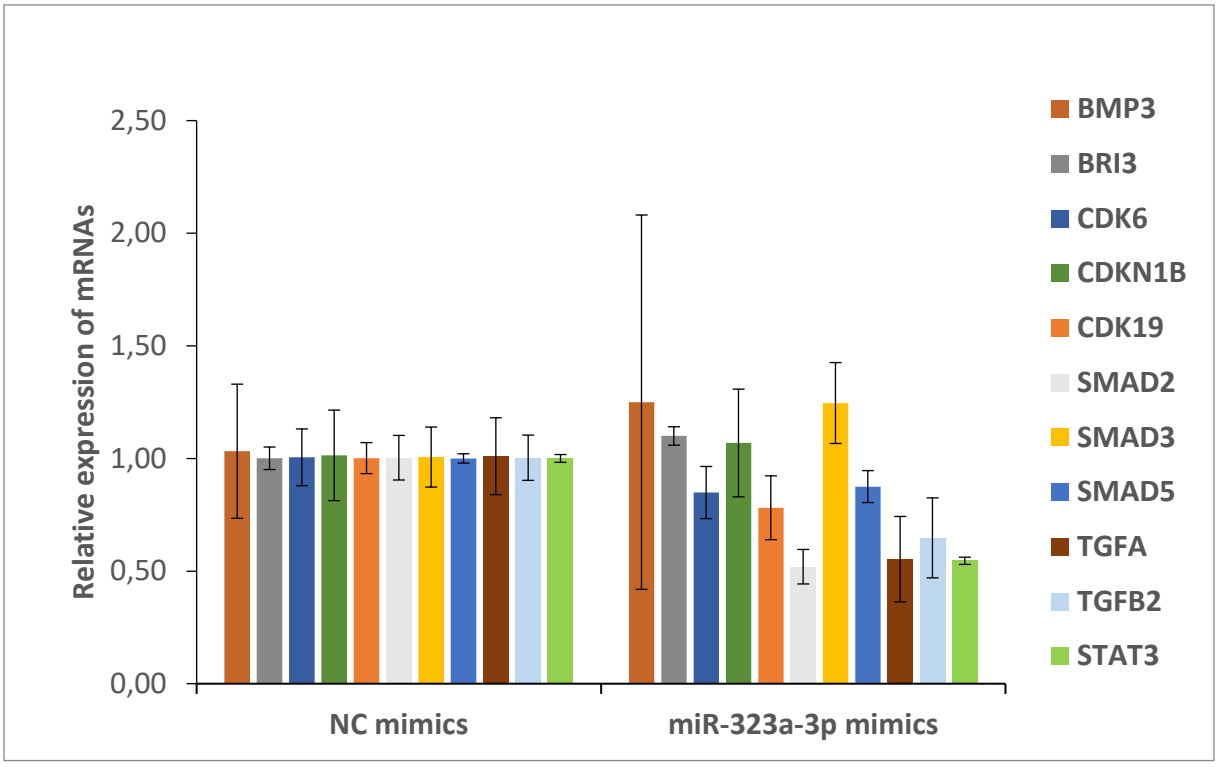

Supplementary figure 3: Screening of selected *miR-323a-3p* targets in the cell line Kelly. **A)** Selected list of predicted or validated (as direct targets by luciferase 3'UTR assay) targets of *miR-323a-3p*. **B)** RT-qPCR analysis for screening of *miR-323a-3p* targets in Kelly cell line transfected with NC or *miR-323a-3p* mimics. The expression of *miR-323a-3p* in NC transfected cells was set to 1 and *miR-4286* served as an endogenous control for miRNAs. Data are presented as mean ± SD of each experiment repeated in triplicates.

References for Supplementary Figure 3

1. Yang L, Xiong Y, Hu X-F, Du Y-H. MicroRNA-323 regulates ischemia/reperfusion injury-induced neuronal cell death by targeting BRI3. International journal of clinical and experimental pathology. 2015;8(9):10725-33.

2. Zhang H, Wang X, Chen X. Potential Role of Long Non-Coding RNA ANRIL in Pediatric Medulloblastoma Through Promotion on Proliferation and Migration by Targeting miR-323. Journal of Cellular Biochemistry. 2017;118(12):4735-44.

3. Ge L, Habiel DM, Hansbro PM, Kim RY, Gharib SA, Edelman JD, et al. miR-323a-3p regulates lung fibrosis by targeting multiple profibrotic pathways. JCI insight. 2016;1(20):e90301-e.

4. Kärner J, Wawrzyniak M, Tankov S, Runnel T, Aints A, Kisand K, et al. Increased microRNA-323-3p in IL-22/IL-17-producing T cells and asthma: a role in the regulation of the TGF-β pathway and IL-22 production. Allergy. 2017;72(1):55-65.

5. Wang C, Liu P, Wu H, Cui P, Li Y, Liu Y, et al. MicroRNA-323-3p inhibits cell invasion and metastasis in pancreatic ductal adenocarcinoma via direct suppression of SMAD2 and SMAD3. Oncotarget. 2016;7(12):14912-24.

Manuscript II

Hsa-miR-193b-3p Sensitizes MCL-1 Primed Neuroblastoma Cells to the BH3 Mimetic ABT-737

Lotte Olsen[1*], Sarah Andrea Roth[1*], Cecilie Løkke[1], Trond Flægstad[2] and Christer Einvik[1,2]

[1] Pediatric Research Group, Department of Clinical Medicine, Faculty of Health Science, UiT The Arctic University of Norway, NO-9037 Tromsø, Norway

[2] Department of Pediatrics, Division of Child and Adolescent Health, UNN – University Hospital of North-Norway, NO-9038 Tromsø, Norway

*Authors have contributed equally to this work.

Abstract

Evading apoptosis is considered a hallmark of cancer. Members of the BCL-2 protein family are important candidate mediators of therapy response and represent viable therapeutic targets for restoring drug sensitivity in neuroblastoma. Many cancer cells develop a selective dependence on one or a few anti-apoptotic proteins for survival, which dictates the sensitivity towards BCL-2 antagonists, such as ABT-737. This is also the case for the pediatric solid cancer neuroblastoma. While BCL-2 primed neuroblastoma cells are sensitive, MCL-1 primed cells are resistant to ABT-737. However, resistance in MCL-1 primed cells may be overcome by MCL-1 silencing. We have previously demonstrated that *miR-193b-3p* downregulates *MCL-1* in neuroblastoma, thus hypothesized that this miRNA may help overcome resistance to ABT-737 in neuroblastoma with primary MCL-1 dependence. Indeed, *miR-193b-3p* increases sensitivity of SH-SY5Y and NLF cells (MCL-1 primed) to ABT-737 by targeting *MCL-1*. At higher ABT-737 concentrations and prolonged exposure, it also reduces the ABT-737-resistance in SK-N-AS cells (BH3-resistant). Conversely, in the BCL-2 primed cell line SMS-KAN *miR-193b-3p* hardly changes the cells' sensitivity to ABT-737. Interestingly, in another BCL-2 primed cell line, CHLA-20 we do see a certain effect, as *miR-193b-3p* alone and in combination with ABT-737 impair growth of this cell line. Therefore, introducing *miR-193b-3p* may represent a novel therapeutic strategy for high-risk neuroblastoma as monotherapy or in combination with small molecule BCL-2-family antagonists

Introduction

Induction of apoptosis occurs through two distinct pathways, the extrinsic and the intrinsic. An intricate balance between anti- and pro-apoptotic members of the BCL-2 family regulates the intrinsic pathway, which is also referred to as the mitochondrial pathway. To date, more than two dozen members of the BCL-2 protein family have been described (1). They are classified into three functional groups according to their anti-apoptotic or pro-apoptotic functions and the number of conserved amino acid sequence regions, commonly referred to as BCL-2 homology (BH) motifs (BH1-BH4) (2, 3). Multi-BH-domain members may either suppress (e.g. BCL-2, MCL-1, BCL-X_L, BCL-W, BFL-1 and BCL-B) or promote (e.g. BAX, BAK) apoptosis. Conversely, BH3-only proteins are exclusively pro-apoptotic, and function through interaction with both anti-apoptotic BCL-2 family members and the pro-apoptotic multi-domain members BAK and BAX. These BH3-only proteins (e.g. PUMA, tBID, BIM, NOXA, HRK, BMF, BIK and BAD) act as stress sensors that are activated through transcriptional or post-transcriptional processes in response to various stimuli. The fate of the cell rests on the balance between anti- and pro-apoptotic family members. When the scale tips in pro-apoptotic favor, apoptogenic proteins (e.g. cytochrome c) are released from the mitochondria to promote activation of caspases, the executioner of apoptosis (4).

Evading apoptosis is considered a hallmark of cancer (5). While tumor-initializing cells find ways to override checkpoints, established cancers produce therapy resistance mechanisms to avoid induction of apoptosis (6). Inherent stressors of malignant cells, like upregulation of oncogenes, high proliferation rate, nutritional deprivation and genomic instability, cause a constant bombardment of death signals (7, 8). In order to evade death, cancer cells mitigate distinct apoptotic signals, and by doing so become dependent on selected cellular features (6). Indeed, high levels of anti-apoptotic proteins, including MCL-1, BCL-2 and BCL-X_L, or silencing of pro-apoptotic members, such as BIM, PUMA and BAX, have been reported in several cancers (3). One particular survival mechanism is to halt death signals by sequestering BH3-only proteins with anti-apoptotic proteins (such as MCL-1 or BCL-2 bound to BIM). Cells are then considered to be “primed for death” because this state allows for rapid induction of apoptosis if the BH3-only activators are liberated (6, 9, 10).

In the childhood cancer neuroblastoma, studies have revealed that cancer cells maintain a competent apoptotic machinery and are primed for death through sequestration of BIM by anti-apoptotic proteins of the BCL-2 protein family. The pattern of BIM priming demonstrates a selective dependence on either MCL-1 or BCL-2 for survival, and predicts the response of

cells to small molecule BCL-2 antagonists such as the BAD mimetic ABT-737 (11, 12). While BCL-2 primed neuroblastoma cells are highly sensitive, MCL-1 primed cell lines are more resistant to BCL-2 antagonists (12). However, recent studies have revealed that *MCL-1* silencing increases the sensitivity of MCL-1 primed neuroblastoma cell lines to ABT-737 (13-15).

MicroRNAs (miRNAs) are small, endogenous RNA molecules that silence gene expression through binding of mRNA (16). In neuroblastoma, *miR-193b-3p* has been found downregulated in cell lines from patients with relapsed disease compared to cell lines from the same patients at diagnosis (17); while patients' data indicate low expression of *miR-193b* in primary tumors (18). Additional functional analyses suggest a tumor suppressive function of the *miR-193b-3p* and we have previously shown that endogenous *miR-193b-3p* downregulates *MCL-1* in neuroblastoma (18). The latter led us to hypothesize that *miR-193b-3p* could sensitize neuroblastoma cells with primary MCL-1 dependency to ABT-737. Indeed, the current study shows that *miR-193b-3p* reduces the apoptotic threshold in MCL-1 primed neuroblastoma cells in combination with ABT-737, partially through *MCL-1*-targeting. Interestingly, the miRNA also has some ability to sensitize cells with a primary BCL-2 addiction and cells formerly described as BH3-resistant (that is, cells where BH3-only proteins do not induce apoptosis, thus suggesting downstream resistance mechanisms).

Materials and Methods

Cell Lines

CHLA-20 cells (from Children's Oncology Group; COG) were grown in Iscove's Modified Dulbecco's Medium (Sigma) supplemented with 20% fetal bovine serum (FBS) (Gibco Thermo Fisher Scientific), 4 mM L-Glutamine (Sigma) and 1 × Insulin-Transferrin-Selenium (Gibco). SH-SY5Y, NLF, SMS-KAN (COG) and SK-N-AS (COG) cell lines were maintained in RPMI-1640 with 2mM L-Glutamine (Sigma) supplemented with 10% FBS. All cell lines were cultured at 37°C in a humidified incubator containing a 5% CO_2 atmosphere. The identity of the cell lines was confirmed by short tandem repeat (STR) profiling by the Center of Forensic Genetics, UiT The Arctic University of Norway, Norway. Cells were tested and confirmed negative for mycoplasma contamination using MycoAlert™ PLUS Mycoplasma Detection Kit (Lonza).

RNA Interference and Plasmids

Negative control (NC) and *miR-193b-3p* (193b) mimics from GenePharma were used to overexpress miRNA. ON TARGETplus non-targeting pool siRNA (siNC) and SMARTpool siRNA against *MCL-1* (siMCL-1) (Dharmacon) were transfected for *MCL-1*-silencing experiments. MCL-1 overexpression plasmid lacking the 3'untranslated region (UTR) was kindly provided by Anthony Faber. Empty pcDNA3.1 vector (Invitrogen) was used as negative control. A miRCURY LNA miRNA Power Target Site Blocker (QIAGEN) was designed to block target recognition of *miR-193b-3p* on the following predicted *MCL-1* sequence: 5'-GGCCAGU-3' (***supplementary figure 1***).

Transient Transfection and Treatment with Drugs

Apart from the experiments using the target site blocker, which were transiently transfected the day after seeding, all neuroblastoma cell lines were reverse transfected using Lipofectamine 2000 (Thermo Fisher Scientific) suspended in Opti-MEM™ (Gibco) according to the manufacturer's instructions. Twenty-five nanomolar of either mimics or siRNAs were used. Plasmids were transfected at a concentration of 0,5 µg/ml. For the target site blocker, a concentration of 5 nM was applied. Twenty-four hours post-transfection, medium was replaced by fresh medium supplemented with indicated concentrations of ABT-737 (Selleck Chemicals). Dimethyl sulfoxide (DMSO) was used as vehicle, and subjected to untreated cells.

Cell Viability Assay

Cell viability was evaluated with alamarBlue® (Thermo Fisher Scientific). Briefly, 1/10th volume of alamarBlue® reagent was added directly to cells in culture and incubated at 37°C for three hours. One hundred microliter of supernatant was then collected from each well, transferred to a black-walled 96-well plate and fluorescence was monitored at 540 nm excitation wavelength and 590 nm emission wavelength in a microplate reader (CLARIOstar, BMG LABTECH).

Caspase Assay

Caspase 3/7 activity as an indicator of apoptosis was determined using the Caspase-Glo 3/7 Assay (Promega). One volume of Caspase-Glo 3/7 reagent was added directly to cells in culture and incubated at room temperature for 90 minutes. One hundred microliter of supernatant was then collected from each well, transferred to a white-walled 96-well plate and luminescence was measured in a microplate reader (CLARIOstar, BMG LABTECH).

Western Blot Analysis

For isolation of protein, cells in suspension were collected and subsequently pooled with the corresponding adherent cells detached by trypsin. After centrifugation at 200 g for 5 min, cell pellets were washed with phosphate-buffered saline (PBS), re-centrifuged and lysed in RIPA buffer (50 mM Tris-HCl pH 8, 150 mM NaCl, 1% NP-40, 0.5% sodium deoxycholate, 0.1% SDS) supplemented with 1 x Protein Inhibitor Cocktail (Roche) and 1 mM dithiothreitol (Sigma-Aldrich). Lysates were cleared with centrifugation, before total protein concentrations were determined using the DC^{TM}Protein Assay Kit (Bio-Rad) according to the manufacturer's recommendation.

An amount of 20-40 µg of protein in NuPAGE® LDS Sample Buffer (Thermo Fisher Scientific) was separated on NuPAGE® Novex 4-12% Bis-Tris precast polyacrylamide gels (Thermo Fisher Scientific) and subsequently electroblotted onto Immobilon-FL PVDF membrane (Millipore). PVDF membranes were blocked in Odyssey blocking buffer (LI-COR Biosciences) for 1 hour at room temperature, and incubated overnight at 4°C with primary antibodies diluted in Odyssey blocking buffer supplemented with SDS and Tween®20 (Sigma-Aldrich). The membranes were washed 4 x 5 min with PBS added 0,1% Tween®20 before and after being treated with the secondary antibodies goat Rabbit IgG (H&L) Antibody DyLight™ 800 Conjugated 1:5000 (Rockland Immunochemicals) and goat anti-mouse IgG (H+L) Alexa Fluor 680 1:5000 (Thermo Fisher Scientific) for 1 hour at room temperature. Antibody-binding

was detected on the Odyssey CLx infrared imaging system (LI-COR). Primary antibody specifications are listed in ***table 1***. For a semi-quantitative determination of protein amounts, images were processed in ImageJ (19) (available at imagej.net) and normalized with actin as a loading control.

Antibody	Epitope	Origin	Dilution	Supplier
PARP-1 (9542)	Human full length and cleaved PARP-1	Rabbit, polyclonal	1:1000	Cell Signaling Technology
MCL-1 (4572S)	Human MCL-1	Rabbit, polyclonal	1:1000	Cell Signaling Technology
Actin (ab3280)	Human actin	Mouse, monoclonal	1:2000	Abcam

Table 1: Primary antibodies used in this study.

Reverse Transcription Quantitative-Polymerase Chain Reaction

Total RNA was isolated using TRIzol® (Thermo Fisher Scientific) according to the manufacturer's instructions. Purity and concentration of RNA was determined photometrically on a NanoDrop™ 2000 spectrophotometer (Thermo Fisher Scientific).

Complementary DNA (cDNA) from miRNA was synthesized using miScript II RT Kit (QIAGEN). In short, 1 µg total RNA was brought to a volume of 12 µl with deionized water. Two microliters of miScript Reverse Transcriptase Mix and 2 µl of miScript Nucleics Mix diluted in 4 µl of 5 x miScript HiSpec Buffer were added to each sample. Reverse transcription (RT) was performed at 37°C for 60 minutes followed by 95°C for 5 minutes to terminate the reaction. The resulting cDNA was diluted with deionized water to achieve a concentration of 1 ng/µl.

MiScript SYBR® Green PCR Kit (QIAGEN) was used for quantitative polymerase chain reaction (qPCR). Each 10 µl reaction composed of 1 µl cDNA equivalent to 1 ng cDNA, 2 µl water, 5 µl QuantiTect SYBR Green, 1 µl 10 x Universal primers and 1 µl 10 x specific miScript primers. Hs_miR-193b_3p (cat. no. MS00031549) and Hs_RNU6-2_11 (cat. no. MS00033740) miScript Primer Assay (QIAGEN) were used to determine *miR-193b-3p* expression and as a reference gene, respectively. Amplifications were carried out in the LightCycler 96 SW 1.1 (Roche). The ΔΔCq method (20) was applied to calculate expression of *miR-193b-3p*. To confirm amplification specificity, a melting curve was generated after the completion of the amplification reaction.

Statistical Analysis

GraphPad Prism 5 was used for statistical analysis and designing of graphs. Data are presented as mean ± standard deviation (SD) of two or more independent experiments. To calculate statistical significance of the observed differences we applied the Student's t-test. P*<0.05 was considered statistically significant.

Results

Priming State of Neuroblastoma Cell Lines Dictates Sensitivity to ABT-737

The BAD analogue ABT-737 (21) has previously been shown to induce more anti-tumorigenic effect on cells and tumors with a primary BCL-2 dependence than those with MCL-1 dependence (6, 22). Subjecting five cell lines that harbor different priming states to increasing concentrations of ABT-737 presented concurring results. By accessing viability (***figure 1A***) and caspase 3/7 activity (***figure 1B***) we observed that SK-N-AS cells, formerly characterized as BH3-resistant (6), are almost unaffected by ABT-737, whereas the BCL-2 primed cell line SMS-KAN is highly sensitive. Although less impervious than SK-N-AS, both SH-SY5Y and NLF (MCL-1 primed) display a resistant profile, as anticipated. CHLA-20 has previously been described as a BCL-2 primed cell line (6), but is not as sensitive to ABT-737 as SMS-KAN. Nevertheless, BH3-resistant and MCL-1 primed cells are less affected by ABT-737 than BCL-2 primed cells.

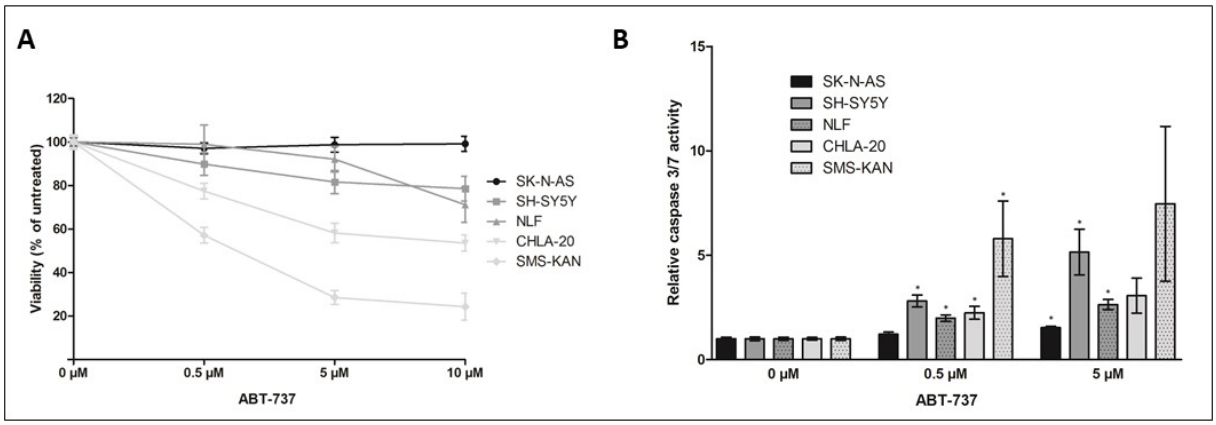

Figure 1: ABT-737 differentially affects the cell viability and caspase 3/7 activity of neuroblastoma cells based on apoptotic priming state. A) Measurement of cell viability of neuroblastoma cells after 24 hours treatment with different concentrations of ABT-737. Cell viability is presented as the percentage of untreated cells. **B)** Caspase 3/7 activity in neuroblastoma cell lines after treatment with different concentrations of ABT-737. Caspase 3/7 activity was calculated relative to untreated cells. Both graphs represent mean ± SD of at least two independent experiments performed in triplicates. *$p \leq 0.05$ marks statistical significance of ABT-737 treatment compared to untreated cells.

Overexpression of *miR-193b-3p* Increases Apoptosis in Neuroblastoma Cells.

We have previously shown that *miR-193b-3p* induces apoptosis in neuroblastoma cells (18). In concordance with this, introduction of *miR-193b-3p* mimics caused poly (ADP-ribose) polymerase-1 (PARP-1) cleavage in all cell lines (***figure 2A, supplementary figure 2***) and increased caspase 3/7 activity in SH-SY5Y, NLF and CHLA-20 by 4.4-, 2.4- and 1.6-fold, respectively (***figure 2B***), which are indicative of apoptosis. No change in caspase activity were observed in SK-N-AS and SMS-KAN.

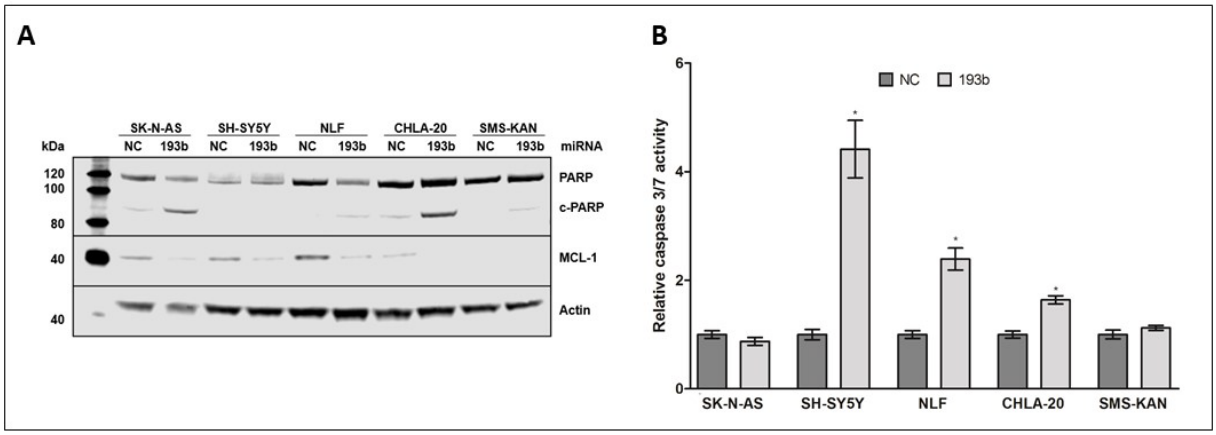

Figure 2: Induction of apoptosis in neuroblastoma cells upon ectopic expression of *miR-193b-3p.* Five neuroblastoma cell lines were transfected with *miR-193b-3p* (193b) or negative control (NC) mimics, and incubated for 48 hours. **A)** Protein expression of full-length PARP-1 (PARP), cleaved PARP-1 (c-PARP), MCL-1 and actin on western blot. Depicted is a representative blot of at least three independent experiments. Quantification of c-PARP is presented in supplementary figure 2A **B)** Caspase 3/7 activity relative to NC-transfected cells. Graph represents mean ± SD of at least two independent experiments performed in triplicates. *$p \leq 0.05$ marks statistical significance of *miR-193b-3p* overexpression.

MiR-193b-3p Sensitizes MCL-1 Primed Cell Lines to ABT-737

Others have demonstrated that small interfering RNA (siRNA)-mediated knockdown of *MCL-1* will increase the sensitivity of MCL-1 primed neuroblastoma cell lines to ABT-737 (13-15). Based on this and our own observation of *miR-193b-3p*-induced *MCL-1* downregulation (***figure 2A*** and (18)), we speculated that *miR-193b-3p* would sensitize MCL-1 primed, but not BCL-2 primed neuroblastoma cells to ABT-737. To investigate this, cells were transfected with either negative control (NC) or *miR-193b-3p* (193b) mimics and treated with different concentrations of ABT-737. Overexpression of *miR-193b-3p* was confirmed by RT-qPCR (***supplementary figure 3***). Exposing SH-SY5Y and NLF cells to 0.5 µM ABT-737 reduced cell viability significantly more in *miR-193b-3p*-transfected cells than in the control cells (***figure 3A and D***). Furthermore, in SH-SY5Y cells 0.5 and 5 µM ABT-737 increased caspase 3/7 activity by 2.8- and 5.2-fold, whereas in *miR-193b-3p* overexpressing cells the caspase 3/7 activity increased by 7.9- and 9.2-fold relative to untreated NC-transfected cells (***figure 3B***). In NLF cells, we also observed greater caspase activity at 0.5 µM ABT-737 in *miR-193b-3p* transfected cells than in NC-transfected cells (***figure 3E***). However, at a higher concentration there was no difference, perhaps indicating a plateau for caspase activity. At all concentrations tested, PARP-1 cleavage increased compared to NC-transfected cells (***figure 3C and F, supplementary figure 4A and B***). This indicates that *miR-193b-3p* restores sensitivity towards ABT-737 through induction of apoptosis in these two MCL-1 primed cell lines.

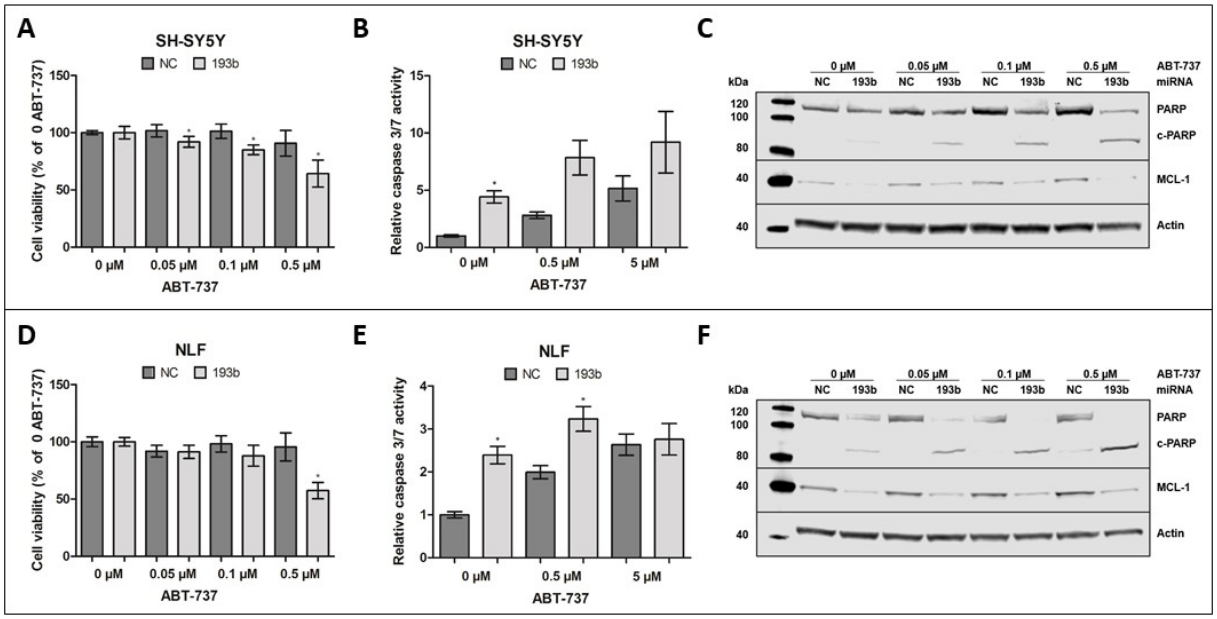

Figure 3: **MCL-1 primed cell lines, SH-SY5Y and NLF, transfected with *miR-193b-3p* mimics and treated with different concentrations of ABT-737.** SH-SY5Y and NLF cells were transfected with *miR-193b-3p* (193b) or negative control (NC) mimics, before being treated with ABT-737 the next day. Twenty-four hours post-treatment cell viability, caspase 3/7 activity and protein expression were measured. **A)** Cell viability measured in SH-SY5Y cells. Cell viability data are normalized to NC- or 193b mimic transfection alone, and therefore, the additional decrease in cell viability observed with combination treatment reflects an interaction between *miR-193b-3p* and ABT-737 treatment. **B)** Caspase 3/7 activity relative to NC-transfected, untreated SH-SY5Y cells. **C)** Western blot presenting full-length PARP-1 (PARP), PARP-1 cleavage (c-PARP), MCL-1 and actin protein expression in SH-SY5Y. Depicted are representative blots of at least three independent experiments. **D)** Cell viability, **E)** caspase 3/7 activity, and **F)** protein expression measured in NLF the same way as in SH-SY5Y. Graphs represent mean ± SD of at least two independent experiments performed in triplicates. *$p \leq 0.05$ marks statistical significance of *miR-193b-3p* overexpression compared to NC-transfected cells with the same treatment. Quantification of c-PARP is presented in supplementary figure 4A and B.

As expected, transfection of *miR-193b-3p* mimics into the known BCL-2 primed cell line SMS-KAN hardly influenced sensitivity to ABT-737. Minimal difference in cell viability or apoptosis were seen between control- and *miR-193b-3p* transfected SMS-KAN cells treated with various concentrations of ABT-737 (***figure 4A-C, supplementary figure 4C***). In the second BCL-2 primed cell line, CHLA-20, viability loss was more profound in ABT-737-treated cells transfected with *miR-193b-3p* than control mimics (***figure 4D***), and PARP-1 cleavage was higher at low drug concentrations (***figure 4F, supplementary figure 4D***). However, although caspase 3/7 activity increased in a dose dependent manner, there was no marked difference between *miR-193b-3p*- and NC-transfected cells (***figure 4E***). Nevertheless, these results indicate an increased sensitization also in this cell line. Furthermore, contrary to SMS-KAN this cell line does express detectable levels of MCL-1 protein (***figure 2A***).

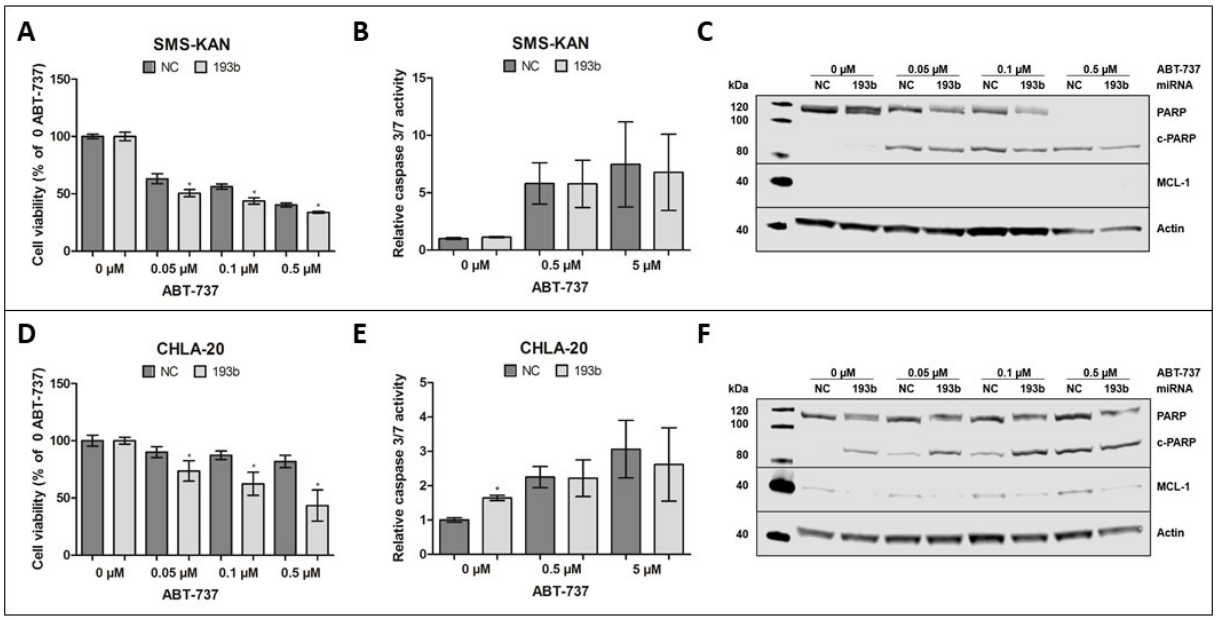

Figure 4: **The BCL-2 primed cell lines, SMS-KAN and CHLA-20, transfected with *miR-193b-3p* mimics and treated with different concentrations of ABT-737.** Measurement of **A)** cell viability **B)** caspase 3/7 activity and **C)** protein expression in SMS-KAN and **D)-F)** CHLA-20 performed in the same way as in figure 3. Graphs represent mean ± SD of at least two independent experiments performed in triplicates. *$p \leq 0.05$ marks statistical significance of *miR-193b-3p* overexpression compared to NC-transfected cells with the same treatment. Depicted western blots are representative blots of at least three independent experiments. Quantification of c-PARP is presented in supplementary figure 4C and D.

In the BH3-resistant cell line SK-N-AS we observed no effect of ABT-737 at concentrations used for the other cell lines. However, at extremely high concentrations (10 µM after 24h exposure, and 5 and 10 µM after 48h exposure) of ABT-737 we observed a minor reduction in the viability of *miR-193b-3p*-transfected cells (***figure 5A, supplementary figure 5***). Interestingly, despite the minimal impact on viability the apoptotic pathway appeared to be activated. Caspase 3/7 activity increased 1.5-fold more in *miR-193b-3p*-transfected than in control cells when subjected to 5 µM ABT-737 (***figure 5B***), whereas augmented PARP-1 cleavage was observed at all concentrations tested (***figure 5C, supplementary figure 4E***). These results demonstrate that higher concentrations and longer treatment-duration of ABT-737 are necessary to sensitize *miR-193b-3p*-transfected SK-N-AS cells. Thus, *miR-193b-3p* overexpressing SK-N-AS cells still display a relatively resistant profile.

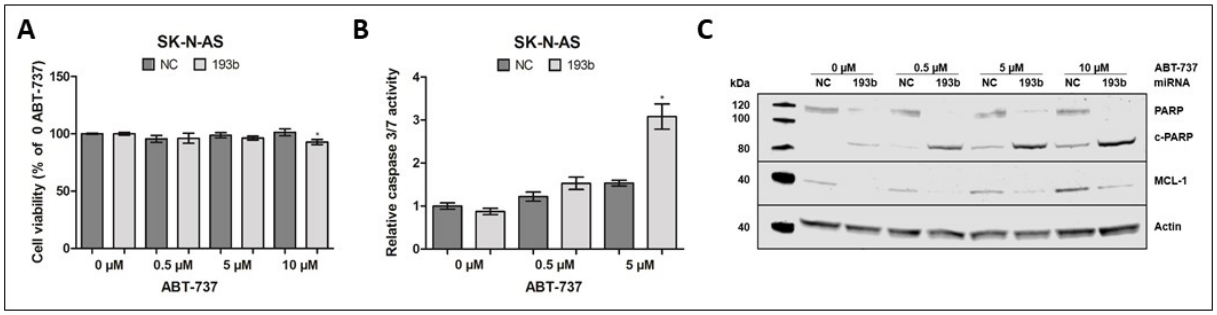

Figure 5: The BH3-resistant cell line, SK-N-AS, transfected with *miR-193b-3p* mimics and treated with different concentrations of ABT-737. Measurement of **A)** cell viability **B)** caspase 3/7 activity and **C)** protein expression in SK-N-AS performed in the same way as in figure 3. Graphs represent mean ± SD of at least two independent experiments performed in triplicates. *p $\leq$ 0.05 marks statistical significance of *miR-193b-3p* overexpression compared to NC-transfected cells with the same treatment. Depicted western blot is a representative blot of at least three independent experiments. Quantification of c-PARP is presented in supplementary figure 4E.

Increased Sensitivity to ABT-737 can be Attributed to *miR-193b-3p* Induced *MCL-1* Downregulation

To investigate if the *miR-193b-3p*-induced sensitization to ABT-737 indeed can be attributed to *MCL-1* downregulation, we first transfected SH-SY5Y, SMS-KAN and CHLA-20 cells with anti-*MCL-1* siRNA (siMCL-1), and evaluated viability and PARP-1 cleavage. All three cell lines presented a phenotype similar to that observed when overexpressing *miR-193b-3p* (***figure 6, supplementary figure 6***). Secondly, co-transfection of *miR-193b-3p* and an MCL-1 overexpression plasmid without the 3'UTR in NLF and SH-SY5Y partially rescued loss of viability induced by ABT-737 and the miRNA in NLF (***figure 7A***), but not in SH-SY5Y (***figure 7B***). However, the SH-SY5Y cells transfected with control plasmid did not show the same level of viability loss that we normally observed when combining *miR-193b-3p* overexpression and ABT-737. The results in NLF indicate that there are *miR-193b-3p* binding sites within the 3'UTR of *MCL-1*, and that this miRNA-mRNA interaction is involved in establishment of the phenotype we observed in MCL-1 primed cells. The target prediction softwares TargetScan (23) (available at targetscan.org) and miRDB (24, 25) (available at mirdb.org) suggest a highly conserved putative site for *miR-193b-3p* in the *MCL-1* 3'UTR (***supplementary figure 1***). In order to block this site, we designed a locked nucleic acid (LNA) antisense oligonucleotide ("target site blocker"; TSB) specific for this miRNA-mRNA interaction. Obstruction of the site revoked the effect on viability from combining *miR-193b-3p* and ABT-737 in both NLF (***figure 7C***) and SH-SY5Y (***figure 7D***). Together, these findings propose that the increased sensitivity to ABT-737 observed after introducing *miR-193b-3p* overexpression can, at least in part, be credited to *MCL-1* downregulation. Moreover, while *miR-193b-3p* reduced viability itself in SH-SY5Y and CHLA-20 (***supplementary figure 7A***), equal viability loss was not observed

with transfection of siMCL-1 (***supplementary figure 7B***), suggesting that *miR-193b-3p* probably convey additional anti-growth effects unrelated to targeting *MCL-1*.

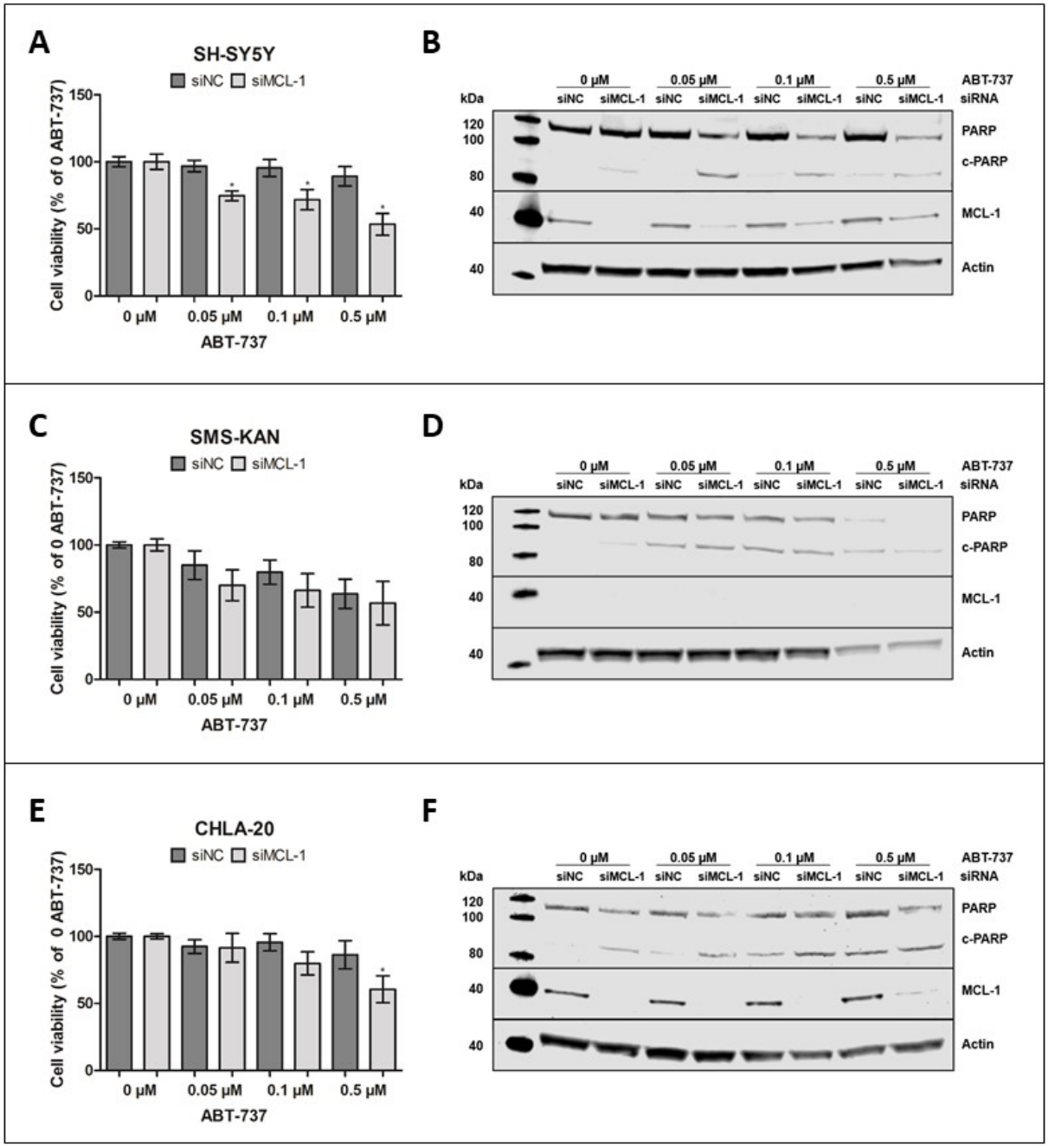

Figure 6: Cells transfected with anti-*MCL-1* siRNA and treated with different concentrations of ABT-737. SH-SY5Y, SMS-KAN and CHLA-20 cells were transfected with anti-MCL-1 (siMCL-1) or negative control (siNC) siRNA, before being treated with different concentrations of ABT-737 the next day. Twenty-four hours post-treatment viability and protein expression were measured. Graphs represent measurement of cell viability in **A)** SH-SY5Y, **C)** SMS-KAN and **E)** CHLA-20. Cell viability data are normalized to NC- or 193b mimic transfection. Graphs represent mean ± SD of at least three independent experiments performed in triplicates. *p $\leq$ 0.05 marks statistical significance of *miR-193b-3p* overexpression compared to NC-transfected cells with the same treatment. Protein expression of full-length PARP-1 (PARP), cleaved PARP-1 (c-PARP), MCL-1 and actin assessed on western blot in the cell lines **B)** SH-SY5Y, **D)** SMS-KAN and **F)** CHLA-20. Depicted western blots are representative blots of at least three independent experiments. Quantification of c-PARP is presented in supplementary figure 6.

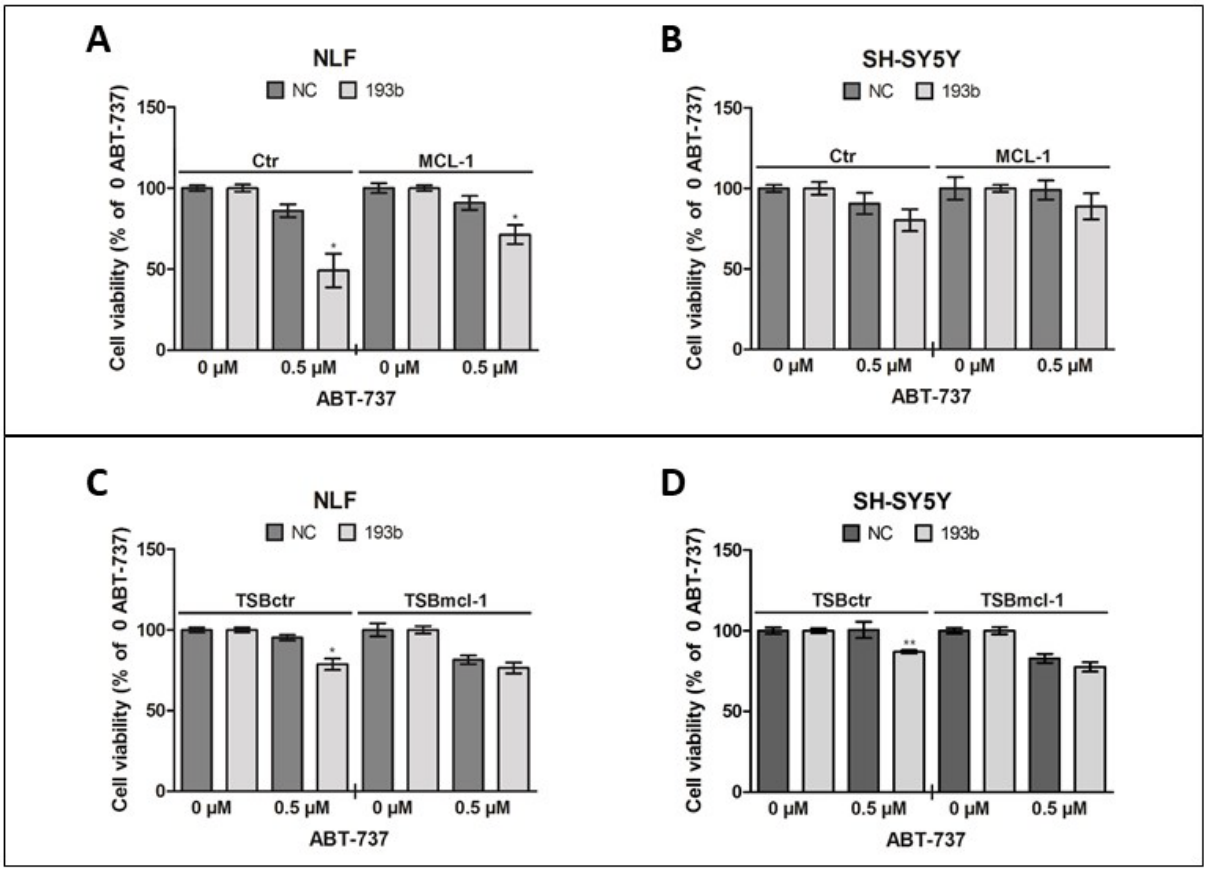

Figure 7: *miR-193b-3p*-mediated repression of *MCL-1* sensitizes MCL-1 primed neuroblastoma cell lines to ABT-737. **A)** NLF and **B)** SH-SY5Y cells were co-transfected with *miR-193b-3p* (193b) or negative control (NC) mimics and an MCL-1 overexpression plasmid lacking the 3'UTR or a control plasmid (Ctr), before being treated with 0.5 µM ABT-737 the next day. Twenty-four hours post-treatment, cell viability was measured. **C)** NLF and **D)** SH-SY5Y cells were co-transfected with 193b or NC mimics and a target site blocker (TSB) that should specifically perturb the *miR-193b-3p/MCL-1* interaction at a predicted site, or a non-targeting control. The cells were treated with 0.5 µM ABT-737. Twenty-four hours post-treatment cell viability was measured. Graphs represent mean ± SD of at least two independent experiments performed in triplicates. Cells not treated with ABT-737 are set to 100%. *$p \leq 0.05$ marks statistical significance of *miR-193b-3p* overexpression compared to NC-transfected cells with the treatment.

Discussion

Survival rate for high-risk neuroblastoma patients is a dismal 40-50%, despite multimodal treatment (26, 27), and progressive therapy resistance is one of the main reasons for treatment failure and relapse in this patient group (28). Finding alternative ways to combat this disease is therefore imperative. Since evasion of apoptosis is a classical feature of malignant cells, creating drugs that can reintroduce apoptosis is an appealing strategy. Small molecule drugs that sequester specific anti-apoptotic proteins to allow abundant pro-apoptotic proteins to transmit death signal have been developed and show promising results.

Induction of apoptosis by the BCL-2 antagonist ABT-737 is carried out by displacement of BCL-2 from BIM, allowing BIM to activate BAX/BAK (6) Our analyzes of the ABT-737 resistance profile in a selection of cell lines support the assumption that sensitivity to this inhibitor is affected by the cell's selective dependence on specific anti-apoptotic proteins. SMS-KAN and CHLA-20 were the most sensitive of the five neuroblastoma cell lines investigated, as expected, since others have demonstrated that they are BCL-2 primed cell lines where BIM is sequestered by BCL-2 (6). The fact that CHLA-20 showed a more resistant phenotype than SMS-KAN can possibly be attributed to low BAX/BAK levels (11). Both NLF and SH-SY5Y probably hold a primary dependence upon MCL-1 (22, 29). In concordance with other studies (22, 29, 30) these cell lines were quite resistant to ABT-737 treatment. Although the primed state of SH-SY5Y has not yet been described *per se*, its parental cell line SK-N-SH is a well-defined MCL-1 primed cell line (11). We therefore presume that the same apply to SH-SY5Y cells. Furthermore, we have previously demonstrated that *miR-193b-3p* induced apoptosis in SH-SY5Y cells by downregulating *MCL-1*, and that siRNA against *MCL-1* increased PARP-1 cleavage (18). These findings support our presumption that SH-SY5Y cells are MCL-1 primed. As anticipated, SK-N-AS was highly resistant to ABT-737. Goldsmith *et al.* have found that the SK-N-AS cell line retain BIM priming similar to MCL-1 primed neuroblastoma cell lines, but shows repressed apoptotic signaling downstream of MCL-1 sequestration, thereby characterizing it as BH3-resistant (11). Thus, treatment of SK-N-AS cells with AT-101, a small molecule antagonist that binds and inhibits MCL-1, had only a minimal effect in SK-N-AS at doses that were cytotoxic to other MCL-1 primed cell lines (12).

Silencing of MCL-1, using siRNA or MCL-1 targeting drugs in cells and tumors dependent on MCL-1, have been shown to increase sensitivity to ABT-737 (13-15). As *miR-193b-3p* targets this anti-apoptotic protein (18, 31-33), we postulated that the miRNA would restore sensitivity to ABT-737 in the two MCL-1 primed cell lines SH-SY5Y and NLF, whereas

BCL-2 primed cells would not be equally affected. Indeed, magnitude of viability loss in the MCL-1 primed cell lines after treatment with 0.5 μM ABT-737 was higher upon *miR-193b-3p* overexpression than in control cells, due to induction of apoptosis, in contrast to SMS-KAN where ABT-737 caused apoptosis and reduced viability regardless of *miR-193b-3p* levels. Interestingly, despite being reported as a BCL-2 primed cell line (6), CHLA-20 did become sensitive to ABT-737 upon *miR-193-3p* overexpression, resembling the MCL-1 primed cell lines SH-SY5Y and NLF. A similar result was observed when CHLA-20 was treated with anti-*MCL-1* siRNAs. The latter indicates that even though this is a predominantly BCL-2 primed cell line, it possibly retains partial dependence on MCL-1, as seen for other cell lines (29). Furthermore, in control cells, we observed that ABT-737 appeared to increase protein expression of MCL-1 in the cell lines that expressed this protein (**figure 3C and F, 4F, 5C**). In breast cancer, a similar observation has been reported for the clinical analogue of ABT-737, ABT-263 (34). This can indicate that the cells compensate for BCL-2 sequestration by increasing MCL-1 expression. In CHLA-20 this compensation can perhaps make cells more dependent on MCL-1 during ABT-737 treatment, thus explaining the more MCL-1 primed-like phenotype similar to SH-SY5Y and NLF. As SMS-KAN do not express MCL-1 at all (**figure 4C**), this compensation does not occur in this cell line. Moreover, we have previously observed that *miR-193b-3p* has a pro-apoptotic effect, independent of MCL-1, in CHLA-20 (18). This was supported by findings where overexpression of MCL-1 did not rescue the apoptogenic effect of *miR-193b-3p.* The inherent trait of miRNAs to bind partially complimentary to its targets yield a vast targetome. Additionally, expression of miRNAs and their targets are highly cell- and tissue specific (35). The increased sensitivity towards ABT-737 in CHLA-20 upon *miR-193b-3p* overexpression is therefore probably explained by the miRNA's influence on both *MCL-1* and other targets.

When measuring viability in SK-N-AS, ectopic *miR-193b-3p* did not sensitize cells to low doses of ABT-737 after 24 hours, but caused a slight reduction in resistance to high doses after 48 hours. These findings are in concordance with a study by Boiani *et al.* where they demonstrated that *MCL-1* silencing using siRNA had no effect on viability in SK-N-AS (14). Despite having no impact on viability at 5 μM, ABT-737 induced both a solid increase in caspase 3/7 activation and PARP-1 cleavage when combined with *miR-193b-3p* overexpression. This may suggest a resistance mechanism downstream of PARP-1 cleavage. Caspase-induced cleavage of PARP-1 results in an 89 kDa and a 24 kDa product. Albeit will the first product promote apoptosis, but the latter can have the opposite effect (36). One could

speculate if an expedited degradation of the larger fragment could cause a propensity towards survival. Regardless, defects in the apoptotic signaling downstream of MCL-1 may explain why *miR-193b-3p* had a reduced effect of ABT-737 sensitivity in SK-N-AS as compared to SH-SY5Y and NLF cells. Taken together, we demonstrate that *miR-193b-3p* sensitizes MCL-1 primed neuroblastoma cell lines to the BCL-2 inhibitor ABT-737.

Since *miR-193b-3p* downregulated *MCL-1*, affected ABT-737 sensitivity primarily in MCL-1 primed cells, and we observed phenotypic similarities between introducing *miR-193b-3p* and siRNA against *MCL-1*, we postulated that *miR-193b-3p*-mediated ABT-737-sensitization takes place through downregulation of *MCL-1*. To confirm this, we co-transfected MCL-1 dependent cells with *miR-193b-3p* and an MCL-1 overexpression plasmid lacking the 3'UTR to analyze if MCL-1 restoration may rescue the *miR-193b-3p*-mediated effect. Surely, viability of *miR-193b-3p* overexpressing NLF cells were improved upon transfection with the MCL-1 plasmid, indicating that *miR-193b-3p* increases sensitivity to ABT-737 through silencing of *MCL-1*. The rescue was not complete, though, suggesting additional mechanisms. Failure to demonstrate the same in SH-SY5Y might be a result of lower transfection efficiency, as magnitude of viability loss were less than we observed with miRNA mimic transfection alone. Yet, reduced binding of endogenous *miR-193b-3p* might be the cause of the augmentation in viability we observe with MCL-1 overexpression. There is a putative binding site for *miR-193b-3p* in the 3'UTR of *MCL-1*, which is functional in breast cancer (31). To determine if this site is functional in neuroblastoma and to see if blocking it would abolish the *miR-193b-3p* effect on ABT-737 sensitivity, we designed LNA antisense oligonucleotides complementary to the *miR-193b-3p* binding site. These target site blockers (TSB) will specifically abrogate the *miR-193b-3p/MCL-1*-interaction if the site is functional (37). Certainly, in both SH-SY5Y and NLF the difference in viability were abolished. Although we have to confirm that the abrogated miRNA-mRNA interaction is the cause of this abolishment and not an off-target effect of the TSB, our results argue that *miR-193b-3p* increases ABT-737 sensitivity of MCL-1 primed cells partially through silencing of *MCL-1*.

Preclinical studies with ABT-737 have revealed a diverse anti-tumor activity in a wide range of cancers, including myeloma (38, 39), glioblastoma (40), acute myeloid and lymphoblastic leukemia (41-43) and neuroblastoma (11, 12, 14, 30, 44). This has led to progression into clinical trials. ABT-263 (Navitoclax), an orally bioavailable derivate of ABT-737, have displayed significantly anti-tumor effect in patients with chronic lymphocytic leukemia (CLL) (3, 45, 46). However, since BCL-X_L has an essential role in apoptosis of

platelets (47), this compound cause thrombocytopenia in the majority of patients (48, 49). To avoid this adverse effect, a modified version (ABT-199; Venetoclax) that exclusively targets BCL-2 has been created (50). This second generation BH3 mimetic is now approved for treatment of patients with CLL and small lymphocytic lymphoma (SLL) (51, 52).

Analogous to *in vitro* observations, preclinical studies in neuroblastoma have demonstrated a low threshold for apoptosis in BCL-2 primed xenografts and limited effect in MCL-1 primed xenografts when exposed to BCL-2 antagonists. However, even though BCL-2 antagonists display a potent anti-tumor effect *in vivo*, it has been shown beneficial to combine it with cytotoxic drugs to simultaneously induce cell death by several distinct mechanisms. Subjecting mice that harbor BCL-2 primed tumors to ABT-737 or ABT-199 monotherapy led to tumor regression and increased overall survival, but complete regression was only observed when the treatment was combined with cyclophosphamide (11, 53). As we and others have shown for MCL-1 primed cells and tumors a compelling strategy to maximizing treatment efficacy and sensitizing intrinsic resistant tumors to BCL-2 antagonists can be to combine them with drugs that neutralize MCL-1. In recent years, miRNA-based anticancer therapeutics have received growing attention, and promising advances indicate that substitution of tumor suppressive miRNAs could become a novel treatment strategy in cancer therapy (54-57). To date, there are limited research done to assess the potential of combining BCL-2 antagonists and miRNA replacement therapy. A study by Lam *et al.* identified a panel of miRNAs that could restore the ability of ABT-263-resistant cells to undergo apoptosis when treated with ABT-263 (58). Another study by Chen *et al.* demonstrated that ABT-737 alone induced apoptosis in melanoma cells, but introduction of *miR-193b-3p* significantly enhanced the effect of ABT-737 (32). Our data support that miRNA replacement therapy in combination with BCL-2-targeting strategies may be a promising therapeutic approach to treat human cancer. Furthermore, although *miR-193b-3p* did not profoundly increase sensitivity of the BCL-2 primed cell line SMS-KAN to ABT-737, it indeed has effect on cell viability. It significantly impairs cell growth by inducing G1 cell cycle arrest (18).

Conclusion

In this study, we have demonstrated how upregulation of *miR-193b-3p* increases sensitivity to the BH3 mimetic ABT-737 in neuroblastoma cells with primary dependence on MCL-1. The results presented here and in our former study advocate a therapeutic potential for *miR-193b-3p* in neuroblastoma, either as monotherapy or in combination with clinical analogues of ABT-737 in MCL-1 dependent tumors.

Declarations

Funding

This study was supported by grants from the UiT The Arctic University of Tromsø, The Northern-Norwegian Health Authorities (Helse Nord), The University Hospital of North Norway (UNN), Barnekreftforeningen and Simon Fougner Hartmanns Familiefond.

Authors' contributions

LO, SR and CE designed the research. LO, SR and CL performed the experimental work. CE and TF supervised the experimental work. LO and SR wrote the manuscript. CE critically amended the manuscript. The final manuscript was read and approved by all the authors.

Acknowledgements

We would like to thank Dr. John Inge Johnsen, Childhood Cancer Research Unit, Department of Women's and Children's Health, Karolinska Institutet, 171 76 Stockholm, Sweden for providing us with the SH-SY5Y cell line, and Dr. Frank Speleman, Center for Medical Genetics Ghent, Cancer Research Institute Ghent, B-9000 Ghent, Belgium for the NLF cell line.

References

1. Warren CFA, Wong-Brown MW, Bowden NA. BCL-2 family isoforms in apoptosis and cancer. Cell Death & Disease. 2019;10(3):177.

2. Vela L, Marzo I. Bcl-2 family of proteins as drug targets for cancer chemotherapy: the long way of BH3 mimetics from bench to bedside. Current opinion in pharmacology. 2015;23:74-81.

3. Delbridge AR, Grabow S, Strasser A, Vaux DL. Thirty years of BCL-2: translating cell death discoveries into novel cancer therapies. Nature reviews Cancer. 2016;16(2):99-109.

4. Suvarna V, Singh V, Murahari M. Current overview on the clinical update of Bcl-2 anti-apoptotic inhibitors for cancer therapy. European Journal of Pharmacology. 2019;862:172655.

5. Hanahan D, Weinberg Robert A. Hallmarks of Cancer: The Next Generation. Cell. 2011;144(5):646-74.

6. Goldsmith KC, Gross M, Peirce S, Luyindula D, Liu X, Vu A, et al. Mitochondrial Bcl-2 family dynamics define therapy response and resistance in neuroblastoma. Cancer Research. 2012;72(10):2565-77.

7. Certo M, Moore VDG, Nishino M, Wei G, Korsmeyer S, Armstrong SA, et al. Mitochondria primed by death signals determine cellular addiction to antiapoptotic BCL-2 family members. Cancer Cell. 2006;9(5):351-65.

8. Montero J, Letai A. Why do BCL-2 inhibitors work and where should we use them in the clinic? Cell Death And Differentiation. 2017;25:56.

9. Delbridge ARD, Grabow S, Strasser A, Vaux DL. Thirty years of BCL-2: translating cell death discoveries into novel cancer therapies. Nature Reviews Cancer. 2016;16:99.

10. García-Sáez AJ. The secrets of the Bcl-2 family. Cell Death And Differentiation. 2012;19:1733.

11. Goldsmith KC, Gross M, Peirce S, Luyindula D, Liu X, Vu A, et al. Mitochondrial Bcl-2 family dynamics define therapy response and resistance in neuroblastoma. Cancer research. 2012;72(10):2565-77.

12. Goldsmith KC, Lestini BJ, Gross M, Ip L, Bhumbla A, Zhang X, et al. BH3 response profiles from neuroblastoma mitochondria predict activity of small molecule Bcl-2 family antagonists. Cell death and differentiation. 2010;17(5):872-82.

13. Lestini BJ, Goldsmith KC, Fluchel MN, Liu X, Chen NL, Goyal B, et al. Mcl1 downregulation sensitizes neuroblastoma to cytotoxic chemotherapy and small molecule Bcl2-family antagonists. Cancer Biol Ther. 2009;8(16):1587-95.

14. Boiani M, Daniel C, Liu X, Hogarty MD, Marnett LJ. The stress protein BAG3 stabilizes Mcl-1 protein and promotes survival of cancer cells and resistance to antagonist ABT-737. The Journal of biological chemistry. 2013;288(10):6980-90.

15. Klymenko T, Brandenburg M, Morrow C, Dive C, Makin G. The Novel Bcl-2 Inhibitor ABT-737 Is More Effective in Hypoxia and Is Able to Reverse Hypoxia-Induced Drug Resistance in Neuroblastoma Cells. Molecular Cancer Therapeutics. 2011;10(12):2373.

16. O'Brien J, Hayder H, Zayed Y, Peng C. Overview of MicroRNA Biogenesis, Mechanisms of Actions, and Circulation. Frontiers in Endocrinology. 2018;9(402).

17. Roth SA, Knutsen E, Fiskaa T, Utnes P, Bhavsar S, Hald ØH, et al. Next generation sequencing of microRNAs from isogenic neuroblastoma cell lines isolated before and after treatment. Cancer Letters. 2016;372(1):128-36.

18. Roth SA, Hald ØH, Fuchs S, Løkke C, Mikkola I, Flægstad T, et al. MicroRNA-193b-3p represses neuroblastoma cell growth via downregulation of Cyclin D1, MCL-1 and MYCN. Oncotarget. 2018;9(26):18160-79.

19. Schindelin J, Arganda-Carreras I, Frise E, Kaynig V, Longair M, Pietzsch T, et al. Fiji: an open-source platform for biological-image analysis. Nature Methods. 2012;9(7):676-82.

20. Livak KJ, Schmittgen TD. Analysis of Relative Gene Expression Data Using Real-Time Quantitative PCR and the 2−ΔΔCT Method. Methods. 2001;25(4):402-8.

21. Oltersdorf T, Elmore SW, Shoemaker AR, Armstrong RC, Augeri DJ, Belli BA, et al. An inhibitor of Bcl-2 family proteins induces regression of solid tumours. Nature. 2005;435(7042):677-81.

22. Goldsmith KC, Lestini BJ, Gross M, Ip L, Bhumbla A, Zhang X, et al. BH3 Response Profiles From Neuroblastoma Mitochondria Predict Activity of Small Molecule Bcl-2 Family Antagonists. Cell death and differentiation. 2010;17(5):872-82.

23. Agarwal V, Bell GW, Nam J-W, Bartel DP. Predicting effective microRNA target sites in mammalian mRNAs. eLife. 2015;4:e05005.

24. Liu W, Wang X. Prediction of functional microRNA targets by integrative modeling of microRNA binding and target expression data. Genome Biology. 2019;20(1):18.

25. Wong N, Wang X. miRDB: an online resource for microRNA target prediction and functional annotations. Nucleic Acids Research. 2014;43(D1):D146-D52.

26. Maris JM. Recent advances in neuroblastoma. The New England journal of medicine. 2010;362(23):2202-11.

27. Pinto NR, Applebaum MA, Volchenboum SL, Matthay KK, London WB, Ambros PF, et al. Advances in Risk Classification and Treatment Strategies for Neuroblastoma. Journal of Clinical Oncology. 2015;33(27):3008-17.

28. Maris JM. Recent Advances in Neuroblastoma. New England Journal of Medicine. 2010;362(23):2202-11.

29. Lestini BJ, Goldsmith KC, Fluchel MN, Liu X, Chen NL, Goyal B, et al. Mcl1 downregulation sensitizes neuroblastoma to cytotoxic chemotherapy and small molecule Bcl2-family antagonists. Cancer biology & therapy. 2009;8(16):1587-95.

30. Klymenko T, Brandenburg M, Morrow C, Dive C, Makin G. The novel Bcl-2 inhibitor ABT-737 is more effective in hypoxia and is able to reverse hypoxia-induced drug resistance in neuroblastoma cells. Molecular cancer therapeutics. 2011;10(12):2373-83.

31. Long J, Ji Z, Jiang K, Wang Z, Meng G. miR-193b Modulates Resistance to Doxorubicin in Human Breast Cancer Cells by Downregulating MCL-1. Biomed Res Int. 2015;2015:373574-.

32. Chen J, Zhang X, Lentz C, Abi-Daoud M, Paré GC, Yang X, et al. miR-193b Regulates Mcl-1 in Melanoma. The American Journal of Pathology. 2011;179(5):2162-8.

33. Mao K, Zhang J, He C, Xu K, Liu J, Sun J, et al. Restoration of miR-193b sensitizes Hepatitis B virus-associated hepatocellular carcinoma to sorafenib. Cancer Letters. 2014;352(2):245-52.

34. Williams MM, Elion DL, Rahman B, Hicks DJ, Sanchez V, Cook RS. Therapeutic inhibition of Mcl-1 blocks cell survival in estrogen receptor-positive breast cancers. Oncotarget. 2019;10(52).

35. Mestdagh P, Lefever S, Pattyn F, Ridzon D, Fredlund E, Fieuw A, et al. The microRNA body map: dissecting microRNA function through integrative genomics. Nucleic Acids Research. 2011;39(20):e136-e.

36. Castri P, Lee Y-j, Ponzio T, Maric D, Spatz M, Bembry J, et al. Poly(ADP-ribose) polymerase-1 and its cleavage products differentially modulate cellular protection through NF-kB-dependent signaling. Biochimica et Biophysica Acta (BBA) - Molecular Cell Research. 2014;1843(3):640-51.

37. Louloupi A, Ørom UAV. Inhibiting Pri-miRNA Processing with Target Site Blockers. In: Ørom UAV, editor. miRNA Biogenesis: Methods and Protocols. New York, NY: Springer New York; 2018. p. 63-8.

38. Trudel S, Stewart AK, Li Z, Shu Y, Liang SB, Trieu Y, et al. The Bcl-2 family protein inhibitor, ABT-737, has substantial antimyeloma activity and shows synergistic effect with dexamethasone and melphalan. Clinical cancer research : an official journal of the American Association for Cancer Research. 2007;13(2 Pt 1):621-9.

39. Kline MP, Rajkumar SV, Timm MM, Kimlinger TK, Haug JL, Lust JA, et al. ABT-737, an inhibitor of Bcl-2 family proteins, is a potent inducer of apoptosis in multiple myeloma cells. Leukemia : official journal of the Leukemia Society of America, Leukemia Research Fund, UK. 2007;21(7):1549-60.

40. Tagscherer KE, Fassl A, Campos B, Farhadi M, Kraemer A, Bock BC, et al. Apoptosis-based treatment of glioblastomas with ABT-737, a novel small molecule inhibitor of Bcl-2 family proteins. Oncogene. 2008;27(52):6646-56.

41. Konopleva M, Contractor R, Tsao T, Samudio I, Ruvolo PP, Kitada S, et al. Mechanisms of apoptosis sensitivity and resistance to the BH3 mimetic ABT-737 in acute myeloid leukemia. Cancer cell. 2006;10(5):375-88.

42. High LM, Szymanska B, Wilczynska-Kalak U, Barber N, O'Brien R, Khaw SL, et al. The Bcl-2 homology domain 3 mimetic ABT-737 targets the apoptotic machinery in acute lymphoblastic leukemia resulting in synergistic in vitro and in vivo interactions with established drugs. Mol Pharmacol. 2010;77(3):483-94.

43. Del Gaizo Moore V, Schlis KD, Sallan SE, Armstrong SA, Letai A. BCL-2 dependence and ABT-737 sensitivity in acute lymphoblastic leukemia. Blood. 2008;111(4):2300-9.

44. Laetsch TW, Liu X, Vu A, Sliozberg M, Vido M, Elci OU, et al. Multiple components of the spliceosome regulate Mcl1 activity in neuroblastoma. Cell death & disease. 2014;5:e1072.

45. Wilson WH, O'Connor OA, Czuczman MS, LaCasce AS, Gerecitano JF, Leonard JP, et al. Navitoclax, a targeted high-affinity inhibitor of BCL-2, in lymphoid malignancies: a phase 1 dose-escalation study of safety, pharmacokinetics, pharmacodynamics, and antitumour activity. The lancet oncology. 2010;11(12):1149-59.

46. Roberts AW, Seymour JF, Brown JR, Wierda WG, Kipps TJ, Khaw SL, et al. Substantial susceptibility of chronic lymphocytic leukemia to BCL2 inhibition: results of a phase I study of navitoclax in patients with relapsed or refractory disease. Journal of clinical oncology : official journal of the American Society of Clinical Oncology. 2012;30(5):488-96.

47. Zhang H, Nimmer PM, Tahir SK, Chen J, Fryer RM, Hahn KR, et al. Bcl-2 family proteins are essential for platelet survival. Cell Death & Differentiation. 2007;14(5):943-51.

48. Gandhi L, Camidge DR, Oliveira MRd, Bonomi P, Gandara D, Khaira D, et al. Phase I Study of Navitoclax (ABT-263), a Novel Bcl-2 Family Inhibitor, in Patients With Small-Cell Lung Cancer and Other Solid Tumors. Journal of Clinical Oncology. 2011;29(7):909-16.

49. Rudin CM, Hann CL, Garon EB, Ribeiro de Oliveira M, Bonomi PD, Camidge DR, et al. Phase II Study of Single-Agent Navitoclax (ABT-263) and Biomarker Correlates in Patients with Relapsed Small Cell Lung Cancer. Clinical Cancer Research. 2012;18(11):3163.

50. Souers AJ, Leverson JD, Boghaert ER, Ackler SL, Catron ND, Chen J, et al. ABT-199, a potent and selective BCL-2 inhibitor, achieves antitumor activity while sparing platelets. Nature Medicine. 2013;19(2):202-8.

51. EMA. Venclyxto: European Medicines Agency; 2019 [Available from: https://www.ema.europa.eu/en/medicines/human/summaries-opinion/venclyxto.

52. US.FDA. FDA approves venetoclax for CLL and SLL: U.S. Food and Drug Administration; 2019 [Available from: https://www.fda.gov/drugs/resources-information-approved-drugs/fda-approves-venetoclax-cll-and-sll.

53. Tanos R, Karmali D, Nalluri S, Goldsmith KC. Select Bcl-2 antagonism restores chemotherapy sensitivity in high-risk neuroblastoma. BMC Cancer. 2016;16:97.

54. Bouchie A. First microRNA mimic enters clinic. Nature biotechnology. 2013;31(7):577.

55. Bader AG. miR-34 - a microRNA replacement therapy is headed to the clinic. Frontiers in genetics. 2012;3:120.

56. Thorsen SB, Obad S, Jensen NF, Stenvang J, Kauppinen S. The therapeutic potential of microRNAs in cancer. Cancer journal (Sudbury, Mass). 2012;18(3):275-84.

57. Iorio MV, Croce CM. MicroRNA dysregulation in cancer: diagnostics, monitoring and therapeutics. A comprehensive review. EMBO molecular medicine. 2012;4(3):143-59.

58. Lam LT, Lu X, Zhang H, Lesniewski R, Rosenberg S, Semizarov D. A microRNA screen to identify modulators of sensitivity to BCL2 inhibitor ABT-263 (navitoclax). Molecular cancer therapeutics. 2010;9(11):2943-50.

Supplementary Figures

	Predicted consequential pairing of target region (top) and miRNA (bottom)
Position 327-334 of MCL1 3' UTR	5' ...UGAGAACAGGAAAGUGGCCAGUA...
hsa-miR-193b-3p	3' UCGCCCUGAAACUCCCGGUCAA

Supplementary figure 1: Putative target site for *miR-193b-3p* on *MCL-1* mRNA. According to the target prediction softwares TargetScan and miRDB there is a target site for human *miR-193b-3p* in the 3'UTR of *MCL-1*. The figure is copied from targetscan.org.

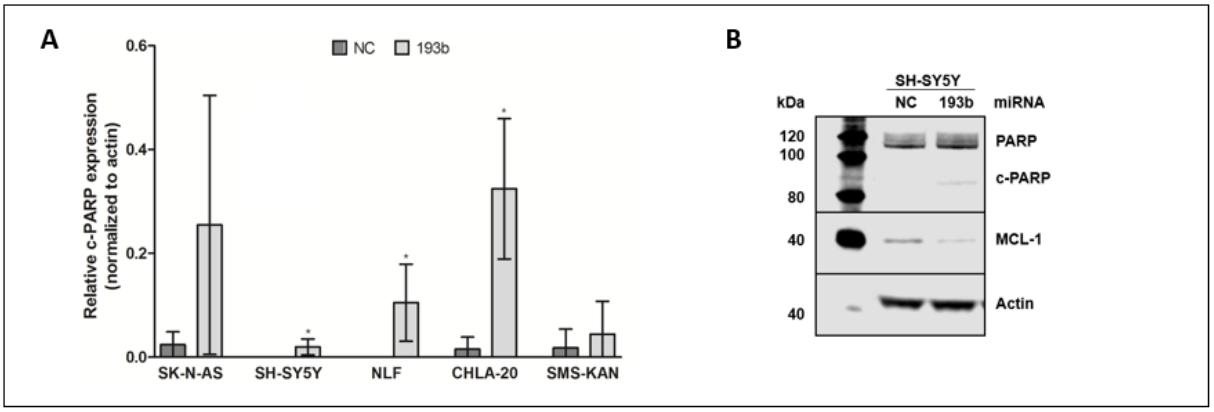

Supplementary figure 2: Relative expression of cleaved PARP-1 on western blot. A) Semi-quantitative ImageJ analyses of at least three western blots presented as relative cleaved PARP-1 protein expression normalized to actin. *p $\leq$0.05 marks statistical significance of *miR-193b-3p* overexpression compared to control cells. Representative blot is depicted in figure 2A. **B)** The same western blot as figure 2A, presented with higher exposure, depicts cleaved PARP-1 (c-PARP) in SH-SY5Y.

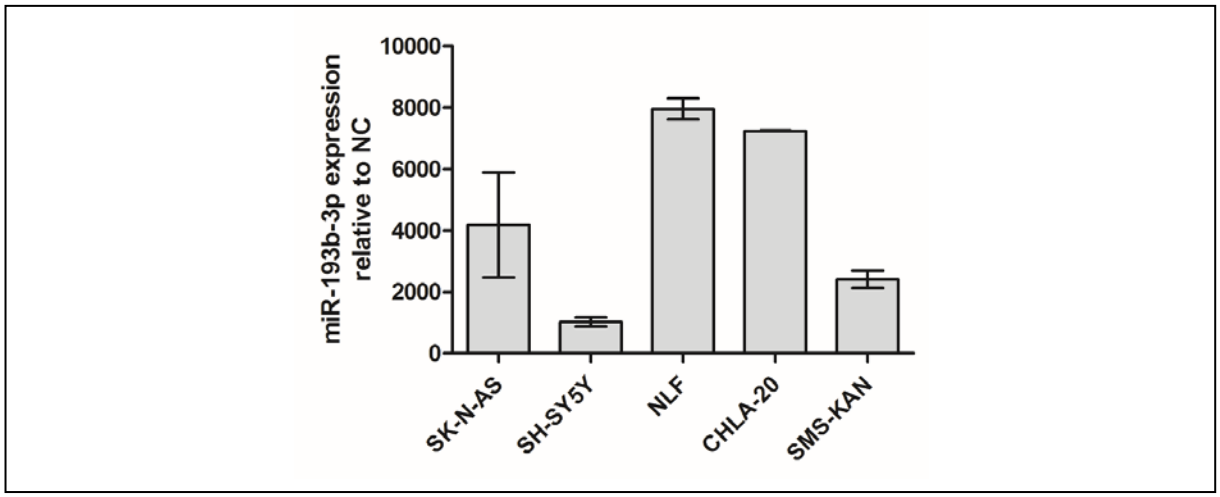

Supplementary figure 3: Confirmation of *miR-193b-3p* overexpression upon transfection with miRNA mimic. SK-N-AS, SH-SY5Y, NLF, CHLA-20 and SMS-KAN cells were transfected with *miR-193b-3p* or NC mimics. Forty-eight hours after transfection *miR-193b-3p* mRNA expression was measured with RT-qPCR. Expression was calculated with the ΔΔCq method using RNU6 as reference gene. Expression is relative to NC-transfected cells. Graph represent mean ± SD of two independent experiments performed in triplicates.

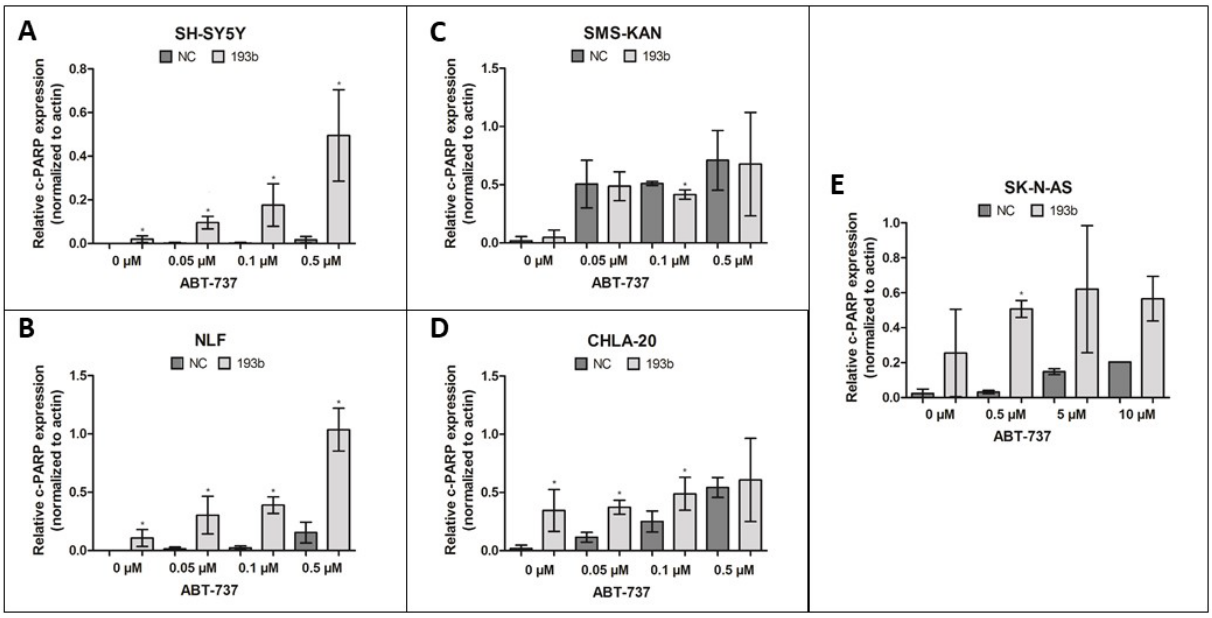

Supplementary figure 4: Relative expression of cleaved PARP-1 on western blot after transfection with miR-193b-3p or NC mimics and treatment with ABT-737. Semi-quantitative ImageJ analyses of at least three western blots, presented as relative cleaved PARP-1 protein expression normalized to actin in **A)** SH-SY5Y, **B)** NLF, **C)** SMS-KAN, **D)** CHLA-20 and **E)** SK-N-AS cells. *p ≤ 0.05 marks statistical significance of *miR-193b-3p* overexpression compared to control cells with the same treatment. Representative blots are depicted in figure 3C (SH-SY5Y), 3F (NLF), 4C (SMS-KAN), 4F (CHLA-20) and 5C (SK-N-AS).

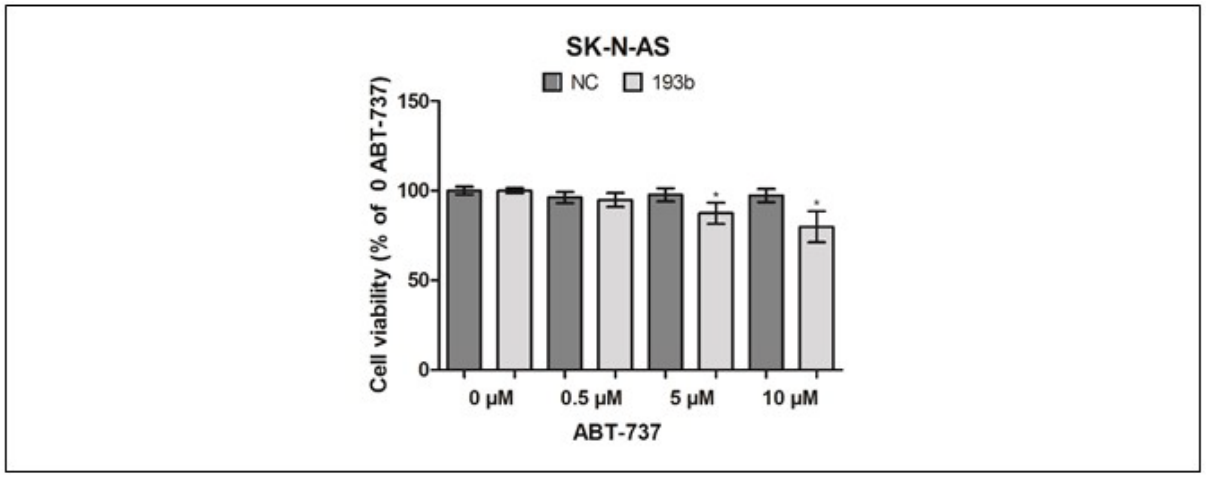

Supplementary figure 5: Cell viability in SK-N-AS cells after transfection with *miR-193b-3p* mimics and 48 hours treatment with ABT-737. SK-N-AS cells were transfected with miR-193b-3p (193b) or negative control (NC) mimics and treated with ABT-737 the next day. Forty-eight hours post-treatment, cell viability was measured. Cell viability data are normalized to NC- or 193b mimic transfection alone. Graph represent mean ± SD of at least three independent experiments performed in triplicates. *p ≤ 0.05 marks statistical significance of *miR-193b-3p* overexpression compared to NC-transfected cells with the same treatment.

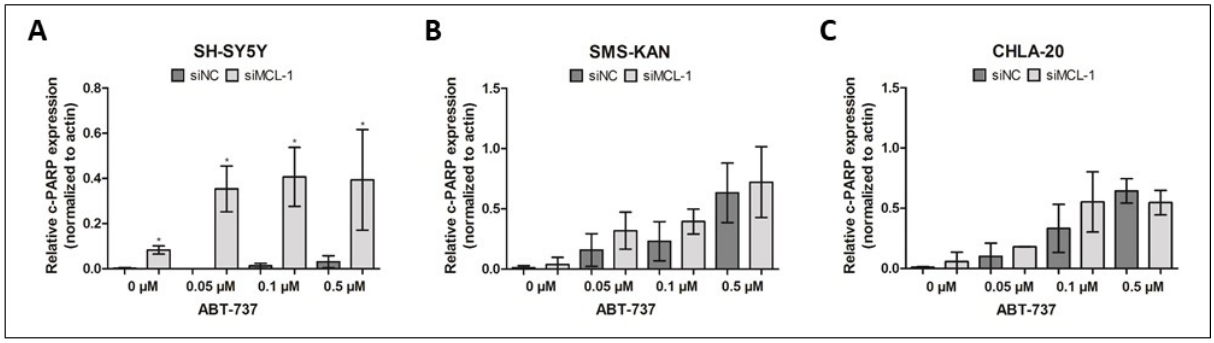

Supplementary figure 6: Relative expression of cleaved PARP-1 on western blot after transfection with anti-*MCL-1* siRNA and treatment with ABT-737. Semi-quantitative ImageJ analyses of at least three western blots, presented as relative cleaved PARP-1 protein expression normalized to actin in **A)** SH-SY5Y, **B)**, SMS-KAN, **C)** CHLA-20. *p ≤ 0.05 marks statistical significance of *MCL-1* downregulation compared to control cells with the same treatment. Representative blots are depicted in figure 6B (SH-SY5Y), 6D (SMS-KAN), 6F (CHLA-20).

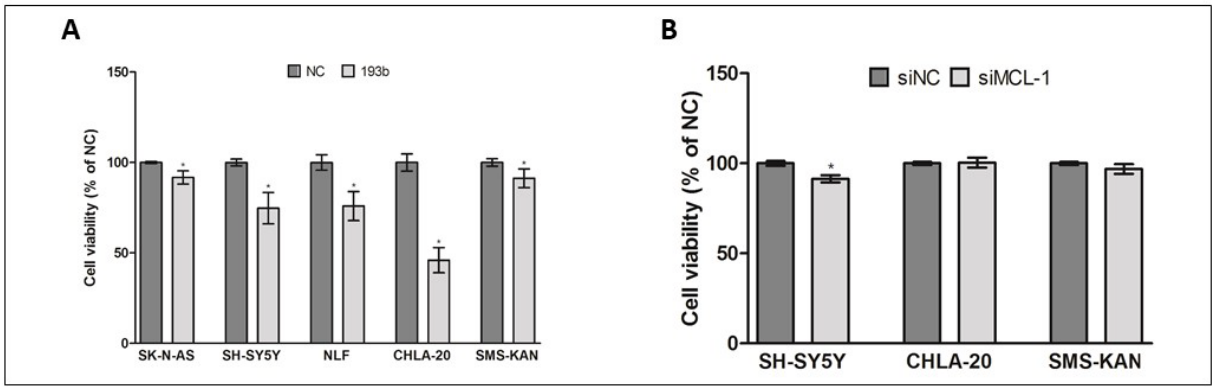

Supplementary figure 7: Cell viability in neuroblastoma cell lines after *miR-193b-3p* overexpression or MCL-1 downregulation. A) Cell viability measured 48 hours after transfection with either *miR-193b-3p* (193b) or negative control (NC) mimics in neuroblastoma cell lines. **B)** Cell viability measured 48 hours after transfection with siRNA directed against *MCL-1* (siMCL-1) or control siRNA (siNC) in three neuroblastoma cell lines. All values are presented as percentage relative to control mimics. Graphs represent mean ± SD of at least three independent experiments performed in triplicates. *p ≤ 0.05 marks statistical significance of *miR-193b-3p* overexpression or *MCL-1* downregulation compared to control cells.

Paper I

Oncogene (2019) 38:2800–2813
https://doi.org/10.1038/s41388-018-0611-7

ARTICLE

Inhibitors of ribosome biogenesis repress the growth of *MYCN*-amplified neuroblastoma

Øyvind H. Hald[1] · Lotte Olsen[2] · Gabriel Gallo-Oller[3] · Lotta Helena Maria Elfman[3] · Cecilie Løkke[2] · Per Kogner[3] · Baldur Sveinbjörnsson[3,4] · Trond Flægstad[1,2] · John Inge Johnsen[3] · Christer Einvik[1,2]

Received: 26 April 2018 / Revised: 27 September 2018 / Accepted: 23 November 2018 / Published online: 12 December 2018

Abstract

Abnormal increases in nucleolar size and number caused by dysregulation of ribosome biogenesis has emerged as a hallmark in the majority of spontaneous cancers. The observed ribosome hyperactivity can be directly induced by the *MYC* transcription factors controlling the expression of RNA and protein components of the ribosome. Neuroblastoma, a highly malignant childhood tumor of the sympathetic nervous system, is frequently characterized by *MYCN* gene amplification and high expression of *MYCN* and *c-MYC* signature genes. Here, we show a strong correlation between high-risk disease, *MYCN* expression, poor survival, and ribosome biogenesis in neuroblastoma patients. Treatment of neuroblastoma cells with quarfloxin or CX-5461, two small molecule inhibitors of RNA polymerase I, suppressed MycN expression, induced DNA damage, and activated p53 followed by cell cycle arrest or apoptosis. CX-5461 repressed the growth of established *MYCN*-amplified neuroblastoma xenograft tumors in nude mice. These findings suggest that inhibition of ribosome biogenesis represent new therapeutic opportunities for children with high-risk neuroblastomas expressing high levels of Myc.

Introduction

Neuroblastoma, a childhood tumor of the peripheral sympathetic nervous system, originates from neural crest cells and usually manifests in the adrenal gland or in a paraspinal location in the abdomen or chest. The clinical features of neuroblastoma are characterized by heterogeneity spanning from spontaneous regression or differentiation with an overall survival of 85–90%, to treatment-refractory progression and metastatic tumors with less than 50% of the patients surviving despite intensive therapies [1]. Currently, no effective therapy exists for patients with recurrent or relapsed neuroblastoma, and new treatment modalities for these patients are urgently needed.

A molecular hallmark of high-risk neuroblastoma is genetic amplification and high expression of the *MYCN* oncogene [2]. Also, single-copy high-risk neuroblastomas frequently show high expression of the *MYCN* homolog *c-MYC* [3]. The MycN and c-Myc proteins are transcription factors, and exert their oncogenic effects through the activation and repression of a wide array of genes controlling fundamental cellular processes, including proliferation, cell growth, metabolism, differentiation, and migration [4].

Ribosomal biogenesis is upregulated in malignant cells, and nucleolar enlargement has been used as a marker for the histopathological diagnosing of cancer for over a century [5]. MycN has been shown to positively regulate the expression of a large set of genes involved in ribosomal biogenesis [6], and also c-Myc is well-established as a driver of this process [7]. In line with these observations, tumor cells from *MYC*-driven neuroblastomas frequently

Supplementary information The online version of this article (https://doi.org/10.1038/s41388-018-0611-7) contains supplementary material, which is available to authorized users.

✉ Christer Einvik
christer.einvik@uit.no

[1] Department of Pediatrics, Division of Child and Adolescent Health, UNN – University Hospital of North-Norway, NO-9038 Tromsø, Norway

[2] Pediatric Research Group, Department of Clinical Medicine, Faculty of Health Science, The Arctic University of Norway – UiT, NO-9037 Tromsø, Norway

[3] Childhood Cancer Research Unit, Department of Women's and Children's Health, Karolinska Institutet, 171 76 Stockholm, Sweden

[4] Molecular Inflammation Research Group, Department of Medical Biology, Faculty of Health Science, The Arctic University of Norway – UiT, NO-9037 Tromsø, Norway

display nucleolar hypertrophy [8, 9]. In recent years, specific inhibitors of ribosomal biogenesis have been developed and characterized. Two small molecular compounds, quarfloxin (CX-3543) and CX-5461, target and inhibit RNA pol I activity. CX-5461 is currently being tested in patients with advanced solid tumors (NCT02719977) and advanced hematological cancer (ACTRN12613001061729) [10]. Quarfloxin has completed phase 1 and 2 trials in patients with advanced solid tumors and lymphomas (NCT00955786) and neuroendocrine/carcinoid tumors (NCT00780663), respectively. Inhibition of RNA pol I activity has been shown to induce apoptosis, nucleolar surveillance signaling, p53 pathway activation, senescence, and pro-death autophagy [11–14].

In this study, we demonstrate a strong correlation between advanced stage disease, high *MYCN* expression levels, and elevated expression of genes involved in ribosome biogenesis in several large neuroblastoma patient cohorts. Based on these observations, we evaluated the effects of quarfloxin and CX-5461, two small molecule inhibitors of ribosome biogenesis in neuroblastoma cell lines and xenografts. Both quarfloxin and CX-5461 are cytotoxic to neuroblastoma cells in nanomolar concentrations and orally administered CX-5461 represses the growth of *MYCN*-amplified neuroblastoma xenografts in mice. Mechanistically, we demonstrate that both compounds induce p53 signaling, cell cycle arrest, DNA damage, and apoptosis of neuroblastoma cells and reduced MycN and RNA pol I activity.

Results

Neuroblastoma tumors with high ribosome biogenesis activity have poor a prognosis

A previous study by Boon et al. showed that the MycN protein enhances the rate of ribosome biogenesis in neuroblastoma cell lines [6]. To investigate how genes regulating ribosome biogenesis correlate with clinical parameters in neuroblastoma, we performed an unsupervised clustering analysis (k-means clustering) to subdivide the tumors in a large neuroblastoma RNAseq dataset (SEQC-498) in two groups according to expression of genes defined by the KEGG pathway "Ribosome Biogenesis in Eukaryotes". The 498 neuroblastoma tumors clustered into two well-defined groups characterized by low (Low-RiBi, $n = 354$) and high (High-RiBi, $n = 144$) expression of ribosome biogenesis genes (Supplementary Figure 1). Eighty-five percent of tumors defined by the High-RiBi group belong to advanced stage disease (INSS 3 and 4) (Fig. 1a). Furthermore, the High-RiBi tumors were characterized by high *MYCN* expression (Fig. 1b). Kaplan–Meier analyses of the two clusters showed that tumors from the High-RiBi group had a very poor overall- and event-free survival (log-rank test, $p = 4.7 \times 10^{-32}$ and $p = 7.4 \times 10^{-20}$, respectively, Figure 1c, d). Similar results were observed for several independent neuroblastoma cohorts investigated (Supplementary Figure 2A–D). These data demonstrate that neuroblastoma tumors with enhanced ribosome biogenesis activity are characterized by high *MYCN* expression, advanced stage disease, and poor prognosis.

Inhibitors of ribosome biogenesis decrease neuroblastoma cell viability

Given that the expression of genes involved in ribosome biogenesis strongly correlated with neuroblastoma high-risk disease and prognosis, we evaluated the effects of two compounds inhibiting RNA polymerase I in a panel of neuroblastoma cells (Supplementary Table 1). Neuroblastoma cells were incubated with an 8-log dose range of CX-5461 (0.0005–5000 nM) or quarfloxin (0.001–10000 nM) for 48 h (Fig. 2a), and absolute IC_{50} values were calculated (Table 1). *MYCN*-amplified (MNA) and wild-type *TP53* (wt-*TP53*) IMR-32 and CHP-134 cells, and *c-MYC* overexpressing/wt-*TP53* CHLA-15 cells, were highly sensitive to the action of both drugs. Also, the IC_{50} of MNA/mut-*TP53* cell lines BE(2)-C and Kelly were substantially lower than those of non-MNA/mut-*TP53* SK-N-AS and SK-N-FI cells.

These data show that quarfloxin and CX-5461 effectively inhibit the growth of neuroblastoma cells in vitro. MNA (or high *c-Myc*) and wt-*TP53* cell lines were found to be more sensitive to these drugs compared with cells with single-copy *MYCN* and inactivating *TP53* mutations.

High MycN expression sensitizes neuroblastoma cell lines to quarfloxin and CX-5461

To further investigate the relationship between MycN expression and ribosome biogenesis in neuroblastoma cell lines, we reanalyzed microarray gene expression data from a previous *MYCN* siRNA experiment on IMR-32 cells performed by Bell et al. [15]. K-means clustering with all genes in the KEGG pathway "Ribosome Biogenesis in Eukaryotes" revealed two distinct clusters defined by a High-RiBi and a Low-RiBi group (Supplementary Figure 3A). The High- and Low-RiBi clusters consisted of samples with high *MYCN* expression (no siRNA, siSCR-16h, and siSCR-48 h) and low *MYCN* expression (siMYCN-16 h and siMYCN-48 h), respectively. The expression of *MYCN* was significantly higher in the High-RiBi cluster compared with the Low-RiBi cluster (Supplementary Figure 3B). These data show that siRNA-mediated knockdown of MycN expression represses the expression of genes involved in ribosome biogenesis.

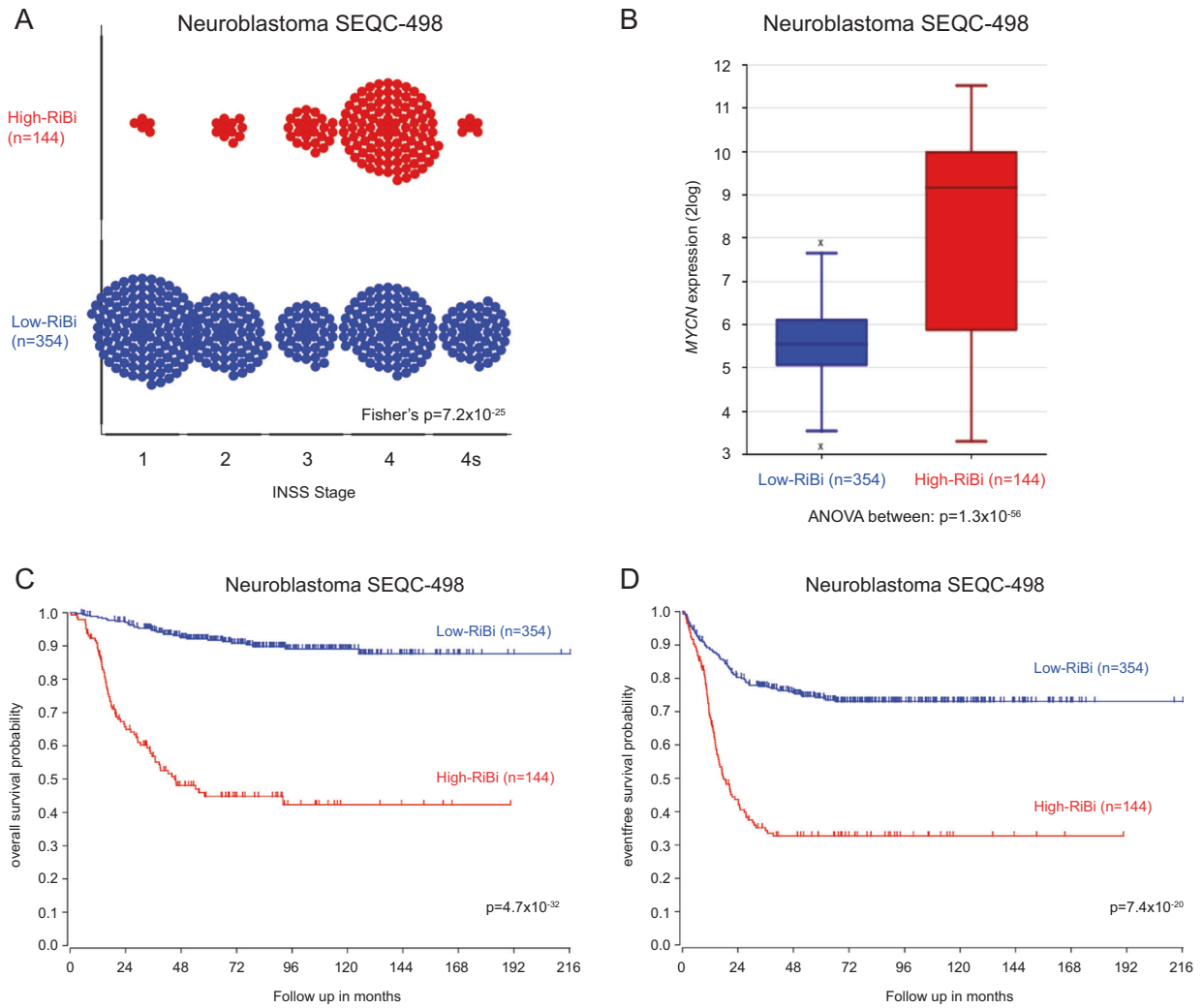

Fig. 1 Neuroblastoma tumors with enhanced ribosome biogenesis activity are characterized by high *MYCN* expression, advanced stage disease, and poor prognosis. **a** Plot showing the distribution of High-RiBi and Low-RiBi neuroblastoma tumors in different INSS stages. **b** Boxplot showing *MYCN* expression in tumors defined by High-RiBi and Low-RiBi. High-RiBi tumors show significantly higher *MYCN* expression. Kaplan–Meier analysis showing overall **c** and event-free **d** survival of neuroblastoma patients defined by High-RiBi and Low-RiBi tumors. The analyses were performed on publically available data (Tumor Neuroblastoma SEQC-498-RNAseq) from R2: Genomic Analysis and Visualization Platform (http://r2.amc.nl)

To functionally investigate the role of MycN on the sensitivity of neuroblastoma cell lines to the ribosome biogenesis inhibitors, we utilized the SHEP-TET21N model system. SHEP-TET21N is a MycN-inducible cell line derived from the parental single-copy *MYCN* human neuroblastoma cell line SHEP [16]. In the presence of 1 µg/mL doxycycline (dox), SHEP-TET21N cells express undetectable levels of MycN, whereas removal of dox induces high MycN expression (Fig. 2b, insert).

High MycN SHEP-TET21N cells grown without dox had a lower IC_{50} value for quarfloxin and CX-5461 compared with their low MycN expressing counterparts treated with 1 µg/mL doxycycline (Fig. 2b, Table 1).

Next, we used two different siRNAs targeting *MYCN* to knockdown MycN expression in the MNA neuroblastoma cell line IMR-32. Cells were transfected with siMYCN-1 and siMYCN-2 (siRNAs targeting *MYCN*) or siNC (a negative control siRNA), and treated with CX-5461 and quarfloxin. Efficient MycN knockdown was confirmed by western blot (Supplementary Figure 4A). After 48 h of drug treatment, both siMYCNs repressed the cytotoxic effect of the drugs when compared with siNC-treated cells (Fig. 2c). Similar results were observed in CHP-134 cells (Supplementary Figure 5).

These data confirm that neuroblastoma cells with high MycN expression are more sensitive to CX-5461 and quarfloxin than cells with low MycN expression.

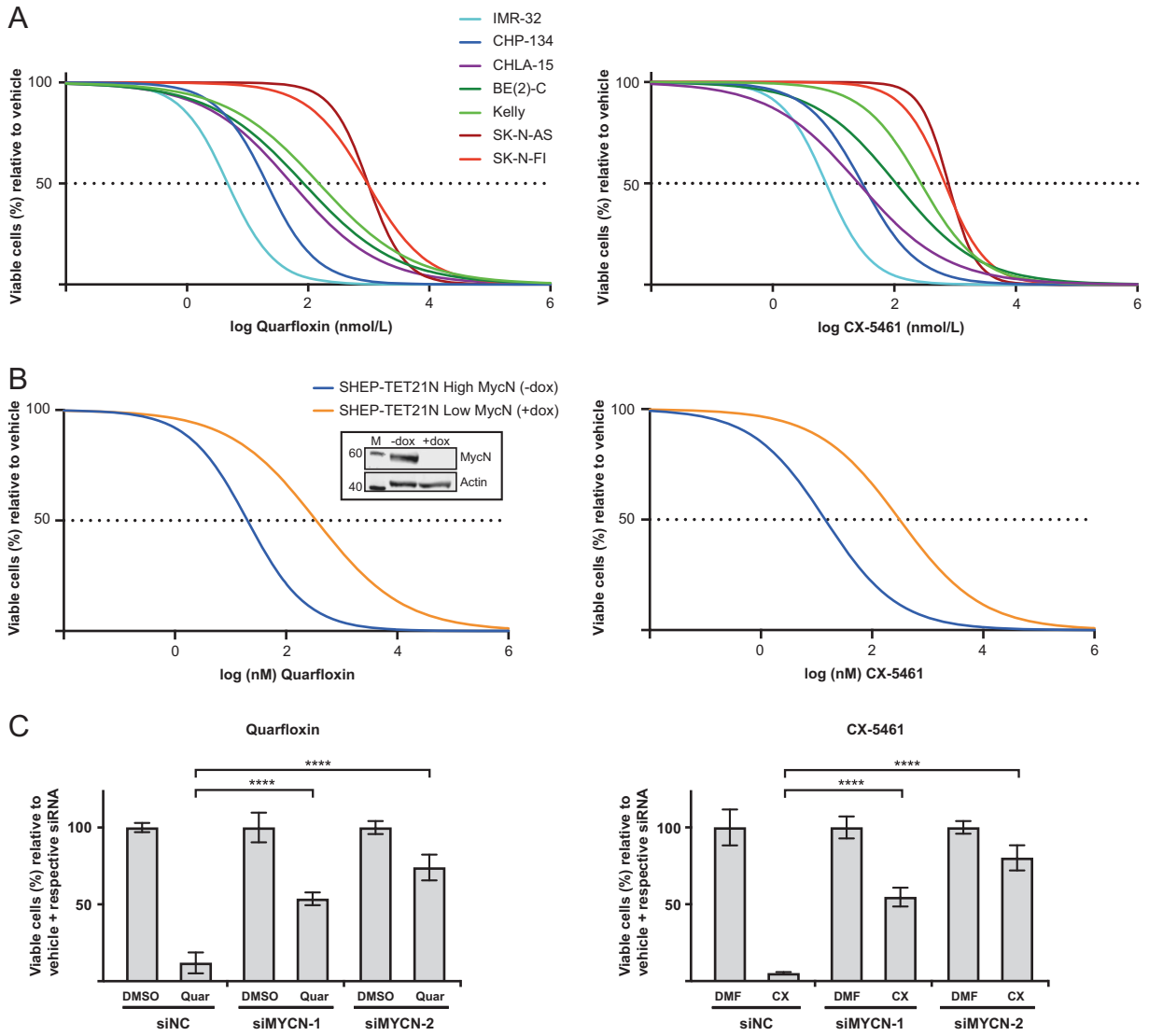

Fig. 2 Cell viability of neuroblastoma cell lines treated with quarfloxin or CX-5461. **a** Cell viability of neuroblastoma cell lines treated with an 8-log fold dose range of quarfloxin (left panel) or CX-5461 (right panel). Absolute half-maximal inhibitory concentrations (IC_{50} values) are shown in Table 1. **b** SHEP-TET21N cells were seeded in the presence (low MycN) or absence (high MycN) of 1 ug/mL doxycycline (dox). On the following day, cells were treated for 48 h with an 8-log fold change dose range of quarfloxin (left panel) or CX-5461 (right panel). IC_{50} values are shown in Table 1. Insert: WB showing MycN expression in absence (-dox) and in presence of dox (+dox). M = marker. Numbers to left indicate MW in kDa. **c** Cell viability of IMR-32 cells transfected with siRNAs (siMYCN-1 and siMYCN-2) targeting *MYCN* or a negative control siRNA (siNC), and treated with 50 nM quarfloxin (left panel) or 75 nM CX-5461 (right panel) for 48 h. The viability of vehicle + respective siRNA was set to 100%, and quarfloxin and CX-5461 treated cells were normalized to their respective controls. DMSO and DMF are vehicle controls to quarfloxin and CX-5461, respectively. For a, b, c; cell viability was measured with the Alamar blue assay. The data represents the mean cell viability and SD of two individual experiments performed in duplicate. (***$p \leq 0.001$; ****$p \leq 0.0001$)

Quarfloxin and CX-5461 induce DNA damage, p53 signaling, cell death, and cell cycle arrest in neuroblastoma cell lines

To investigate the mechanisms underlying the observed growth repression of neuroblastoma cells treated with quarfloxin and CX-5461, we analyzed several cell lines for the presence of apoptotic markers. First, we assessed the presence of the 89 kDa cleaved PARP (c-PARP) fragment and p53 on western blots of protein extracts isolated from cells treated with 150 nM quarfloxin or 230 nM of CX-5461 or 0.1% vehicle (DMSO and DMF, respectively). For all the wt-*TP53* cell lines tested (IMR-32, CHP-134, and CHLA-15), we detected increased presence of c-PARP and induction of the p53 protein after 24 h of treatment (Fig. 3a). On the contrary, mut-*TP53* cells (Kelly, SK-N-AS, and BE(2)-C) showed no significant increase in c-PARP or p53 expression. We further confirmed these observations by

Table 1 Half-maximal inhibitory concentration (IC50 values) from neuroblastoma cell lines treated with quarfloxin and CX-5461

Cell line	*MYCN* status	*TP53* status	IC50 (nM)±SD	
			Quarfloxin	CX-5461
IMR-32	Amp.	Wt	5.0 ± 2.2	7.6 ± 0.21
CHP-134	Amp.	Wt	23.0 ± 14.7	40.1 ± 13.9
CHLA-15	Non-amp.	Wt	54.0 ± 3.7	25.8 ± 2.2
BE(2)-C	Amp.	Mut	84.3 ± 5.0	106.9 ± 2.4
Kelly	Amp.	Mut	150.1 ± 33.7	275.6 ± 29.7
SK-N-AS	Non-amp.	Mut	965.2 ± 122.8	747.5 ± 65.8
SK-N-FI	Non-amp.	Mut	967.6 ± 178.8	618.3 ± 99.1
SHEP-TET21N -dox	Exogenous, high MycN	Wt	20.2 ± 0.03	14.4 ± 2.8
SHEP-TET21N + dox	Exogenous, low MycN	Wt	357.2 ± 151.5	311.8 ± 9.1

Data from two independent experiments each consisting of two biological replicates per concentration. SD is the standard deviation between the individual experiments

showing that two representative wt-*TP53* neuroblastoma cells (IMR-32 and CHLA-15) treated with quarfloxin or CX-5461 had increased expression of the 17/19 kDa cleaved-Caspase-3 (c-Casp-3) and induction of p21 protein and mRNA expression (Fig. 3b, Supplementary Figure 6). Enhanced c-Casp-3 or p21 expression was not observed in the mut-*TP53* neuroblastoma cell lines BE(2)-C and SK-N-AS treated with quarfloxin or CX-5461 (Fig. 3b).

Next, we used flow cytometry to analyze representative wt-*TP53* and mut-*TP53* neuroblastoma cell lines for the apoptotic marker Annexin V after treatment with quarfloxin or CX-5461. As shown in Fig. 3c, an increase in the proportion of Annexin V-positive cells after treatment with quarfloxin or CX-5461 was only observed in the wt-*TP53* cell lines IMR-32 and CHLA-15.

To further confirm the importance of functional p53 on the cytotoxic effect observed upon exposure of neuroblastoma cell lines to quarfloxin and CX-5461, we performed knockdown of *TP53* using two siRNAs (siTP53-1 and siTP53-2, Supplementary Figure 4B). When p53 expression was repressed by siTP53-1 and siTP53-2 in IMR-32 cells, the cytotoxic effect of quarfloxin and CX-5461 was reduced (Fig. 3d) and c-PARP was almost completely abolished (Fig. 3e). A similar, but less prominent, reduction in cell viability upon p53 knockdown was observed in CHP-134 cells (Supplementary Figure 5). Induction of functional p53 signaling by quarfloxin or CX-5461 was validated using a p53-responsive luciferase assay [17]. Only the wt-*TP53* cell lines (IMR-32 and CHLA-15) showed a significant increase in luciferase activity, indicating induction of functional p53 expression in cells exposed to CX-5461 or quarfloxin (Fig. 3f).

However, when we reconstituted functional p53 in BE(2)-C cells by exogenous overexpression of wt-p53, we did not observe a rescue in viability (Supplementary Figure 7A) or increased apoptosis (Supplementary Figure 7B) upon treatment with quarfloxin or CX-5461.

To further understand the growth impairing effects of quarfloxin and CX-5461 in the cell lines failing to undergo apoptosis, we evaluated cell cycle distribution profiles in BE(2)-C and SK-N-AS cells after treatment with these compounds. Both cell lines showed an accumulation in the G2/M-phase of the cell cycle after 24 h exposure to the drugs (Fig. 4a).

Genotoxic stress is a major activator of p53 signaling, therefore we investigated whether quarfloxin and CX-5461 have the propensity to induce DNA damage in neuroblastoma cell lines. In order to assess this, we evaluated the presence of DNA damage biomarker γ-H2A.X on western blots from several neuroblastoma cell lines. In all cell lines tested, we detected an increase of this marker, compared with vehicle-treated cells (Fig. 4b).

Together these results show that CX-5461 and quarfloxin induced DNA damage and impaired growth of neuroblastoma cells by apoptosis in wt-*TP53* cells and G2/M-arrest in mut-*TP53* cells.

Quarfloxin and CX-5461 reduce the expression of MycN and pre-rRNA (47S-rRNA)

To further explore how the RNA pol I inhibitors influence the biology of *MYCN*-amplified neuroblastoma cells, we examined the effect of quarfloxin and CX-5461 on MycN expression in several different *MYCN*-amplified neuroblastoma cell lines. MycN was downregulated in IMR-32 and CHP-134 cells, but not in mut-*TP53* BE(2)-C and Kelly cells after 48 h of drug treatment (Fig. 5a).

As quarfloxin and CX-5461 originally were characterized as direct inhibitors of RNA pol I activity, we assessed the ability of quarfloxin and CX-5461 to suppress the expression of RNA pol I transcript 47S-rRNA. The 47S-rRNA contains the 5'ETS of rDNA genes, which is the first region to be processed with fast kinetics, and is therefore often used as a proxy for the pre-rRNA transcriptional activity of RNA pol I [18]. To our surprise, quarfloxin and CX-5461 concentrations, which effectively induced DNA damage, cell death, p53 signaling, and cell cycle arrest, did not downregulate the expression of 47S-rRNA after 24 h of treatment (Fig. 5b). However, a downregulation of 47S-rRNA was observed after 24 h with a 10-fold increase of the quarfloxin or CX-5461 doses (Fig. 5c). In order to investigate other components of the ribosomal subunits, we measured the expression of mature rRNAs (18S-, 5.8S-, and

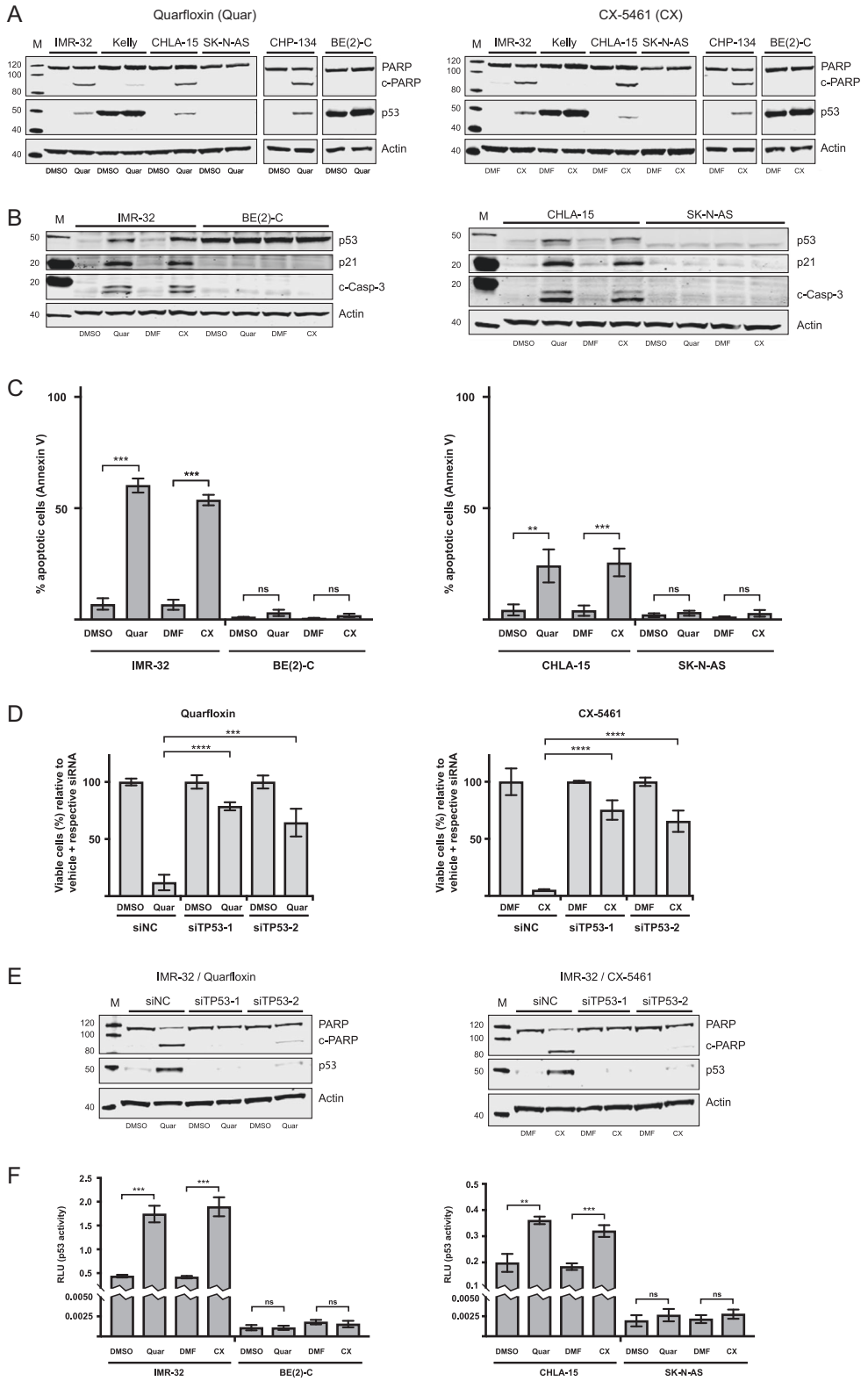

28S-rRNA) and a subset of ribosomal proteins (RPL13A, RPL32, RPS5, and RPS19) in IMR-32 cells exposed to low and high doses of quarfloxin or CX-5461. Similar to our observations of 47S-rRNA expression, no significant changes were observed for the other components of ribosomal subunits when IMR-32 cells were exposed to the low

◀ **Fig. 3** Quarfloxin and CX-5461 induce p53-dependent apoptosis in *TP53*-wt neuroblastoma cells. **a** Representative western blot (WB) for the assessment of cleaved PARP (c-PARP) and p53 expression in neuroblastoma cell lines treated for 24 h with 150 nM quarfloxin (left panel) or 230 nM CX-5461 (right panel) or 0.1% vehicle (DMSO and DMF, respectively). **b** Representative WB evaluation of cleaved-Caspase-3 (c-Casp-3), p53, and p21 expression in neuroblastoma cell lines treated as in **a**. **c** FACS analysis of Annexin V-positive neuroblastoma cells after 24 h treatment with 150 nM quarfloxin or 230 nM CX-5461 or vehicle. The data represents the mean and SD of representative experiments performed with two biological replicates pr. condition (ns, not significant; $^{**}p \le 0.01$; $^{***}p \le 0.001$). **d** p53 induction sensitizes neuroblastoma cells to quarfloxin and CX-5461. The day after transfection with siRNAs targeting *TP53* (siTP53-1 and siTP53-2), 50 nM quarfloxin (left panel) or 75 nM CX-5461 (right panel) were added and cell viability was measured 48 h after treatment. The viability of vehicle + respective siRNA was set to 100%, and quarfloxin and CX-5461 treated cells were normalized against their respective controls. The data represents the mean cell viability and s.d. of two individual experiments performed in duplicate ($^{***}p \le 0.001$; $^{****}p \le 0.0001$). **e** Representative WB assessing c-PARP levels after p53 knockdown. IMR-32 cells were reverse transfected with siTP53-1 and siTP53-2, and treated with 150 nM quarfloxin (left panel) or 230 nM CX-5461 (right panel) for 24 h before harvesting and immunoblotting. **f** Assessment of p53 transcriptional activity. Neuroblastoma cells were co-transfected immediately after seeding with a p53-responsive firefly luciferase reporter (pg13) and CMV-renilla luciferase. 150 nM quarfloxin or 230 nM CX-5461 were added the following day and cells were treated for 24 h before harvesting and analysis. Pg-13 expression was normalized to Renilla expression (RLU) and the data shown represents the mean of one experiment with three biological replicates and is representative of two independent experiments (ns, not significant; $^{**}p \le 0.01$; $^{***}p \le 0.001$)

cytotoxic doses of the inhibitors, except a minor reduction in expression of RPL32. However, when the same cells were exposed to 10-fold higher doses of quarfloxin and CX-5461, we measured increased levels of 18S-rRNA and 28S-rRNA. A similar increase was observed for ribosomal proteins RPL13A and RPS5 (Supplementary Figure 8).

CX-5461 represses the growth of neuroblastoma xenografts

Since quarfloxin and CX-5461 show almost identical effects in all neuroblastoma cell lines tested and because CX-5461 is currently in clinical trials, we decided to limit our preclinical in vivo investigations to CX-5461. In order to evaluate the therapeutic potential of CX-5461 in vivo, NMRI *nu/nu* mice with established IMR-32 or BE(2)-C xenograft tumors were treated by oral administration of CX-5461. In both models, a significant decrease of tumor growth was observed, with treated IMR-32 tumors reduced to 38% (Fig. 6a) and BE(2)-C to 69% (Fig. 6b) at the end of treatment compared with their respective control groups.

Histological analysis of tissue sections from treated tumors revealed a pale appearance with regional necrosis, hemorrhage and significant increase in damaged cells with disintegrated cytoplasm (Fig. 6c, Supplementary Figure 9). In addition, higher number of apoptotic cell bodies and fragmented nuclei were evident as confirmed by immunohistochemical detection of c-Casp-3 (Fig. 6d) and γ-H2A.X (Fig. 6e) levels in tumors from mice treated with CX-5461 compared with control tumors. Furthermore, compared with control tumors, treatment was associated with a prominent reduction in staining of the cell proliferation marker Ki-67 (Fig. 6f) and reduced levels of MycN protein (Fig. 6g). These histological features were in particular evident in tumor tissue from the *MYCN*-amplified IMR-32 xenograft. The data suggest an inhibitory effect of CX-5461 on tumor proliferation by induction of a DNA damage response and apoptosis.

Discussion

Despite intensive treatment modalities, the survival of patients with high-risk neuroblastoma is still around 50%. The major marker attributed to high-risk neuroblastoma is *MYCN* gene amplification and high-risk neuroblastoma patients without *MYCN*-amplification frequently exhibit high expression of either MycN, c-Myc, or Myc signature genes [19]. Our analysis of publicly available gene expression RNAseq and microarray data, show that high-risk neuroblastoma with high *MYCN* expression strongly correlates to elevated expression of genes involved in ribosome biogenesis and poor patient survival. Several observations have shown that c-Myc is an important regulator of ribosome biogenesis by affecting the expression of ribosomal genes as well as auxiliary factors important in ribosome biogenesis [7]. Also, elevated MycN expression has been suggested to augment the expression of several genes involved in ribosome biogenesis and protein synthesis [6]. Similarly, we found that siRNA-mediated down-regulation of MycN expression resulted in reduced expression of genes involved in ribosome biogenesis. Hyperactive ribosome biogenesis, which morphologically can be detected by an increase in nucleolar size and number, is a hallmark for the majority of cancers and is frequently associated with poor prognosis [5]. In neuroblastoma, poorly differentiated cells exhibit increased number of nucleolar organizer regions [20] suggesting increased proliferation and elevated ribosome biogenesis. Furthermore, neuroblastomas with high expression of MycN or c-Myc have been shown to exhibit enlarged nucleoli [8, 9]. Together, these data suggest that inhibition of ribosome biogenesis in neuroblastoma should be tested as a treatment option for neuroblastoma patients expressing high levels of MycN and/or c-Myc. In the present study, we show that treatment with quarfloxin or CX-5461, two small molecule inhibitors of RNA polymerase I, inhibited the growth of neuroblastoma cells with IC_{50} at nanomolar concentrations.

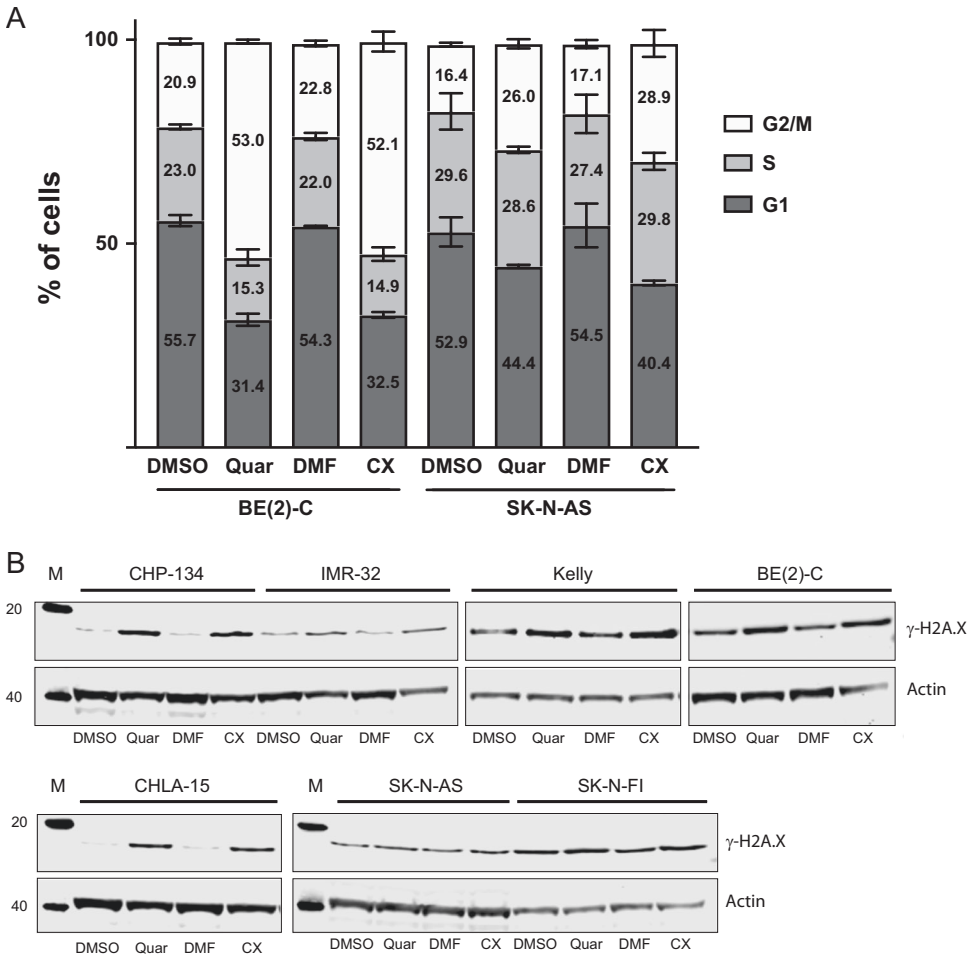

Fig. 4 Analysis of cell cycle distribution and DNA damage in neuroblastoma cell lines. **a** Quarfloxin and CX-5461 induce G2/M-arrest in *TP53*-mutated neuroblastoma cell lines. Flow cytometry analysis of cell cycle distribution in neuroblastoma cell lines BE(2)-C and SK-N-AS after 24 h treatment with 150 nM quarfloxin or 230 nM CX-5461. The data represent the mean percentage and SD of cells in G1, S, and G2/M phases from two individual experiments, each performed with two biological replicates. **b** Quarfloxin and CX-5461 induce DNA damage in neuroblastoma cell lines. Representative western blot of DNA damage marker γ-H2A.X in neuroblastoma cell lines exposed to 150 nM quarfloxin or 230 nM CX-5461 for 24 h

Neuroblastoma cells expressing high levels of *MYCN* or *c-MYC* were significantly more sensitive to treatment with these compounds. We also show that both drugs reduce the levels of MycN protein and that wt-*TP53* neuroblastoma cell lines activate p53 signaling and undergo apoptosis, whereas mut-*TP53* cells undergo cell cycle arrest in the G2/M-phase. Previously, CX-5461 has been shown to prevent initiation of rRNA synthesis by RNA polymerase I through inhibiting the binding of the transcription factor SL1 to the rDNA promoter, with subsequent release of free ribosomal proteins and activation of the nucleolar stress pathway promoting the activation of p53 signaling [21]. Exogenous addition of wt-*TP53* cDNA by transient transfection did not result in increased effects of CX-5461 or quarfloxin in BE(2)-C cells, a neuroblastoma cell line expressing high levels of mutant *TP53* (*TP53mut C135F*). *TP53*-C135F lies within the DNA-binding domain of the p53 protein (UniProt.org) and confers a loss of function to the p53 protein as demonstrated by loss of p53 transactivation activity [22]. In fact, the C135F-mutated version of p53 from SK-N-BE(2) cells has been shown to exert a moderate dominant negative effect on wt-p53 transcriptional activity [23]. Hence, the reason for the lack of increased effects of CX-5461 or quarfloxin in BE(2)-C could be caused by the presence of high levels of endogenous mutant-p53 protein that interferes with the exogenous wt-p53 during complex formation and binding to DNA, resulting in an incomplete restoration of the transactivation activity [24]. This also partly explains that we observed an increase in p21 expression in wt-*TP53* transfected cells but no increase in apoptotic marker (c-PARP) or rescue of cell viability. Together, this can, at least partly, explain the differential effects observed in neuroblastoma cells containing wt-*TP53* versus those cells with mutated *TP53*.

Destabilization of MycN or c-Myc proteins mediated by RNA polymerase I inhibitors has also been established by others [25, 26]. In our study, we did not observe reduction of MycN expression in the *TP53*-mutated cell lines Kelly and BE(2)-C, whereas MycN was robustly downregulated in wt-*TP53* IMR-32 and CHP-134 (Fig. 5a). A similar observation was very recently reported by Niemas-Teshiba et al. [21]. In this study, a low dose of CX-5461 (250 nM) efficiently repressed MycN expression in wt-*TP53* LAN5 cells after 24 h exposure, whereas a fourfold higher dose (1000 nM), only led to a very slight suppression of MycN in *TP53*-mutated Kelly cells. This differential response to the

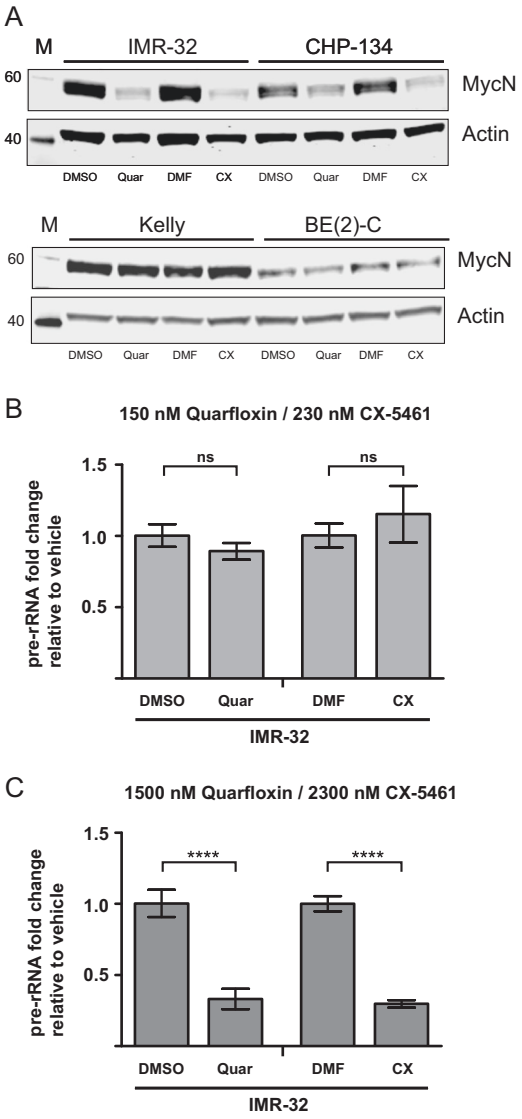

Fig. 5 Analysis of MycN and pre-rRNA expression in neuroblastoma cells treated with quarfloxin and CX-5461. **a** The protein levels of MycN are depleted in neuroblastoma cells with functional p53 upon treatment with quarfloxin or CX-5461. Representative western blot showing MycN protein levels in wt-*TP53* IMR-32 and CHP-134 (upper panel) and *TP53*-mutated Kelly and BE(2)-C (lower panel) cells after 48 h treatment with 150 nM quarfloxin or 230 nM CX-5461. **b** Expression of 47S-rRNA (pre-rRNA) in IMR-32 cells treated for 24 h with low doses of quarfloxin (150 nM) and CX-5461(230 nM). **c** Expression of 47S-rRNA (pre-rRNA) in IMR-32 cells treated for 24 h with high doses of quarfloxin (1500 nM) and CX-5461(2300 nM). ns, not significant; ****$p \le 0.0001$

drugs with regards to MycN expression could be explained by several possible mechanisms. Kelly and BE(2)-C cells have been characterized as drug-resistant cell lines whereas IMR-32 and CHP-134 are drug sensitive [27–29]. Therefore, the difference in MycN downregulation caused by CX-5461 and quarfloxin might be due to enhanced drug efflux caused by high levels of transporter molecules present in Kelly and BE(2)-C cells. In fact, the multifunctional drug transporter protein RALBP1/RLIP76 has been shown to be repressed by p53 in neuroblastoma cells expressing wt-p53. In contrast, SK-N-BE(2) cells expressing mutant-p53 showed overexpression of RALBP1/RLIP76 and increased drug resistance [30]. Another mechanism contributing to the difference in MycN expression could be explained by effects on the MycN degradation machinery. The FBXW7 E3-ubiquitin ligase is an important regulator of MycN stability in neuroblastoma cells [31]. In a study by Burmakin et al., reactivation of p53 by RITA was shown to induce a rapid and substantial downregulation of MycN via FBXW7-mediated proteasomal degradation in neuroblastoma cells [31]. Furthermore, reports from both ovarian and gastric cancers have shown that FBXW7 is downregulated in *TP53*-mutated tumors [32, 33]. When a dominant negative (R175H) p53 was overexpressed in wt-*TP53* ovarian cancer cell lines, the expression of FBXW7 was suppressed.

Interestingly, the *c-MYC* gene contains a G-quadruplex motif in its gene promoter and *MYCN* contains a G-quadruplex in intron 1, a region shown to be important for the transcriptional activation of this gene [34–36]. Quarfloxin has previously been described as a G-quadruplex stabilizer and reduces rRNA synthesis through disruption of the interaction between putative G-quadruplex structures in the rDNA and nucleolin [13]. Stabilization of G-quadruplexes in promoter regions has been shown to inhibit transcription, thereby providing another potential mechanism of *MYC* gene suppression by quarfloxin and CX-5461 [37].

Both quarfloxin and CX-5461 have previously been described as RNA polymerase I inhibitors [12, 13]. In our experiments, we did not observe any change in expression of 47S-rRNA when IMR-32 cells were exposed to quarfloxin and CX-5461 at doses which effectively induced DNA damage, cell death, p53 signaling, and cell cycle arrest (Fig. 5b). In addition, the expression of other components of the ribosomal subunits (mature rRNAs and ribosomal proteins) was also unaffected by this treatment (Supplementary Figure 8A and 8C). We therefore conclude that treatment with low cytotoxic doses of quarfloxin and CX-5461 does not significantly inhibit ribosomal biogenesis in *MYCN*-amplified neuroblastoma cell lines. However, when the cells were exposed to 10-fold higher doses of the drugs, we observed a marked downregulation of 47S-rRNA expression (Fig. 5c). These high concentrations of quarfloxin and CX-5461 also increased the levels of 18S-rRNA, 28S-rRNA, RPL13A, and RPS5 (Supplementary Figure 8B and 8D). We do not have a reasonable biological explanation for the discrepancy observed during exposure of high doses of the drugs. From the raw Cq values, we observe a significant increase, indicating reduced levels, of the mRNA housekeeping genes (*SDHA* and *ACTB*), 5.8S- and 47 S rRNA when cells were exposed to high doses of the drugs. This may explain the apparent increase of 18S- and 28S-rRNA

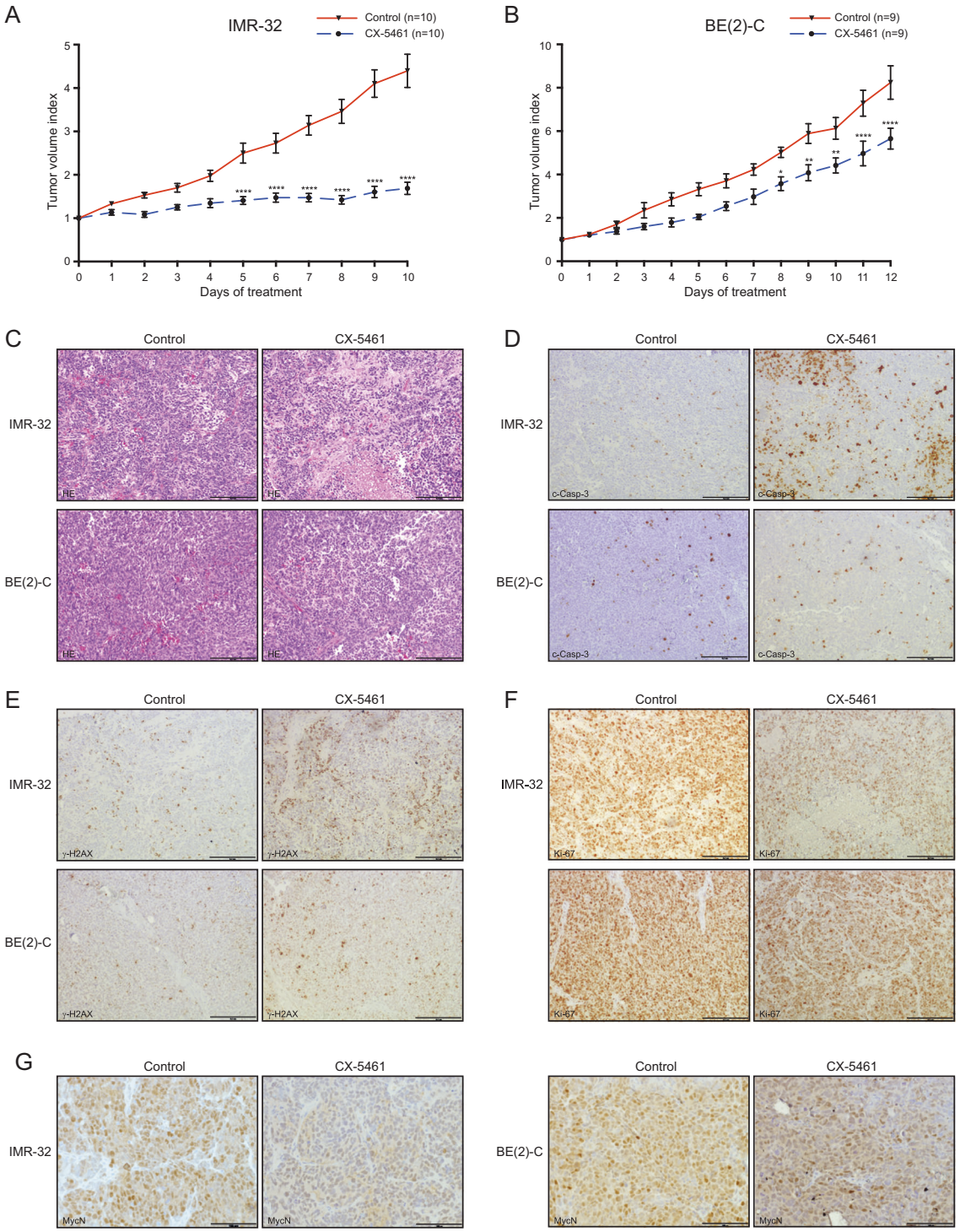

Fig. 6 CX-5461 inhibits neuroblastoma xenograft growth in vivo. **a** Comparison of tumor growth in IMR-32 xenograft bearing mice receiving no treatment ($n = 10$) or CX-5461 ($n = 10$) for 3–6 consecutive days and then every third days for 10 days. Tumor volume index (TVI) means with SEM is displayed (****$p \le 0.0001$). **b** Comparison of tumor growth (tumor volume index; TVI) in BE(2)-C engrafted mice receiving no treatment ($n = 9$) or CX-5461 ($n = 9$) every third day for 12 days. TVI means with SEM is displayed (*$p \le 0.05$; **$p \le 0.01$; ****$p \le 0.0001$). **c** Sections of dissected tumors were analyzed by hematoxylin and eosin (H&E) staining. IMR-32 xenografts sections deriving from mice treated with CX-5461 demonstrated areas with necrotic tissues, which was less evident in corresponding BE(2)-C xenografts, and **d** immunohistochemical staining with antibodies to detect the apoptotic marker c-Casp-3, **e** the DNA damage marker γ-H2A.X, **f** the proliferation marker Ki-67, and **g** MycN. Scalebar = 100 μm

measurements as a normalization artifact, rather than increased expression of these highly expressed and very stable rRNAs. A similar observation was reported in a study by Xu et al., demonstrating that these drugs caused synthetic lethality in BRCA1/2-deficient breast and ovarian cancers at doses which did not inhibit RNA pol I activity [38]. This study uncovered a novel mechanism of action for these drugs through causing replication-dependent ssDNA damage and subsequent growth arrest and apoptosis by stabilization of G-quadruplex structures in the genomic DNA. We demonstrate DNA damage in all neuroblastoma cell lines tested after treatment with quarfloxin and CX-5461, and in vivo DNA damage after CX-5461 treatment of nude mice bearing neuroblastoma xenografts. Our findings suggest that quarfloxin and CX-5461 cause cellular toxicity through a process involving stabilization of G-quadruplexes. The initial characterization studies by Drygin et al. described quarfloxin and CX-5461 as non-genotoxic using the Ames and Comet assay [12, 13]. This is in contrast to our results and the findings of Xu et al. [38] Furthermore, reports by Negi et al. and Quin et al. have shown that CX-5461 induces the ATM/ATR signaling pathway leading to a G2/M-phase cell cycle arrest [39, 40]. ATM and ATR are crucial sensors of DNA damage and activate the DNA damage response upon the presence of dsDNA or ssDNA breaks, respectively [41]. Negi et al. [39] demonstrated the enhancement of apoptosis in leukemia cells when co-treating with VE-822, an ATR inhibitor, and CX-5461. These results suggest that CX-5461 induces ssDNA damage, and show that co-targeting DNA damage response pathways can be utilized to overcome potential resistance to this agent.

CX-5461 significantly inhibited the growth of established *MYCN*-amplified neuroblastoma grown as xenografts in nude mice. Growth suppression was more pronounced in tumors harboring wt-*TP53* (IMR-32) compared with neuroblastoma containing mutated *TP53* (BE(2)-C). These results further support the notion that RNA polymerase I inhibitors activate p53 signaling and that p53 activation is one mechanism for the growth inhibiting effects seen by RNA polymerase I inhibitors in tumor cells.

Taken together, RNA polymerase I inhibitors are promising agents that should be further investigated in clinical studies as a treatment options for neuroblastoma patients with high expression of MycN or c-Myc.

Materials and methods

Cell culture

All cells were grown in a humidified incubator at 37 °C with 5% CO_2. BE(2)-C, SK-N-AS, CHP-134, Kelly and SHEP-TET21N cells were maintained in RPMI-1640 supplemented with 10% sterile-filtered fetal bovine serum (FBS). IMR-32 and SK-N-FI were grown in low glucose DMEM supplemented with 10% FBS and 1% non-essential amino acids (NEAA). CHLA-15 cells were grown in IMDM with 20% FBS, 1x ITS, and 4 nM L-glutamine. All cell identities were confirmed by short tandem repeat analysis, and the cells were regularly checked to be mycoplasma-free.

Chemicals

CX-5461 (Selleckchem) was resuspended in dimethylformamide (DMF) to a 5 mM stock. Quarfloxin (AdooQ) was resuspended in DMSO to a stock of 10 mM as recommended by the manufacturers. Aliquots of both chemicals were kept at −80 °C and were thawed and diluted in their respective vehicles (DMF or DMSO) for working solutions. The concentration of vehicle never exceeded 0.1%. For animal studies, CX-5461 was dissolved in 50 mM NaH_2PO_4 (pH 4.3) at 5 mg/mL.

Viability assays

For IC_{50} experiments, cells grown in 24-well plates were treated with an 8-log dose range of quarfloxin and CX-5461 in a total volume of 500 µL/well for 48 h before the addition of 50 µL Alamar blue reagent (Thermo Fisher) directly to the wells. Cells were incubated at 37 °C for an additional 2 h and 100 µL of media was transferred to a black-walled 96-well plate and fluorescence was measured at 540 nm excitation and 590 nm emission wavelengths using a micro plate reader (CLARIOstar). The raw data was normalized to vehicle treated, and IC_{50} was calculated using the Prism 7 software and the equation: log(inhibitor) vs. normalized response—Variable slope. All experiments were repeated twice with two biological replicates.

Flow cytometry

For cell cycle distribution profiling, cells were treated for 24 h in the presence of vehicle or 150 nM quarfloxin or 230 nM CX-5461. Floating and adherent cells (trypsination) were harvested and subsequently fixed and permeabilized in ice-cold 70% EtOH. Fixed cells were subsequently stained in PBS containing 50 µg/mL Propidium Iodide (PI) and 100 µg/mL RNaseA for 30 min protected from light at room temperature and then placed on ice. PI-stained cells were analyzed using a BD LSR Fortessa, and cell cycle data were further analyzed using FlowJo v.10 with the Watson model for evaluation of cell cycle distribution.

For the Annexin V apoptosis assay, cells were treated for 24 h in the presence of vehicle or 150 nM quarfloxin or 230 nM CX-5461 and analyzed using the FITC Annexin V Apoptosis Detection Kit according to the manufacturer's instructions (BD Biopharmigen). Annexin V-positive cells were detected using a BD LSR Fortessa.

Western blotting

Cells were treated with vehicle, quarfloxin, or CX-5461 as indicated. At harvesting, floating cells and adherent cells (trypsination) were collected for analysis. Protein isolation and blotting were performed essentially as previously described using NuPAGE 4–12% bis-tris precast polyacrylamide gels and Immobilon-PVDF membranes (Millipore) [42]. For western blots containing Caspase-3 and p21, 4–20% Tris-Glycine gels (Lonza) were used for better separation of these low MW proteins. Primary antibodies used in this study were mouse monoclonal anti-MycN (sc-53993, Santa Cruz Biotechnology, CA, USA), mouse monoclonal anti-p53 (sc-126, Santa Cruz Biotechnology, CA, USA), rabbit monoclonal anti-p21 (#2947, Cell Signaling Technology, MA, USA), rabbit polyclonal anti-PARP (#9542, Cell Signaling Technology, MA, USA), rabbit polyclonal anti-Caspase-3 (#9662, Cell Signaling Technology, MA, USA), mouse monoclonal anti-γ-H2A.X (05–636, Merck Millipore, MA, USA), rabbit polyclonal anti-actin (A2066, Sigma-Aldrich, MO, USA) and mouse monoclonal anti-actin (AB3280, Abcam, Cambridge, UK). Membranes were detected using the Odyssey Infrared Imaging system (LI-COR).

RT-qPCR

Floating and adherent cells were lysed in 1 mL of Qiazol (Qiagen), 0.2 mL of chloroform was added for phase separation, and RNA was precipitated overnight from 0.4 mL of the aqueous phase 1:1 in isopropanol at −20 °C. The RNA pellet was washed twice in ice-cold 75% EtOH and resuspended in TE-buffer (10 mM Tris-HCl, 1 mM disodium EDTA, pH 8.0). RNA quality and quantity was assesed using the Nanodrop 2000. In total, 1200 ng of RNA was reverse transcribed using the High Capacity cDNA kit w/RNase inhibitor (Thermo Fisher). Each RT-qPCR reaction (20 µL) contained 12.5 ng of cDNA in 5 µL, 10 µL of Power SYBR (Thermo Fisher), 0.8 µL of 5 µM F+R primers, and 4.2 µL of nuclease-free H_2O. Amplification of cDNA was carried out using a LightCycler 96 SW 1.1 (Roche). Relative expression of transcript levels was evaluated using the ddCT method with the geometric mean of two housekeeping genes (*SDHA* and *ACTB*). Expression of rRNA transcripts was normalized using the geometric mean of all rRNA transcripts according to [43]. Primer sequences were; SDHA: forward 5′-CTGATGAGACAAGATGTGGTG-3′, reverse 5′-CAATCTCCCTTCAATGTACTCC-3′, ACTB: forward 5′-CACCATGTACCCTGGCATT-3′, reverse 5′-ACGGAGTACTTGCGCTCAG-3′, p21: forward 5′-GCAGACCAGCATGACAGATTT-3′, reverse 5′-GGATTAGGGCTTCCTCTTGGA-3′, 47S-rRNA: forward 5′-CCGCGCTCTACCTTACCTAC-3′, reverse 5′-GCATGGCTTAATCTTTGAGACAAG-3′, 5.8S-rRNA: forward 5′-ACTCGGCTCGTGCGTC-3′, reverse: 5′-GCGACGCTCAGACAGG-3′, 18S-rRNA: forward 5′-GTAACCCGTTGAACCCCATT-3′, reverse 5′-CCATCCAATCGGTAGTAGCG-3′, 28S-rRNA: forward 5′-GGGTGGTAAACTCCATCTAAGG-3′, reverse 5′-GCCCTCTTGAACTCTCTCTTC-3′, RPL13A: forward 5′-TAAACAGGTACTGCTGGGCCG-3′, reverse 5′-CTCGGGAAGGGTTGGTGTTC-3′, RPL32: forward 5′-TACGACCCATCAGCCCTTGC-3′, reverse 5′-CATGATGCCGAGAAGGAGATGG-3′, RPS5: forward 5′-ATCATCAACAGTGGTCCCCG-3′, reverse 5′-AGATGGCCTGGTTCACACG-3′, RPS19: forward 5′-AAACCCCGTCGTTCCCTTTC-3′, reverse 5′ GCTTCCCGGACTTTTTGAGG-3′.

p53 activity assays

Cells in 12-well plates were reverse transfected using Lipofectamine 2000 (Thermo Fisher) with 0.5 µg p53 transcriptional reporter (PG13) (Addgene), (originally published in Ref. [17]) and 0.02-µg pCMV-Renilla luc (Promega). On the next day, cells were treated with vehicles or 150 nM quarfloxin or 230 nM CX-5461. After 24 h of treatment, cells were collected in 200 µL 1x PLB buffer, and luciferase activity was measured using the Dual-Luciferase Reporter Assay according to the instructions from the manufacturer (Promega). PG13 firefly activity was normalized to renilla (RLU).

siRNA transfections and *TP53* overexpression

Transfections were carried out using Lipofectamine 2000 and were performed essentially as described [44]. The following siRNAs were used (all from Qiagen): AllStars Negative Control siRNA (siNC), Hs_MYCN_4 FlexiTube siRNA (siMYCN_1), Hs_MYCN_6 FlexiTube siRNA (siMYCN_2), Hs_TP53_3 FlexiTube siRNA (siTP53_1), and Hs_TP53_9 FlexiTube siRNA (siTP53_2). Final concentrations of the respective siRNAs were 20 nM in all the experiments. The wt-p53 overexpression plasmid was a kind gift from Dr. Ugo Moens, University of Tromsø, Norway, empty vector was pCMV-XL4 (Origene). Final DNA plasmid concentration was 1 µg/mL of media.

Xenografts

Four-to-six-week-old female Sca:NMRI *nu/nu* mice (Scanbur, Stockholm, Sweden) were maintained in pathogen-free conditions and given free access to sterile water and food. For BE(2)-C xenografts, 10×10^6 cells were injected subcutaneously on the right flank under isoflurane anesthesia and for IMR-32 9×10^6 cells in 50% Matrigel were injected following the same procedure. Tumors were measured every day with a digital caliper and tumor volume (mL) was calculated as $\text{volume} = \text{width}^2 \times \text{length} \times 0.44$. When

tumors reached ≥ 0.15 ml, mice were randomized into treatment with CX-5461 or control groups (no treatment). Mice in the treatment groups received 50 mg/kg CX-5461 by oral gavage every third day for 12 days for BE(2)-C or 3–6 consecutive days and then every third day for 10 days for IMR-32. Tumor volume index (TVI) was determined by dividing the tumor volume of each day by the starting volume (day 0). TVIs from treated and untreated tumors were compared in GraphPad Prism 7 using repeated measures two-way ANOVA with Bonferroni correction and p-values ≤ 0.05 were considered statistically significant. No significant weight changes were observed in both untreated and treated groups. At autopsy, tumors were fixed in 4% paraformaldehyde (PFA) at 4 °C for 24 h and then kept in 70% EtOH at 4 °C before further analysis. All animal experiments were approved by the regional ethics committee for animal research (N231/14), appointed and under the control of the Swedish Board of Agriculture and the Swedish Court. The animal experiments presented herein were in accordance with national regulations (SFS 1988:534, SFS 1988:539, and SFS 1988:541).

Immunohistochemistry

Formalin-fixed and paraffin-embedded tissue sections were deparaffinized in xylene and graded alcohols, hydrated, and washed in a phosphate-buffered saline (PBS). After antigen retrieval in a sodium citrate buffer (pH 6) in a microwave oven, the endogenous peroxidase was blocked by 0.3% H_2O_2 for 15 min. Sections were incubated overnight at 4 °C with primary antibodies anti-γ-H2A.X (#9718 Cell Signal Technology, MA, USA), anti-cleaved Caspase-3 (Asp175) (Cell signaling Technology, MA, USA) or anti-Ki-67 (SP6, Neomarkers, CA, USA), respectively. As a secondary antibody, the anti-rabbit-horseradish peroxidase (HRP) SignalStain Boost IHC detection kit was used (# 8114, Cell Signaling Technology, MA, USA). For the assessment of MycN expression, a monoclonal mouse anti-MycN antibody was used (sc-53993, Santa Cruz Biotechnology, CA, USA). As a secondary antibody, anti-mouse EnVision-HRP (Dako, Agilent Technologies, Inc., Santa Clara, CA, USA) was used. A matched isotype control was also used as a control for nonspecific background staining.

Statistical analysis

Differences between two groups were compared using the two-sided Student's t test. Differences in treated and untreated xenograft tumor volume indexes were studied using repeated measures two-way ANOVA with Bonferroni correction. All statistical analysis was done using the GraphPad Prism 7 software and a result was considered statistically significant when $p \le 0.05$.

Acknowledgements This work was supported by the Norwegian Childhood Cancer Society (Barnekreftforeningen), The Northern-Norwegian Health Authorities (Helse Nord), the Simon Fougner Hartmanns Familiefond, the Swedish Childhood Cancer Foundation, the Swedish Cancer Foundation, the Swedish Foundation for Strategic Research (www.nnbcr.se) and The Cancer Research Foundations of Radiumhemmet. We wish to thank Dr. Emma Bell for kindly providing the siMYCN IMR-32 microarray data.

Compliance with ethical standards

Conflict of interest The authors declare that they have no conflict of interest.

References

1. Cole KA, Maris JM. New strategies in refractory and recurrent neuroblastoma: translational opportunities to impact patient outcome. Clin Cancer Res. 2012;18:2423–8.
2. Maris JM. Recent advances in neuroblastoma. N Engl J Med. 2010;362:2202–11.
3. Westermann F, Muth D, Benner A, Bauer T, Henrich KO, Oberthuer A, et al. Distinct transcriptional MYCN/c-MYC activities are associated with spontaneous regression or malignant progression in neuroblastomas. Genome Biol. 2008;9:R150.
4. Ruiz-Perez MV, Henley AB, Arsenian-Henriksson M. The MYCN protein in health and disease. Genes. 2017;8:E113
5. Pelletier J, Thomas G, Volarevic S. Ribosome biogenesis in cancer: new players and therapeutic avenues. Nat Rev Cancer. 2018;18:51–63.
6. Boon K, Caron HN, van Asperen R, Valentijn L, Hermus MC, van Sluis P, et al. N-myc enhances the expression of a large set of genes functioning in ribosome biogenesis and protein synthesis. EMBO J. 2001;20:1383–93.
7. van Riggelen J, Yetil A, Felsher DW. MYC as a regulator of ribosome biogenesis and protein synthesis. Nat Rev Cancer. 2010;10:301–9.
8. Kobayashi C, Monforte-Munoz HL, Gerbing RB, Stram DO, Matthay KK, Lukens JN, et al. Enlarged and prominent nucleoli may be indicative of MYCN amplification: a study of neuroblastoma (Schwannian stroma-poor), undifferentiated/poorly differentiated subtype with high mitosis-karyorrhexis index. Cancer. 2005;103:174–80.
9. Wang LL, Suganuma R, Ikegaki N, Tang X, Naranjo A, McGrady P, et al. Neuroblastoma of undifferentiated subtype, prognostic significance of prominent nucleolar formation, and MYC/MYCN protein expression: a report from the Children's Oncology Group. Cancer. 2013;119:3718–26.
10. Harrison SJ, Khot A, Brajanovski N, Cameron D, Hein N, McArthur GA, et al. A phase 1, open-label, dose escalation,

safety, PK and PD study of a first in class Pol1 inhibitor (CX-5461) in patients with advanced hematologic malignancies (HM). J Clin Oncol. 2015;33:e22212-e.
11. Bywater MJ, Poortinga G, Sanij E, Hein N, Peck A, Cullinane C, et al. Inhibition of RNA polymerase I as a therapeutic strategy to promote cancer-specific activation of p53. Cancer Cell. 2012;22:51–65.
12. Drygin D, Lin A, Bliesath J, Ho CB, O'Brien SE, Proffitt C, et al. Targeting RNA polymerase I with an oral small molecule CX-5461 inhibits ribosomal RNA synthesis and solid tumor growth. Cancer Res. 2011;71:1418–30.
13. Drygin D, Siddiqui-Jain A, O'Brien S, Schwaebe M, Lin A, Bliesath J, et al. Anticancer activity of CX-3543: a direct inhibitor of rRNA biogenesis. Cancer Res. 2009;69:7653–61.
14. Li L, Li Y, Zhao J, Fan S, Wang L, Li X. CX-5461 induces autophagy and inhibits tumor growth via mammalian target of rapamycin-related signaling pathways in osteosarcoma. Onco Targets Ther. 2016;9:5985–97.
15. Bell E, Lunec J, Tweddle DA. Cell cycle regulation targets of MYCN identified by gene expression microarrays. Cell cycle (Georgetown, Tex). 2007;6:1249–56.
16. Lutz W, Stohr M, Schurmann J, Wenzel A, Lohr A, Schwab M. Conditional expression of N-myc in human neuroblastoma cells increases expression of alpha-prothymosin and ornithine decarboxylase and accelerates progression into S-phase early after mitogenic stimulation of quiescent cells. Oncogene. 1996;13:803–12.
17. el-Deiry WS, Tokino T, Velculescu VE, Levy DB, Parsons R, Trent JM, et al. WAF1, a potential mediator of p53 tumor suppression. Cell. 1993;75:817–25.
18. Popov A, Smirnov E, Kovacik L, Raska O, Hagen G, Stixova L, et al. Duration of the first steps of the human rRNA processing. Nucleus (Austin, Tex). 2013;4:134–41.
19. Johnsen JI, Dyberg C, Fransson S, Wickstrom M. Molecular mechanisms and therapeutic targets in neuroblastoma. Pharmacol Res. 2018;131:164–76.
20. Egan M, Raafat F, Crocker J, Williams D. Comparative study of the degree of differentiation of neuroblastoma and mean numbers of nucleolar organiser regions. J Clin Pathol. 1988;41:527–31.
21. Hein N, Hannan KM, George AJ, Sanij E, Hannan RD. The nucleolus: an emerging target for cancer therapy. Trends Mol Med. 2013;19:643–54.
22. Gonin-Laurent N, Gibaud A, Huygue M, Lefevre SH, Le Bras M, Chauveinc L, et al. Specific TP53 mutation pattern in radiation-induced sarcomas. Carcinogenesis. 2006;27:1266–72.
23. Goldschneider D, Horvilleur E, Plassa LF, Guillaud-Bataille M, Million K, Wittmer-Dupret E, et al. Expression of C-terminal deleted p53 isoforms in neuroblastoma. Nucleic Acids Res. 2006;34:5603–12.
24. Bykov VJN, Eriksson SE, Bianchi J, Wiman KG. Targeting mutant p53 for efficient cancer therapy. Nat Rev Cancer. 2018;18:89–102.
25. Niemas-Teshiba R, Matsuno R, Wang LL, Tang XX, Chiu B, Zeki J, et al. MYC-family protein overexpression and prominent nucleolar formation represent prognostic indicators and potential therapeutic targets for aggressive high-MKI neuroblastomas: a report from the children's oncology group. Oncotarget. 2018;9:6416–32.
26. Lee HC, Wang H, Baladandayuthapani V, Lin H, He J, Jones RJ, et al. RNA polymerase I inhibition with CX-5461 as a novel therapeutic strategy to target MYC in multiple myeloma. Br J Haematol. 2017;177:80–94.
27. Xue C, Haber M, Flemming C, Marshall GM, Lock RB, MacKenzie KL, et al. p53 determines multidrug sensitivity of childhood neuroblastoma. Cancer Res. 2007;67:10351–60.
28. Keshelava N, Zuo JJ, Chen P, Waidyaratne SN, Luna MC, Gomer CJ, et al. Loss of p53 function confers high-level multidrug resistance in neuroblastoma cell lines. Cancer Res. 2001;61:6185–93.
29. Schroeder U, Bernt KM, Lange B, Wenkel J, Jikai J, Shabat D, et al. Hydrolytically activated etoposide prodrugs inhibit MDR-1 function and eradicate established MDR-1 multidrug-resistant T-cell leukemia. Blood. 2003;102:246–53.
30. Singhal J, Yadav S, Nagaprashantha LD, Vatsyayan R, Singhal SS, Awasthi S. Targeting p53-null neuroblastomas through RLIP76. Cancer Prev Res (Phila, Pa). 2011;4:879–89.
31. Otto T, Horn S, Brockmann M, Eilers U, Schuttrumpf L, Popov N, et al. Stabilization of N-Myc is a critical function of Aurora A in human neuroblastoma. Cancer Cell. 2009;15:67–78.
32. Kitade S, Onoyama I, Kobayashi H, Yagi H, Yoshida S, Kato M, et al. FBXW7 is involved in the acquisition of the malignant phenotype in epithelial ovarian tumors. Cancer Sci. 2016;107:1399–405.
33. Yokobori T, Mimori K, Iwatsuki M, Ishii H, Onoyama I, Fukagawa T, et al. p53-Altered FBXW7 expression determines poor prognosis in gastric cancer cases. Cancer Res. 2009;69:3788–94.
34. Siddiqui-Jain A, Grand CL, Bearss DJ, Hurley LH. Direct evidence for a G-quadruplex in a promoter region and its targeting with a small molecule to repress c-MYC transcription. Proc Natl Acad Sci USA. 2002;99:11593–8.
35. Trajkovski M, da Silva MW, Plavec J. Unique structural features of interconverting monomeric and dimeric G-quadruplexes adopted by a sequence from the intron of the N-myc gene. J Am Chem Soc. 2012;134:4132–41.
36. Suenaga Y, Kaneko Y, Matsumoto D, Hossain MS, Ozaki T, Nakagawara A. Positive auto-regulation of MYCN in human neuroblastoma. Biochem Biophys Res Commun. 2009;390:21–6.
37. Rhodes D, Lipps HJ. G-quadruplexes and their regulatory roles in biology. Nucleic Acids Res. 2015;43:8627–37.
38. Xu H, Di Antonio M, McKinney S, Mathew V, Ho B, O'Neil NJ, et al. CX-5461 is a DNA G-quadruplex stabilizer with selective lethality in BRCA1/2 deficient tumours. Nat Commun. 2017;8:14432.
39. Negi SS, Brown P. rRNA synthesis inhibitor, CX-5461, activates ATM/ATR pathway in acute lymphoblastic leukemia, arrests cells in G2 phase and induces apoptosis. Oncotarget. 2015;6:18094–104.
40. Quin J, Chan KT, Devlin JR, Cameron DP, Diesch J, Cullinane C, et al. Inhibition of RNA polymerase I transcription initiation by CX-5461 activates non-canonical ATM/ATR signaling. Oncotarget. 2016;7:49800–18.
41. Smith J, Tho LM, Xu N, Gillespie DA. The ATM-Chk2 and ATR-Chk1 pathways in DNA damage signaling and cancer. Adv Cancer Res. 2010;108:73–112.
42. Henriksen JR, Haug BH, Buechner J, Tomte E, Lokke C, Flaegstad T, et al. Conditional expression of retrovirally delivered anti-MYCN shRNA as an in vitro model system to study neuronal differentiation in MYCN-amplified neuroblastoma. BMC Dev Biol. 2011;11:1.
43. Karahan G, Sayar N, Gozum G, Bozkurt B, Konu O, Yulug IG. Relative expression of rRNA transcripts and 45S rDNA promoter methylation status are dysregulated in tumors in comparison with matched-normal tissues in breast cancer. Oncol Rep. 2015;33:3131–45.
44. Roth S, Hald Ø, Fuchs S, Løkke C, Mikkola I, Flaegstad T. et al. MicroRNA-193b-3p represses neuroblastoma cell growth via downregulation of Cyclin D1, MCL-1 and MYCN. Oncotarget. 2018;9:18160–79.

Supplementary Table 1: Genetic characteristics of neuroblastoma cell lines used in this study

Cell line	Stage	Origin	Treatment	*MYCN*-amplified	*TP53*	1p del	11q del	17q gain	References
BE(2)-C	4	Bone marrow	YES	YES	MUT	YES	NO	NO	[1, 2]
Kelly	4	Bone marrow	YES	YES	MUT	YES	YES	YES	[3, 4]
IMR-32	unknown	Abdomen	NO	YES	WT	YES	YES	YES	[5]
CHP-134	4	Lymph node (primary: adrenal)	YES	YES	WT	YES	NO	YES	[6]
SK-N-FI		Bone marrow	YES	NO	MUT	NO	?	?	[8]
CHLA-15	4	Primary	NO	NO	WT	?	?	?	[7, 9]
SK-N-AS	4	Bone marrow (primary: adrenal)	YES	NO	MUT	YES	YES	NO	[1, 10, 11]
MYCN-inducible neuroblastoma cell line:									
SHEP-Tet21N		Derived from SHEP (substrate adherent subtype of SK-N-SH)		+dox: OFF -dox: ON	WT				[12]

1. Thiele, C.J., *Neuroblastoma Cell Lines*, in *Neuroblastoma*, J.H.C. Culture. 1998: Lancaster, UK. p. 21-53.

2. Tweddle, D.A., A.J. Malcolm, N. Bown, A.D. Pearson*, et al.*, *Evidence for the development of p53 mutations after cytotoxic therapy in a neuroblastoma cell line*. Cancer Res, 2001. **61**(1): p. 8-13.

3. Gogolin, S., V. Ehemann, G. Becker, L.M. Brueckner*, et al.*, *CDK4 inhibition restores G(1)-S arrest in MYCN-amplified neuroblastoma cells in the context of doxorubicin-induced DNA damage.* Cell Cycle, 2013. **12**(7): p. 1091-104.

4. Piskareva, O., H. Harvey, J. Nolan, R. Conlon*, et al.*, *The development of cisplatin resistance in neuroblastoma is accompanied by epithelial to mesenchymal transition in vitro.* Cancer Lett, 2015. **364**(2): p. 142-55.

5. Tumilowicz JJ, Nichols WW, Cholon JJ, Greene AE. *Definition of a continuous human cell line derived from neuroblastoma*. Cancer Res. 1970 Aug;30(8):2110-8.

6. Schlesinger HR, Gerson JM, Moorhead PS, Maguire H, Hummeler K. *Establishment and characterization of human neuroblastoma cell lines*. Cancer Res. 1976 Sep;36(9 pt.1):3094-100.

7. Keshelava, N., R.C. Seeger, S. Groshen, and C.P. Reynolds, *Drug resistance patterns of human neuroblastoma cell lines derived from patients at different phases of therapy.* Cancer Res, 1998. **58**(23): p. 5396-405.

8. Helson, L., Nisselbaum, J., Helson, C., Majeranowski, A., and Johnson, G. A. *Biological markers in neuroblastoma and other pediatric neoplasias*. In: W. Davis, K. R. Harrap, and G. Stathopoulos (eds.), Human Cancer. Its Characterization and Treatment, pp. 86–94. Princeton: Excerpta Medica, 1980.

9. Keshelava, N., E. Davicioni, Z. Wan, L. Ji*, et al.*, *Histone deacetylase 1 gene expression and sensitization of multidrug-resistant neuroblastoma cell lines to cytotoxic agents by depsipeptide.* J Natl Cancer Inst, 2007. **99**(14): p. 1107-19.

10. Caren, H., H. Kryh, M. Nethander, R.M. Sjoberg*, et al.*, *High-risk neuroblastoma tumors with 11q-deletion display a poor prognostic, chromosome instability phenotype with later onset.* Proc Natl Acad Sci U S A, 2010. **107**(9): p. 4323-8.

11. Goldschneider, D., E. Horvilleur, L.F. Plassa, M. Guillaud-Bataille*, et al.*, *Expression of C-terminal deleted p53 isoforms in neuroblastoma.* Nucleic Acids Res, 2006. **34**(19): p. 5603-12.

12. Lutz W, Stohr M, Schurmann J, Wenzel A, Lohr A, Schwab M. *Conditional expression of N-myc in human neuroblastoma cells increases expression of alpha-prothymosin and ornithine decarboxylase and accelerates progression into S-phase early after mitogenic stimulation of quiescent cells.* Oncogene. 1996;13(4):803-12.

SUPPLEMENTARY FIGURE 1

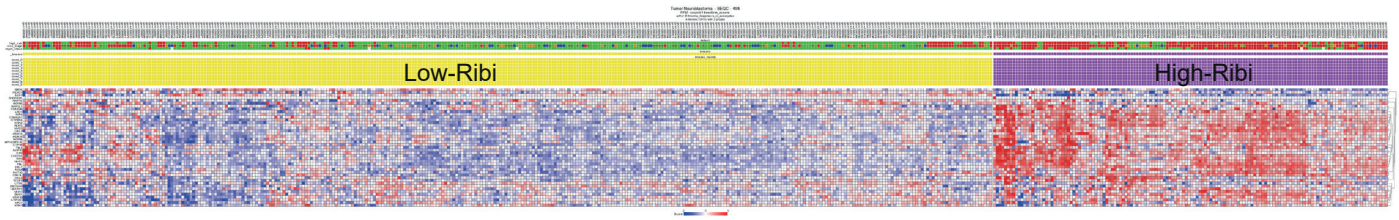

SUPPLEMENTARY FIGURE 2

A

Neuroblastoma Versteeg-88

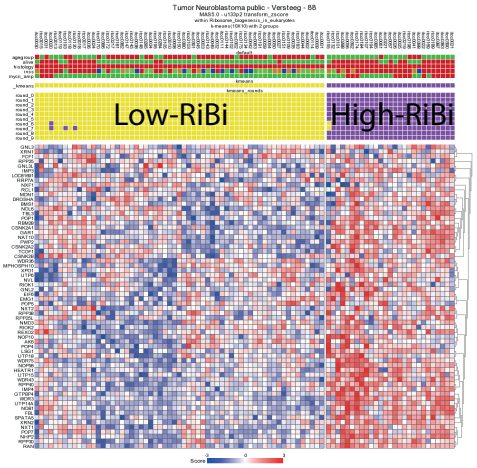

K-means clustering, 2 groups
"ribosome biogenesis in eukaryotes"

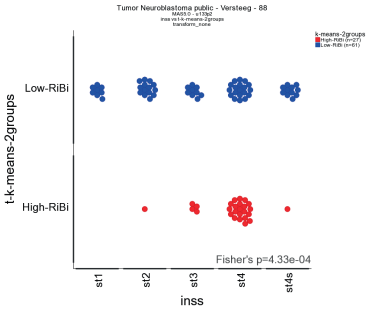

Distribution of High-RiBi and Low-RiBi tumors in INSS tumor stages

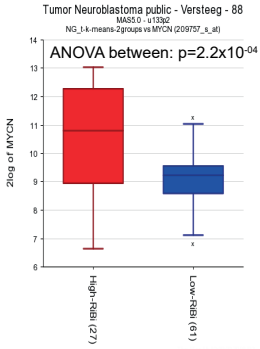

MYCN expression in High-RiBi and Low-RiBi tumors

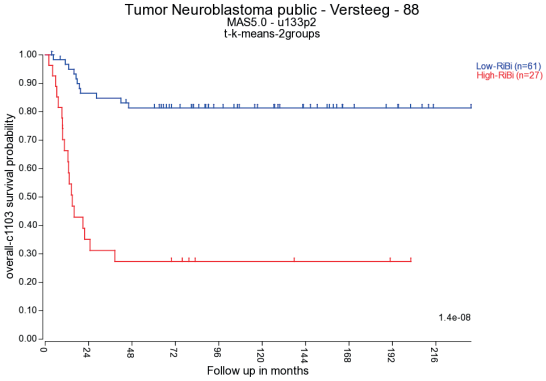

Overall survival between Low-Ribi and High-RiBi tumors

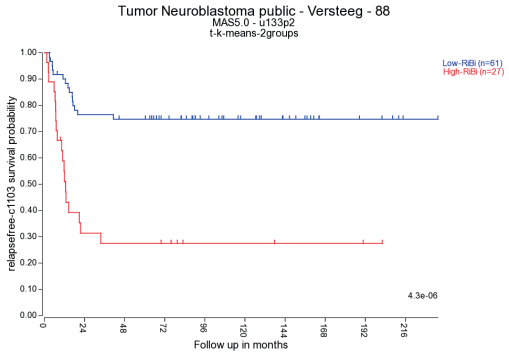

Relapsefree survival between Low-Ribi and High-RiBi tumors

B

Neuroblastoma Maris-101

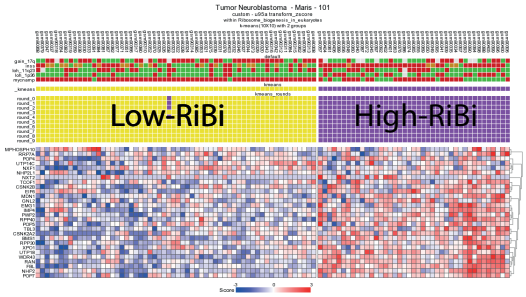

K-means clustering, 2 groups
"ribosome biogenesis in eukaryotes"

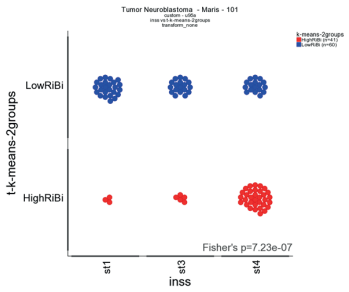

Distribution of High-RiBi and Low-RiBi tumors in INSS tumor stages

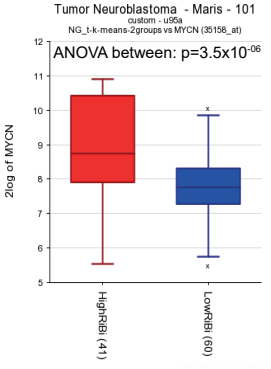

MYCN expression in High-RiBi and Low-RiBi tumors

C

Neuroblastoma Oberthuer-251

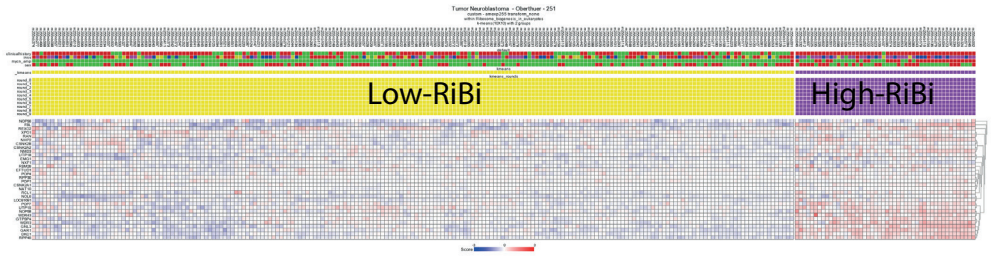

2 color array containing negative values. To avoid filter out, K-mean's settings were as follow:
-floor value: -500
-range: 0
-max exp: -500

K-means clustering, 2 groups
"ribosome biogenesis in eukaryotes"

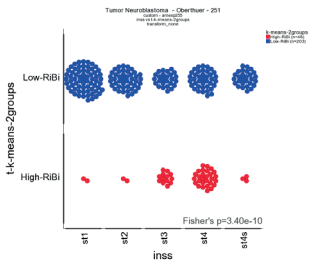

Distribution of High-RiBi and Low-RiBi tumors in INSS tumor stages

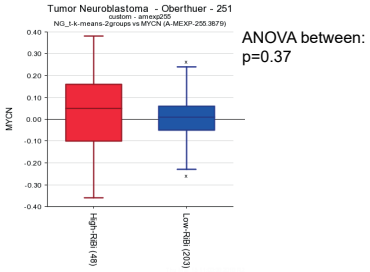

ANOVA between: p=0.37

MYCN expression in High-RiBi and Low-RiBi tumors

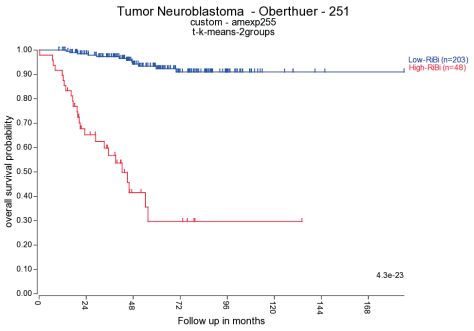

Overall survival between Low-Ribi and High-RiBi tumors

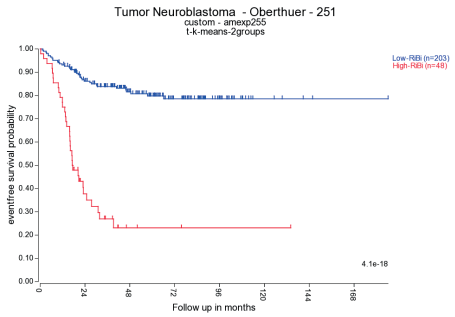

Eventfree survival between Low-Ribi and High-RiBi tumors

D

Neuroblastoma non-*MYCN*-amplified - Seeger-102

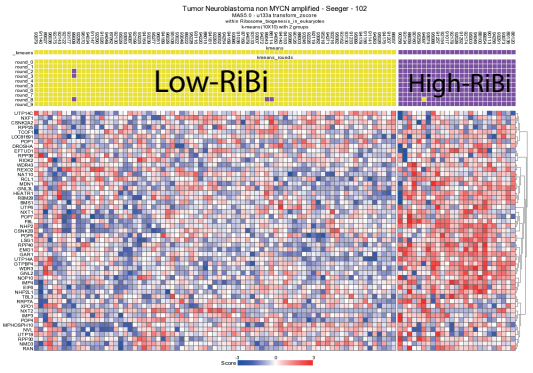

K-means clustering, 2 groups
"ribosome biogenesis in eukaryotes"

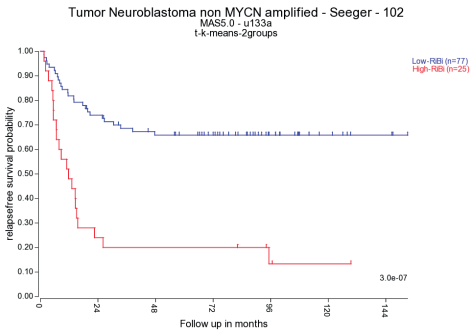

Relapsefree survival between Low-Ribi and High-RiBi tumors

SUPPLEMENTARY FIGURE 3

A

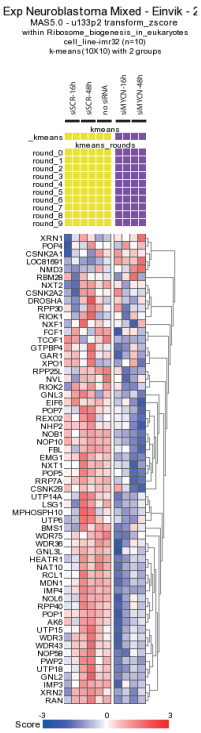

B

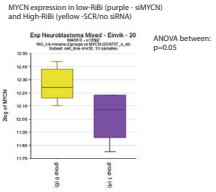

SUPPLEMENTARY FIGURE 4

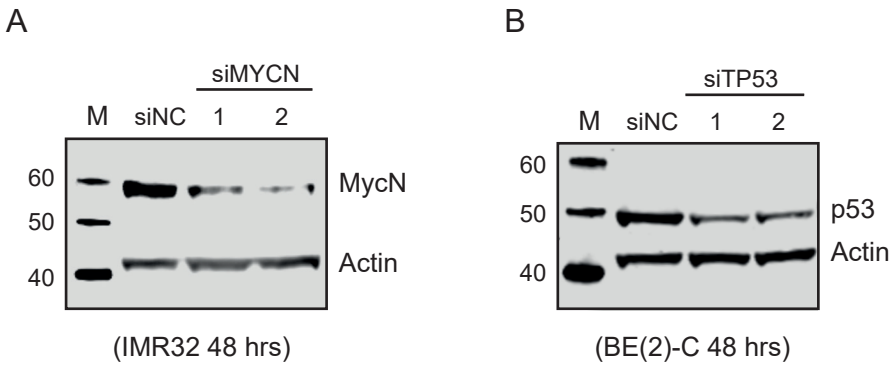

SUPPLEMENTARY FIGURE 5

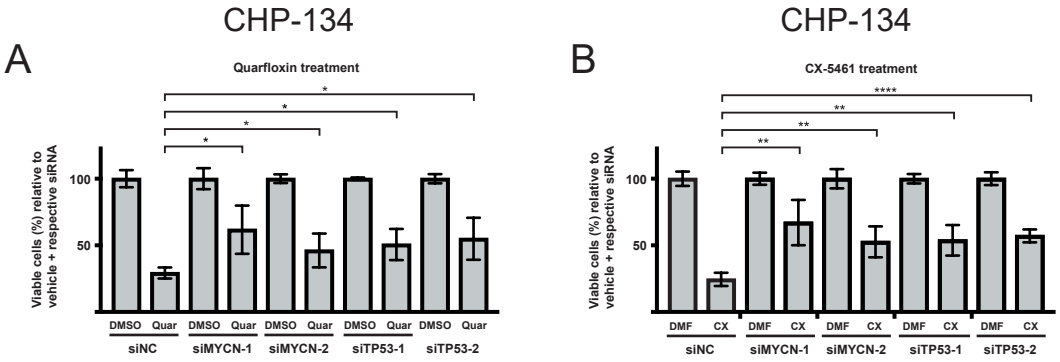

SUPPLEMENTARY FIGURE 6

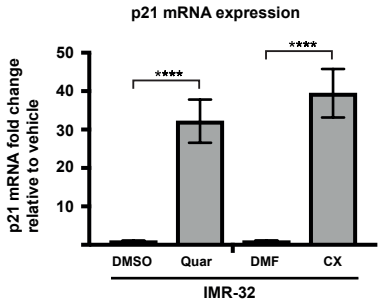

SUPPLEMENTARY FIGURE 7

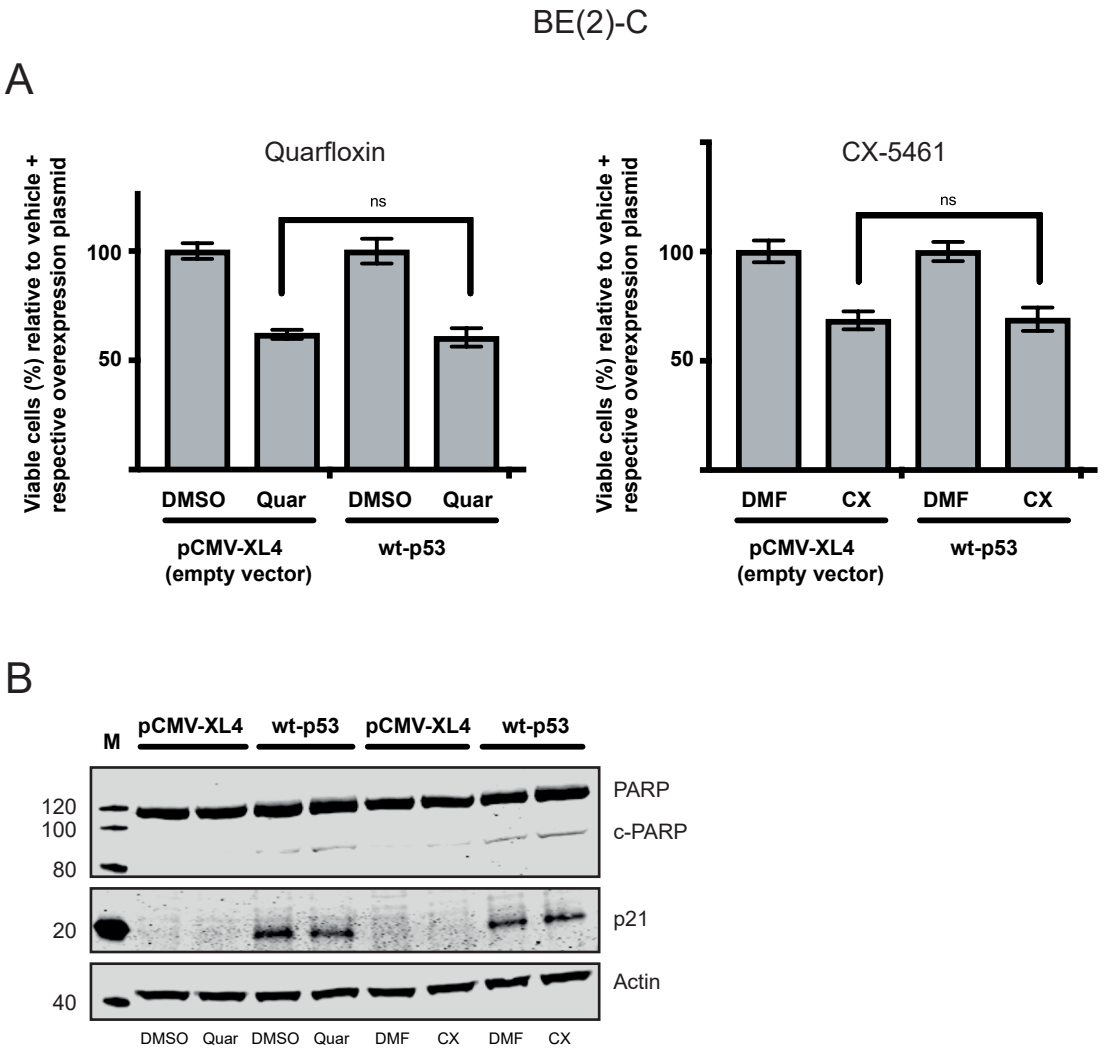

SUPPLEMENTARY FIGURE 8

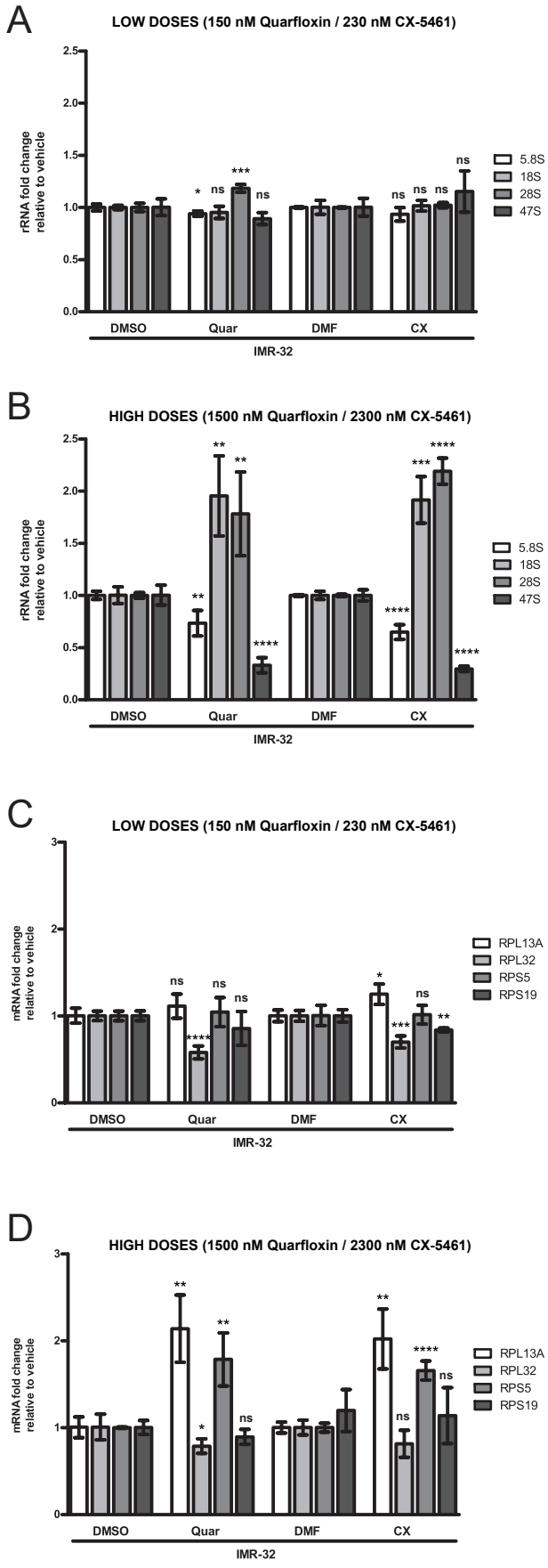

SUPPLEMENTARY FIGURE 9